Contribution to the discretization of sliding mode differentiators

José Eduardo Carvajal Rubio

Thèse de doctorat

Pour obtenir le grade de Docteur de

l'UNIVERSITÉ POLYTECHNIQUE HAUTS-DE-FRANCE,

l'INSA HAUTS-DE-FRANCE

et CENTRO DE INVESTIGACIÓN Y DE ESTUDIOS AVANZADOS DEL IPN

Discipline, spécialité :

Automatique, Genie Informatique

Présentée et soutenue par José Eduardo CARVAJAL RUBIO.

à Cinvestav, Mexique

Ecole doctorale : ED PHF

Equipe de recherche, Laboratoire : LAMIH-UMR CNRS 8201 et Cinvestav

Contribution à la discrétisation des différentiateurs par modes glissants

JURY

Président du Jury	CASTILLO TOLEDO, Bernardino	PR. CINVESTAV
Rapporteur	BARBOT, Jean Pierre	PR. ENSEA
Rapporteur	BOTERO CASTRO, Hector	PR. National University of Colombia
Examinatrice	LALEG KIRATI, Taous-Meriem	MCF. KAUST
Examinatrice	ORTEGA CISNEROS, Susana	PR. CINVESTAV
Co-encadrant	DJEMAI, Mohamed	PR. UPHF, INSA HdF
Co-directeur	DEFOORT, Michaël	PR. UPHF
Co-directeur	LOUKIANOV, Alexander	PR. CINVESTAV
Invité	SÁNCHEZ TORRES, Juan Diego	Dr. ITESO
Invité	RUIZ LEON, José Javier	PR. CINVESTAV

Contribution to the discretization of sliding mode differentiators

Jose Eduardo Carvajal Rubio

A thesis submitted for the degree of Doctor of Philosophy in partial fulfilment of the requirements of

EL CENTRO DE INVESTIGACIÓN Y DE ESTUDIOS AVANZADOS DEL IPN,

l'UNIVERSITÉ POLYTECHNIQUE HAUTS-DE-FRANCE,

l'INSA HAUTS-DE-FRANCE

Research undertaken in the Laboratory of Automatic Control at CINVESTAV, and LAMIH UMR CNRS 8201

December 2022

JURY

President of the Jury	CASTILLO TOLEDO, Bernardino	PR. CINVESTAV
Reviewer	BARBOT, Jean Pierre	PR. ENSEA
Reviewer	BOTERO CASTRO, Hector	PR. National University of Colombia
Examiner	LALEG KIRATI, Taous-Meriem	MCF. KAUST
Examiner	ORTEGA CISNEROS, Susana	PR. CINVESTAV
Co-supervisor	DJEMAI, Mohamed	PR. UPHF, INSA HdF
Co-director	DEFOORT, Michaël	PR. UPHF
Co-director	LOUKIANOV, Alexander	PR. CINVESTAV
Invited	SÁNCHEZ TORRES, Juan Diego	PR. ITESO
Invited	RUIZ LEON, José Javier	PR. CINVESTAV

Titre: Contribution to the discretization of sliding mode differentiators

Résumé: Ce travail vise à concevoir des algorithmes en temps discret permettant d'estimer les dérivés successives d'un signal bruité. Dans un premier temps, nous avons introduit et analysé une réalisation explicite et implicite en temps discret du différenciateur homogène en temps continu. Le différenciateur implicite en temps discret n'est pas anticipatif et repose sur une estimation de l'unique racine positive d'un polynôme, qui dépend des états et de l'entrée du système. La stabilité de ces réalisations est étudiée en utilisant la notion d'homogénéité. Une implémentation efficace est également proposée pour réduire la complexité temporelle de l'algorithme. Dans un second temps, nous avons introduit et analysé des réalisations explicites et implicites pour le différenciateur filtré exact robuste en temps continu. Une version explicite, basée sur la discrétisation exacte des systèmes linéaires avec un bloqueur d'ordre zéro, est introduit. Cependant, la présence de termes d'ordre élevé dans la dynamique du filtre peut provoquer une instabilité de l'erreur d'estimation pour les signaux avec des dérivées non bornées. Par conséquent, une version modifiée est proposée, visant à supprimer cet inconvénient. Sur la base de ce schéma, une version implicite est dérivée. On montrera, en utilisant la propriété d'homogénéité, qu'après un temps fini, les différenciateurs explicites et implicites en temps discret préservent la précision de celui en temps continu malgré la présence de bruit de mesure. Sur la base de ces résultats, un contrôleur basé sur le différentiateur filtré est élaboré en utilisant les mesures bruitées et échantillonnées. Une analyse de la stabilité en boucle fermée est fournie pour un système de type chaîne d'intégrateurs avec mesures échantillonnées et bruitées. Des résultats de simulation sont effectués pour comparer les méthodes de discrétisation proposées avec d'autres schémas existants pour mettre en évidence, par exemple, ses avantages en termes de précision lorsque des périodes d'échantillonnage relativement grandes sont considérées. Une validation expérimentale est réalisée sur le convertisseur abaisseur de tension DC-DC.

Mots-Clés: Discrétisation implicite; Différenciateur robuste; Modes glissants à temps discret; Systèmes homogènes; Différenciation en ligne; Contrôle du mode coulissant; Stabilisation du retour de sortie.

Title: Contribution to the discretization of sliding mode differentiators

Abstract: This work aims to design discrete-time realization to estimate the successive time derivatives of a noisy signal. Explicit and implicit realizations in discrete-time of the continuous-time homogeneous differentiator are introduced and analyzed. The discrete-time implicit differentiator is non anticipative and relies on an estimate of the unique positive root of a polynomial, which depends on the states and the input of the system. The stability of these realizations is studied using the notion of homogeneity. An efficient implementation is also proposed to reduce the time complexity of the implicit version. Secondly, we introduced and analyzed explicit and implicit realizations for the continuous-time robust exact filtering differentiator. An explicit version, based on the exact discretization of linear systems with a zero order hold, is introduced. However, the presence of high order terms in the filter dynamics can cause instability of the estimation error for signals with unbounded derivatives. Therefore, a modified version is proposed, aimed at eliminating this drawback. Based on this scheme, an implicit version is derived. It is shown, using the property of homogeneity, that after a finite time, the explicit and implicit realizations preserve the accuracy of the continuous counterpart despite the presence of measurement noise. Based on these results, a controller based on the filtered differentiator is built using the sampled noisy measurements. A closed-loop stability analysis is provided for a chain-of-integrators system with sampled and noisy measurements. Simulation results are performed to compare the proposed discretization methods with other existing schemes to highlight, for instance, its advantages in terms of accuracy when relatively large sampling periods are considered. An experimental validation is carried out on the DC-DC buck converter.

Keywords: Implicit discretization; Robust differentiator; Discrete-time sliding modes; Homogeneous Systems; Online differentiation; Sliding mode control; Output feedback stabilization.

Contents

List of Notations

- $\mathbb{R}$ Set of real numbers.
- $\mathcal{N}_C(x)$ Normal cone to the set C at a point $x \in \mathbb{R}^n$.
- $\sigma_C(x)$ Support function of a non-empty compact convex set C at a point $x \in \mathbb{R}^n$.
- $\mathbb{R}^+$ Set of positive real numbers.
- $\mathbb{R}^-$ Set of negative real numbers.
- $\text{proj}_M[C; y]$ Orthogonal projection at a point $y \in \mathbb{R}^n$, for a positive definite matrix M and a closed non empty convex set C.
- $\text{sign}(x)$ Set-valued function sign.
- τ Sampling time.
- $\boldsymbol{\Lambda_m}(\alpha)$ Dilation matrix.
- n Number of estimated derivatives.
- $f_0(t)$ Function at least n times differentiable.
- $\Delta(t)$ Measurement noise.
- $\boldsymbol{e}_i$ Canonical vectors i.
- $\mathbb{K}_{i,n}$ Kolmogorov constants.
- σ_i Estimation error of the derivative i.
- λ_i Gains of the differentiator.
- $\lfloor \cdot \rceil^x$ $\lfloor \cdot \rceil^x = |\cdot|^x \,\text{sign}(\cdot)$ for $x \geq 0$.
- $\Psi_{i,n}(\cdot)$ $\Psi_{i,n}(\cdot) = -\lambda_{n-i} L^{\frac{i+1}{n+1}} \lfloor \cdot \rceil^{\frac{n-i}{n+1}}$.

List of Acronyms

- HEDD Homogeneous explicit discrete-time differentiator.
- HIDD Homogeneous implicit discrete-time differentiator.
- EDFD Explicit discrete-time filtering differentiator.
- MEDFD Modified explicit discrete-time filtering differentiator.
- MIDFD Modified implicit discrete-time filtering differentiator.
- HIDD Implicit discretization of the homogeneous differentiator.
- HDD Homogeneous discrete-time differentiator.
- GHDD Generalized homogeneous discrete-time differentiator.
- I-A0-SD Implicit discrete time realization of the arbitrary order standard differentiator.
- IHDD Implicit homogeneous discrete-time differentiator.

Acknowledgements

First I want to thank all my family, for the unconditional support they have always given me in all the projects and goals.

I would like to express my sincere gratitude to my supervisors Pr. Michaël Defoort, and Pr. Alexander Loukianov for their continuous support throughout the duration of my thesis, as well as their valuable suggestions and guidance. I would also like express my immense thanks to my co-supervisor Pr. Mohamed Djemai and Pr. Juan Diego Sánchez Torres for their availability, for sharing their experience and for their extremely valuable support. Specifically, I want to thank Pr. Juan Diego Sánchez Torres because he proposed the initial topic of the thesis, he helped me to contact Pr. Michaël Defoort and formalize the cooperation between Cinvestav and UPHF. I could not have asked for better supervisors.

I would also like to thank all of my friends and colleagues for the past 3 years both in UPHF and CINVESTAV, for their friendship, cooperation and support. Particularly, I would like to thank to Martin Alarcon Carbajal, Dr. David Enrique Castro Palazuelos and Dr. Guillermo Javier Rubio Astorga for its collaboration in the implementation of the algorithms proposed in this work.

A very special thanks to Pr. Jean-Pierre Barbot and Pr. Hector Antonio Botero Castro for agreeing to examine and review my work. Furthermore, thanks to Pr. Bernardino Castillo Toledo, Pr. Taous-Meriem Laleg Kirati, Pr. Susana Ortega Cisneros and Pr. José Javier Ruiz León agreeing to be part of the jury. I am very appreciative and honoured.

Furthermore, I would like to thank CONACyT for the scholarship provided during this investigation to the student with No. CVU 555845, and to CINVESTAV for the provided resources.

Finalement, je tiens à remercier mon financeur du côté UPHF, la région Hauts-de-France, qui a permis que ces travaux de thèse, soient possibles.

Declaration

I declare that the work contained in this thesis has only been submitted for the cotutelle dual award under the cotutelle agreement between CINVESTAV and Université Polytechnique Hauts-de-France and has not been submitted for any other award and that it is all my own work. I also confirm that this work fully acknowledges opinions, ideas and contributions from the work of others.

Name: José Eduardo Carvajal Rubio
Date: 10/10/2022

General Introduction

Motivation

Sliding-modes are widely used to design and implement observer [Utkin *et al.* 2009, Kim 2010, Lienhardt *et al.* 2007, Ren *et al.* 2019] due to their finite-time convergence, accuracy and robustness properties with respect to uncertainties [Utkin *et al.* 2009, Edwards & Spurgeon 1998]. One of its main disadvantages is the chattering effect [Levant 2010], which might be cause by measurement noise, delays, inadequate discretization and hysteresis effects [Levant 2010].

In many control engineering applications, real-time differentiation of a noisy signal is required [Atassi & Khalil 2000, Levant 2003] (e.g., PID and output-feedback controllers, observers, supervision, ...). The main challenge concerning the design of real-time differentiators is the trade-off between exactness and noise filtration performances [Rodrigues & Oliveira 2018]. For instance, the explicit Euler differentiator amplifies the effect of measurement noise. Therefore, measurement noises with small magnitude may significantly affect the estimate of the signal derivatives. To deal with this issue, linear filters (i.e., a combination of low-pass filter and ideal differentiator) were investigated. However, they require an appropriate tuning of the parameters according to noise characteristics and only guarantee asymptotic time convergence of the differentiaton errors. To alleviate these limitations, continuous-time homogeneous differentiators based on sliding modes have been proposed to estimate the first n derivatives of a noisy signal under the assumption of athe existence of a known Lipschitz constant for the n-th derivative of the free-noise signal [Levant 2003]. Several proofs and numerical studies show that such differentiators present excellent robustness properties to bounded noises and exact finite-time convergence in the absence of noise. Furthermore, these attractive properties motivate their application in several applications [Kaveh & Shtessel 2008, Shtessel *et al.* 2007, Iqbal *et al.* 2011].

Recently, in [Levant & Livne 2019], a continuous-time filtering differentiator has been investigated to improve the accuracy compared with the standard one [Levant 2003], under a specific class of noises. Mainly, for bounded noises, it presents the same accuracy as the standard one. In contrast to the standard differentiator, the robust exact filtering differentiator rejects the effects of some large noises after a finite time. Furthermore, this differentiator can filter out unbounded noises composed of signals of global filtering order $j \in \mathbb{N}$, where j is less than or equal to the filtering order of the differentiator.

A discrete-time version of the standard differentiator is needed to implement a controller or an observer on a digital device. However, an improper discretization may result in eliminating the properties of its continuous-time counterpart or undesirable behavior due to, for instance, numerical chattering [Polyakov *et al.* 2019] or the asymptotic accuracy of the continuous-time differentiator [Livne & Levant 2014]. Therefore, some discrete-time sliding mode schemes have been introduced and applied in several works [Polyakov *et al.* 2019, Drakunov & Utkin 1990, Utkin 1994, Kikuuwe & Fujimoto 2006, Su *et al.* 2000]. In particular, for the standard differentiator and robust exact filtering differentiator, some explicit discrete-time realizations have been proposed in [Levant & Livne 2019, Livne & Levant 2014, Koch *et al.* 2020, Barbot *et al.* 2020, Carvajal-Rubio *et al.* 2021a, Carvajal-Rubio *et al.* 2020b, Hanan

et al. 2020, Mojallizadeh *et al.* 2021] to preserve properties of the respective continuous-time system using different methodologies. The discrete-time filtering differentiator, proposed in [Levant & Livne 2019], corresponds to an Euler discretization with Taylor-like terms for the states that estimate the signal derivatives. Similarly, the scheme presented in [Hanan *et al.* 2020] preserves the accuracy of the filtering differentiator.

Recently, other discrete-time schemes that rely on an implicit discretization have been introduced [Brogliato *et al.* 2019, Luo *et al.* 2019, Huber *et al.* 2013]. It has been shown that such discrete-time realizations preserve the existing properties of the continuous-time sliding mode algorithms and reduce the numerical chattering. Contrary to many explicit discretization methods, implicit ones do not significantly reduce the performance for large sampling times in terms of robustness properties to matched perturbations and accuracy while not being sensitive to control gain variations. Nevertheless, they require a more elaborate scheme compared with their explicit counterparts. A pioneer work [Drakunov & Utkin 1990] has presented an implicit discretization for the scalar case where the disturbance is required to be known. Then, other works, [Brogliato *et al.* 2019, Huber *et al.* 2013] have introduced a time discretization of the original plant and an implicit discretization of the controller, where the unperturbed plant is analyzed to obtain a causal controller. Moreover, implicit time-discretization schemes have been derived for twisting and super-twisting controllers [Brogliato *et al.* 2019, Huber *et al.* 2019], finite-time and fixed-time systems [Polyakov *et al.* 2019], where the stability properties are preserved. The implicit discrete-time super-twisting [Brogliato *et al.* 2019] has presented convergence to the origin in a finite number of steps for the unperturbed case.

At last, a control law often needs the derivatives of noisy signals (i.e., the measurements). Hence, several works consider the design of sliding mode differentiator-based controllers due to finite-time property (see [Oliveira *et al.* 2017, Castañeda *et al.* 2021] for instance). However, differentiators require high gains to deal with the system uncertainties when they are used in a closed-loop. It is even more difficult when high-order differentiators are needed since it yields the sensitivity of the closed-loop system with respect to measurement noise and discretization effect. It should be highlighted that the sampled-data sliding mode differentiator-based control design is not well-investigated in the literature.

Objective

The main objectives of this thesis are to design new discrete-time realizations for the continuous-time homogeneous and filtering differentiators such that they

- allow for large sampling periods without a significant decrease of the performances,
- reduce the numerical chattering,
- preserve the continuous-time properties of continuous-time counterpart, for instance, the finite-time convergence and perturbation rejection,

- provide good robustness properties with respect to measurement noises.

Furthermore, a sampled-data sliding mode differentiator based controller is designed which guarantees that the associated closed-loop discrete-time system is stable.

Contributions of the thesis

The main contributions of this work are the following

- To introduce explicit and implicit discrete-time realizations of the continuous-time homogeneous differentiator.
- To introduce explicit and implicit discrete-time realizations of the continuous-time robust exact filtering differentiator.
- The unique solution of the implicit differentiators is non-anticipative, relies on a root finding method and preserves the properties of the continuous-time differentiators.
- The stability property of the proposed schemes are analyzed using homogeneity property.
- The cubic convergence of the Halley's method for the implicit differentiator is demonstrated.
- An efficient implementation is proposed to reduce the time complexity for the implicit method.
- A sampled-data sliding mode differentiator based controller is designed.
- The link between the disturbance bound and the observer parameters of the filtering differentiator is discussed.
- A stability analysis of the closed-loop system combining the robust exact filtering observer and a saturated output feedback controller is provided for integrator chains with sampled data.
- Comparisons between the proposed implicit and explicit discrete-time realizations with other existing schemes, highlighting that the implicit scheme supersedes the explicit one are provided.
- Comparisons between the implicit discrete-time closed-loop differentiator and the explicit one [Levant & Livne 2019] are given to highlight the advantages in terms of accuracy of the proposed scheme.
- Experiments are conducted on the DC-DC buck converter to show the effectiveness of the proposed scheme.

Organization

The thesis is divided as follows.

- In Chapter 1, some preliminaries on set-valued functions, generalized equations, homogeneous systems are recalled. Explicit and implicit discretization methods are discussed. The differentiation problem is introduced and some continuous-time differentiators are recalled. At last, some existing discrete-time realizations of the standard differentiator are reported. All these concepts will be very useful to derive the main results in the following Chapters.

- In Chapter 2, two discrete-time realizations of the homogeneous differentiator, i.e. an explicit and an implicit one, namely HEDD and HIDD are introduced. Furthermore, its main properties are studied and it is demonstrated that they preserve the accuracy of their continuous-time counterparts after a finite time. An implementation strategy is proposed for the implicit discrete-time realization, which is non-anticipative and includes a root-finding method based on Halley's method. Different methodologies are also discussed to obtain an efficient implementation, in terms of time complexity, of the implicit discrete-time differentiator which rely on the Horner's method and the Shaw-Traub algorithm. Simulation results using the proposed interpolation methods were carried out to show a noticeable improvement compared to a direct implementation. A comparison analysis of discrete-time realizations of the robust exact differentiator with existing ones is provided. It was shown that HIDD exhibits the best performance for a free-noise case and in the presence of noise. Furthermore, HIDD supersedes HEDD, consistent with the implicit and explicit time discretization of other continuous-time systems.

- Chapter 3 is focused on novel explicit and implicit realizations for the continuous-time robust exact filtering differentiator [Levant & Livne 2019]. First, a time discretization of the robust exact filtering differentiator based on the Matching approach is investigated. It relies on the stabilization of a pseudo linear discrete-time system. Then, an explicit discrete-time filtering differentiator, based on the exact discretization of linear systems with a zero-order holder, is introduced. However, the presence of high-order terms in the filter dynamics may cause instability of the estimation error for signals with unbounded derivatives. Hence, a modified explicit discrete-time filtering differentiator is proposed, aiming to remove such a drawback of the exact discretization. Based on this scheme, an implicit version is derived. It will shown, using the homogeneity property, that after a finite time, the explicit and implicit discrete-time filtering differentiators preserve the accuracy of the continuous-time one despite the presence of measurement noise. Finally, some simulation results include comparisons between the proposed implicit and explicit discrete-time realizations with other existing schemes, highlighting that the implicit scheme supersedes the explicit one.

- In Chapter 4, the stabilization problem for perturbed chain of integrators using sampled noisy measurements is investigated. First, an implicit discrete-time

realization of the robust exact filtering differentiator is derived to include some additional terms related to the control input. An appropriate output feedback control law is then derived. The stability of the closed-loop system is studied. A comparison between the implicit discrete-time closed-loop differentiator and the explicit one [Levant & Livne 2019] is given to highlight the advantages in terms of accuracy of the proposed scheme. At last, experiments are conducted on the DC-DC buck converter to show the effectiveness of the proposed scheme.

- In Chapter 5, the obtained results are summarised and possible future research directions are given.

Publication

The above contributions were presented in the following international journal papers:

- J. E. Carvajal-Rubio, J. D. Sanchez-Torres, M. Defoort, M. Djemai, and A. G. Loukianov. "Implicit and Explicit Exact Discretization of Homogeneous Differentiators", International Journal of Robust and Nonlinear Control, March. 2021, doi:10.1002/rnc.5505.

- J. E. Carvajal-Rubio, J. D. Sanchez-Torres, M. Defoort, M. Djemai, and A. G. Loukianov. "On the Efficient Implementation of an Implicit Discrete-Time Differentiator", WSEAS Transactions on Circuits and Systems, vol. 20, pp. 70-74, 2021.

- J. E. Carvajal-Rubio, M. Defoort, J. D. Sanchez-Torres, M. Djemai, and A. G. Loukianov. "Implicit and explicit discrete-time realizations of the robust exact filtering differentiator", Journal of the Franklin Institute, vol. 359, pp 3951-3978, May 2022, doi: 10.1016/j.jfranklin.2022.03.007.

- M. A. Alarcon-Carbajal, J. E. Carvajal-Rubio, J. D. Sanchez-Torres, D. E. Castro-Palazuelos, and G. J. Rubio-Astorga. "An Output Feedback Discrete-Time Controller for the DC-DC Buck Converter", Energies, vol. 15, July 2022, doi: 10.3390/en15145288.

- J. E. Carvajal-Rubio, M. A. Alarcon-Carbajal, J. D. Sanchez-Torres, M. Defoort, G. J. Rubio-Astorga, D. E. Castro-Palazuelos, M. Djemai, and A. G. Loukianov. "Robust Discrete-Time Output Feedback Stabilization of Integrator Chains", International Journal of Robust and Nonlinear Control, 2022.

Additionally, the following conference papers were published:

- J.E. Carvajal-Rubio, A. G. Loukianov, J. D. Sanchez-Torres, M. Defoort. "On the discretization of a class of homogeneous differentiators", 16th International Conference on Electrical Engineering, Computing Science and Automatic Control, 2019, doi: 10.1109/ICEEE.2019.8884567.

- J. E. Carvajal-Rubio, J. D. Sanchez-Torres, M. Defoort, A. G. Loukianov. "On the Discretization of Robust Exact Filtering Differentiators", 21st IFAC World Congress, 2020.
- J. E. Carvajal-Rubio, J. D. Sanchez-Torres, M. Defoort, A. G. Loukianov and M. Djemai. "Discretization of the Robust Exact Filtering Differentiator Based on the Matching Approach", 17th International Conference on Electrical Engineering, Computing Science and Automatic Control, 2020, doi:10.1109/CCE50788.2020.9299184v .

CHAPTER 1

Preliminaries and state of the art

In this chapter, some preliminaries, used to derive the main results in the following Chapters, are given. First, before describing some basics on time discretization, we recall some concepts and definitions related to set-valued functions and generalized equations. Then, we introduce some existing discretization methods (explicit and implicit ones). One can note that the implicit discretization of first order sliding mode schemes preserve the properties of continuous-time sliding mode one to the digital implementation setting. However, the study of high order sliding mode schemes require some concepts as homogeneity. Hence, Section 1.2 will focus on homogeneous systems, the associated convergence properties and robustness properties with respect to delays, measurement noise and disturbances. The differentiation problem is introduced in Section 1.3. Furthermore, two continuous-time homogeneous differentiators are presented (i.e., the robust exact differentiator also called standard differentiator and the robust exact filtering differentiator). One can note that the continuous-time homogeneous differentiators include integration and continuous-time measurements. To implement these differentiators on a digital device, a proper discretization is required. Hence, in Section 1.4, some existing discrete-time realizations of the standard differentiator are reported.

1.1 Time discretization

Before describing some basics on time discretization, let us recall some concepts related to set-value functions and generalized equations.

1.1.1 Set-valued functions

In this section, the set-valued functions and selections are defined. Both concepts are used to obtain the implicit time discretizations of Chapters 2 and 3. A set-valued function is defined as follows:

Definition 1.1 *[Hiriart-Urruty & Lemaréchal 2004] A mapping $\boldsymbol{F}$ of $\boldsymbol{x} \in \mathbb{R}^n$ associated to a subset of $\mathbb{R}^m$ is called a set-valued function. This mapping is represented with the notation:*

$$\mathbb{R}^n \ni \boldsymbol{x} \longmapsto \boldsymbol{F}(\boldsymbol{x}) \subseteq \mathbb{R}^m, \tag{1.1}$$

or also as

$$\boldsymbol{F} : \mathbb{R}^n \rightrightarrows \mathbb{R}^m. \tag{1.2}$$

The domain of $\boldsymbol{F}$, $dom(\boldsymbol{F})$, is the set of $\boldsymbol{x} \in \mathbb{R}^n$ such that $\boldsymbol{F}(x) \neq \emptyset$. The image of a set-valued function F is the union of all the sets $\boldsymbol{F}(x) \subseteq \mathbb{R}^m$ with $\boldsymbol{x} \in \mathbb{R}^n$. The graph of $\boldsymbol{F}$, $gr(\boldsymbol{F})$, is defined as the union of the sets $\{\boldsymbol{x}\} \times \boldsymbol{F}(\boldsymbol{x}) \subseteq \mathbb{R}^n \times \mathbb{R}^m$, where $\boldsymbol{x}$ belongs to the domain of $\boldsymbol{F}$. A remarkable concept related to set-valued functions is the selection of $\boldsymbol{F}$

Definition 1.2 *A selection of $\boldsymbol{F}$ is a function $f : dom(\boldsymbol{F}) \mapsto \mathbb{R}^n$ with $f(x) \in \boldsymbol{F}(\boldsymbol{x})$ for all $\boldsymbol{x} \in \mathbb{R}^n$.*

Concerning set-valued functions, the upper semi-continuous concept is defined as follows:

Definition 1.3 *A set-value function $\boldsymbol{F}$ is upper semi-continuous in $x_0 \in \mathbb{R}^n$ if for any open set A such that $\boldsymbol{F}(x_0) \subseteq A$, then $\boldsymbol{F}(x) \subseteq A$ for all x close enough to x_0.*

Example 1.1 *An example of an upper semi-continuous in 0 is:*

$$\boldsymbol{F}(x) \begin{cases} \{0\} & \text{if} \quad x \neq 0, \\ [-1, 1] & \text{if} \quad x = 0. \end{cases} \tag{1.3}$$

■

The main difference between a real valued function and a set-valued function is that a real valued function maps from one element of $\mathbb{R}^n$ to an element in $\mathbb{R}^m$, whereas a set-valued maps from one element of $\mathbb{R}^n$ to one or more elements in $\mathbb{R}^m$. In this work, some set-valued functions are used, e.g., the sign function and the normal cone. The first one is defined as, let $x \in \mathbb{R}$ then

$$\text{sign}(x) = \begin{cases} 1 & \text{if} \quad x > 0, \\ [-1, 1] & \text{if} \quad x = 0, \\ -1 & \text{if} \quad x < 0. \end{cases} \tag{1.4}$$

Notice that $\text{sign}(x)$ is a set-valued function because it maps from 0 to the set $[-1, 1]$ and it is upper semi-continuous. On the other hand, the following two set-valued functions are defined [Bachem *et al.* 2012]:

Definition 1.4 *Let $C \in \mathbb{R}^n$ be a convex and close set, then the normal cone to the set C at a point $x \in \mathbb{R}^n$ is defined as:*

$$\mathcal{N}_C(x) = \begin{cases} \emptyset & \text{if} \quad x \neq C, \\ \{y \mid \langle y, c - x \rangle \leqq 0 \quad \forall c \in C & \text{if} \quad x \notin C. \end{cases} \tag{1.5}$$

Definition 1.5 *A support function of a non-empty compact convex set C, is given as:*

$$\sigma_C(x) = \sup_{v \in C} \langle x, v \rangle. \tag{1.6}$$

With respect to normal cone, the support function is the set of all the normal vectors to C in x. Furthermore, the set-valued functions $\partial\sigma_C(x)$ (where δ denotes the subdifferential) and $\mathcal{N}_C(x)$ are inverse mapping. The above means that:

$$x \in \partial\sigma_C(y) \Leftrightarrow y \in \mathcal{N}_C(x), \quad \forall x, y \in \mathbb{R}^n. \tag{1.7}$$

In particular, when $C = [-1, 1]$ and defining the normal cone in $\mathbb{R}$, $\sigma_{[-1,1]}(x) = |x|$, $\partial\sigma_{[-1,1]}(x) = \text{sign}(x) = \partial|x|$. Hence, the normal cone to C is given as:

$$\mathcal{N}_{[-1,1]}(x) = \begin{cases} \mathbb{R}^+ & \text{if} \quad x = 1, \\ 0 & \text{if} \quad x \in (-1, 1), \\ \mathbb{R}^- & \text{if} \quad x = -1. \end{cases} \tag{1.8}$$

The inverse mapping of the set-valued function sign (1.4), is the normal cone (1.8), i.e.,

$$x \in \text{sign}(y) \Leftrightarrow y \in \mathcal{N}_{[-1,1]}(x). \tag{1.9}$$

Let C be a closed non empty convex set. The following relation is useful to solve generalized equations, which are defined hereafter:

$$M(x - y) \in -\mathcal{N}_C(x) \Leftrightarrow x = \text{proj}_M[C; y], \tag{1.10}$$

where $x \in \mathbb{R}^n$, $y \in \mathbb{R}^n$ and M is positive definite symmetric matrix. The orthogonal projection is defined as:

$$\text{proj}_M[C; y] = \text{argmin}_{z \in C} \frac{1}{2}(z - y)^\top M(z - y). \tag{1.11}$$

Let $F : \mathbb{R}^n \rightrightarrows \mathbb{R}^m$ be a set-valued function. F is (strictly) monotone if for any x, $y \in \text{dom}(\mathbf{F}) \subseteq \mathbb{R}^n$ (with $x \neq y$) and $x' \in \mathbf{F}(x), y' \in \mathbf{F}(y)$, the following inequalities are satisfied:

$$\langle x - y, x' - y' \rangle \geq 0 \quad (\langle x - y, x' - y' \rangle > 0). \tag{1.12}$$

Moreover, if there exists an $\alpha > 0$ such that

$$\langle x - y, x' - y' \rangle \geq \alpha \|x - y\|, \tag{1.13}$$

Then, the set-valued function F is strongly monotone. Additionally, if there exists $\xi > 1$ such that

$$\langle x - y, x' - y' \rangle \geq \alpha \|x - y\|^\xi, \tag{1.14}$$

then F is ξ-monotone in C. It is possible to determine if a set-valued function F has these properties with the following propositions [Facchinei & Pang 2003]:

Proposition 1.1

[Facchinei & Pang 2003] A mapping $F : C \subseteq \mathbb{R}^n \mapsto \mathbb{R}^n$ is:

- pseudo monotone in C if for all the vectors x and $y \in C$,

$$(x-y)^T F(y) \geq 0 \Rightarrow (x-y)^T F(x) \geq 0, \tag{1.15}$$

- monotone in C if

$$(F(x)-F(y))^T (x-y) \geq 0, \quad \forall x, y \in C, \tag{1.16}$$

- strictly monotone in C if

$$(F(x)-F(y))^T (x-y) > 0, \quad \forall x, y \in C, \tag{1.17}$$

- ξ-monotone in C with a $\xi > 1$, if there exists a constant $d > 0$ such that:

$$(F(x)-F(y))^T (x-y) \geq d\|x-y\|^{\xi}, \quad \forall x, y \in C, \tag{1.18}$$

- strong monotone in C if there exists a constant $d > 0$ such that:

$$(F(x)-F(y))^T (x-y) \geq d\|x-y\|^2, \quad \forall x, y \in C. \tag{1.19}$$

Proposition 1.2

[Facchinei & Pang 2003] Let $F : D \subseteq \mathbb{R}^n \mapsto \mathbb{R}^n$ be continuously differentiable in the close set D. The following statements hold true:

- F if monotone in D if and only if its jacobian is semi definite positive for all x en D.
- F is strictly monotone in D if its jacobian is uniformly positive.
- F is strong monotone in D if and only if its jacobian is uniformly positive definite for all x in D, i.e., there exists a constant $d > 0$ such that:

$$y^T JF(x) y \geq d\|y\|^2, \quad \forall y \in \mathbb{R}^n, \ \ \forall x \in D. \tag{1.20}$$

1.1.2 Generalized Equations

The generalized equations have some similarities with the differential equations. The main difference is that the right-side of these equations is a set-valued function. Specif-

ically, in the dissertation, we consider the following structure:

$$\mathbf{0} \in f(x) + \mathcal{N}_C(x), \tag{1.21}$$

where C is a closed convex set and $f : \mathbb{R}^n \mapsto \mathbb{R}^n$. Equivalently, the generalized equation (1.21) can be represented as:

$$-f(x) \in \mathcal{N}_C(x). \tag{1.22}$$

The generalized equation (1.21) is called variational inequality. Note that the solutions of the generalized equations have to belong to the set C. An alternative structure of the generalized equation is the following one:

$$x \in C \text{ and } \langle f(x), x' - x \rangle \geq 0, \ \forall x' \in C. \tag{1.23}$$

The following corollaries and Theorems are important for generalized equations.

Corollary 1.1.1 *[Facchinei & Pang 2003] Let $C \subseteq \mathbb{R}^n$ be a non-empty compact convex set and $f : C \mapsto \mathbb{R}^n$ be a continuous mapping. Then, the set of solutions of the variational inequality (1.23) is not empty and compact.*

Corollary 1.1.2 *[Facchinei & Pang 2003] Let $C \subseteq \mathbb{R}^n$ be closed and convex, and $F : \mathbb{C} \mapsto \mathbb{R}^n$ be continuous. If there exits a vector x^{ref} in C such that:*

$$F(x)^T(x - x^{ref}) \geq 0, \ \ \forall x \in C, \tag{1.24}$$

then the variational inequality (1.23) has a solution.

Theorem 1.1.1

[Facchinei & Pang 2003] Let $C \subseteq \mathbb{R}^n$ be closed and convex and $f : C \mapsto \mathbb{R}^n$ be continuous.

- If f is strictly monotone in C, the varitional inequality (1.23) has at least one solution.
- If f is ξ-monotone in C with $\xi > 1$, the variational inequality (1.23) have a unique solution.

1.1.3 Time discretization

Two adjectives are commonly used to characterize an integration method: explicit and implicit. In the following, we will explain these concepts and existing discretization methods.

Definition 1.6 *Let*

$$\boldsymbol{x}_{k+1} = \boldsymbol{x}_k + \boldsymbol{F}(t_k, t_{k+1}, x_{k+1}, x_k) \tag{1.25}$$

a temporal discretization of the continuous-time system:

$$\dot{\boldsymbol{x}} = \boldsymbol{f}(\boldsymbol{x}, t) \tag{1.26}$$

where $t_k = t = \tau k$ *with* $k = 0, 1, \cdots$, *and the difference between* t_{k+1} *and* t_k *is the sampling time* τ. *Hence,*

- *A time discretization is implicit if* F *in Equation* (1.25), *depends only on the quantities* t_k, t_{k+1}, x_{k+1}.
- *A time discretization is explicit if* F *in Equation* (1.25), *depends only on the quantities* t_k, t_{k+1}, x_k.
- *A time discretization is semi-implicit (half-implicit) if* F *in Equation* (1.25), *depends only on the quantities* t_k, t_{k+1}, x_k, x_{k+1}.

One can mention that the implicit and semi-implicit time discretization show good results with set-valued function. Hereafter, an example of an implicit time discretization of a continuous-time system is presented.

Example 1.2 *Let us consider the following system*

$$\dot{x} = u(t) + d(x, t), \tag{1.27}$$

where $d(x, t)$ *is an unknown bounded disturbance with* $|d(x, t)| \leq L$ *and* L *is known. Moreover,* $x(0) = x_0 \in \mathbb{R}$. *The control input* $u(t)$ *is defined as:*

$$u(t) = -\lambda(t), \quad \lambda(t) \in Gsign(x(t)), \tag{1.28}$$

where $u(t)$ *is a selection of the set-valued function and the solution of system* (1.27) *is understood in the Filippov sense, i.e., in the origin* $x(t) = 0$ *there exists a value* $\delta(t)$ *such that* $u(t) = -d(x, t)$. *Now, the system can be time discretizated using the exact discretization or the Euler method. Using the last method, one gets*

$$\begin{aligned} x_{k+1} &= x_k + \tau u_k + \tau d_k, \\ u_k &= -Gsign(x_k), \end{aligned} \tag{1.29}$$

where u_k *is constant in* $t \in [t_k, t_{k+1})$. *To obtain an implicit realization, a modified copy of the explicit system* (1.29) *is used as follows:*

$$\begin{aligned} x_{k+1} &= x_k + \tau u_{k+1} + \tau d_k, \\ \widetilde{x}_{k+1} &= x_k + \tau u_{k+1}, \\ u_{k+1} &= -\lambda_{k+1}, \\ \lambda_{k+1} &\in Gsign(\widetilde{x}_{k+1}). \end{aligned} \tag{1.30}$$

Notice that $\widetilde{x}_{k+1}$ *is defined using the unperturbated system. To implement* u_{k+1}, *the unperturbed system is used and the following generalized equations are obtained:*

$$\begin{aligned} \widetilde{x}_{k+1} - x_k &\in -\tau Gsign(\widetilde{x}_{k+1}), \\ \lambda_{k+1} &\in Gsign(\widetilde{x}_{k+1}). \end{aligned} \tag{1.31}$$

or equivalently:

$$\begin{aligned} 0 &\in -\widetilde{x}_{k+1} + x_k - \tau G sign(\widetilde{x}_{k+1}), \\ 0 &\in -\lambda_{k+1} + G sign(\widetilde{x}_{k+1}). \end{aligned} \tag{1.32}$$

From the relation (1.10), one obtains the following generalized equations:

$$\begin{aligned} &-\frac{\widetilde{x}_{k+1} - x_k}{\tau G} \in sign(\widetilde{x}_{k+1}), \\ &\widetilde{x}_{k+1} \in \mathcal{N}_{[-1,1]}\left(-\frac{\widetilde{x}_{k+1} - x_k}{\tau G}\right) = -\mathcal{N}_{[-1,1]}\left(\frac{\widetilde{x}_{k+1} - x_k}{\tau G}\right). \end{aligned} \tag{1.33}$$

Let $M = \tau G$, $x = \frac{\widetilde{x}_{k+1} - x_k}{\tau G}$, $y = -\frac{x_k}{\tau G}$, then using the relation (1.10), one obtains that $\widetilde{x}_{k+1}$ is given as:

$$\begin{aligned} \text{proj}_{\tau G}\left[[-1,1]; -\tfrac{x_k}{\tau G}\right] &= \text{argmin}_{z\in[-1,1]} \tfrac{1}{2}\left(z + \tfrac{x_k}{\tau G}\right) \tau G \left(z + \tfrac{x_k}{\tau G}\right), \\ \text{proj}_{\tau G}\left[[-1,1]; -\tfrac{x_k}{\tau G}\right] &= \begin{cases} -1 & \text{if} \quad x_k > \tau G, \\ -x_k/\tau G & \text{if } x \in [-\tau G, \tau G], \\ 1 & \text{if } x_k < -\tau G, \end{cases} \\ \tilde{x}_{k+1} &= x_k + \tau G \,\text{proj}_{\tau G}\left[[-1,1]; -\tfrac{x_k}{\tau G}\right]. \end{aligned} \tag{1.34}$$

One can modify the second generalized equation in (1.31) as follows:

$$\begin{aligned} \tilde{x}_{k+1} &\in \mathcal{N}_{[-1,1]}\left(\lambda_{k+1}/G\right), \\ x_k + \tau u_k &\in \mathcal{N}_{[-1,1]}\left(\lambda_{k+1}/G\right), \\ x_k - \tau\lambda_{k+1} &\in \mathcal{N}_{[-1,1]}\left(\lambda_{k+1}/G\right), \\ \lambda_{k+1} - \tfrac{x_k}{\tau} &\in -\mathcal{N}_{[-1,1]}\left(\lambda_{k+1}/G\right), \\ \tfrac{\lambda_{k+1}}{G} - \tfrac{x_k}{\tau G} &\in -\mathcal{N}_{[-1,1]}\left(\lambda_{k+1}/G\right). \end{aligned} \tag{1.35}$$

Similar to $\widetilde{x}_{k+1}$, the selection λ_{k+1} is obtained with $M = 1$, $x = \frac{\lambda_{k+1}}{G}$, $y = \frac{x_k}{\tau G}$:

$$\lambda_{k+1} = G \,\text{proj}_1\left[[-1,1]]; \frac{x_k}{\tau G}\right]. \tag{1.36}$$

Therefore, both variables are defined as:

$$\begin{aligned} &\tilde{x}_{k+1} = x_k + \tau G \,\text{proj}_{\tau G}\left[[-1,1]; -\tfrac{x_k}{\tau G}\right], \\ &u_k = -\lambda_{\mathrm{k+1}} = \mathrm{G}\,\text{proj}_1\left[[-1,1]; -\tfrac{x_k}{\tau G}\right], \\ &\text{proj}_{\tau G}\left[[-1,1]; -\tfrac{x_k}{\tau G}\right] = \begin{cases} -1 & \text{if} \quad x_k > \tau G, \\ -x_k/\tau G & \text{if} \quad x \in [-\tau G, \tau G], \\ 1 & \text{if} \quad x_k < -\tau G. \end{cases} \end{aligned} \tag{1.37}$$

Some remarkable properties of the control law (1.37) with system (1.30) are:

- *The control law u_{k+1} is unique and is non-anticipative. It is due to that the functions of the generalized equation are strictly monotone.*
- *In the unperturbed case, the origin of the discrete-time system is globally Lyapunov stable, with the same continuous-time Lyapunov function.*

- *With an adequate selection of the gain G, the solutions of the perturbed system converge to the discrete-time sliding mode surface $\sum_d = \{(x_k, u_k) | \widetilde{x}_{k+1} = 0\}$ in a finite number of steps and it stays forever.*

- *In the sliding mode surface $\sum_d$, one obtains $u_k = -d_{k+1}$ and $x_k = \tau d_{k-1}$. Moreover, the disturbance is attenuated with a factor τ and the control law almost compensates for the disturbance with a delay τ.*

- *$\widetilde{x}_{k+1}$ is understood as a virtual sliding variable, and u_{k+1} as a selection of the set-valued function sign.*

- *If the trajectories of the systems are far from the origin, the explicit and implicit control laws are equal, and the difference is obtained near to the sliding surface $\sum_d$.*

■

1.2 Homogeneous systems

It should be noted that the implicit discretization of first order sliding mode schemes preserve the properties of continuous-time sliding mode one to the digital implementation setting. However, the study of high order sliding mode schemes require some concepts as homogeneity.

1.2.1 Definitions and illustrative examples

An homogeneous system is invariant with respect to a coordinates-time transformation, in specific, it is a dilation symmetry.

Example 1.3 *Figures 1.1-1.2 show the behavior of the system $\dot{x} = -|x|^{1/2} sign(x)$, which is homogeneous with respect to the transformation $(t, x) \mapsto (\alpha t, \alpha^2 x)$ with $\alpha > 0$. The trajectory of $x(t, 1)$ is obtained with the initial condition $x_0 = 1$, while $x(t, \alpha^2 1)$ is obtained with the initial condition $x(0) = \alpha^2(1) = \alpha^2(x_0)$, where $\alpha = 2$.*

Using the mapping $(x) \mapsto (\alpha^2 x)$, the trajectory of the system obtained with $x_0 = 1$ has the same values than with $x_0 = \alpha^2$. The unique difference between both trajectories is the time when these values are obtained. It is because the transformation includes the time, which is $t \mapsto \alpha t$. As $\alpha = 2$, then the red trajectory at time t_a is obtained with the blue trajectory at time $\alpha t_a = 2t_a$ in Figure 1.2.

■

In order to present a definition of homogeneous systems, the following coordinates transformation is introduced $\boldsymbol{x} \mapsto \boldsymbol{\Lambda_m}(\alpha)\boldsymbol{x}$, where $\boldsymbol{\Lambda_m}(\alpha)$ is a linear mapping $\mathbb{R}^n \mapsto \mathbb{R}^n$

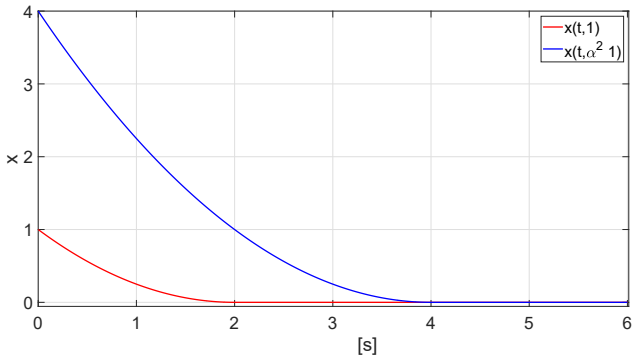

Figure 1.1: Homogeneous system with different initial conditions.

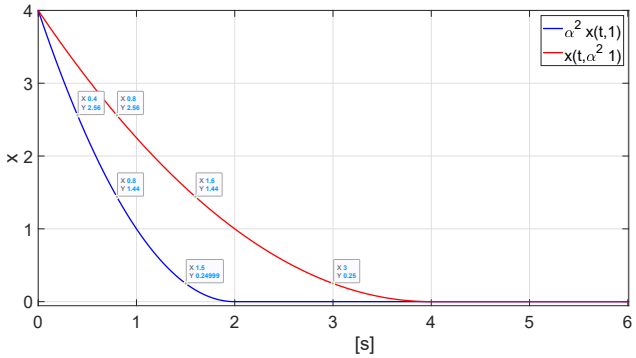

Figure 1.2: Comparison of the trajectories under the coordinate transformation.

defined with the following dilation matrix:

$$\boldsymbol{\Lambda}_{\boldsymbol{m}}(\alpha) = \begin{bmatrix} \alpha^{m_0} & 0 & \cdots & 0 & 0 \\ 0 & \alpha^{m_1} & \cdots & 0 & 0 \\ \vdots & \vdots & \ddots & \vdots & \vdots \\ 0 & 0 & \cdots & \alpha^{m_{n-2}} & 0 \\ 0 & 0 & \cdots & 0 & \alpha^{m_{n-1}} \end{bmatrix}. \tag{1.38}$$

In this matrix, m_i, which is positive, is the weight of the coordinate x_i, and the vector of weights is defined as $\boldsymbol{m} = [m_0 \quad m_1 \quad \cdots \quad m_{n-2} \quad m_{n-1}]^T$. Furthermore, $\boldsymbol{\Lambda}_{\boldsymbol{m}}(\alpha)$ can be expressed as $e^{m_i s} = \alpha^{m_i}$, where $s \in \mathbb{R}$. The most common matrix dilation are the uniform dilation (Leonhard Euler) and the weighted matrix [Zubov 1958]. For the uniform dilation, $m_i = 1$ and therefore $\boldsymbol{\Lambda}_{\boldsymbol{m}}(\alpha) = \alpha \boldsymbol{I}_n$. In the case of the weighted dilation, $\boldsymbol{\Lambda}_{\boldsymbol{m}}(\alpha)$ is defined as in Equation (1.38) where the weights could not be equal.

Concerning a function, its weight is known as homogeneity degree, which is represented as $\deg(x) = m_i$. Then, the following definition is presented [Shtessel *et al.* 14]:

Definition 1.7 *A function $f : \mathbb{R}^n \to \mathbb{R}$ is homogeneous of degree $q \in \mathbb{R}$, $\deg(f) = q$, with a dilation $\boldsymbol{\Lambda}_{\boldsymbol{m}}$, if for any $\alpha > 0$, the equality $f(\boldsymbol{\Lambda}_{\boldsymbol{m}}(\alpha)\boldsymbol{x}) = \alpha^q f(\boldsymbol{x})$ is kept.*

Example 1.4 *Let* $g(x) = -x^v$*, one can select* m_0 *as* $m_0 = 1$*, then* $\deg(g) = v$*. If is selected as* $\deg(x_0) = 3$ *and* $\deg(x_1) = 2$*, the function* $g(x_0, x_1) = -|x_0|^{1/3} sign(x_0) - |x_1|^{1/2} sign(x_1)$ *is homogeneous of degree 1.*
■

Let f and g be homogeneous functions in $\boldsymbol{x} \in \mathbb{R}^n \neq 0$, and k be a constant then the following properties are fulfilled:

- The function $f + g$ is an homogeneous function if and only if $\deg(f) = \deg(g)$.
- If $k \neq 0$, $\deg(k) = 0$.
- $\deg(fg) = \deg(f)\deg(g)$.
- $\deg(f/g) = \deg(f) - \deg(g)$.
- $\deg(kf) = \deg(f)$.
- $\deg(\frac{\partial f}{\partial x_i}) = \deg(f) - \deg(x_i)$.

In the case of a vector field, then the following definition is presented:

Definition 1.8 *A vector field* $\boldsymbol{f} : \mathbb{R}^n \to \mathbb{R}^n$ *is homogeneous of degree* $q \in \mathbb{R}$, $\deg(\boldsymbol{f}) = q$*, with the dilation* $\boldsymbol{\Lambda_m}$*, if for any* $\alpha > 0$*, the equality* $f(\boldsymbol{\Lambda_m}(\alpha)\boldsymbol{x}) = \alpha^q \boldsymbol{\Lambda_m}(\alpha) f(\boldsymbol{x})$ *is kept.*

Example 1.5 *Let the vector field* $\boldsymbol{f}(\boldsymbol{x})$ *and the dilation matrix* $\boldsymbol{\Lambda_m}$ *defined as:*

$$\begin{aligned} \boldsymbol{f}(\boldsymbol{x}) &= \begin{pmatrix} x_2 \\ -x_1^{1/3} - |x_2|^{1/2} \, sign(x_2) \end{pmatrix}, \\ \boldsymbol{\Lambda_m}(\alpha) &= \begin{bmatrix} \alpha^3 & 0 \\ 0 & \alpha^2 \end{bmatrix}. \end{aligned} \tag{1.39}$$

Hence $\deg(x_1) = 3$ *and* $\deg(x_2) = 2$*. If* $\deg(\boldsymbol{f}) = -1$ *is proposed, it is easy to see that* $\deg(f_1) = \deg(x_1) - 1 = 2$ *and* $\deg(f_2) = \deg(x_2) - 1 = 1$*. The above is obtained since* $f_1(\boldsymbol{\Lambda_m}(\alpha)\boldsymbol{x}) = \alpha^2 f_1(\boldsymbol{x})$ *and* $f_2(\boldsymbol{\Lambda_m}(\alpha)\boldsymbol{x}) = \alpha f_2(\boldsymbol{x})$*.* ■

Concerning differential inclusions and equations, the following definition is presented:

Definition 1.9 *Let* $\boldsymbol{f} : \mathbb{R}^n \to \mathbb{R}^n$*, the differential equation:*

$$\dot{\boldsymbol{x}} = \boldsymbol{f}(\boldsymbol{x}) \tag{1.40}$$

is homogeneous of degree $q \in \mathbb{R}$, $\deg(\boldsymbol{f}) = q$*, with the dilation* $\boldsymbol{\Lambda_m}$*, if the inclusion is invariant with respect to the coordinates-time transformation* $\boldsymbol{G}_\alpha : (t, \boldsymbol{x}) \mapsto (\alpha^{-q} t, \boldsymbol{\Lambda_m}(\alpha)\boldsymbol{x})$.

Definition 1.10 *Let the set-valued function* $\boldsymbol{F}(\boldsymbol{x}) \subset \mathbb{R}^n$ *and* $\boldsymbol{x} \in \mathbb{R}^n$*, the differential inclusion:*

$$\dot{\boldsymbol{x}} \in \boldsymbol{F}(\boldsymbol{x}) \tag{1.41}$$

is homogeneous of degree $q \in \mathbb{R}$, $\deg(\boldsymbol{F}) = q$*, with the dilation* $\boldsymbol{\Lambda_m}$*, if the inclusion is invariant with respect to the coordinates-time transformation* $\boldsymbol{G}_\alpha : (t, \boldsymbol{x}) \mapsto (\alpha^{-q}t, \boldsymbol{\Lambda_m}(\alpha)\boldsymbol{x})$.

The above conditions in previous definitions are equivalent to satisfy the following equations:

$$\boldsymbol{f}(\boldsymbol{x}) = \alpha^{-q}\boldsymbol{\Lambda_m}^{-1}(\alpha)\boldsymbol{f}(\boldsymbol{\Lambda_m}(\alpha)\boldsymbol{x}), \tag{1.42}$$

and in the case of differential inclusions:

$$\boldsymbol{F}(\boldsymbol{x}) = \alpha^{-q}\boldsymbol{\Lambda_m}^{-1}(\alpha)\boldsymbol{F}(\boldsymbol{\Lambda_m}(\alpha)\boldsymbol{x}). \tag{1.43}$$

Example 1.6 *The following system is homogeneous system of degree* -1*:*

$$\begin{aligned} \dot{x}_1 &= x_2, \\ \dot{x}_2 &= -|x_1|^{1/3} sign(x_1) - |x_2|^{1/2}\, sign(x_2), \end{aligned} \tag{1.44}$$

where $\deg(x_1) = 3$, $\deg(x_2) = 2$ *and* $\deg(t) = 1$*. On the other hand, the system*

$$\dot{x} = -x^v, \tag{1.45}$$

is homogeneous of degree $v - 1$ *with* $\deg(x) = 1$. ■

1.2.2 Convergence properties

In order to investigate the properties of homogeneous systems, the globally uniformly finite-time stable and globally fixed-time stable systems are defined.

Considering the system:

$$\dot{\boldsymbol{x}} = \boldsymbol{f}(t, \boldsymbol{x}(t)), \qquad \boldsymbol{x}(0) = \boldsymbol{x}_0, \tag{1.46}$$

where $x \in \mathbb{R}^n$, $\boldsymbol{f} : \mathbb{R}^n \to \mathbb{R}^n$ is an upper semi-continuous mapping. Furthermore, it is assumed that the unique equilibrium point of the system is the origin and the solutions of the system are understood in the Filippov sense.

Definition 1.11 *The origin of system* (1.46) *is* ***globally uniformly finite-time stable*** *if it is globally uniformly asymptotically stable and there is a locally bounded function* $T_f : \mathbb{R}^n \to \mathbb{R}_+ \cup \{0\}$*, such that the solutions of the system are kept in the origin* $\forall t \geq T_f(x(0))$*. The function* T_f *is called the* ***settling-time function****.*

Definition 1.12 *The origin of system* (1.46) *is* ***globally fixed-time stable*** *if it is globally uniformly finite-time stable and its settling-time* T_f *is globally bounded, i.e,* $\exists T_{max} \in \mathbb{R}_+$ *such that* $T_f(\boldsymbol{x}(0)) \leq T_{max}$, $\forall \boldsymbol{x}(0) \in \mathbb{R}^n$*.*

One relevant result of homogeneous systems was presented in [Bhat & Bernstein 1997] and given as follows.

Theorem 1.2.1

[Bhat & Bernstein 1997] Let $\dot{\boldsymbol{x}} = \boldsymbol{f}(\boldsymbol{x})$ be a homogeneous differential equation with homogeneous degree q, and where $\boldsymbol{f}$ is a vector field $\boldsymbol{f} : \mathbb{R}^n \to \mathbb{R}^n$. The origin is a finite-time stable equilibrium point if and only if the system is asymptotically stable and $q < 0$.

Example 1.7 *[Bhat & Bernstein 1997] Let the system:*

$$\begin{aligned} \dot{x}_1 &= x_2, \\ \dot{x}_2 &= \frac{u}{m}, \end{aligned} \tag{1.47}$$

with $m > 0$ and u defined as $u = -|x_1|^{\beta} sign(x_1) - |x_2|^{\frac{\beta}{2-\beta}} sign(x_2)$, where $\beta \in (0, 1)$. One can note that the system is homogeneous of negative degree $(\beta - 1)$ with respect to the transformation $(t, x_1, x_2) \mapsto (\alpha^{-(\beta-1)}t, \alpha^{(2-\beta)}x_1, \alpha x_2)$. The above comes from the fact that

$$\begin{aligned} &\left(\alpha^{-(\beta-1)}\right)\left(\alpha^{(\beta-2)}\right) f_1(\alpha^{(2-\beta)}x_1, \alpha x_2) = f_1\left(x_1, x_2\right), \\ &\left(\alpha^{-(\beta-1)}\right)\left(\alpha^{-1}\right) f_2(\alpha^{(2-\beta)}x_1, \alpha x_2) = \alpha^{-\beta}\frac{\alpha^{\beta}(-|x_1|^{\beta} sign(x_1) - |x_2|^{\frac{\beta}{2-\beta}} sign(x_2))}{m}, \\ &\left(\alpha^{-(\beta-1)}\right)\left(\alpha^{-1}\right) f_2(\alpha^{(2-\beta)}x_1, \alpha x_2) = f_2(x_1, x_2). \end{aligned} \tag{1.48}$$

Using the candidate Lyapunov function $V(x_1, x_2) = \frac{1}{2}mx_2^2 + \frac{2-\beta}{2}|x_1|^{\frac{2}{2-\beta}}$, one gets $\dot{V}(x_1, x_2) = -|x_2|^{1+\beta} \leq 0$. As the time derivative of the Lyapunov function is semi-definite negative, the invariant belonging to the set$M : \{(x_1, x_2)|x_2 = 0\}$ is given by $S : \{(x_1, x_2)|x_1 = 0, x_2 = 0\}$. Therefore, from the LaSalle's invariance principle, the system is asymptotically stable. At last, from Theorem 1.2.2, the system is finite-time stable. A simulation with $\beta = 0.5$, $\boldsymbol{x}(0) = (1, -2)$ and $m = 2$ is presented in Figure 1.3.

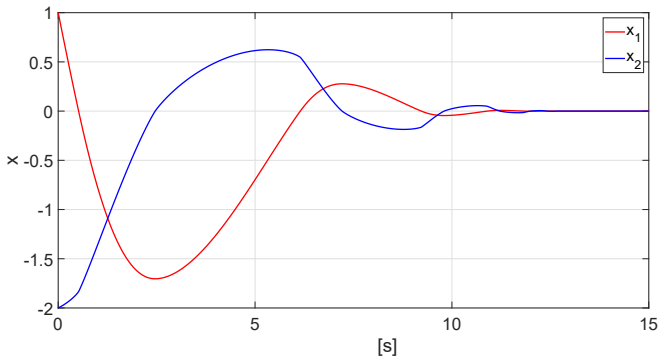

Figure 1.3: Homogeneous system with negative degree.

One can see that the system converges in a finite-time to the origin. If $\beta = 1$, then the system converges asymptotically but it is not finite-time stable. The above can be seen in Figure 1.4.

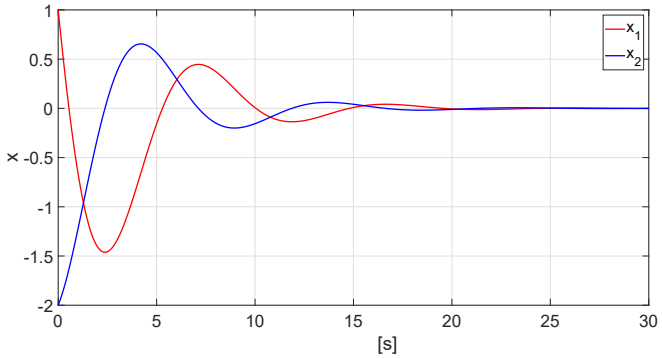

Figure 1.4: Homogeneous system with homogeneity degree 0.

■

Example 1.8 *Let the system $\dot{x} = -|x|^v sign(x)$, which is homogeneous of degree $v-1$. Considering $v = 1/3$, the system is homogeneous with a negative degree and finite-time stable. The trajectories of the system is given as:*

$$x\left(t, x(0)\right) = \begin{cases} \left(|x(0)|^{\frac{2}{3}} - \frac{2}{3}t\right)^{\frac{3}{2}} & \text{if } t \in \left[0, \frac{3}{2}|x(0)|^{\frac{2}{3}}\right) \\ 0 & \text{if } t \geq \frac{3}{2}|x(0)|^{\frac{2}{3}} \end{cases}, \tag{1.49}$$

The simulation results of the system $\dot{x} = -|x|^{\frac{1}{3}} sign(x)$, with the initial condition -2 are presented in Figure 1.5. From the above initial condition, $T_f(-2) = 2.3811\,\text{sec}$, as it can be seen in Figure 1.5.

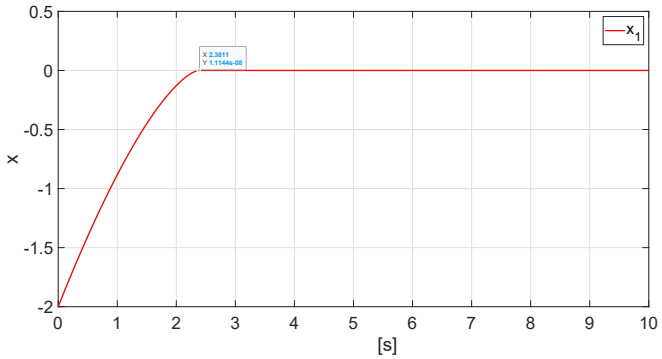

Figure 1.5: Homogeneous system with homogeneous degree $-2/3$.

If $v = 1$, the system is homogeneous of degree 0 and converges exponentially to the origin, as it can be seen in Figure 1.6.

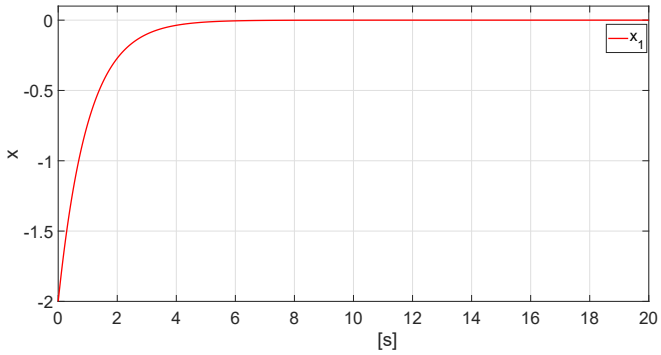

Figure 1.6: Homogeneous system of degree 0.

In the case of positive degree, e.g., $v > 1$*. the trajectories of the system converge to a vicinity of the origin in fixed time. The settling time is independent of the initial condition. If we defined the following vicinity, the settling time can be calculated as follows:*

$$|x(t, x(0))| < r, \qquad \forall t > \frac{1}{r^{v-1}(v-1)}. \tag{1.50}$$

with $r > 0$*. In Figure 1.7 the system is simulated with* $v = 2$ *and three initial conditions. The above equation shows that for* $t > 1$*, the trajectories for any initial conditions, reach this vicinity* $|x(t, x(0))| < 1$*.*

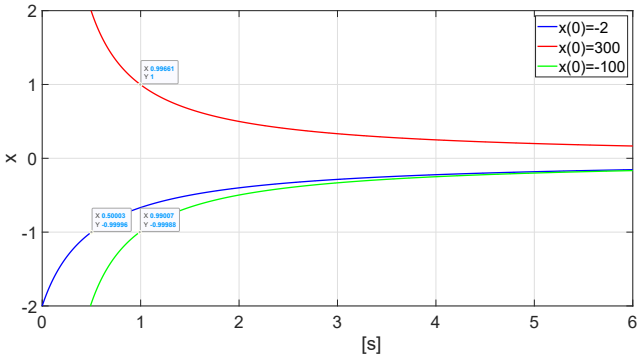

Figure 1.7: Homogeneous system of degree 1.

■

The above is a property of homogeneous systems with positive degree, where the origin is locally uniformly asymptotic stable. In such case, the origin is globally uniformly practically fixed-time stable [Polyakov 2020], as defined hereafter.

Definition 1.13 *[Polyakov 2011] The origin of system (1.46) is globally uniformly practically fixed-time stable if* $\forall r > 0\ \exists T(r) > 0 : ||\boldsymbol{x}(t, \boldsymbol{x}(0))|| < r$*,* $\forall t \geq T(r)$*,* $\forall x(0) \in \mathbb{R}^n$

Additionally, with both properties (i.e. positive and negative degree), one can obtain a fixed-time stable system as illustrated in the following example.

Example 1.9 *Let the system*

$$\dot{x} = u, \tag{1.51}$$

where u is defined as

$$u = \begin{cases} -|x|^{1/2} sign(x) & if\ |x| \leq 1, \\ -|x|^{3/2} sign(x) & if\ |x| > 1. \end{cases} \tag{1.52}$$

If $|x| > 1$, the system trajectories are equal to the trajectories of an homogeneous system with a positive degree $q = \frac{1}{2}$, whereas if $|x| \leq 1$, the system trajectories are equal to the trajectories of an homogeneous system with a negative degree $q = -\frac{1}{2}$. Hence, the trajectories obtained with $|x(0)| > 1$ converge to the region $|x| \leq 1$ at $t \leq T_1 = 2\,\text{sec}$, whereas the trajectories with the initial condition $|x| \leq 1$ converge to the origin at $t \leq T_2(x) = 2\sqrt{|x(0)|}$. Therefore, for any initial condition the system converges to the origin at $t_c \leq T_1 + T_2(1) = T_{max} = 4\,\text{sec}$. According to the about result, the following Figure shows the convergence to the region and the origin with different initial conditions.

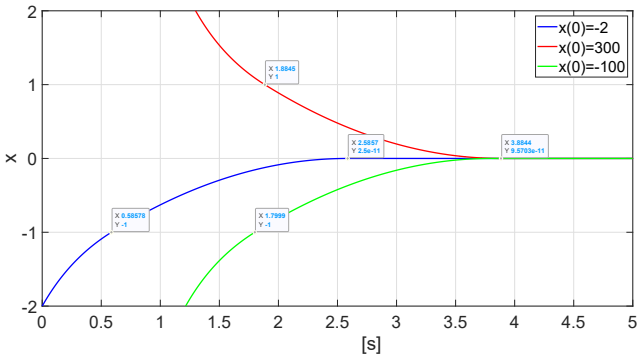

Figure 1.8: Fixed-time stable system.

■

1.2.3 Robustness properties with respect to delays and measurement noise

In the case of differential homogeneous finite-time stable inclusions, they present robustness properties with respect to delays and measurement noises. The following corollary shows this property.

Corollary 1.2.1 *[Levant 2005] Let $\dot{\boldsymbol{x}} \in \boldsymbol{F}(\boldsymbol{x}) \subset \mathbb{R}^n$ be a homogeneous differential inclusion with the weight vector $\boldsymbol{m} = [m_1 \quad m_2 \quad \cdots \quad m_{n-1} \quad m_n]^T$, with a homogeneity degree $q < 0$, $\deg(t) = -q$ and where the solutions of the system are understood in the*

Filippov sense. Furthermore, the system is assumed to be globally uniformly finite-time stable and $\boldsymbol{x}(t)$ *is defined for any* $t \geq -\rho^{-q}$ *(*$\rho > 0$*), with the initial condition* $\boldsymbol{x}(t) = \boldsymbol{\xi}(t)$, $t \in [-\rho^{-q}, 0]$. *Consider measurement noise with magnitude* $\beta_i \rho^{m_i}$ *for each component. Then, if* $\boldsymbol{x}(t)$ *is any solution of the perturbed inclusion:*

$$\dot{\boldsymbol{x}} \in \boldsymbol{F}(x_1(t-\rho^{-q}) + \beta_1 \rho^{m_1}[-1,1], \cdots, x_n(t-\rho^{-q}) + \beta_n \rho^{m_n}[-1,1]), \tag{1.53}$$

the inequalities $|x_i| \leq \mu_i \rho^{m_i}$ *are satisfied in finite-time, where the constants* $\mu_i > 0$, *are independent of* ρ *and* $\boldsymbol{\xi}(t)$.

To show the robustness properties with respect to delays and measurement noise of homogeneous systems, the following example is presented.

Example 1.10 *Let the system*

$$\begin{aligned} \dot{x} &= u(x), \\ u(x) &= -|x|^{1/3} sign(x). \end{aligned} \tag{1.54}$$

In the presence of a bounded measurement noise $\Delta(t)$, *(*$|\Delta(t)| \leq \delta$ *with* $\delta \geq 0$*), the control input becomes* $u(x + \Delta(t))$. *Hence, one obtains the following differential inclusion:*

$$\begin{aligned} \dot{x} &\in u(x + \rho^3[-1,1]), \\ \rho &= \delta^{1/3}, \end{aligned} \tag{1.55}$$

The trajectories of the system converge to a region $|x| \leq \mu\delta$. *The above can be seen in Fig. 1.9.*

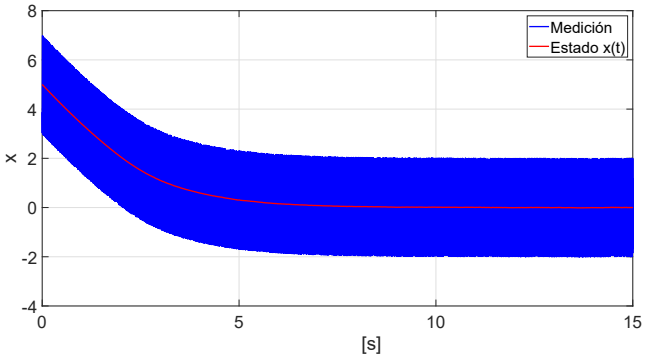

Figure 1.9: Homogeneous system with bounded measurement noise.

On the other hand, if there exists delay in the states, then the following differential inclusion is obtained:

$$\begin{aligned} \dot{x} &\in u(x(t-\rho^2)), \\ \rho &= (\tau_r)^{1/2}, \end{aligned} \tag{1.56}$$

where τ_r *is the measurement delay. A simulation is presented in Figure 1.10.*

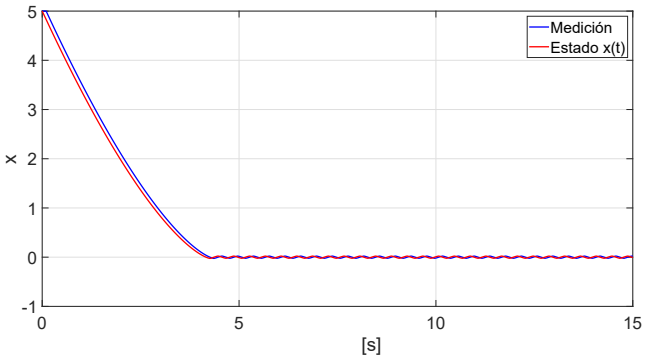

Figure 1.10: Homogeneous system with measurement delay.

If both are presented in the system, then the system obtains the structure:

$$\begin{aligned} \dot{x} &\in u(x(t-\rho^2[-1,1]) + \rho^3[-1,1]), \\ \rho &= max\left\{(\tau_r)^{1/2}, \delta^{1/3}\right\}. \end{aligned} \tag{1.57}$$

The behavior of the system is showed in Figure 1.11.

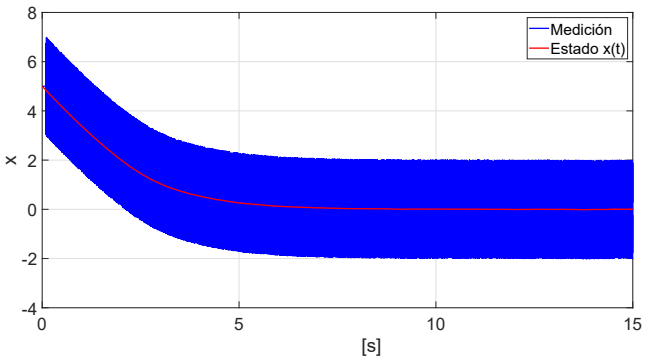

Figure 1.11: Homogeneous system with measurement noise and delay.

■

1.2.4 Robustness properties with respect to disturbances

Similar to Corollary 1.2.1, the following result allows to analyze the convergence of a perturbed homogeneous system. Let us define the following disturbed differential inclusion:

$$\begin{aligned} &\dot{\boldsymbol{x}} \in \boldsymbol{F}(\boldsymbol{x}(t), \boldsymbol{\gamma}), \quad \boldsymbol{x} \in \mathbb{R}^n, \quad \boldsymbol{\gamma} \in \mathbb{R}^\mu, \\ &\boldsymbol{\gamma} = (\gamma_1, \gamma_2, \cdots, \gamma_\eta), \quad \boldsymbol{\gamma}_j \in \mathbb{R}^{\mu_j}, , \quad \mu = \mu_1 + \cdots + \mu_\eta. \end{aligned} \tag{1.58}$$

where $\boldsymbol{\gamma}$ is the disturbance vector. Furthermore, the following assumptions are used:

- The set field $\boldsymbol{F}(\boldsymbol{x}, \boldsymbol{\gamma}) \subset \mathbb{R}^n$ is a non-empty compact convex set-valued function, upper-semicontinuous at all points $(\boldsymbol{x}, \boldsymbol{0})$, $\boldsymbol{x} \in \mathbb{R}^n$, $\boldsymbol{0} \in \mathbb{R}^\mu$.

- The undisturbed inclusion $\dot{\boldsymbol{x}} \in \boldsymbol{F}(\boldsymbol{x}, \boldsymbol{0})$ is finite-time stable and homogeneous of degree $q < 0$ where the dilation is $\boldsymbol{\Lambda_m}(\alpha)$, and $m_i > 0$, $m_i > -q$.
- The differential inclusion (1.58) is homogeneous with respect to the disturbance variable, where $\deg(\gamma_{j,i}) = w_{i,j} > 0$. The above means that, $\boldsymbol{F}(\boldsymbol{x}, \boldsymbol{\gamma}) = \alpha^{-q}\boldsymbol{\Lambda_m^{-1}}(\alpha)\boldsymbol{F}(\boldsymbol{\Lambda_m}(\alpha)\boldsymbol{x}, \alpha^{w_{1,1}}\gamma_{1,1}, \cdots, \alpha^{w_{\mu,\mu_j}}\gamma_{\mu,\mu_j})$.

Moreover, $\boldsymbol{\gamma}$ are assumed be particular elements of set-valued homogeneous disturbance, $\boldsymbol{\Gamma}(\boldsymbol{x}, \rho)$ with a properly defined magnitude parameter ρ, which satisfies the following conditions:

- $\Gamma_i(\boldsymbol{x}, \rho)$ is a set-valued function with non-empty compact values, $\boldsymbol{x} \in \mathbb{R}^m$, $\rho \geq 0$.
- The disturbance satisfies the homogeneity condition $\forall\ \alpha, \rho \geq 0$, $\forall \boldsymbol{x} \in \mathbb{R}^n$: $\Gamma_i(\boldsymbol{\Lambda_m}(\alpha)\boldsymbol{x}, \alpha^{w_\rho}\rho) = \boldsymbol{\Lambda_l}(\alpha)\Gamma_i(\boldsymbol{x}, \rho)$, where the weights of the dilation $\boldsymbol{\Lambda_l}$ are positive and Γ_i is vanishing with respect to ρ.
- Γ_i monotonously increases with respect to the parameter ρ, in the sense that for any $\boldsymbol{x}$ the inequality, $0 \leq \rho \leq \hat{\rho}$ implies that $\Gamma_i(\boldsymbol{x}, \rho) \subset \Gamma_i(\boldsymbol{x}, \hat{\rho})$.
- Γ_i is Hausdorff-continuous in ρ, $\boldsymbol{x}$ at the points with $\rho = 0$.

Additionally, the following initial condition is used in the inclusion (1.58):

$$\boldsymbol{x} = \xi(t), \quad t \in [-\tau, 0], \quad \xi \in \Xi(\tau, \rho, x_0), \tag{1.59}$$

which satisfies the following assumptions:

- $\boldsymbol{\Xi}(\tau, \rho, x_0)$, $\boldsymbol{x} \in \mathbb{R}^n$, τ, $\rho \geq 0$ is a set of bounded Lebesgue measurable functions of time, $\xi(t) \in \mathbb{R}^n$, $t \in [-\tau, 0]$, $\xi(0) = \boldsymbol{x}$.
- Initial-condition sets satisfy the homogeneity condition in the sense that transformation establishes the one-to-one correspondence $\xi(t) \to \boldsymbol{\Lambda_m}(\alpha)\boldsymbol{\xi}(t)$ between the functions of the sets $\boldsymbol{\Xi}(\tau, \rho, \boldsymbol{x})$ and $\boldsymbol{\Xi}(\alpha^q, \alpha^{w_p}\rho, \boldsymbol{\Lambda_m}(\alpha)\boldsymbol{x})$.
- For any $\boldsymbol{x}$, if $0 \leq \tau \leq \hat{\tau}$, $0 \leq \rho \leq \hat{\rho}$ then the functions $\boldsymbol{\Xi}(\hat{\tau}, \hat{\rho}, \boldsymbol{x})$ restricted to the time $[-\tau, 0]$ include the functions of $\boldsymbol{\Xi}(\tau, \rho, \boldsymbol{x})$.
- The initial conditions are uniformly continuous at $\tau = 0$, $\rho = 0$.

The above initial conditions can be fulfilled if the dynamics of the system are not affected by the value of the states for $t < 0$. Using the above conditions the following theorem and lemma are derived.

Theorem 1.2.2

[Levant & Livne 2016] There exists constants μ_i such that after a finite-time transient, indefinitely extendable solutions of the disturbed differential inclusion (1.58) enter to the region $|x_i(t)| \leq \mu_i\delta^{m_i}$, $\rho = \max\left\{\rho^{1/w_p}, \tau^{1/q}\right\}$ and remain there.

Lemma 1.1 *[Levant & Livne 2016] Let $q = w_p = 1$, then all solutions of the disturbed differential inclusion (1.58) after a finite-time transient enter to the region $|x_i(t)| \leq \mu_i\delta^{m_i}$ and remain there.*

1.3 Differentiation of continuous-time signals

In many control engineering applications, real-time differentiation of a noisy signal is required [Atassi & Khalil 2000, Levant 2003] (e.g., PID and output-feedback controllers, observers, ...). The main challenge concerning the design of real-time differentiators is the trade-off between exactness and noise filtration performances [Rodrigues & Oliveira 2018]. For instance, the explicit Euler differentiator amplifies the effect of measurement noise. Therefore, measurement noises with small magnitude can significantly affect the estimate of the signal derivatives. To deal with this issue, linear filters (i.e., a combination of low-pass filter and ideal differentiator) were investigated. However, they require an appropriate tuning of the parameters according to noise characteristics and only guarantee asymptotic time convergence of the differentiaton errors. To alleviate these limitations, different methods have been proposed, such as high gain observers [Vasiljevic & Khalil 2008], algebraic differentiators based on the analysis of the Fourier transform of the kernels [Othmane *et al.* 2021], homogeneous sliding mode-based differentiators [Levant 2003], fixed-time differentiator [Moreno 2021, Moulay *et al.* 2022] and filtering sliding mode differentiator [Levant & Livne 2019, Jbara *et al.* 2021].

In this section, we will recall two continuous-time homogeneous differentiators which present exact differentiation and excellent robustness properties to bounded noises and disturbances. These two differentiator will be the basis of our main contributions in the next Chapters.

1.3.1 Problem Statement

The objective of a differentiator is obtain the first n derivatives of a function using its measurement, which usually is noisy. This function is represented as $f_0(t)$, $f_0 : \mathbb{R} \to \mathbb{R}$ and its measurement is represented as $f(t) = f_0(t) + \Delta(t)$, where $\Delta(t)$ is the measurement noise. To achieve this objective, the following assumptions are required.

Assumption 1.3.1 *The function $f_0(t)$ is at least n times differentiable, and its n-th derivative has a known constant Lipschitz $L \geq 0$.*

Assumption 1.3.2 *The measurement noise $\Delta(t)$ is a bounded Lebesgue measurable noise, i.e., there exists $\delta \geq 0$ such that $|\Delta(t)| \leq \delta$.*

From Assumption 1.3.1, one can deduce that $f_0^{(n+1)}(t) \in [-L, L]$ for almost any time. Additionally, the following assumption about the measurement noise can be used instead of Assumption 1.3.2 to improve the estimation of the standard differentiator.

Assumption 1.3.3 *([Levant & Livne 2019]) The measurement noise consists of n_f+1 components, $\Delta(t) = \Delta_0(t) + \Delta_1(t) + \cdots + \Delta_{n_f}(t)$, where each $\Delta_j(t)$ (possibly unbounded), $j = 0, 1, \cdots, n_f$, is a signal of global filtering order j and the jth-order integral magnitude $\varepsilon_j \geq 0$.*

The definition of a signal of global filtering order j was presented in [Levant & Livne 2019] as follows:

Definition 1.14 *[Levant & Livne 2019] A function $\Delta_j(t)$, $\Delta_j : [0,\infty) \to \mathbb{R}$, is a signal of global filtering order $j \geq 0$, if Δ_j is a locally integrable Lebesgue-measurable function, and there exists a globally bounded solution $\beta_j(t)$ of the equation $\beta_j^{(j)}(t) = \Delta_j(t)$. Any number exceeding $\sup|\beta_j(t)|$ is called a jth-order global integral magnitude of Δ_j.*

Here, n_f is referenced as the filtering order. Note that if a noise signal satisfies Assumption 1.3.2 then it trivially satisfies Assumption 1.3.3 with $n_f = 0$ and $\varepsilon_0 = \delta$.

To estimate the first n derivatives of a signal $f_0(t)$, a state space representation is used. The state variables are defined as $x_i = f_0^{(i)}(t)$ and $\boldsymbol{x} = \begin{bmatrix} x_0 & x_1 & x_2 & \cdots & x_n \end{bmatrix}^T \in \mathbb{R}^{n+1}$. The following representation is obtained:

$$\dot{\boldsymbol{x}} = \boldsymbol{A}\boldsymbol{x} + \boldsymbol{e}_{n+1} f_0^{(n+1)}(t); \quad f_0(t) = \boldsymbol{e}_1^T \boldsymbol{x}, \tag{1.60}$$

with the canonical vectors $\boldsymbol{e}_i = [0 \ \cdots \ 0 \ 1 \ 0 \ \cdots \ 0]^T$ (here the element "1" is in the position i), and $\boldsymbol{A}$ is the following nilpotent matrix:

$$\boldsymbol{A} = \begin{bmatrix} 0 & 1 & 0 & \cdots & 0 \\ 0 & 0 & 1 & \cdots & 0 \\ \vdots & \vdots & \vdots & \ddots & \vdots \\ 0 & 0 & 0 & \cdots & 1 \\ 0 & 0 & 0 & \cdots & 0 \end{bmatrix}.$$

As $f_0^{(n+1)}(t)$ is unknown in system (1.60), the estimation of the state requires strong observability. Since the triple $\left(\boldsymbol{A}, \boldsymbol{e}_{n+1}, \boldsymbol{e}_1^T\right)$ is strongly observable [Kratz 1995], the representation (1.60) gives the possibility to estimate the time derivatives of $f_0(t)$ through the design of a state observer.

1.3.2 Robust exact sliding mode differentiator

It is worth noting that sliding mode differentiators guarantee the robust finite time estimations of the first n derivatives of a signal with bounded $(n+1)-$th derivative with interesting robustness properties with respect to measurement noise.

Let us define the signed power function as follows. For $\gamma \geq 0$ and $x \in \mathbb{R}$, the signed power γ of x is defined as $\lfloor x \rceil^\gamma = |x|^\gamma \operatorname{sign}(x)$. With the purpose of estimating the state of system (1.60), in [Levant 2003] a homogeneous continuous-time differentiator is proposed. Its non-recursive form is given as follows:

$$\begin{aligned} \dot{z}_0 &= -\lambda_n L^{\frac{1}{n+1}} \lfloor z_0 - f(t) \rceil^{\frac{n}{n+1}} + z_1, \\ \dot{z}_1 &= -\lambda_{n-1} L^{\frac{2}{n+1}} \lfloor z_0 - f(t) \rceil^{\frac{n-1}{n+1}} + z_2, \\ &\vdots \\ \dot{z}_n &= -\lambda_0 L \lfloor z_0 - f(t) \rceil^0, \end{aligned} \tag{1.61}$$

where $\boldsymbol{z} = \begin{bmatrix} z_0 & z_1 & z_2 & \ldots & z_n \end{bmatrix}^T$ is an estimate of the vector $\boldsymbol{x}$ in finite time and where the parameters $\lambda_i > 0$ are adequate parameters [Shtessel *et al.* 14].

Remark 1.3.1 *Since* $\lfloor z_0 - f(t) \rceil^0$ *is a set-valued function at* $z_0 = f$*, the solutions of the system are understood in the Filippov sense [Filippov 88].*

With the absence of noise, the differentiator (1.61) can be represented as:

$$\begin{aligned}
\dot{z}_0 &= -\lambda_n L^{\frac{1}{n+1}} \lfloor z_0 - f_0(t) \rceil^{\frac{n}{n+1}} + z_1, \\
\dot{z}_1 &= -\lambda_{n-1} L^{\frac{2}{n+1}} \lfloor z_0 - f_0(t) \rceil^{\frac{n-1}{n+1}} + z_2, \\
&\vdots \\
\dot{z}_n &= -\lambda_0 L \lfloor z_0 - f_0(t) \rceil^0 .
\end{aligned} \tag{1.62}$$

If Assumption 1.3.2 is satisfied, the differentiator (1.61) has the following accuracy $\left| z_i(t) - f_0^{(i)}(t) \right| = O\left(\delta^{(n+1-i)/(n+1)}\right)$ [Shtessel *et al.* 14]. With discrete-time measurements, $z_0 - f(t)$ is changed with $z_0(t_k) - f(t_k)$ where $t_k \leq t < t_{k+1}$ and $t_{k+1} - t_k = \tau \geq 0$ (τ is a constant sampling time). With discrete-time measurements and in the absence of noise, the differentiator has the following accuracy $\left| z_i(t) - f_0^{(i)}(t) \right| = O\left(\tau^{(n-i+1)}\right)$ [Levant 2003]. If both phenomenons occur, the differentiator obtains the asymptotic accuracy $|z_i(t) - f_0^{(i)}(t)| \leq \mu_i L \rho^{n+1-i}$ for $i = 0, 1, 2, \cdots, n$, with $\rho = \max\left\{(\delta/L)^{1/n+1}, \tau\right\}$ and $\mu_i \geq 1$ [Levant *et al.* 2017].

For $\tau = 0$ and under Assumptions 1.3.1-1.3.2, the standard differentiator has an optimal asymptotic accuracy, i.e., only μ_i could be improved [Levant *et al.* 2017]. Nevertheless, if the signal is m-th differentiable, with $m > n$ and $f_0^{(m)}(t)$ has a Lipschitz constant L_m, then, its accuracy can be improved with a differentiator of order m instead of n. Concerning the parameters μ_i, their best possible values are defined by the Kolmogorov constants ($\mu_i \geq \mathbb{K}_{i,n} 2^{\frac{i}{n+1}}$)[Levant *et al.* 2017], which satisfy the inequalities $1 \leq \mathbb{K}_{i,n} \leq \frac{\pi}{2}$.

Let us now rewrite system (1.62) using the estimation errors

$$\sigma_i = z_i - x_i, \quad \text{for } i = 0, 1, \ldots, n. \tag{1.63}$$

Hence, differentiator (1.62) becomes

$$\dot{\boldsymbol{z}} = \boldsymbol{A}\boldsymbol{z} + \boldsymbol{u}(\sigma_0), \tag{1.64}$$

where $\boldsymbol{u}(\sigma_0)$ is considered as the input vector of the observer and is defined as follows:

$$\begin{aligned}
\boldsymbol{u}(\sigma_0) &= \left[\Psi_{0,n}(\sigma_0) \;\; \Psi_{1,n}(\sigma_0) \;\; \cdots \;\; \Psi_{n,n}(\sigma_0)\right]^T, \\
\Psi_{i,n}(\cdot) &= -\lambda_{n-i} L^{\frac{i+1}{n+1}} \lfloor \cdot \rceil^{\frac{n-i}{n+1}}, \\
\Psi_{n,n}(\cdot) &\in -\lambda_0 L \operatorname{sign}(\cdot).
\end{aligned} \tag{1.65}$$

Let $\boldsymbol{\sigma} = \boldsymbol{z} - \boldsymbol{x}$ be the vector of the estimations errors. Then, the dynamics of the errors can be represented as:

$$\dot{\boldsymbol{\sigma}} = \boldsymbol{A}\boldsymbol{\sigma} + \boldsymbol{u}(\sigma_0) - \boldsymbol{e}_{n+1} f_0^{(n+1)}(t). \tag{1.66}$$

In the absence of noise and using $f_0^{(n+1)}(t) \in [-L, L]$, system (1.66) can be rewritten as:

$$\begin{aligned} \dot{\sigma}_i &= \sigma_{i+1} + \Psi_{i,n}(\sigma_0), \quad i = 0, \ldots, n-1, \\ \dot{\sigma}_n &\in \Psi_{n,n}(\sigma_0) + [-L, L]. \end{aligned}$$

Defining $\bar{\sigma}_i = \sigma_i / L$ and $\bar{\sigma}_n = \sigma_n / L$, one obtains:

$$\begin{aligned} \dot{\bar{\sigma}}_i &= \bar{\sigma}_{i+1} + \frac{\Psi_{i,n}(\bar{\sigma}_0)}{L^{\frac{i+1}{n+1}}}, \quad i = 0, \ldots, n-1, \\ \dot{\bar{\sigma}}_n &\in \frac{\Psi_{n,n}(\bar{\sigma}_0)}{L} + [-1, 1]. \end{aligned} \tag{1.67}$$

or in a compact form as:

$$\dot{\bar{\boldsymbol{\sigma}}} \in \boldsymbol{C}_n(\bar{\boldsymbol{\sigma}}). \tag{1.68}$$

Concerning the selection of the parameters λ_i, the following assumption is considered.

Assumption 1.3.4 *[Levant 2003] The parameters λ_0, λ_1, $\cdots$, λ_n are constants and such that the differential inclusion (1.68) is asymptotically stable.*

Remark 1.3.2 *Let $m_0 = n+1$, $m_1 = n$, $\cdots$, $m_n = 1$, then for all $\alpha > 0$, and $\bar{\boldsymbol{\sigma}} \in \mathbb{R}^{n+1}$, $\boldsymbol{C}_n(\bar{\boldsymbol{\sigma}}) = \alpha \boldsymbol{\Lambda}_{\boldsymbol{m}}^{-1}(\alpha) \boldsymbol{C}_n(\boldsymbol{\Lambda}_{\boldsymbol{m}}(\alpha) \bar{\boldsymbol{\sigma}})$. Therefore, the differential inclusion (1.68) is invariant with respect to the transformation $(t, \bar{\boldsymbol{\sigma}}) \mapsto (\alpha t, \boldsymbol{\Lambda}_{\boldsymbol{m}}(\alpha) \bar{\boldsymbol{\sigma}})$. Hence, the inclusion (1.68) is a homogeneous system with a homogeneous degree -1. Hence, from Assumption 1.3.4, it is finite-time stable.*

Sequences of parameters λ_i, which satisfy 1.3.4, are presented for any $0 \leq n \leq 7$ in [Levant 2018]. On the other hand, the parameters λ_i are not unique. Indeed, they can be built from any $\lambda_0 > 1$ [Levant 2003, Shtessel *et al.* 14]. One can obtain different sequences in [Reichhartinger *et al.* 2017] and a methodology to obtain that parameters can be found in [Jbara *et al.* 2020].

1.3.3 Robust Exact Filtering Differentiator

Recently, a novel homogeneous differentiator was presented in [Levant & Livne 2019]. Although the standard differentiator has good performance under Assumptions 1.3.1, 1.3.2 and 1.3.4, the robust exact filtering differentiator improves the accuracy of the standard differentiator with less restrictive noise assumptions (i.e., Assumption 1.3.3). It is given as:

$$\begin{aligned} \dot{w}_{j_f}(t) &= \Psi_{j_f-1,m}(w_1(t)) + w_{j_f+1}(t), \\ \dot{w}_{n_f}(t) &= \Psi_{n_f-1,m}(w_1(t)) + z_0(t) - \bar{x}_0(t), \\ \dot{z}_{j_d}(t) &= \Psi_{n_f+j_d,m}(w_1(t)) + z_{j_d+1}(t), \\ \dot{z}_n(t) &= \Psi_{m,m}(w_1(t)). \\ j_f &= 1, 2, \cdots, n_f - 1. \quad j_d = 0, 1, 2, \cdots, n-1. \end{aligned} \tag{1.69}$$

where $m = n + n_f$, and the parameters λ_j are selected as in (1.62). n_f is greater than or equal to the filtering orders of the signals $\Delta_j(t)$ that compose $\Delta(t)$. For $n_f = 0$, the robust exact filtering differentiator becomes the standard differentiator (1.62).

Using the estimation errors (1.63), one obtains:

$$\begin{aligned}
\dot{w}_{j_f}(t) &= \Psi_{j_f-1,m}\left(w_1(t)\right) + w_{j_f+1}(t),\\
\dot{w}_{n_f}(t) &= \Psi_{n_f-1,m}\left(w_1(t)\right) + \sigma_0(t) - \Delta\left(t\right),\\
\dot{\sigma}_{j_d}(t) &= \Psi_{n_f+j_d,m}\left(w_1(t)\right) + \sigma_{j_d+1}(t),\\
\dot{\sigma}_n(t) &= \Psi_{m,m}\left(w_1(t)\right) + x_0^{(n+1)}(t).\\
j_f &= 1, 2, \cdots, n_f - 1. \quad j_d = 0, 1, 2, \cdots, n-1.
\end{aligned} \tag{1.70}$$

Let $\omega_j(t)$ be defined as:

$$\omega_j(t) = w_j(t) + \sum_{l=n_f-j+1}^{n_f} \beta_l^{(l+j-n_f-1)}(t), \tag{1.71}$$

where $\beta_j^{(j)}(t) = \Delta_j(t)$. Therefore, (1.70) can be rewritten as:

$$\begin{aligned}
\dot{\omega}_{j_f}(t) &= \Psi_{j_f-1,m}\left(\omega_1(t) - \beta_{n_f}^{(0)}(t)\right) + \omega_{j_f+1}(t) - \beta_{n_f-j_f}^{(0)}(t),\\
\dot{\omega}_{n_f}(t) &= \Psi_{n_f-1,m}\left(\omega_1(t) - \beta_{n_f}^{(0)}(t)\right) + \sigma_0(t) - \beta_0^{(0)}\left(t\right),\\
\dot{\sigma}_{j_d}(t) &= \Psi_{n_f+j_d,m}\left(\omega_1(t) - \beta_{n_f}^{(0)}(t)\right) + \sigma_{j_d+1}(t),\\
\dot{\sigma}_n(t) &\in \Psi_{m,m}\left(\omega_1(t) - \beta_{n_f}^{(0)}(t)\right) + \left[-L, L\right].\\
j_f &= 1, 2, \cdots, n_f - 1. \quad j_d = 0, 1, 2, \cdots, n-1.
\end{aligned} \tag{1.72}$$

Let $\bar{\omega}_j = \omega_j / L$, $\bar{\sigma}_j(t) = \sigma_j(t)/L$ and

$$\rho = \max\left[\left(\frac{\varepsilon_0}{L}\right)^{\frac{1}{n+1}}, \left(\frac{\varepsilon_1}{L}\right)^{\frac{1}{n+2}}, \cdots, \left(\frac{\varepsilon_{n_f}}{L}\right)^{\frac{1}{m+1}}\right], \tag{1.73}$$

it allows to obtain the inclusions:

$$\begin{aligned}
\dot{\bar{\omega}}_{j_f}(t) &\in \frac{\Psi_{j_f-1,m}\left(\bar{\omega}_1(t) + \rho^{m+1}\left[-1,1\right]\right)}{L^{\frac{j_f}{m+1}}} + \bar{\omega}_{j_f+1}(t) + \rho^{m+1-j_f}\left[-1,1\right],\\
\dot{\bar{\omega}}_{n_f}(t) &\in \frac{\Psi_{n_f-1,m}\left(\bar{\omega}_1(t) + \rho^{m+1}\left[-1,1\right]\right)}{L^{\frac{n_f}{m+1}}} + \bar{\sigma}_0(t) + \rho^{n+1}\left[-1,1\right],\\
\dot{\bar{\sigma}}_{j_d}(t) &\in \frac{\Psi_{n_f+j_d,m}\left(\bar{\omega}_1(t) + \rho^{m+1}\left[-1,1\right]\right)}{L^{\frac{n_f+j_d+1}{m+1}}} + \bar{\sigma}_{j_d+1}(t),\\
\dot{\bar{\sigma}}_n(t) &\in \frac{\Psi_{m,m}\left(\bar{\omega}_1(t) + \rho^{m+1}\left[-1,1\right]\right)}{L} + \left[-1,1\right].\\
j_f &= 1, 2, \cdots, n_f - 1. \quad j_d = 0, 1, 2, \cdots, n-1.
\end{aligned} \tag{1.74}$$

The inclusions (1.74) correspond to a perturbed finite-time stable homogeneous error dynamics (1.68) of mth-order instead of nth-order. Furthermore,

the error dynamics system (1.74) is homogeneous with respect to the transformation $\left(t, \rho, \bar{\omega}_1, \ldots, \bar{\omega}_{n_f}, \bar{\sigma}_0, \ldots, \bar{\sigma}_n\right) \mapsto \left(\alpha t, \alpha\rho, \alpha^{m+1}\bar{\omega}_1, \ldots, \alpha^{n+2}\bar{\omega}_{n_f}, \alpha^{n+1}\bar{\sigma}_0, \ldots, \alpha\bar{\sigma}_n\right)$, with homogeneity degree -1 and where $\deg(\bar{\omega}_j) = m + 2 - j$, $\deg(\bar{\sigma}_j) = n + 1 - j$, $\deg(\rho) = 1$ and $\deg(t) = 1$. If Assumptions 1.3.1 and 1.3.3 hold, the continuous-time filtering differentiator (1.69) presents the following accuracy:

$$|\sigma_j(t)| \leq \mu_j L \rho^{n+1-j}, \quad \mu_j > 0, \quad j = 0, 1, 2, \cdots, n. \tag{1.75}$$

In the case of bounded noise, the accuracy (1.75) becomes (1.69). The advantage of using the robust exact filtering differentiator (1.69) instead of the standard one (1.62), is that (1.69) improves the accuracy of (1.62).

1.4 State of the art

The continuous-time robust exact differentiators given previously include integration and continuous-time measurements. To implement these differentiators on a digital device, a proper discretization is required. Hence, hereafter, some existing discrete-time realizations of the standard differentiator (1.61) and the robust exact filtering differentiator (1.69) are presented. Furthermore, the differentiators proposed in [Livne & Levant 2014, Koch & Reichhartinger 2018, Koch *et al.* 2020], are carefully discussed in the following subsections.

1.4.1 Forward Euler Discretization

In the case of discrete-time measurements of the input signal $f(t)$, the differentiator (1.61) for $t \in [t_k, t_{k+1})$ can be represented as:

$$\begin{aligned} \dot{z}_i &= z_{i+1} + \Psi_{i,n}\left(z_0(t_k) - f(t_k)\right), \quad i = 0, \ldots, n-1, \\ \dot{z}_n &= \Psi_{n,n}\left(z_0(t_k) - f(t_k)\right). \end{aligned} \tag{1.76}$$

By applying the one-step Euler method, the above differentiator is given by the following form:

$$\begin{aligned} z_{i,k+1} &= z_{i,k} + \tau\Psi_{i,n}\left(z_{0,k} - f_k\right) + \tau z_{i+1,k}, \\ z_{n,k+1} &= z_{n,k} + \tau\Psi_{n,n}\left(z_{0,k} - f_k\right), \end{aligned} \tag{1.77}$$

where $\tau = t_{k+1} - t_k > 0$, $z_i(t_k) = z_{i,k}$, $z_i(t_{k+1}) = z_{i,k+1}$ and $f(t_k) = f_k$. Subtracting $f_0^{(i)}(t_{k+1})$ and using Taylor expansion of $f_0^{(i)}(t_{k+1})$ with the Lebesgue-integral remainder form, it yields the following estimation error

$$\begin{aligned} \sigma_{i,k+1} \in& \sigma_{i,k} + \tau\sigma_{i+1,k} + \tau\Psi_{i,n}\left(\sigma_{0,k} + [-\delta, \delta]\right) - \frac{\tau^2}{2} f_0^{(i+2)}(\xi_{i,k}), \\ \sigma_{n-1,k+1} \in& \sigma_{n-1,k} + \tau\sigma_{n,k} - \frac{\tau^2}{2}[-L, L] + \tau\Psi_{n-1,n}\left(\sigma_{0,k} + [-\delta, \delta]\right), \\ \sigma_{n,k+1} \in& \sigma_{n,k} + \tau\Psi_{n,n}\left(\sigma_{0,k} + [-\delta, \delta]\right) - \tau[-L, L], \end{aligned} \tag{1.78}$$

where $\sigma_{i,k} = z_{i,k} - f_{0,k}^{(i)}$, $i = 0, 1, \ldots, n-2$ and $\xi_{i,k} \in [t_k, t_{k+1}]$. Notice that for $n = 1$ the above inclusion is homogeneous with respect to the transformation

$$(t_k, \delta, \sigma_0, \ldots, \sigma_n) \mapsto \left(\lambda t_k, \lambda^{n+1}\delta, \lambda^{n+1}\sigma_0, \ldots, \lambda\sigma_n\right), \tag{1.79}$$

whereas the differentiator obtained using Euler method looses the homogeneity property for $n \geq 2$. In [Livne & Levant 2014], it was demonstrated that if the unknown function $f_0(t)$ is n-smooth function for $n \geq 1$ (i.e., $|f_0^{(j)}(t)| \leq D_j$ for $j = 2, 3, \ldots, n, n+1$ and $D_{n+1} = L$), $\Delta(t)$ is a Lebesgue measurable noise bounded by a constant δ, then the accuracy of the differentiator (1.77) is given by:

$$\begin{aligned} |z_{i,k} - f_{0,k}^{(i)}| &\leq \mu_i \rho^{n-i+1}, \\ \rho &= \max_{j=2,3,\ldots,n+1} \left\{ \left(\frac{\tau}{2} D_j\right)^{\frac{1}{n-j+2}}, \tau, \delta^{\frac{1}{n+1}} \right\}, \end{aligned} \tag{1.80}$$

for $i = 0, 1, \ldots, n$ and where the coefficients μ_i only depend on the differentiator parameters $\lambda_0, \ldots, \lambda_n, L$. Notice that it does not preserve the ultimate accuracy of the differentiator (1.62) with discrete measurements.

1.4.2 Homogeneous Discrete-time Differentiator (HDD)

Let us consider the same assumptions as previously, i.e. the unknown function $f_0(t)$ is n-smooth function for $n \geq 1$ (i.e., $|f_0^{(j)}(t)| \leq D_j$ for $j = 2, 3, \ldots, n, n+1$ and $D_{n+1} = L$), $\Delta(t)$ is a Lebesgue measurable noise bounded by a constant δ. In [Livne & Levant 2014], an explicit discretization of the homogeneous differentiator (1.61) is proposed as follows:

$$\boldsymbol{z}_{k+1} = \boldsymbol{\Phi}(\tau)\, \boldsymbol{z}_k + \tau \boldsymbol{u}_k, \tag{1.81}$$

with

$$\begin{aligned} \boldsymbol{u}_k &= \begin{bmatrix} \Psi_{0,n}(z_{0,k} - f_k) \\ \Psi_{1,n}(z_{0,k} - f_k) \\ \vdots \\ \Psi_{n,n}(z_{0,k} - f_k) \end{bmatrix}, \\ \boldsymbol{\Phi}(\tau) &= \begin{bmatrix} 1 & \tau & \frac{\tau^2}{2!} & \cdots & \frac{\tau^{n-1}}{(n-1)!} & \frac{\tau^n}{n!} \\ 0 & 1 & \tau & \cdots & \frac{\tau^{n-2}}{(n-2)!} & \frac{\tau^{n-1}}{(n-1)!} \\ \vdots & \vdots & \vdots & \ddots & \vdots & \vdots \\ 0 & 0 & 0 & \cdots & 1 & \tau \\ 0 & 0 & 0 & \cdots & 0 & 1 \end{bmatrix}. \end{aligned} \tag{1.82}$$

Then, the accuracy of the HDD (1.81) is given as:

$$\begin{aligned} |z_i - f_0^{(i)}| &\leq \mu_i \rho^{n-i+1}, \\ \rho &= \max\left\{\tau, \delta^{\frac{1}{n+1}}\right\}, \end{aligned} \tag{1.83}$$

where as in the Euler method, the coefficients μ_i only depend on the differentiator parameters $\lambda_0, \ldots, \lambda_n, L$. Unlike the differentiator (1.77), the differentiator (1.81) preserves the ultimate accuracy of the differentiator (1.62) with discrete measurements and the homogeneity property. At last, some robustness properties with respect to variable sampling time are guaranteed.

1.4.3 Matching Discrete-time Differentiator

In [Koch & Reichhartinger 2018], a discrete-time version of the differentiator (1.62) is presented. It has the following form:

$$\boldsymbol{z}_{k+1} = \boldsymbol{\Phi}(\tau)\,\boldsymbol{z}_k + \boldsymbol{\lambda}(\sigma_{0,k})\,\sigma_{0,k}, \tag{1.84}$$

where $\boldsymbol{\Phi}(\tau)$ is the same matrix as in equation (1.82). Furthermore, the matrix $\boldsymbol{\lambda}(\sigma_{0,k})$ is designed with the purpose of placing the eigenvalues of the matrix $\boldsymbol{\Phi}(\tau) - \boldsymbol{\lambda}(\sigma_{0,k})\,\boldsymbol{e}_1^T$, which is the matrix present in the dynamics of the observation error dynamics obtained from (1.84):

$$\boldsymbol{\sigma}_{k+1} = \left[\boldsymbol{\Phi}(\tau) + \boldsymbol{\lambda}(\sigma_{0,k})\,\boldsymbol{e}_1^T\right]\boldsymbol{\sigma}_k + \boldsymbol{h}_k, \tag{1.85}$$

In order to solve the eigenvalue placement problem, the Ackerman's formula is used by mapping the continuous-time eigenvalues to the discrete-time domain and the matching approach ([Franklin *et al.* 1998]). Then, $\boldsymbol{\lambda}(\sigma_{0,k})$ is given as:

$$\begin{aligned}
&\boldsymbol{\lambda}(\sigma_{0,k}) = \chi\left(\boldsymbol{\Phi}(\tau), \sigma_{0,k}\right)\boldsymbol{S}_o^{-1}\boldsymbol{e}_{n+1},\\
&\chi\left(\boldsymbol{\Phi}(\tau), \sigma_{0,k}\right) = \prod_{i=0}^{n}\left(\boldsymbol{\Phi}(\tau) - q_i(\sigma_{0,k})\,\boldsymbol{I}\right),\\
&\boldsymbol{S}_o = \begin{bmatrix} \boldsymbol{e}_1^T \\ \boldsymbol{e}_1^T\boldsymbol{\Phi}(\tau) \\ \vdots \\ \boldsymbol{e}_1^T\boldsymbol{\Phi}^n(\tau) \end{bmatrix}, \quad q_i(\sigma_{0,k}) = e^{\tau p_i\left|\sigma_{0,k}\right|^{\frac{n}{n+1}-1}},
\end{aligned} \tag{1.86}$$

where p_i are the continuous poles of the differentiator, $\boldsymbol{I}$ is the identity matrix of dimensions $((n+1)\times(n+1))$. Although, a close form can be obtained for (1.86), a more complex form can be obtained if different poles are considered.

Notice that the differentiator (1.84) has been designed for the free-noise case. For the free-noise case, it presents some relevant properties such as insensitivity to an overestimation of the parameter L, preservation of the accuracy of the continuous differentiator ($|\sigma_{i,k}| = O(\tau^{n-i+1})$) and a hyper-exponential stability (the definition can be founded in [Clempner & Yu 17]). However, there is no convergence proof in the case of measurement noise.

1.4.4 Generalized Homogeneous Discrete-time Differentiator (GHDD)

In [Koch *et al.* 2020], a discrete-time version of the differentiator (1.62) is presented. It has the following form:

$$\boldsymbol{z}_{k+1} = \boldsymbol{\Phi}(\tau)\,\boldsymbol{z}_k + \tau\boldsymbol{P}(\tau)\,\boldsymbol{u}_k, \tag{1.87}$$

where $\boldsymbol{u}_k$ and $\boldsymbol{\Phi}(\tau)$ are expressed as in equation (1.82), and with a constant sampling time τ. Furthermore, matrix $\boldsymbol{P}(\tau)$ is given as:

$$\boldsymbol{P}(\tau) = \begin{bmatrix} 1 & 0 & 0 & 0 & \cdots & 0 & 0 \\ 0 & 1 & \beta_{2,3}\tau & \beta_{2,4}\tau^2 & \cdots & \beta_{2,n}\tau^{n-1} & \beta_{2,n+1}\tau^n \\ 0 & 0 & 1 & \beta_{3,4}\tau & \cdots & \beta_{3,n}\tau^{n-2} & \beta_{3,n+1}\tau^{n-1} \\ \vdots & \vdots & \vdots & \vdots & \ddots & \vdots & \vdots \\ 0 & 0 & 0 & 0 & \cdots & 1 & \beta_{n,n+1}\tau \\ 0 & 0 & 0 & 0 & \cdots & 0 & 1 \end{bmatrix} \tag{1.88}$$

where the parameters $\beta_{i,j}$ are constant, such $\boldsymbol{P}$ satisfies the condition:

$$\boldsymbol{\Phi}(\tau)\boldsymbol{P}(\tau) = \boldsymbol{P}(\tau)(I + \tau A) \tag{1.89}$$

In specific, in [Koch *et al.* 2020], the following matrices $\boldsymbol{P}(\tau)$ are defined for the GHDD of order $n \leq 5$:

$$\begin{aligned} P_1(\tau) &= \begin{bmatrix} 1 & 0 \\ 0 & 1 \end{bmatrix} \\ P_2(\tau) &= \begin{bmatrix} 1 & 0 & 0 \\ 0 & 1 & -\frac{1}{2}\tau \\ 0 & 0 & 1 \end{bmatrix} \\ P_3(\tau) &= \begin{bmatrix} 1 & 0 & 0 & 0 \\ 0 & 1 & -\frac{1}{2}\tau & \frac{1}{3}\tau^2 \\ 0 & 0 & 1 & -\tau \\ 0 & 0 & 0 & 1 \end{bmatrix} \\ &\vdots \\ P_5(\tau) &= \begin{bmatrix} 1 & 0 & 0 & 0 & 0 & 0 \\ 0 & 1 & -\frac{1}{2}\tau & \frac{1}{3}\tau^2 & -\frac{1}{4}\tau^3 & \frac{1}{5}\tau^4 \\ 0 & 0 & 1 & -\tau & \frac{11}{12}\tau^2 & -\frac{5}{6}\tau^3 \\ 0 & 0 & 0 & 1 & -\frac{3}{2}\tau & \frac{7}{4}\tau^2 \\ 0 & 0 & 0 & 0 & 1 & -2\tau \\ 0 & 0 & 0 & 0 & 0 & 1 \end{bmatrix} \end{aligned} \tag{1.90}$$

Moreover, in [Koch *et al.* 2020], a proof of convergence even in the presence of noise has been provided. It has been demonstrated that the GHDD (1.87) preserves the ultimate accuracy of the differentiator (1.62) with discrete measurements, i.e.,

$$\begin{aligned} &|\sigma_{i,k}| \leq \mu_i \rho^{n-i+1}, \\ &\rho = \max\left\{\tau, (\delta/L)^{\frac{1}{n+1}}\right\}. \end{aligned} \tag{1.91}$$

where the coefficients μ_i only depend on the differentiator parameters $\lambda_0, \ldots, \lambda_n, L$

1.4.5 Implicit discretization of the standard differentiator

Recently, some implicit and semi-implicit discrete-time realizations have been investigated (see for instance [Mojallizadeh *et al.* 2021]). They have been obtained from

the standard differentiator (1.61), HDD (1.81), GHDD (1.87) and the forward Euler discretization (1.77).

Implicit discrete time realization of the Arbitrary Order Standard Differentiator (I-AO-SD)

Taking into account the forward Euler discretization (1.77), the following scheme is proposed:

$$\begin{aligned} z_{i,k+1} &= z_{i,k} + \tau \Psi_{i,n}\left(\sigma_{0,k+1}\right) + \tau z_{i+1,k+1}, \\ z_{n,k+1} &\in z_{n,k} + \tau \Psi_{n,n}\left(\sigma_{0,k+1}\right), \end{aligned} \tag{1.92}$$

where $i = 0, 1, \cdots, n-1$. To obtain the implicit variable $\sigma_{0,k+1}$ at time t_k, the following generalized equation is obtained from (1.92):

$$\begin{aligned} g(\sigma_{0,k+1}) &\in -\tau^{n+1}\lambda_0 L \operatorname{sign}(\sigma_{0,k+1}), \\ g(\sigma_{0,k+1}) &= \sigma_{0,k+1} + \sum_{l=0}^{n-1}\left(\tau^{l+1}\lambda_{n-l}\left\lfloor \sigma_{0,k+1}\right\rceil^{\frac{n-l}{n+1}}\right) + b_k, \\ b_k &= -\sum_{l=0}^{n}\tau^l z_{l,k} + f_{k+1}, \\ \xi(\sigma_{0,k+1}) &= g^{-1}(\sigma_{0,k+1}). \end{aligned} \tag{1.93}$$

Remark 1.4.1 *It is important to note that the resolution of the generalized equation at time t_k needs the computation of b_k using f_{k+1}. The above implies that the differentiator needs to be implemented with a delay τ or by replacing b_k with b_{k-1}, which reduces its accuracy [Mojallizadeh et al. 2021]. As it will be seen, the implicit differentiators presented in [Mojallizadeh et al. 2021] requires f_{k+1}.*

From the generalized equation, one obtains the following implementation for the implicit differentiator (1.92):

- Case 1: $b_k < -\tau^{n+1}\lambda_0 L$. Hence, $\sigma_{0,k+1} > 0$. In this case, it is calculated $X_k = \sigma_{0,k+1}^{\frac{1}{n+1}}$ and $\operatorname{sign}(\sigma_{0,k+1}) = \xi_k = 1$, where X_k is the root of the following equation with respect to θ_k:

$$\theta_k^{n+1} + \sum_{l=0}^{n-1}\left(\tau^{l+1}\lambda_{n-l}L^{\frac{l+1}{n+1}}\theta_k^{n-l}\right) + b_k + \tau^{n+1}L = 0. \tag{1.94}$$

- Case 2: $b_k \in [-\tau^{n+1}\lambda_0 L, \tau^{n+1}\lambda_0 L]$. Hence, $\sigma_{0,k+1} = 0$. In this case, $\operatorname{sign}(\sigma_{0,k+1}) = [-1, 1]$, and $\xi_k = -\frac{b_k}{\tau^{n+1}\lambda_0 L}$.

- Case 3: $b_k > \tau^{n+1}\lambda_0 L$. Hence, $\sigma_{0,k+1} < 0$. In this case, it is calculated as $X_k = (-\sigma_{0,k+1})^{\frac{1}{n+1}}$ and $\operatorname{sign}(\sigma_{0,k+1}) = \xi_k = 1$, where X_k is the root of the following equation with respect to θ_k:

$$-\theta_k^{n+1} - \sum_{l=0}^{n-1}\left(\tau^{l+1}\lambda_{n-l}L^{\frac{l+1}{n+1}}\theta_k^{n-l}\right) + b_k - \tau^{n+1}L = 0. \tag{1.95}$$

Then, the I-AO-SD (1.92) is implemented with ξ_k instead of $\operatorname{sign}(\sigma_{0,k+1})$.

Implicit homogeneous discrete-time differentiator (IHDD)

From the homogeneous discrete-time differentiator (HDD) (1.81), the following implicit scheme is proposed:

$$\begin{aligned} z_{i,k+1} &= z_{i,k} + \tau \Psi_{i,n}\left(\sigma_{0,k+1}\right) + \sum_{j=1}^{n-i} \frac{\tau^j}{j!} z_{j+1,k+1}, \\ z_{n,k+1} &\in z_{n,k} + \tau \Psi_{n,n}\left(\sigma_{0,k+1}\right). \end{aligned} \tag{1.96}$$

where $i = 0, 1, \cdots, n-1$. Similar to (1.93), one obtains the following generalized equation:

$$\begin{aligned} g(\sigma_{0,k+1}) &\in -\tau^{n+1}\lambda_0 L m_n \text{sign}(\sigma_{0,k+1}), \\ g(\sigma_{0,k+1}) &= \sigma_{0,k+1} + \sum_{l=0}^{n-1} \left(m_l \tau^{l+1} \lambda_{n-l} \left\lfloor \sigma_{0,k+1} \right\rceil^{\frac{n-l}{n+1}} \right) + b_k, \\ b_k &= -\sum_{l=0}^{n} m_l \tau^l z_{l,k} + f_{k+1}, \\ \xi(\sigma_{0,k+1}) &= g^{-1}(\sigma_{0,k+1}). \end{aligned} \tag{1.97}$$

$\sigma_{0,k+1}$ and ξ_k are implemented solving the generalized equation as in the previous case.

As it was mentioned previously, the main drawback of both implicit differentiators is that they require measurements at time t_{k+1} to estimate the state at time t_k (see Remark 1.4.1). Furthermore, the convergence proof is only given in the noise-free case and assuming that $f^{n+1}(t) = 0$. In Chapters 2-3 implicit discrete-time realizations are introduced in order to alleviate these disadvantages.

1.5 Conclusion

In this chapter, some preliminaries on set-valued functions, generalized equations, homogeneous systems have been recalled. Explicit and implicit discretization methods have been discussed. The differentiation problem has been introduced and some continuous-time differentiators have been recalled. At last, some existing discrete-time realizations of the standard differentiator have been reported. All these concepts will be very useful to derive the main results in the following Chapters.

CHAPTER 2

Explicit and implicit discretizations of homogeneous differentiator

A discrete-time realization of the standard differentiator is needed to implement a controller or an observer on a digital device. However, an improper discretization may result in eliminating the properties of its continuous-time counterpart or undesirable behavior due to, for instance, numerical chattering [Polyakov *et al.* 2019] or the asymptotic accuracy of the continuous-time differentiator [Livne & Levant 2014]. Therefore, some discrete-time sliding mode schemes have been introduced and applied in several works [Polyakov *et al.* 2019, Drakunov & Utkin 1990, Utkin 1994, Kikuuwe & Fujimoto 2006, Su *et al.* 2000]. In particular, for the homogeneous differentiator, some explicit discrete-time realizations have been proposed in [Livne & Levant 2014, Koch *et al.* 2020, Barbot *et al.* 2020, Mojallizadeh *et al.* 2021] to preserve properties of the respective continuous-time system using different methodologies.

Contrary to many explicit discretization methods, implicit ones do not significantly reduce the performance for large sampling times in terms of robustness properties to matched perturbations and accuracy while not being sensitive to control gain variations. Nevertheless, they require a more elaborate scheme compared with their explicit counterparts. A pioneer work [Drakunov & Utkin 1990] has presented an implicit discretization for the scalar case where the disturbance is required to be known. Then, other works, [Brogliato *et al.* 2019, Huber *et al.* 2013] have introduced a time discretization of the original plant and an implicit discretization of the controller, where the unperturbed plant is analyzed to obtain a causal controller. Moreover, implicit time-discretization schemes have been derived for twisting and super-twisting controllers [Brogliato *et al.* 2019, Huber *et al.* 2019], finite-time and fixed-time systems [Polyakov *et al.* 2019], where the stability properties are preserved. The implicit discrete-time super-twisting [Brogliato *et al.* 2019] has presented convergence to the origin in a finite number of steps for the unperturbed case. A detailed comparison between explicit and implicit schemes has been given in [Huber *et al.* 2013]. Remarkable experimental results have been provided in [Huber *et al.* 2016b, Wang *et al.* 2015, Huber *et al.* 2016a, Huber *et al.* 16]. Such discrete-time realizations preserve the continuous-time desirable properties of the sliding mode algorithms while

reducing numerical chattering at the output and input. Furthermore, most of the mentioned works do not significantly reduce the performance for large sampling times, allowing suitable robustness properties to matched bounded disturbances and being not sensitive to control gain variations. In contrast, the above properties may not be valid for an explicit discretization. Nevertheless, their main drawback is a more elaborate procedure than the explicit counterpart.

The main contributions of this chapter are to introduce and analyze an explicit and implicit discrete-time realization of the continuous-time homogeneous differentiator. First, an explicit discrete-time version of the continuous-time homogeneous differentiator is proposed. Based on this scheme, an implicit discrete-time differentiator is obtained. It is non-anticipative and relies on a root-finding method. Furthermore, in this paper, the properties of the proposed schemes are analyzed using homogeneity. It will be shown that the estimation errors of the explicit and implicit differentiators, as defined in this work, converge to a vicinity of the origin. An efficient implementation is also proposed to reduce the time complexity of the algorithm. At last, simulation results are performed to compare the proposed implicit discretization method with other existing schemes to highlight, for instance, its advantages in terms of accuracy when relatively large sampling periods are considered.

2.1 Explicit Discretization of the Homogeneous Differentiator (HEDD)

Let $x_{i,k} = x_i(t_k)$ and $\boldsymbol{x}_k = [x_{0,k}, \ldots, x_{n,k}]^T$. Then, the system

$$\boldsymbol{x}_{k+1} = \boldsymbol{\Phi}(\tau)\,\boldsymbol{x}_k + \boldsymbol{h}_k(\tau) \tag{2.1}$$

is a discrete-time representation of system (1.60). It is obtained similarly to [Koch & Reichhartinger 2018] by using Taylor series expansion with Lagrange's remainders [Firey 1960]. For this system, since $\boldsymbol{A}$ is a nilpotent matrix, $\boldsymbol{\Phi}(\tau) = e^{\boldsymbol{A}\tau}$ is defined as:

$$\boldsymbol{\Phi}(\tau) = \begin{bmatrix} 1 & \tau & \frac{\tau^2}{2!} & \cdots & \frac{\tau^{n-1}}{(n-1)!} & \frac{\tau^n}{n!} \\ 0 & 1 & \tau & \cdots & \frac{\tau^{n-2}}{(n-2)!} & \frac{\tau^{n-1}}{(n-1)!} \\ \vdots & \vdots & \vdots & \ddots & \vdots & \vdots \\ 0 & 0 & 0 & \cdots & 1 & \tau \\ 0 & 0 & 0 & \cdots & 0 & 1 \end{bmatrix}. \tag{2.2}$$

If $f_0^{(n+1)}(t)$ is an absolutely continuous function, then $\boldsymbol{h}_k(\tau)$ is given as:

$$\boldsymbol{h}_k(\tau) = \begin{bmatrix} \frac{\tau^{n+1}}{(n+1)!} f_0^{(n+1)}(\theta_n) & \frac{\tau^n}{n!} f_0^{(n+1)}(\theta_{n-1}) & \cdots & \tau f_0^{(n+1)}(\theta_0) \end{bmatrix}^T, \tag{2.3}$$

with $\theta_i \in (t_k, t_{k+1})$. For a discontinuous function $f_0^{(n+1)}(t)$, the equation (2.3) is replaced with the following equation:

$$\boldsymbol{h}_k(\tau) \in \begin{bmatrix} \frac{\tau^{n+1}}{(n+1)!}[-L, L] & \frac{\tau^n}{n!}[-L, L] & \cdots & \tau[-L, L] \end{bmatrix}^T. \tag{2.4}$$

This result is obtained from Theorems 3.16, 7.6, and 7.7 presented in [Apostol 1967]. Similar to (2.1), system

$$\boldsymbol{z}_{k+1} = \boldsymbol{\Phi}(\tau)\,\boldsymbol{z}_k + \boldsymbol{B}^*(\tau)\,\boldsymbol{u}(\sigma_{0,k}), \tag{2.5}$$

with $z_{i,k} = z_i(t_k)$, $\boldsymbol{z}_k = [z_{0,k}, \ldots, z_{n,k}]^T$, is a discrete-time representation of system (1.64). Assuming that $\boldsymbol{u}(\sigma_0)$ is constant on $[t_k, t_{k+1})$, the matrix $\boldsymbol{B}^*(\tau)$ is as follows:

$$\boldsymbol{B}^*(\tau) = \int_{t_k}^{t_{k+1}} e^{\boldsymbol{A}(t_{k+1}-\xi)} d\xi = \begin{bmatrix} \tau & \frac{\tau^2}{2!} & \frac{\tau^3}{3!} & \cdots & \frac{\tau^n}{n!} & \frac{\tau^{n+1}}{(n+1)!} \\ 0 & \tau & \frac{\tau^2}{2!} & \cdots & \frac{\tau^{n-1}}{(n-1)!} & \frac{\tau^n}{n!} \\ \vdots & \vdots & \vdots & \ddots & \vdots & \vdots \\ 0 & 0 & 0 & \cdots & \tau & \frac{\tau^2}{2!} \\ 0 & 0 & 0 & \cdots & 0 & \tau \end{bmatrix}. \tag{2.6}$$

Thus, considering the form of $\boldsymbol{\Phi}(\tau)$ in (2.2), $\boldsymbol{B}^*(\tau)$ in (2.6) and a constant $\sigma_0(t)$ for $[t_k, t_{k+1})$, system (2.5) is an exact discretization of the differentiator (1.64) in the sense of exact discretization of linear systems [Kazantzis & Kravaris 1999]. However, in practice, the earlier assumption ($\sigma_0(t)$ is constant for $[t_k, t_{k+1})$) is not satisfied. Hence, it is only used to propose the discrete-time realization, but it is not used in its stability proof presented in the next section. Concerning the sampling time, the following assumption is used in the next sections:

Assumption 2.1.1 *The sampling time τ is a positive constant and the input of the differentiator, $f(t)$, is measured in the instant of time $t_k = k\tau$ for $k = 0, 1, 2, 3, \cdots$.*

Under Assumptions 1.3.1, 1.3.2, 1.3.4 and 2.1.1, and based on the discrete-time realization (2.5), the following discrete-time injections provide the final form for the explicit discretization of the differentiator (1.64), caller hereafter HEDD:

$$\boldsymbol{u}(\sigma_{0,k}) = [\Psi_{0,n}(\sigma_{0,k}) \quad \Psi_{1,n}(\sigma_{0,k}) \quad \cdots \quad \Psi_{n,n}(\sigma_{0,k})]^T, \tag{2.7}$$

where $\Psi_{i,n}(\cdot)$ is defined as in the Equation (1.65).

Remark 2.1.1 *The discrete-time differentiator (2.5)-(2.7) has a similar structure to that proposed in the differentiators (1.81), (1.84) and (1.87). The main difference is that for HDD, given in eq. (1.81), $\boldsymbol{B}^*(\tau)$ is given as $\boldsymbol{B}^*(\tau) = \tau\boldsymbol{I}$, where $\boldsymbol{I}$ is an identity matrix of appropriate dimensions, and in [Koch & Reichhartinger 2018], $\boldsymbol{B}^*(\tau)\,\boldsymbol{u}(\sigma_{0,k})$ are the injection terms obtained by placing the eigenvalues of the discrete-time error system. The Matching differentiator, given in eq. (1.84), can be written in the form of (2.7) with a different matrix $\boldsymbol{B}^*(\tau)$. The discrete-time differentiators HDD, Matching and HEDD can be seen as particular cases of the discrete-time differentiator proposed in [Barbot et al. 2020]. Note that in [Barbot et al. 2020], the convergence of the estimation error using the explicit discrete-time differentiator (2.5) has been investigated even for variable sampling times.*

Let $\sigma_{i,k} = \sigma_i(t_k)$ and $\boldsymbol{\sigma}_k = [\sigma_{0,k}, \ldots, \sigma_{n,k}]^T$. Using Equations (2.1) and (2.7), the discrete-time estimation error system has the form:

$$\boldsymbol{\sigma}_{k+1} = \boldsymbol{\Phi}(\tau)\,\boldsymbol{\sigma}_k + \boldsymbol{B}^*(\tau)\,\boldsymbol{u}(\sigma_{0,k}) - \boldsymbol{h}_k(\tau). \tag{2.8}$$

Furthermore, in the presence of measurement noise, the estimation error dynamics become

$$\boldsymbol{\sigma}_{k+1} = \boldsymbol{\Phi}(\tau)\,\boldsymbol{\sigma}_k + \boldsymbol{B}^*(\tau)\,\boldsymbol{u}(\sigma_{0,k} - \Delta_k) - \boldsymbol{h}_k(\tau), \tag{2.9}$$

where $\Delta_k = \Delta(t_k)$. As $\Delta_k \in [-\delta, \delta]$ and $f_0^{(n+1)}(t) \in [-L, L]$, one obtains

$$\begin{aligned}\boldsymbol{\sigma}_{k+1} \in & \boldsymbol{\Phi}(\tau)\,\boldsymbol{\sigma}_k + \boldsymbol{B}^*(\tau)\,\boldsymbol{u}(\sigma_{0,k} + [-\delta, \delta]) + \ldots \\ & \ldots + \begin{bmatrix} \dfrac{\tau^{n+1}}{(n+1)!}[-L, L] & \dfrac{\tau^n}{n!}[-L, L] & \cdots & \tau[-L, L] \end{bmatrix}^T = \boldsymbol{\varpi}_k(\tau, \delta, \boldsymbol{\sigma}).\end{aligned} \tag{2.10}$$

Lemma 2.1 *The system (2.10) is homogeneous with respect to the transformation* $(\tau, \delta, \sigma_0, \ldots, \sigma_n) \mapsto (\alpha\tau, \alpha^{n+1}\delta, \alpha^{n+1}\sigma_0, \ldots, \alpha\sigma_n)$*, for all* $\alpha \in \mathbb{R}^+$*.*

Proof *Since* $\boldsymbol{\Lambda}_{\boldsymbol{m}}^{-1}(\alpha)\,\boldsymbol{A}\boldsymbol{\Lambda}_{\boldsymbol{m}}(\alpha) = \alpha^{-1}\boldsymbol{A}$*, the following equalities are obtained:*

$$\boldsymbol{A}\boldsymbol{\Lambda}_{\boldsymbol{m}}(\alpha) = \alpha^{-1}\boldsymbol{\Lambda}_{\boldsymbol{m}}(\alpha)\,\boldsymbol{A}, \tag{2.11}$$

$$\boldsymbol{A}^i\boldsymbol{\Lambda}_{\boldsymbol{m}}(\alpha) = \alpha^{-i}\boldsymbol{\Lambda}_{\boldsymbol{m}}(\alpha)\,\boldsymbol{A}^i, \tag{2.12}$$

$$\boldsymbol{\Lambda}_{\boldsymbol{m}}(\alpha)\,\boldsymbol{\Phi}(\tau) = \boldsymbol{\Phi}(\alpha\tau)\,\boldsymbol{\Lambda}_{\boldsymbol{m}}(\alpha), \tag{2.13}$$

$$\boldsymbol{\Lambda}_{\boldsymbol{m}}(\alpha)\,\boldsymbol{B}^*(\tau) = \alpha^{-1}\boldsymbol{B}^*(\alpha\tau)\,\boldsymbol{\Lambda}_{\boldsymbol{m}}(\alpha), \tag{2.14}$$

$$\boldsymbol{u}\left(\alpha^{n+1}\sigma_{0,k} + \left[-\alpha^{n+1}\delta, \alpha^{n+1}\delta\right]\right) = \alpha^{-1}\boldsymbol{\Lambda}_{\boldsymbol{m}}(\alpha)\,\boldsymbol{u}(\sigma_{0,k} + [-\delta, \delta]), \tag{2.15}$$

$$\begin{aligned}&\begin{bmatrix} \dfrac{(\alpha\tau)^{n+1}}{(n+1)!}[-L, L] & \dfrac{(\alpha\tau)^n}{n!}[-L, L] & \cdots & \alpha\tau[-L, L] \end{bmatrix}^T = \ldots \\ &\boldsymbol{\Lambda}_{\boldsymbol{m}}(\alpha)\begin{bmatrix} \dfrac{\tau^{n+1}}{(n+1)!}[-L, L] & \dfrac{\tau^n}{n!}[-L, L] & \cdots & \tau[-L, L] \end{bmatrix}^T.\end{aligned} \tag{2.16}$$

Equation (2.12) is obtained from Equation (2.11) when it is multiplied by $\boldsymbol{A}$ *recursively. Equations (2.13) and (2.14) are obtained from Equations (2.3), (2.6) and (2.12), whereas Equation (2.15) is obtained from Equation (2.7). Let* $m_0 = n + 1$*,* $m_1 = n$*,* $\cdots$ *and* $m_n = 1$ *then*

$$\begin{aligned}&\boldsymbol{\varpi}_k\left(\alpha\tau, \alpha^{n+1}\delta, \boldsymbol{\Lambda}_{\boldsymbol{m}}(\alpha)\,\boldsymbol{\sigma}\right) = \boldsymbol{\Phi}(\alpha\tau)\,\boldsymbol{\Lambda}_{\boldsymbol{m}}(\alpha)\,\boldsymbol{\sigma}_k + \ldots \\ &\ldots + \boldsymbol{B}^*(\alpha\tau)\,\boldsymbol{u}\left(\alpha^{n+1}\sigma_{0,k} + \alpha^{n+1}[-\delta, \delta]\right) + \ldots \\ &\ldots + \begin{bmatrix} \dfrac{(\alpha\tau)^{n+1}}{(n+1)!}[-L, L] & \dfrac{(\alpha\tau)^n}{n!}[-L, L] & \cdots & \alpha\tau[-L, L] \end{bmatrix}^T, \\ &= \boldsymbol{\Lambda}_{\boldsymbol{m}}(\alpha)\left(\boldsymbol{\Phi}(\tau)\,\boldsymbol{\sigma}_k + \boldsymbol{B}^*(\tau)\,\boldsymbol{u}(\sigma_{0,k} + [-\delta, \delta]) + \ldots\right. \\ &\left.\ldots + \begin{bmatrix} \dfrac{\tau^{n+1}}{(n+1)!}[-L, L] & \dfrac{\tau^n}{n!}[-L, L] & \cdots & \tau[-L, L] \end{bmatrix}^T\right), \\ &= \boldsymbol{\Lambda}_{\boldsymbol{m}}(\alpha)\,\boldsymbol{\varpi}_k(\tau, \delta, \boldsymbol{\sigma}).\end{aligned} \tag{2.17}$$

From Equation (2.17), $\boldsymbol{\Lambda}_{\boldsymbol{m}}^{-1}(\alpha)\,\boldsymbol{\varpi}_k\left(\alpha\tau, \alpha^{n+1}\delta, \boldsymbol{\Lambda}_{\boldsymbol{m}}(\alpha)\,\boldsymbol{\sigma}\right) = \boldsymbol{\varpi}_k(\tau, \delta, \boldsymbol{\sigma})$ *and therefore inclusion (2.10) is invariant with respect to the transformation* $(\tau, \delta, \sigma_0, \ldots, \sigma_n) \mapsto (\alpha\tau, \alpha^{n+1}\delta, \alpha^{n+1}\sigma_0, \ldots, \alpha\sigma_n)$ *and homogeneous.*

Remark 2.1.2 *The discrete-time system* (2.10) *preserves the homogeneity degrees of the differential inclusion* (1.68)*, i.e.,* $\deg(\bar{\sigma}_i) = \deg(\sigma_{i,k}) = m_i$ *and* $\deg(t) = \deg(\tau) = 1$.

2.2 Implicit Discretization of the Homogeneous Differentiator (HIDD)

Now, based on the realization of the previous section, HEDD, an implicit scheme is designed.

2.2.1 Design of HIDD

Under Assumptions 1.3.1, 1.3.2, 1.3.4 and 2.1.1, an implicit discretization is performed for the continuous-time differentiator (1.62). First, $\sigma_{0,k}$ is replaced with $\sigma_{0,k+1}$ in Equation (2.7), i.e.,

$$\boldsymbol{u}\left(\sigma_{0,k+1}\right) = \left[\Psi_{0,n}(\sigma_{0,k+1}) \quad \Psi_{1,n}(\sigma_{0,k+1}) \quad \cdots \quad \Psi_{n,n}(\sigma_{0,k+1})\right]^T. \tag{2.18}$$

Therefore, the following implicit discrete-time systems are obtained:

$$\begin{aligned} \boldsymbol{z}_{k+1} &= \boldsymbol{\Phi}\left(\tau\right)\boldsymbol{z}_k + \boldsymbol{B}^*\left(\tau\right)\boldsymbol{u}\left(\sigma_{0,k+1}\right), \\ \boldsymbol{\sigma}_{k+1} &= \boldsymbol{\Phi}\left(\tau\right)\boldsymbol{\sigma}_k + \boldsymbol{B}^*\left(\tau\right)\boldsymbol{u}\left(\sigma_{0,k+1}\right) - \boldsymbol{h}_k\left(\tau\right). \end{aligned} \tag{2.19}$$

However, one should highlight that $\sigma_{0,k+1}$ cannot be obtained from the second equation of (2.19) due to the impossibility to measure the state variables $x_{1,k}$, $x_{2,k}$, $\cdots$, $x_{n,k}$ and vector $\boldsymbol{h}_k\left(\tau\right)$. Therefore, these terms are considered as perturbations for the estimation process of $\sigma_{0,k+1}$. It allows to estimate $\sigma_{0,k+1}$ as:

$$\sigma_{0,k+1} = \sigma_{0,k} + \tau\Psi_{0,n}\left(\sigma_{0,k+1}\right) + \sum_{l=1}^{n}\frac{\tau^l}{l!}\left(z_{l,k} + \frac{\tau}{l+1}\Psi_{l,n}\left(\sigma_{0,k+1}\right)\right). \tag{2.20}$$

Equation (2.20) is only valid for $x_{l,k} = 0$ and $h_{0,k} = 0$, with $l = 1, \cdots, n$. Similar to [Brogliato *et al.* 2020] and [Acary *et al.* 2012], to implement the discrete-time observer (2.19), the intermediate variable $\widetilde{\sigma}_{0,k+1}$ is proposed as a copy of $\sigma_{0,k+1}$ in Equation (2.20):

$$\widetilde{\sigma}_{0,k+1} = \sigma_{0,k} + \tau\Psi_{0,n}\left(\widetilde{\sigma}_{0,k+1}\right) + \sum_{l=1}^{n}\frac{\tau^l}{l!}\left(z_{l,k} + \frac{\tau}{l+1}\Psi_{l,n}\left(\widetilde{\sigma}_{0,k+1}\right)\right). \tag{2.21}$$

$\widetilde{\sigma}_{0,k+1}$ emulates the behavior of $\sigma_{0,k+1}$ with a constant $f_0(t)$ and without measurement noise. To compute $\widetilde{\sigma}_{0,k+1}$, from Equation (2.21) a generalized equation with unknown $\widetilde{\sigma}_{0,k+1}$ is obtained:

$$\widetilde{\sigma}_{0,k+1} + a_n\left\lfloor\widetilde{\sigma}_{0,k+1}\right\rceil^{\frac{n}{n+1}} + \cdots + a_1\left\lfloor\widetilde{\sigma}_{0,k+1}\right\rceil^{\frac{1}{n+1}} + b_k \in -a_0\text{sign}(\widetilde{\sigma}_{0,k+1}), \tag{2.22}$$

where $b_k = -\sigma_{0,k} - \sum_{l=1}^{n}\frac{\tau^l}{l!}z_{l,k}$ and $a_l = \frac{\tau^{n-l+1}}{(n-l+1)!}\lambda_l L^{\frac{n-l+1}{n+1}}$, $l = 0, \ldots, n$. A new support variable is introduced: $\xi_k \in \text{sign}(\widetilde{\sigma}_{0,k+1})$, which can be understood as a selection of

the set-valued signal. Now, $\chi_n(\zeta)$ and its inverse mapping, with $\zeta \in \mathbb{R}$. The first is defined as:

$$\chi_n(\zeta) = \zeta + a_n \lfloor \zeta \rceil^{\frac{n}{n+1}} + \cdots + a_1 \lfloor \zeta \rceil^{\frac{1}{n+1}} + b_k. \tag{2.23}$$

The inverse mapping $\chi_n^{-1}(y)$ is obtained as follows:

$$\begin{aligned} &\chi_n(\zeta) = \zeta + a_n \lfloor \zeta \rceil^{\frac{n}{n+1}} + \cdots + a_1 \lfloor \zeta \rceil^{\frac{1}{n+1}} + b_k = y, \\ &\zeta + a_n \lfloor \zeta \rceil^{\frac{n}{n+1}} + \cdots + a_1 \lfloor \zeta \rceil^{\frac{1}{n+1}} = y - b_k. \end{aligned} \tag{2.24}$$

As it can be seen in the above equation, the sign of the left side is positive when ζ is positive and it is negative if ζ is negative. Therefore, if $y - b_k$ is positive, then ζ is positive, if $y - b_k$ is negative then ζ is negative. It allows to rewrite the left side of the above equation as:

- If $y > b_k$, then

$$\zeta + a_n \zeta^{\frac{n}{n+1}} + \cdots + a_1 \zeta^{\frac{1}{n+1}} = y - b_k. \tag{2.25}$$

- If $y < b_k$, then

$$\zeta - a_n (-\zeta)^{\frac{n}{n+1}} - \cdots - a_1 (-\zeta)^{\frac{1}{n+1}} = y - b_k. \tag{2.26}$$

- If $y = b_k$, then $\zeta + a_n \lfloor \zeta \rceil^{\frac{n}{n+1}} + \cdots + a_1 \lfloor \zeta \rceil^{\frac{1}{n+1}} = 0$, which implies that $\zeta = 0$. If $\zeta \in \mathbb{R} \setminus \{0\}$ then the left side of the equation is positive or negative but is not 0.

Defining r as $r = \zeta^{\frac{1}{n+1}}$ and $r = (-\zeta)^{\frac{1}{n+1}}$ in the first two cases respectively, one defines the inverse mapping $\chi_n^{-1}(\zeta)$ as follows:

- If $y > b_k$, then $\chi_n^{-1}(y) = (r_0)^{n+1}$ where r_0 is the positive root of the polynomial:

$$p(r) = r^{n+1} + a_n r^n + \cdots + a_1 r + (b_k - y). \tag{2.27}$$

- If $y < b_k$, then $\chi_n^{-1}(y) = -(r_0)^{n+1}$ con r_0 where r_0 is the positive root of the polynomial:

$$p(r) = r^{n+1} + a_n r^n + \cdots + a_1 r - (b_k - y). \tag{2.28}$$

- If $y = b_k$, then $\chi_n^{-1}(y) = 0$.

Polynomials (2.27) and (2.28) are obtained if the equations are equal to 0. Additionally, the change of variables implies that r is positive, and therefore ζ is defined with a positive root, and its negatives and complex roots are avoided. Moreover, (2.27) and (2.28) are polynomials without zero coefficients. As the parameters a_i are positive, there is a unique change of sign in the sequence of coefficient of the polynomials (2.27) and (2.28). Hence, according to the Descartes's rule of signs [Aleksandrov *et al.* 1999], both polynomials have a unique positive root.

One of the main properties of the inverse mapping $\chi_n^{-1}(\zeta)$ is that it is continuous for all $\zeta \in \mathbb{R}$, and monotonically increasing if $\zeta \neq b_k$. The above comes from the fact that $\frac{d\chi_n(\zeta)}{d\zeta} > 0$ for $\zeta \neq 0$, therefore $\frac{d\chi_n^{-1}(\zeta)}{d\zeta} > 0$ for all $\zeta \neq b_k$, which is the unique point that mapping to 0 the inverse mapping.

The mapping $\chi_n(\zeta)$ and its inverse mapping $\chi_n^{-1}(y)$, allow to represent the problem of calculating $\widetilde{\sigma}_{0,k+1}$ and ξ_k with the following generalized equations:

$$\begin{aligned} \xi_k \in \operatorname{sign}(\widetilde{\sigma}_{0,k+1}) \Leftrightarrow \widetilde{\sigma}_{0,k+1} \in \mathcal{N}_{[-1,1]}(\xi_k), \\ \chi_n(\widetilde{\sigma}_{0,k+1}) = -a_0\xi_k \Leftrightarrow \widetilde{\sigma}_{0,k+1} = \chi_n^{-1}(-a_0\xi_k), \\ \chi_n^{-1}(-a_0\xi_k) \in \mathcal{N}_{[-1,1]}(\xi_k). \end{aligned} \tag{2.29}$$

In summary, one has the following generalized equations:

$$\begin{aligned} \chi_n\left(\widetilde{\sigma}_{0,k+1}\right) \in -a_0 \operatorname{sign}(\widetilde{\sigma}_{0,k+1}), \\ \chi_n^{-1}\left(-a_0\xi_k\right) \in \mathcal{N}_{[-1,1]}\left(\xi_k\right), \\ \xi_k \in \operatorname{sign}(\widetilde{\sigma}_{0,k+1}). \end{aligned} \tag{2.30}$$

$\widetilde{\sigma}_{0,k+1}$ and ξ_k correspond to the solution of the generalized equations (2.30). A graphic representation of the generalized equations (2.30) are showed in Figure (2.1), where $\tau = 0.5$, $L = 100$, $n = 3$. The intersection between $\chi_3^{-1}(-a_0\xi_k)$ and $\mathcal{N}_{[-1,1]}(\xi_k)$ correspond to the solution of the generalized equations for any value of b_k, in specific, the solutions is represented as $(\xi_k^*, \sigma_{k+1}^*)$ in Figure 2.1.

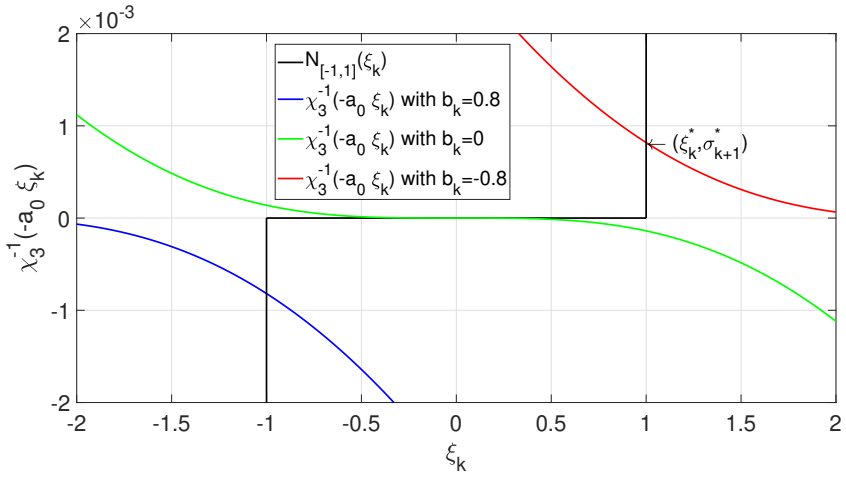

Figure 2.1: Graphic representation of the generalized equation $\chi_n^{-1}\left(-a_0\xi_k\right) \in \mathcal{N}_{[-1,1]}\left(\xi_k\right)$ with $\tau = 0.5$, $L = 100$, $n = 3$.

Using the properties of the inverse mapping $\chi_n^{-1}(\zeta)$, one obtains the following theorem:

Theorem 2.2.1

The generalized equation $\chi_n^{-1}\left(-a_0\xi_k\right) \in \mathcal{N}_{[-1,1]}\left(\xi_k\right)$ has a unique solution for any $b_k \in \mathbb{R}$.

Proof *First, the generalized equations* $\chi_n^{-1}(-a_0\xi_k) \in \mathcal{N}_{[-1,1]}(\xi_k)$ *can be rewritten as follows:*

$$\begin{aligned}
&\chi_n^{-1}(-a_0\xi_k) \in \mathcal{N}_{[-1,1]}(\xi_k),\\
&0 \in -\chi_n^{-1}(-a_0\xi_k) + \mathcal{N}_{[-1,1]}(\xi_k),\\
&0 \in -\chi_n^{-1}(y) + \mathcal{N}_{[-1,1]}\left(-\frac{y}{a_0}\right),\\
&0 \in -\chi_n^{-1}(y) + \mathcal{N}_{[-a_0,a_0]}(-y),\\
&0 \in -\chi_n^{-1}(y) - \mathcal{N}_{[-a_0,a_0]}(y),\\
&0 \in \chi_n^{-1}(y) + \mathcal{N}_{[-a_0,a_0]}(y).
\end{aligned} \tag{2.31}$$

Here the variable y *is given as* $y = -a_0\xi_k$*. As* $\frac{d\chi_n(\zeta)}{d\zeta} > 0$ *with* $\zeta \neq b_k$*, and from Preposition 1.1.1 and Theorem 1.1.2, one can demonstrate that if* $b_k \notin [-a_0, a_0]$ *then* $\chi_n^{-1}(\zeta)$ *is strictly monotone and therefore the generalized equation has at least one solution. With* $b_k \in [-a_0, a_0]$*,* $\frac{d\chi_n(\zeta)^{-1}}{d\zeta}$ *is semi definite positive and the Corollary 1.1.2 is used, with* $x^{ref} = b_k$*. Due to the fact that* $\chi_n^{-1}(\zeta) > 0$ *with* $\zeta > 0$ *and* $\chi_n^{-1}(\zeta) < 0$ *with* $\zeta < 0$*, it can be deduce that:*

$$\chi_n^{-1}(\zeta)(\zeta - b_k) \geq 0, \quad \forall \zeta \in [-a_0, a_0], \tag{2.32}$$

and from Corollary 1.1.2, the generalized equation has a solution. Ultimately, it is demonstrated that this solution is unique. In order to demonstrate it, it is assumed that there are two different solutions of the generalized equations, ζ_1*, and* ζ_2*, it implies that:*

$$\chi_n^{-1}(\zeta_1)(\zeta' - \zeta_1) \geq 0, \quad \chi_n^{-1}(\zeta_2)(\zeta' - \zeta_2) \geq 0, \quad \forall \zeta' \in [-a_0, a_0]. \tag{2.33}$$

Substituting ζ' *with* ζ_2 *and* ζ_1 *respectively and with both inequalities, one obtains:*

$$\begin{aligned}
&\chi_n^{-1}(\zeta_1)(\zeta_2 - \zeta_1) \geq 0, \quad && \chi_n^{-1}(\zeta_2)(\zeta_1 - \zeta_2) \geq 0, \quad && \zeta_1 \neq \zeta_2,\\
&\chi_n^{-1}(\zeta_1)(\zeta_1 - \zeta_2) \leq 0, \quad && -\chi_n^{-1}(\zeta_2)(\zeta_1 - \zeta_2) \leq 0, \quad && \zeta_1 \neq \zeta_2,\\
&\left(\chi_n^{-1}(\zeta_1) - \chi_n^{-1}(\zeta_2)\right)(\zeta_1 - \zeta_2) \leq 0, && && \zeta_1 \neq \zeta_2.
\end{aligned} \tag{2.34}$$

As $\frac{\chi_n^{-1}(\zeta)}{d\zeta} > 0$ *for* $\zeta \neq b_k$*,* $\chi_n^{-1}(b_k) = 0$*,* $\chi_n^{-1}(\zeta) > 0$ *for* $\zeta > b_k$ *and* $\chi_n^{-1}(\zeta) < 0$ *for* $\zeta < b_k$*, then:*

$$\left(\chi_n^{-1}(\zeta_1) - \chi_n^{-1}(\zeta_2)\right)(\zeta_1 - \zeta_2) > 0. \tag{2.35}$$

A contradiction is obtained, and it concludes the proof.

Now the unique solution of the generalized equations (2.30) is given in the following lemma:

Lemma 2.2 *Let* $a_i > 0$*,* $\widetilde{\sigma}_{0,k+1} \in \mathbb{R}$ *and* $\xi_k \in [-1, 1]$*, then the solution of the inclusions (2.30) is the unique pair* $(\widetilde{\sigma}_{0,k+1}, \xi_k)$ *which is defined according to the following cases:*

- *If* $b_k > a_0$, *then* $\xi_k = \{-1\}$ *and* $\widetilde{\sigma}_{0,k+1} = -(r_0)^{n+1} \in \mathbb{R}^-$ *where* r_0 *is the unique positive root of the following polynomial:*

$$p(r) = r^{n+1} + a_n r^n + \cdots + a_1 r + (-b_k + a_0). \tag{2.36}$$

- *If* $b_k \in [-a_0, a_0]$, *then* $\widetilde{\sigma}_{0,k+1} = 0$ *and* $\xi_k = \left\{-\frac{b_k}{a_0}\right\}$.

- *If* $b_k < -a_0$, *then* $\xi_k = \{1\}$ *and* $\widetilde{\sigma}_{0,k+1} = r_0^{n+1} \in \mathbb{R}^+$ *where* r_0 *is the unique positive root of the following polynomial:*

$$p(r) = r^{n+1} + a_n r^n + \cdots + a_1 r + (b_k + a_0). \tag{2.37}$$

Proof *As a result of Equation (2.23),* $\chi(\zeta)$ *presents the following properties:*

$$\begin{cases} \chi(\zeta) > b_k & \text{if} \quad \zeta > 0, \\ \chi(\zeta) = b_k & \text{if} \quad \zeta = 0, \\ \chi(\zeta) < b_k & \text{if} \quad \zeta < 0. \end{cases} \tag{2.38}$$

The following three cases are based on the values of b_k *and* a_0*:*

- *Case 1:* $b_k > a_0$

  From Equations (2.30) and (2.38), one can conclude that $\widetilde{\sigma}_{0,k+1} < 0$. *It yields*

$$\widetilde{\sigma}_{0,k+1} - a_n(-\widetilde{\sigma}_{0,k+1})^{\frac{n}{n+1}} - \cdots - a_1(-\widetilde{\sigma}_{0,k+1})^{\frac{1}{n+1}} + b_k = a_0. \tag{2.39}$$

  Defining $r = (-\widetilde{\sigma}_{0,k+1})^{\frac{1}{n+1}}$, *one can obtain* $p(r) = 0$, *where* $p(r)$ *is the polynomial (2.36). It has only one positive root due to its structure with one sign change in the sequence coefficients. Hence,* $\widetilde{\sigma}_{0,k+1} = -(r_0)^{n+1}$, *where* r_0 *is the positive root of Equation (2.36). Since* $b_k > -a_0\xi_k$, *for all* $\xi_k \in [-1, 1]$, $\beta(-a_0\xi_k) = c$ *for some* $c \in \mathbb{R}^-$. *Therefore, one obtains* $\xi_k = \{-1\}$.

- *Case 2:* $b_k < -a_0$

  From Equations (2.30) and (2.38), one can conclude that $\widetilde{\sigma}_{0,k+1} > 0$. *It yields*

$$\widetilde{\sigma}_{0,k+1} + a_n(\widetilde{\sigma}_{0,k+1})^{\frac{n}{n+1}} + \cdots + a_1(\widetilde{\sigma}_{0,k+1})^{\frac{1}{n+1}} + b_k = a_0. \tag{2.40}$$

  As the previous case, one can demonstrate that $\xi_k = \{1\}$ *and* $\widetilde{\sigma}_{0,k+1} = (r_0)^{n+1}$ *where* r_0 *is the unique positive root of Equation (2.37).*

- *Case 3:* $b_k \in [-a_0, a_0]$

  From Equations (2.30) and (2.38), one can conclude that $\widetilde{\sigma}_{0,k+1} = 0$. *Inclusion (2.30) yields*

$$\xi_k \in sign(\beta(-a_0\xi_k)). \tag{2.41}$$

  If $\xi_k > -\frac{b_k}{a_0}$, *Equation (2.41) becomes* $\xi_k = \{-1\}$. *Hence, a contradiction appears. Similarly, if* $\xi_k < -\frac{b_k}{a_0}$, *a contradiction appears. Therefore, the pair* $\left(0, \left\{\frac{-b_k}{a_0}\right\}\right)$ *is the unique solution.*

Remark 2.2.1 *It could be noted that* $p((b_k - a_0)^{\frac{1}{n+1}}) > 0$ *for polynomial* (2.36) *and* $p((-b_k - a_0)^{\frac{1}{n+1}}) > 0$ *for* (2.37)*. Furthermore, for both polynomials,* $p(0) < 0$*. Therefore,* $r_0 \in \left[0, (b_k - a_0)^{\frac{1}{n+1}}\right]$ *for* $b_k > a_0$ *and* $r_0 \in \left[0, (-b_k - a_0)^{\frac{1}{n+1}}\right]$ *for* $b_k < -a_0$*. It should be highlighted that* r_0 *is unique for these two cases. Therefore,* $\widetilde{\sigma}_{0,k+1}$ *and* ξ_k *always exist for all* $b_k \in \mathbb{R}$ *and* $a_0 \neq 0$*. Additionally, the parameters* a_j *can be calculated previous to implement the implicit differentiator, but* b_k *has to be updated at the time instant* t_k*.*

The proposed implicit discrete-time realizations of the homogeneous differentiator are expressed as follows:

$$\begin{aligned} \boldsymbol{z}_{k+1} &= \boldsymbol{\Phi}(\tau)\,\boldsymbol{z}_k + \boldsymbol{B}^*(\tau)\,\boldsymbol{v}(\widetilde{\sigma}_{0,k+1}), \\ \boldsymbol{v}(\widetilde{\sigma}_{0,k+1}) &= [\Psi_{0,n}(\widetilde{\sigma}_{0,k+1}) \;\; \cdots \;\; \Psi_{n,n}(\widetilde{\sigma}_{0,k+1})]^T, \\ \Psi_{i,n}(\widetilde{\sigma}_{0,k+1}) &= -\lambda_{n-i} L^{\frac{i+1}{n+1}} |\widetilde{\sigma}_{0,k+1}|^{\frac{n-i}{n+1}} \xi_k. \end{aligned} \tag{2.42}$$

At time t_k, the unique pair $(\widetilde{\sigma}_{0,k+1}, \xi_k)$ is computed according to Lemma 2.2. Furthermore, from Lemma 2.2, one can conclude that the proposed discrete-time differentiator (2.42) is non-anticipative. Since the discrete-time differentiator (2.42) uses ξ_k instead of $\text{sign}(\cdot)$, $\boldsymbol{v}(\cdot)$ is used instead of $\boldsymbol{u}(\cdot)$ in the the discrete-time differentiator (2.42). The difference between the functions $\boldsymbol{u}(\widetilde{\sigma}_{0,k+1})$ and $\boldsymbol{v}(\widetilde{\sigma}_{0,k+1})$ comes from their evaluation at $\widetilde{\sigma}_{0,k+1} = 0$. Indeed, at $\widetilde{\sigma}_{0,k+1} = 0$, $\boldsymbol{e}_{n+1}\boldsymbol{u}(\widetilde{\sigma}_{0,k+1}) \in [-\lambda_0 L, \lambda_0 L]$, whereas $\boldsymbol{e}_{n+1}\boldsymbol{v}(\widetilde{\sigma}_{0,k+1}) = \left\{-\frac{\lambda_0 L b_k}{a_0}\right\}$. Although measurement noise is absent in Equation (2.21) and Lemma 2.2, in practice $\sigma_{0,k}$ is not available. Hence, in practice, $\sigma_{0,k} - \Delta_k$ is used instead of $\sigma_{0,k}$. This fact modifies the variable b_k, the polynomials (2.36) and (2.37), and consequently, the behavior of $\widetilde{\sigma}_{0,k+1}$. The effect of the measurement noise on $\widetilde{\sigma}_{0,k+1}$ is studied in the next subsection.

2.2.2 Implementation of HIDD

In this subsection, an implementation scheme of the algorithm of the proposed implicit discrete-time realization of the homogeneous differentiator (2.42) is presented:

Require: $n \geq 0$, L, λ_i, τ
  $m \leftarrow 0$
  while $(m \leq n)$ **do**
    $a_m \leftarrow \frac{\tau^{n-m+1}}{(n-m+1)!}\lambda_m L^{\frac{n-m+1}{n+1}}$
    $m \leftarrow m + 1$
  end while
  $m \leftarrow 0$
  while $(m \leq n)$ **do**
    $z_m \leftarrow 0$ ▷ The states z_i are initialized.
    $m \leftarrow m + 1$
  end while
  $m \leftarrow 0$
  while (1) **do**
    $f_k \leftarrow f(m\tau)$ ▷ The measurement of $f(t)$ is obtained.

$b_k \leftarrow -(z_0 - f_k) - \sum_{l=1}^{n} \frac{\tau^l}{l!} z_l$
if $(b_k > a_0)$ **then**
  $r \leftarrow \left(\frac{b_k - a_0}{2}\right)^{1/(n+1)}$
  $j \leftarrow 0$
  while $(j < 3)$ **do** ▷ Computation of the unique positive root.
    $p \leftarrow r^{n+1} + a_n r^n + \cdots + a_1 r + (-b_k + a_0)$
    $dp \leftarrow (n+1)\, r^n + n a_n r^{n-1} + \cdots + a_1$
    $ddp \leftarrow n\,(n+1)\, r^{n-1} + \cdots + 2a_2$
    $r \leftarrow r - \frac{2p(dp)}{2(dp)^2 - p(ddp)}$
    $j \leftarrow j + 1$
  end while
  $\xi_k \leftarrow -1$
end if
if $(b_k < -a_0)$ **then**
  $r \leftarrow \left(\frac{-b_k - a_0}{2}\right)^{1/(n+1)}$
  $j \leftarrow 0$
  while $(j < 3)$ **do** ▷ Computation of the unique positive root.
    $p \leftarrow r^{n+1} + a_n r^n + \cdots + a_1 r + (b_k + a_0)$
    $dp \leftarrow (n+1)\, r^n + n a_n r^{n-1} + \cdots + a_1$
    $ddp \leftarrow n\,(n+1)\, r^{n-1} + \cdots + 2a_2$
    $r \leftarrow r - \frac{2p(dp)}{2(dp)^2 - p(ddp)}$
    $j \leftarrow j + 1$
  end while
  $\xi_k \leftarrow 1$
end if
if $(b_k > -a_0)$ and $(b_k < a_0)$ **then**
  $r \leftarrow 0$
  $\xi_k \leftarrow -\frac{b_k}{a_0}$
end if
$j \leftarrow 0$
while $(j \leq n)$ **do**
  $u_j \leftarrow -\lambda_{n-j} L^{\frac{j+1}{n+1}} r^{n-j} \xi_k$
  $j \leftarrow j + 1$
end while
$j \leftarrow 0$
while $(j \leq n)$ **do** ▷ The estimation at the time $t = m\tau$ are obtained
  $z_{j,M} = \sum_{l=j}^{n} \frac{\tau^{l-j}}{(l-j)!} z_{l,k} + \frac{\tau^{l-j+1}}{(l-j+1)!} u_l$
  $j \leftarrow j + 1$
end while
$j \leftarrow 0$
while $(j \leq n)$ **do** ▷ The states are updated for the next measurement.
  $z_j = z_{j,M}$
  $j \leftarrow j + 1$
end while

end while

The above algorithm allows to clarify how to implement the HIDD.

2.3 Stability analysis of the differentiator based on the standard differentiator

In this section the stability properties of the explicit and implicit discrete-time differentiators ((2.5) and (2.42)) are derived.

2.3.1 Stability analysis of the differentiator HEDD

First, the stability of the discrete-time differentiator HEDD (2.5) is studied. Based on the results obtained in [Livne & Levant 2014, Barbot *et al.* 2020, Levant & Livne 2016], one can obtain the following theorem:

Theorem 2.3.1

Let $\boldsymbol{z}_k$ be generated with the explicit discrete-time differentiator (2.5). Under Assumptions 1.3.1-2.1.1, there exist constants $\mu_i > 0$, $i = 0, 1, 2, \cdots, n$ such that after a finite-time transient, the following inequalities are fulfilled:

$$\begin{aligned} |z_{i,k} - x_{i,k}| &\leq \mu_i L \rho^{n+1-i}, \\ \rho &= \max\left\{\tau, \left(\frac{\delta}{L}\right)^{\frac{1}{n+1}}\right\}, \end{aligned} \tag{2.43}$$

where the coefficients μ_i only depend on the differentiator parameters $\lambda_0, \ldots, \lambda_n$.

It is important to mention that Theorem 2.3.1 is a particular case of Theorem 4 in [Barbot *et al.* 2020].

Proof *Under Assumptions 1.3.1, 1.3.2, 1.3.4, 2.1.1 and as* $\Delta_k \in [-\delta, \delta]$*, the error system* (2.10) *can be expressed as:*

$$\begin{aligned} \sigma_{i,k+1} \in \sigma_{i,k} + \tau\Psi_{i,n}\left(\sigma_{0,k} + [-\delta, \delta]\right) + \sum_{j=1}^{n-i} \frac{\tau^j}{j!}\sigma_{j+i,k} + \ldots \\ \ldots + \frac{\tau^{j+1}}{(j+1)!}\Psi_{j+i,n}\left(\sigma_{0,k} + [-\delta, \delta]\right) + \frac{\tau^{n-i+1}}{(n-i+1)!}[-L, L], \\ \sigma_{n,k+1} \in \sigma_{n,k} + \tau\Psi_{n,n}\left(\sigma_{0,k} + [-\delta, \delta]\right) + \tau[-L, L], \end{aligned} \tag{2.44}$$

with $i = 0, 1, \ldots, n-1$. *Using* $\bar{\sigma}_{i,k} = \sigma_{i,k}/L$, *the above inclusion can be rewritten as:*

$$\begin{aligned}
\bar{\sigma}_{i,k+1} \in \bar{\sigma}_{i,k} + \tau \frac{\Psi_{i,n}\left(\bar{\sigma}_{0,k} + \left[-\frac{\delta}{L}, \frac{\delta}{L}\right]\right)}{L^{\frac{i+1}{n+1}}} + \ldots \\
\ldots + \sum_{j=1}^{n-i} \frac{\tau^j}{j!} \bar{\sigma}_{j+i,k} + \frac{\tau^{j+1}}{(j+1)!} \frac{\Psi_{j+i,n}\left(\bar{\sigma}_{0,k} + \left[-\frac{\delta}{L}, \frac{\delta}{L}\right]\right)}{L^{\frac{j+i+1}{n+1}}} + \frac{\tau^{n-i+1}}{(n-i+1)!}[-1,1], \\
\bar{\sigma}_{n,k+1} \in \bar{\sigma}_{n,k} + \tau \frac{\Psi_{n,n}\left(\bar{\sigma}_{0,k} + \left[-\frac{\delta}{L}, \frac{\delta}{L}\right]\right)}{L} + \tau[-1,1].
\end{aligned} \tag{2.45}$$

Define the piecewise linear continuous-time function $\boldsymbol{s}(t) = [s_0(t)\ s_1(t)\ \ldots\ s_n(t)]^T$ *such that* $\boldsymbol{s}(t)$ *describes the solution of* (2.45) *(with* $\boldsymbol{s}_k = \boldsymbol{s}(t_k) = \bar{\sigma}(t_k)$*) and is defined as:*

$$\begin{aligned}
\boldsymbol{s}(t) &= \boldsymbol{s}_k + (t - t_k)\boldsymbol{w}_k, \\
\boldsymbol{w}_k &\in \boldsymbol{G}(\boldsymbol{s}_k, \tau),
\end{aligned} \tag{2.46}$$

with $\boldsymbol{G}(\boldsymbol{s}_k, \tau) = [G_0(\boldsymbol{s}_k, \tau)\ \ G_1(\boldsymbol{s}_k, \tau)\ \ \cdots\ \ G_n(\boldsymbol{s}_k, \tau)]^T$, *and* $t \in [t_k, t_{k+1})$

$$\begin{aligned}
G_i(\boldsymbol{s}_k, \tau) = \frac{\Psi_{i,n}\left(s_{0,k} + \left[-\frac{\delta}{L}, \frac{\delta}{L}\right]\right)}{L^{\frac{i+1}{n+1}}} + \sum_{j=1}^{n-i} \frac{\tau^{j-1}}{j!} s_{j+i,k} + \ldots \\
\ldots + \frac{\tau^j}{(j+1)!} \frac{\Psi_{j+i,n}\left(s_{0,k} + \left[-\frac{\delta}{L}, \frac{\delta}{L}\right]\right)}{L^{\frac{j+i+1}{n+1}}} + \frac{\tau^{n-i}}{(n-i+1)!}[-1,1], \\
G_n(\boldsymbol{s}_k, \tau) = \frac{\Psi_{n,n}\left(s_{0,k} + \left[-\frac{\delta}{L}, \frac{\delta}{L}\right]\right)}{L} + [-1,1].
\end{aligned}$$

Note that each solution of (2.45) *satisfies* (2.46) *in the sense that for all* $t \in [t_k, t_{k+1})$, *there is a* $\boldsymbol{w}_k$ *such that* $\boldsymbol{s}(t_k) = \bar{\boldsymbol{\sigma}}_k$ *for any* k. *Due to* (2.46) *and as* $\boldsymbol{s}(t_k)$ *presents a piecewise constant derivative,* $\boldsymbol{s}(t_k)$ *satisfies the following inclusion:*

$$\begin{aligned}
\dot{s}_i \in \frac{\Psi_{i,n}\left(s_{0,k} + \left[-\frac{\delta}{L}, \frac{\delta}{L}\right]\right)}{L^{\frac{i+1}{n+1}}} + \sum_{j=1}^{n-i} \frac{\tau^{j-1}}{j!} s_{j+i,k} + \ldots \\
\ldots + \frac{\tau^j}{(j+1)!} \frac{\Psi_{j+i,n}\left(s_{0,k} + \left[-\frac{\delta}{L}, \frac{\delta}{L}\right]\right)}{L^{\frac{j+i+1}{n+1}}} + \frac{\tau^{n-i}}{(n-i+1)!}[-1,1], \\
\dot{s}_n \in \frac{\Psi_{n,n}\left(s_{0,k} + \left[-\frac{\delta}{L}, \frac{\delta}{L}\right]\right)}{L} + [-1,1].
\end{aligned} \tag{2.47}$$

Let the disturbance intensity ρ *defined as* $\rho = \max\left\{\tau, (\delta/L)^{\frac{1}{n+1}}\right\}$. *Any solution*

of inclusion (2.46) almost everywhere satisfies the differential inclusion:

$$\begin{aligned}
\dot{s}_i \in & \frac{\Psi_{i,n}\left(s_0\left(t-\rho\left[0,1\right]\right)+\rho^{n+1}\left[-1,1\right]\right)}{L^{\frac{i+1}{n+1}}}+\dots \\
& \dots+s_{i+1}\left(t-\rho\left[0,1\right]\right)+\sum_{j=2}^{n-i}\frac{\rho^{j-1}}{j!}s_{j+i}\left(t-\rho[0,1]\right)\left[-1,1\right]+\dots \\
& \dots+\sum_{j=1}^{n-i}\frac{\rho^{j}}{(j+1)!}\frac{\Psi_{j+i,n}\left(s_0\left(t-\rho\left[0,1\right]\right)+\rho^{n+1}\left[-1,1\right]\right)}{L^{\frac{j+i+1}{n+1}}}\left[-1,1\right]\dots \\
& \dots+\frac{\rho^{n-i}}{(n-i+1)!}\left[-1,1\right], \\
\dot{s}_n \in & \frac{\Psi_{n,n}\left(s_0\left(t-\rho\left[0,1\right]\right)+\rho^{n+1}\left[-1,1\right]\right)}{L}+\left[-1,1\right].
\end{aligned} \tag{2.48}$$

In compact form, Equation (2.48) can be summarized as:

$$\dot{\boldsymbol{s}} \in \boldsymbol{C}\left(\boldsymbol{s}(t-\rho[0,1]),\boldsymbol{\Gamma}(\rho,\boldsymbol{s}(t-\rho[0,1]))\right), \tag{2.49}$$

where $\boldsymbol{C}$ *has been defined in (1.68) and* $\boldsymbol{\Gamma}\left(\rho,\boldsymbol{s}(t)\right) = \left[\Gamma_0\left(\rho,\boldsymbol{s}(t)\right)\ \ \Gamma_1\left(\rho,\boldsymbol{s}(t)\right)\ \ \cdots\ \ \Gamma_n\left(\rho,\boldsymbol{s}(t)\right)\right]^T$ *is given as:*

$$\begin{aligned}
\Gamma_0\left(\rho,s(t)\right) =& \rho^{n+1}\left[-1,1\right], \\
\Gamma_i\left(\rho,s(t)\right) =& \frac{\rho^{n-i+1}}{(n-i+2)!}\left[-1,1\right]+\sum_{j=2}^{n-i+1}\frac{\rho^{j-1}}{j!}s_{j+i-1}\left(t\right)\left[-1,1\right]+\dots \\
& \dots+\sum_{j=1}^{n-i+1}\frac{\rho^{j}}{(j+1)!}\frac{\Psi_{j+i-1,n}\left(s_0\left(t\right)\right)}{L^{\frac{j+i}{n+1}}}\left[-1,1\right], \\
\Gamma_n\left(\rho,s(t)\right) =& \frac{\rho}{2!}\left[-1,1\right]+\frac{\rho}{2!}\frac{\Psi_{n,n}\left(s_0\left(t\right)\right)}{L}\left[-1,1\right],
\end{aligned} \tag{2.50}$$

for $i=1,\cdots,n-1$. *Notice that* $\boldsymbol{\Gamma}\left(0,s(t)\right)=\{0\}$, *which means that* $\boldsymbol{\Gamma}\left(\rho,s(t)\right)$ *is vanishing with respect to* ρ. *Furthermore, the following equalities hold:*

$$\begin{aligned}
\left(\lambda\rho\right)^{n+1}\left[-1,1\right] &= \lambda^{n+1}\rho^{n+1}\left[-1,1\right], \\
\frac{\left(\lambda\rho\right)^{n-i+1}}{(n-i+2)!}\left[-1,1\right] &= \lambda^{n-i+1}\frac{\rho^{n-i+1}}{(n-i+2)!}\left[-1,1\right], \\
\frac{\left(\lambda\rho\right)^{j-1}}{j!}\lambda^{n-i-j+2}s_{j+i-1}\left(t\right)\left[-1,1\right] &= \lambda^{n-i+1}\frac{\rho^{j-1}}{j!}s_{j+i-1}\left(t\right)\left[-1,1\right], \\
\frac{\left(\lambda\rho\right)^{j}}{(j+1)!}\frac{\Psi_{j+i-1,n}\left(\lambda^{n+1}s_0\left(t\right)\right)}{L^{\frac{j+i}{n+1}}}\left[-1,1\right] &= \lambda^{n-i+1}\frac{\rho^{j}}{(j+1)!}\frac{\Psi_{j+i-1,n}\left(s_0\left(t\right)\right)}{L^{\frac{j+i}{n+1}}}\left[-1,1\right].
\end{aligned} \tag{2.51}$$

Let $\rho\leq\widetilde{\rho}$, *the inequality* $\rho^{n+1}\leq\widetilde{\rho}^{n+1}$ *is obtained and therefore* $\rho^{n+1}\left[-1,1\right]\subset$

$\widetilde{\rho}^{n+1}[-1,1]$. *In a similar way the following relations are obtained:*

$$\begin{aligned}\frac{\rho^{n-i+1}}{(n-i+2)!}[-1,1] &\subset \frac{\widetilde{\rho}^{n-i+1}}{(n-i+2)!}[-1,1],\\ \frac{\rho^{j-1}}{j!}s_{j+i-1}(t)[-1,1] &\subset \frac{\widetilde{\rho}^{j-1}}{j!}s_{j+i-1}(t)[-1,1],\\ \frac{\rho^{j}}{(j+1)!}\frac{\Psi_{j+i-1,n}(s_0(t))}{L^{\frac{j+i}{n+1}}}[-1,1] &\subset \frac{\widetilde{\rho}^{j}}{(j+1)!}\frac{\Psi_{j+i-1,n}(s_0(t))}{L^{\frac{j+i}{n+1}}}[-1,1].\end{aligned} \tag{2.52}$$

As result of homogeneity property of $\Gamma_i(\rho,s)$*, it is Hausdorff-continous (for more details see [Livne & Levant 2014]). To investigate the stability properties of the solutions of* (2.49)*, one needs to study the properties of* $\boldsymbol{\Gamma}(\rho,\boldsymbol{s}(t))$*, which is considered as a disturbance. Using homogeneity properties and classical relations, it is straightforward to see that:*

- $\Gamma_i(\rho,\boldsymbol{s}(t))$ *is a set-valued function with non-empty compact values for* $\boldsymbol{s}(t)\in\mathbb{R}^{n+1}$ *and* $\rho\geq 0$*, for* $i=0,1,\cdots,n$*.*
- *The disturbance satisfies the homogeneity condition, for all* $\alpha,\rho\geq 0$*, for all* $\boldsymbol{s}(t)\in\mathbb{R}^{n+1}$*,* $\Gamma_i(\alpha^{-q}\rho,\boldsymbol{\Lambda_m}(\alpha)\boldsymbol{s}(t)) = \alpha^{n-i+1}\Gamma_i(\rho,\boldsymbol{s}(t))$ *with* $q=-1$ *and* $\Gamma_i(0,\boldsymbol{s}(t))=\{0\}$*.*
- $\Gamma_i(\rho,\boldsymbol{s}(t))$ *monotonously increases with respect to parameter* ρ *in the sense that for any* $\boldsymbol{s}(t)$ *the inequality* $0\leq\rho\leq\widetilde{\rho}$ *implies* $\boldsymbol{\Gamma}(\rho,\boldsymbol{s}(t))\subset\boldsymbol{\Gamma}(\widetilde{\rho},\boldsymbol{s}(t))$*.*
- $\Gamma_i(\rho,\boldsymbol{s}(t))$ *is Hausdorff-continuous in* ρ*,* $\boldsymbol{s}(t)$ *at the points with* $\rho=0$*. , i.e., for any* $e_i>0$ *there exists* $\widetilde{\rho}$ *such that if* $0\leq\rho\leq\widetilde{\rho}$*,* $||s(t)||\leq r$ *then the Hausdorff distance of the set from the origin satisfies* $d_{\mathrm{Hs}}(\Gamma_i(\rho,\boldsymbol{s}(t)),\{0\})\leq e_i$*.*

From inclusion (2.49)*, one can easily deduce the following properties:*

- *The set field* $\boldsymbol{C}(\boldsymbol{s},\boldsymbol{\Gamma}(\rho,\boldsymbol{s}))\subset\mathbb{R}^{n+1}$ *is a non-empty compact convex set valued function, upper-semicontinuous at all point* $(\boldsymbol{s},\boldsymbol{0})$*,* $\boldsymbol{s}\in\mathbb{R}^{n+1}$*,* $\boldsymbol{0}\in\mathbb{R}^{n+1}$*.*
- *The undisturbed inclusion* $\dot{\boldsymbol{s}}\in\boldsymbol{C}(s,\boldsymbol{0})$ *is finite-time stable and homogeneous of degree* $q=-1$*. The corresponding homogeneity dilation* $\boldsymbol{\Lambda_m}(\alpha)$*:* $(s_0,\ldots,s_n)\mapsto(\alpha^{m_0}s_0,\ldots,\alpha^{m_n}s_n)$ *defines the weights* $m_0,m_1,\ldots,m_{n-1},m_n>0$ *with* $m_i\geq 1$*.*
- $\boldsymbol{C}(\boldsymbol{s},\boldsymbol{\Gamma}(\rho,\boldsymbol{s}(t)))$ *is homogeneous with respect to the transformation* $(t,\boldsymbol{s},\boldsymbol{\Gamma}(\rho,\boldsymbol{s}(t)))\mapsto(\alpha^{-q}t,\boldsymbol{\Lambda_m}(\alpha)\boldsymbol{s},\boldsymbol{\Lambda_m}(\alpha)\boldsymbol{\Gamma}(\rho,\boldsymbol{s}(t)))$ *since* $\boldsymbol{C}(\boldsymbol{s},\boldsymbol{\Gamma}(\rho,\boldsymbol{s}(t))) = \alpha^{-q}\boldsymbol{\Lambda_m}^{-1}(\alpha)\boldsymbol{C}(\boldsymbol{\Lambda_m}(\alpha)\boldsymbol{s},\boldsymbol{\Lambda_m}(\alpha)\boldsymbol{\Gamma}(\rho,\boldsymbol{s}(t)))$*.*

Since the first sampling time is performed at $t_0=0$*, the dynamics of* (2.49) *is not affected by the state values for* $t<0$*. Under the above properties and Theorem 1.2.4, one can deduce that after a finite-time transient, all indefinitely extendable solutions of the perturbed differential inclusion* (2.49) *enter and remain inside the region* $|s_i(t)|\leq\mu_i\rho^{m_i}$ *with* $\mu_i>0$ *and* $\rho=\max\left\{\tau,\left(\frac{\delta}{L}\right)^{\frac{1}{n+1}}\right\}$*. This concludes the proof.*

From Theorem 2.3.1, one can see that the HEDD preserves the asymptotic accuracy of its continuous-time counterpart.

2.3.2 Stability Analysis for HIDD

Before analyzing the stability properties of the proposed implicit discrete-time differentiator (2.42), an implicit discrete-time error system is derived. $\varepsilon_{i,k}$ is defined as $\varepsilon_{i,k} = z_{i,k+1} - x_{i,k}$, for $i = 0, 1, 2, \cdots, n$. These variables allow to demonstrate the convergence of $z_{i,k+1}$ to a vicinity of $x_{i,k}$. If there is no estimation error on $\widetilde{\sigma}_{0,k+1}$ and no noise, one can obtain:

$$\begin{aligned}\boldsymbol{\varepsilon}_{0,k} = \sigma_{0,k} + \tau z_{1,k} + \frac{\tau^2}{2!} z_{2,k} + \cdots + \frac{\tau^n}{n!} z_{n,k} + \tau \Psi_{0,n}\left(\widetilde{\sigma}_{0,k+1}\right) + \ldots \\ \ldots + \frac{\tau^2}{2!} \Psi_{1,n}\left(\widetilde{\sigma}_{0,k+1}\right) + \cdots + \frac{\tau^{n+1}}{(n+1)!} \Psi_{n,n}\left(\widetilde{\sigma}_{0,k+1}\right).\end{aligned} \tag{2.53}$$

Comparing Equations (2.21) and (2.53), one can deduce that $\widetilde{\sigma}_{0,k+1} = \varepsilon_{0,k}$. To obtain the properties of HIDD for a noisy input, b_k^N is defined as $b_k^N = b_k + \Delta_k$, $\widetilde{\sigma}_{0,k+1}^N$ as:

$$\widetilde{\sigma}_{0,k+1}^N = \sigma_{0,k} - \Delta_k + \tau \Psi_{0,n}\left(\widetilde{\sigma}_{0,k+1}^N\right) + \sum_{l=1}^{n} \frac{\tau^l}{l!} \left(z_{l,k} + \frac{\tau}{l+1} \Psi_{l,n}\left(\widetilde{\sigma}_{0,k+1}^N\right)\right), \tag{2.54}$$

and $\xi_k^N \in \operatorname{sign}(\widetilde{\sigma}_{0,k+1}^N)$. b_k^N, $\widetilde{\sigma}_{0,k+1}^N$ and ξ_k^N are the counterpart of b_k, $\widetilde{\sigma}_{0,k+1}$ and ξ_k for a noisy input and without an estimation error of r_0. As there is no analytical equation for the roots, an interpolation method is used to estimate r_0 and an estimation error of r_0 could be present. Following a similar process applied to obtain Lemma 2.2, $\widetilde{\sigma}_{0,k+1}^N$ and ξ_k^N are computed as:

- If $b_k^N > a_0$, then $\xi_k^N = \{-1\}$ and $\widetilde{\sigma}_{0,k+1}^N = -\left(r_0^N\right)^{n+1} \in \mathbb{R}^-$, where r_0^N is the unique positive root of the following polynomial:
$$q(r) = r^{n+1} + a_n r^n + \cdots + a_1 r + \left(-b_k^N + a_0\right). \tag{2.55}$$
- If $b_k^N \in [-a_0, a_0]$, then $\widetilde{\sigma}_{0,k+1}^N = 0$ and $\xi_k^N = \left\{-\frac{b_k^N}{a_0}\right\}$.
- If $b_k^N < -a_0$, then $\xi_k^N = \{1\}$ and $\widetilde{\sigma}_{0,k+1}^N = \left(r_0^N\right)^{n+1} \in \mathbb{R}^+$, where r_0^N is the unique positive root of the following polynomial:
$$q(r) = r^{n+1} + a_n r^n + \cdots + a_1 r + \left(b_k^N + a_0\right). \tag{2.56}$$

One can mention that in the absence of noise, the polynomials (2.36) and (2.37) are the same as the polynomials (2.55) and (2.56). Note that if τ tends to zero, the roots of the polynomials (2.55) and (2.56) tend to $(\sigma_{0,k} - \Delta_k)^{\frac{1}{n+1}}$ and $(-\sigma_{0,k} + \Delta_k)^{\frac{1}{n+1}}$, respectively. In contrast, for the polynomials (2.36) and (2.37), its roots tend to $(\sigma_{0,k})^{\frac{1}{n+1}}$ and $(-\sigma_{0,k})^{\frac{1}{n+1}}$, therefore $\widetilde{\sigma}_{0,k+1}$ tends to $\sigma_{0,k}$. As there is no analytical expression for the roots r_0, in practice, they are estimated with an interpolation method. Therefore, the estimation of $\widetilde{\sigma}_{0,k+1}^N$ is estimated as follows:

$$\hat{\widetilde{\sigma}}_{0,k+1}^N = \begin{cases} -(\hat{r}_0^N)^{n+1} & \text{if} \quad b_k^N > a_0 \\ 0 & \text{if} \quad b_k^N \in [-a_0, a_0] \\ (\hat{r}_0^N)^{n+1} & \text{if} \quad b_k^N < -a_0 \end{cases}, \tag{2.57}$$

where $\hat{r}_0^N$ is the estimation of r_0^N. In a noise case and with an estimation error of r_0^N, $\hat{\tilde{\sigma}}_{0,k+1}^N$ and ξ_k^N are implemented in the implicit discrete-time realization (2.42) instead of $\tilde{\sigma}_{0,k+1}$ and ξ_k. Under these conditions, $\varepsilon_{0,k}$ becomes:

$$\varepsilon_{0,k} = \sigma_{0,k} - \Delta_k + \tau\Psi_{0,n}\left(\hat{\tilde{\sigma}}_{0,k+1}^N\right) + \sum_{l=1}^{n} \frac{\tau^l}{l!}\left(z_{l,k} + \frac{\tau}{l+1}\Psi_{l,n}\left(\hat{\tilde{\sigma}}_{0,k+1}^N\right)\right). \tag{2.58}$$

To determine the effect of the estimation error of r_0 and the measurement noise over the behavior of $\varepsilon_{i,k}$, the variable θ_k is introduced as $\theta_k = \varepsilon_{0,k} - \hat{\tilde{\sigma}}_{0,k+1}^N$, or equivalently as:

$$\theta_k = E_{1,k} + E_{2,k}, \tag{2.59}$$

which is constant during the time interval $[t_k, t_{k+1})$. Here, $E_{1,k}$, $E_{2,k}$ and $E_{3,k}$ are defined as:

$$\begin{aligned} E_{1,k} &= \tilde{\sigma}_{0,k+1}^N - \hat{\tilde{\sigma}}_{0,k+1}^N, \\ E_{2,k} &= \varepsilon_{0,k} - \tilde{\sigma}_{0,k+1}^N, \\ E_{3,k} &= r_0^N - \hat{r}_0^N. \end{aligned} \tag{2.60}$$

$E_{3,k}$ is the estimation error of the roots r_0^N, and it is considered equal to zero for $b_k^N \in [-a_0, a_0]$. $E_{3,k}$ depends on the implemented root-finding method, the initial condition of the estimate, τ and b_k^N. Nevertheless, if its estimation converges monotonically to r_0^N, and its initial condition belong to $\left[0, \left(b_k^N - a_0\right)^{1/(n+1)}\right]$ for $b_k^N > a_0$ and $\left[0, \left(-b_k^N - a_0\right)^{1/(n+1)}\right]$ for $b_k^N < -a_0$, then $\hat{r}_0^N > 0$ and $E_{3,k}$ is bounded with $|E_{3,k}| \leq \left(b_k^N - a_0\right)^{1/(n+1)}$ or $|E_{3,k}| \leq \left(-b_k^N - a_0\right)^{1/(n+1)}$, respectively. $E_{1,k}$ represents the estimation error of the variable $\tilde{\sigma}_{0,k+1}^N$ and it can be represented as:

$$E_{1,k} = \begin{cases} -(r_0^N)^{n+1} + (r_0^N - E_{3,k})^{n+1} & \text{if} \quad b_k^N > a_0 \\ 0 & \text{if} \quad b_k^N \in [-a_0, a_0] \\ (r_0^N)^{n+1} - (r_0^N - E_{3,k})^{n+1} & \text{if} \quad b_k^N < -a_0 \end{cases}, \tag{2.61}$$

whereas $E_{2,k}$ corresponds to the difference between $\varepsilon_{0,k}$ and $\tilde{\sigma}_{0,k+1}^N$ and it is given as:

$$E_{2,k} = \Delta_k + \sum_{l=0}^{n} -\frac{\tau^{l+1}}{(l+1)!}\lambda_{n-l} L^{\frac{l+1}{n+1}} \left(\left\lfloor \hat{\tilde{\sigma}}_{0,k+1}^N \right\rceil^{\frac{n-l}{n+1}} - \left\lfloor \tilde{\sigma}_{0,k+1}^N \right\rceil^{\frac{n-l}{n+1}} \right), \tag{2.62}$$

Note that the effect of $E_{3,k}$ over $E_{2,k}$ is attenuated by τ. Hence, due to the presence of measurement noise and numerical errors in the root-finding method, the following assumption is considered.

Assumption 2.3.1 *$\hat{r}_0^N > 0$ and $\theta(t)$ is a bounded noise with $|\theta(t)| \leq \kappa$ for all $t \geq 0$ and with an unknown real number $\kappa > 0$.*

As $\hat{r}_0^N > 0$, one can deduce that

$$\begin{aligned}
|E_{1,k}| &\leq |E_{3,k}| \left| e_1^n (r_0^N)^n + \cdots + e_n^n (E_{3,k})^{n-1} (r_0^N) + (E_{3,k})^n \right|, \\
|E_{2,k}| &\leq |\Delta_k| + \frac{\tau^n}{n!} \lambda_1 L^{\frac{n}{n+1}} |E_{3,k}| + \ldots \\
&\quad \ldots + \sum_{l=0}^{n-2} \frac{\tau^{l+1}}{(l+1)!} \lambda_{n-l} L^{\frac{l+1}{n+1}} |E_{3,k}| \left| e_1^{n-l-1} (r_0^N)^{n-l-1} + \ldots \right. \\
&\quad \left. \ldots + \cdots + e_{n-l-1}^{n-l-1} (E_{3,k})^{n-l-2} (r_0^N) + (E_{3,k})^{n-l-1} \right|,
\end{aligned} \tag{2.63}$$

where the constants e_j^n are the coefficients of the well-known Pascal's triangle with a respective change of sign, i.e., $e_j^n = (-1)^j \frac{(n+1)!}{j!(n-j+1)!}$. In equation (2.63), $r_0^N = 0$ for $b_k^N \in [-a_0, a_0]$.

Remark 2.3.1 *Clearly, if $E_{3,k} = 0$ for all $t \geq 0$, then $E_{1,k} = 0$, $E_{2,k} = \theta_k = \Delta_k$ and Assumption 2.3.1 is fulfilled. The above is satisfied if $b_k \in [-a_0, a_0]$ for all $t \geq 0$. Due to Equation (2.60), there is not a $\kappa > 0$ such that the Assumption 2.3.1 is satisfied for all $\tau > 0$, $\delta > 0$, $z_{1,k}, z_{2,k}, \ldots, z_{n,k}, \sigma_{0,k}, E_{3,k} \in \mathbb{R}$. However, from the continuity of the right-hand side of (2.63) with respect to $E_{3,k}$, one can deduce the following fact. For any r_0 and $\kappa \geq \delta$, there is a maximum tolerable error $M_{E_{3,k}} \geq 0$ such that $|\theta_k| \leq \kappa$ if $|E_{3,k}| \leq M_{E_{3,k}}$. It justifies Assumption 2.3.1.*

Under Assumption 2.3.1, $\xi_k^N \in \operatorname{sign}(\hat{\tilde{\sigma}}_{0,k+1}^N)$. It comes from the fact that $\hat{r}_0^N > 0$ and therefore the sign of $\tilde{\sigma}_{k+1}^N$ depends on b_k^N and a_0, in the same way that $\tilde{\sigma}_{0,k+1}^N$. As $\hat{\tilde{\sigma}}_{0,k+1}^N$ is implemented instead of $\tilde{\sigma}_{0,k+1}$, $\boldsymbol{v}\left(\tilde{\sigma}_{0,k+1}\right)$ in the discrete-time system (2.42) becomes $\boldsymbol{v}\left(\hat{\tilde{\sigma}}_{0,k+1}^N\right)$, where $\boldsymbol{v}(\cdot)$ is defined in Equation (2.42). Due to Equations (2.59) and (2.60), and the discrete-time systems (2.1) and (2.42), $\boldsymbol{\sigma}_{k+1}$ is expressed as:

$$\boldsymbol{\sigma}_{k+1} = \boldsymbol{\Phi}(\tau)\, \boldsymbol{\sigma}_k + \boldsymbol{B}^*(\tau)\, \boldsymbol{v}(\varepsilon_{0,k} - \theta_k) - \boldsymbol{h}_k(\tau). \tag{2.64}$$

Defining $\boldsymbol{\varepsilon} = [\varepsilon_{0,k}\ \varepsilon_{1,k}\ \ldots\ \varepsilon_{n,k}]^T$ the following equations are obtained:

$$\begin{aligned}
\boldsymbol{\varepsilon}_k &= (\boldsymbol{\Phi}(\tau) - \boldsymbol{I})\boldsymbol{z}_k + \boldsymbol{B}^*(\tau)\, \boldsymbol{v}(\varepsilon_{0,k} - \theta_k) + \boldsymbol{\sigma}_k, \\
\boldsymbol{\varepsilon}_k &= \boldsymbol{\Phi}(\tau)\, \boldsymbol{\sigma}_k + \boldsymbol{B}^*(\tau)\, \boldsymbol{v}(\varepsilon_{0,k} - \theta_k) + (\boldsymbol{\Phi}(\tau) - \boldsymbol{I})\, \boldsymbol{x}_k.
\end{aligned} \tag{2.65}$$

The above equations can be rewritten as:

$$\begin{aligned}
\boldsymbol{\varepsilon}_{k+1} &= (\boldsymbol{\Phi}(\tau) - \boldsymbol{I})\boldsymbol{z}_{k+1} + \boldsymbol{B}^*(\tau)\, \boldsymbol{v}(\varepsilon_{0,k+1} - \theta_{k+1}) + \boldsymbol{\sigma}_{k+1}, \\
\boldsymbol{\varepsilon}_k - (\boldsymbol{\Phi}(\tau) - \boldsymbol{I})\, \boldsymbol{x}_k &= \boldsymbol{\Phi}(\tau)\, \boldsymbol{\sigma}_k + \boldsymbol{B}^*(\tau)\, \boldsymbol{v}(\varepsilon_{0,k} - \theta_k).
\end{aligned} \tag{2.66}$$

Equations (2.64) and (2.66) yield:

$$\begin{aligned}
\boldsymbol{\varepsilon}_{k+1} &= (\boldsymbol{\Phi}(\tau) - \boldsymbol{I})\boldsymbol{z}_{k+1} + \boldsymbol{B}^*(\tau)\, \boldsymbol{v}(\varepsilon_{0,k+1} - \theta_{k+1}) + \boldsymbol{\Phi}(\tau)\, \boldsymbol{\sigma}_k + \ldots \\
&\quad \ldots + \boldsymbol{B}^*(\tau)\, \boldsymbol{v}(\varepsilon_{0,k} - \theta_k) - \boldsymbol{h}_k(\tau), \\
&= (\boldsymbol{\Phi}(\tau) - \boldsymbol{I})\boldsymbol{z}_{k+1} + \boldsymbol{B}^*(\tau)\, \boldsymbol{v}(\varepsilon_{0,k+1} - \theta_{k+1}) + \boldsymbol{\varepsilon}_k - \ldots \\
&\quad \ldots - (\boldsymbol{\Phi}(\tau) - \boldsymbol{I})\, \boldsymbol{x}_k - \boldsymbol{h}_k(\tau), \\
&= (\boldsymbol{\Phi}(\tau) - \boldsymbol{I})\boldsymbol{\varepsilon}_k + \boldsymbol{B}^*(\tau)\, \boldsymbol{v}(\varepsilon_{0,k+1} - \theta_{k+1}) + \boldsymbol{\varepsilon}_k - \boldsymbol{h}_k(\tau), \\
&= \boldsymbol{\Phi}(\tau)\, \boldsymbol{\varepsilon}_k + \boldsymbol{B}^*(\tau)\, \boldsymbol{v}(\varepsilon_{0,k+1} - \theta_{k+1}) - \boldsymbol{h}_k(\tau).
\end{aligned} \tag{2.67}$$

Therefore, under Assumptions 1.3.1, 1.3.2, 1.3.4, 2.1.1 and 2.3.1, the error system using the proposed implicit discrete-time differentiator (2.42) is represented as:

$$\begin{aligned}
&\boldsymbol{\varepsilon}_{k+1} = \boldsymbol{\Phi}(\tau)\,\boldsymbol{\varepsilon}_k + \boldsymbol{B}^*(\tau)\,\boldsymbol{v}(\varepsilon_{0,k+1} - \theta_{k+1}) - \boldsymbol{h}_k(\tau),\\
&\boldsymbol{v}(\varepsilon_{0,k+1} - \theta_{k+1}) = \left[\Psi_{0,n}(\varepsilon_{0,k+1} - \theta_{k+1}) \;\cdots\; \Psi_{n,n}(\varepsilon_{0,k+1} - \theta_{k+1})\right]^T,\\
&\Psi_{i,n}(\varepsilon_{0,k+1} - \theta_{k+1}) = -\lambda_{n-i} L^{\frac{i+1}{n+1}} |\varepsilon_{0,k+1} - \theta_{k+1}|^{\frac{n-i}{n+1}}\, \xi^N_{k+1},\\
&\xi^N_{k+1} \in \operatorname{sign}(\varepsilon_{0,k+1} - \theta_{k+1}).
\end{aligned} \tag{2.68}$$

This form will be useful to study the stability properties under the discrete-time differentiator (2.42). Note that θ_{k+1} is considered as the measurement noise for the discrete-time error system (2.68). Similarly to (2.10), as $\theta_{k+1} \in [-\kappa, \kappa]$ and $f_0^{(n+1)}(t) \in [-L, L]$, the estimation error dynamics can be expressed as the following inclusion:

$$\begin{aligned}
\boldsymbol{\varepsilon}_{k+1} \in &\boldsymbol{\Phi}(\tau)\,\boldsymbol{\varepsilon}_k + \boldsymbol{B}^*(\tau)\,\boldsymbol{v}(\varepsilon_{0,k+1} + [-\kappa, \kappa]) + \ldots\\
&\ldots + \left[\frac{\tau^{n+1}}{(n+1)!}[-L, L] \quad \frac{\tau^n}{n!}[-L, L] \quad \cdots \quad \tau[-L, L]\right]^T.
\end{aligned} \tag{2.69}$$

Lemma 2.3 *The system (2.69) is homogeneous with respect to the transformation* $(\tau, \kappa, \varepsilon_0, \ldots, \varepsilon_n) \mapsto (\alpha\tau, \alpha^{n+1}\kappa, \alpha^{n+1}\varepsilon_0, \ldots, \alpha\varepsilon_n)$*, for all* $\alpha \in \mathbb{R}^+$.

Proof *The proof is omitted since it is similar to that of Lemma 2.1.*

Remark 2.3.2 *System (2.69) preserves the homogeneity degrees of the differential inclusion (1.68), i.e.,* $\deg(\bar{\sigma}_i) = \deg(\varepsilon_{i,k}) = m_i$ *and* $\deg(t) = \deg(\tau) = 1$*. However, it is not homogeneous with respect to the transformation* $(\tau, \delta, \sigma_0, \ldots, \sigma_n) \mapsto (\alpha\tau, \alpha^{n+1}\delta, \alpha^{n+1}\sigma_0, \ldots, \alpha\sigma_n)$.

It is important to mention that system (2.69) describes the behavior of $\widetilde{\sigma}^N_{0,k+1}$, which matches with the results presented in Lemma 2.2. Indeed, from the system (2.69), one obtains

$$\varepsilon_{0,k+1} = -h_{0,k} + \sum_{l=0}^{n} \frac{\tau^l}{l!}\varepsilon_{l,k} + \frac{\tau^{l+1}}{(l+1)!}\Psi_{l,n}(\varepsilon_{0,k+1} - \theta_{k+1}). \tag{2.70}$$

Subtracting $E_{2,k+1}$ the following equations are obtained:

$$\begin{aligned}
\varepsilon_{0,k+1} - E_{2,k+1} &= -E_{2,k+1} - h_{0,k} + \sum_{l=0}^{n} \frac{\tau^l}{l!}\varepsilon_{l,k} + \frac{\tau^{l+1}}{(l+1)!}\Psi_{l,n}\left(\hat{\widetilde{\sigma}}^N_{0,k+2}\right),\\
\widetilde{\sigma}^N_{0,k+2} &= -\Delta_{k+1} - h_{0,k} + \sum_{l=0}^{n} \frac{\tau^l}{l!}\varepsilon_{l,k} + \frac{\tau^{l+1}}{(l+1)!}\Psi_{l,n}\left(\widetilde{\sigma}^N_{0,k+2}\right).
\end{aligned} \tag{2.71}$$

Let $\bar{b}^N_{k+1} = \Delta_{k+1} + h_{0,k} - \sum_{l=0}^{n} \frac{\tau^l}{l!}\varepsilon_{l,k}$. Taking into account that $\varepsilon_{l,k} = z_{l,k+1} - x_{l,k}$, then $\bar{b}^N_{k+1}$ can be expressed as:

$$\bar{b}^N_{k+1} = \Delta_{k+1} + h_{0,k} + \sum_{l=0}^{n} \frac{\tau^l}{l!}x_{l,k} - \sum_{l=0}^{n} \frac{\tau^l}{l!}z_{l,k+1} = \Delta_{k+1} - \sigma_{0,k+1} - \sum_{l=1}^{n} \frac{\tau^l}{l!}z_{l,k+1} = b^N_{k+1}. \tag{2.72}$$

Then, $\widetilde{\sigma}^N_{0,k+2}$ can be expressed as:

$$\widetilde{\sigma}^N_{0,k+2} = -b^N_{k+1} + \sum_{l=0}^{n} \frac{\tau^{l+1}}{(l+1)!} \Psi_{l,n} \left(\widetilde{\sigma}^N_{0,k+2} \right). \tag{2.73}$$

Under Assumption 2.3.1, $\xi^N_{k+1} \in \operatorname{sign}(\widetilde{\sigma}^N_{0,k+2})$. Similar to Lemma 2.2, one obtains that the behavior of $\widetilde{\sigma}^N_{0,k+2}$ and ξ^N_{k+1} are given as:

- If $b^N_{k+1} > a_0$, then $\xi^N_{k+1} = \{-1\}$ and $\widetilde{\sigma}^N_{0,k+2} = -\left(r^N_0\right)^{n+1} \in \mathbb{R}^-$, where r^N_0 is the unique positive root of the following polynomial:

$$q(r) = r^{n+1} + a_n r^n + \cdots + a_1 r + \left(-b^N_{k+1} + a_0 \right). \tag{2.74}$$

- If $b^N_{k+1} \in [-a_0, a_0]$, then $\widetilde{\sigma}^N_{0,k+2} = 0$ and $\xi^N_{k+1} = \left\{ -\frac{b^N_{k+1}}{a_0} \right\}$.

- If $b^N_{k+1} < -a_0$, then $\xi^N_{k+1} = \{1\}$ and $\widetilde{\sigma}^N_{0,k+2} = \left(r^N_0\right)^{n+1} \in \mathbb{R}^+$, where r^N_0 is the unique positive root of the following polynomial:

$$q(r) = r^{n+1} + a_n r^n + \cdots + a_1 r + \left(b^N_{k+1} + a_0 \right). \tag{2.75}$$

Now, the following theorem will establish the stability properties of the implicit discrete-time differentiator.

Theorem 2.3.2

Let $\boldsymbol{z}_k$ be generated with the implicit discrete-time differentiator (2.42) and the parameters $\lambda_0, \ldots, \lambda_n$ be such that the inclusion (1.68) is finite-time stable. Under Assumptions 1.3.1, 1.3.2, 1.3.4, 2.1.1 and 2.3.1, there exist constants $\mu_i > 0$, $i = 0, 1, 2, \cdots, n$ such that after a finite-time transient, the following inequalities are fulfilled:

$$\begin{aligned} &|z_{i,k+1} - x_{i,k}| \leq \mu_i L \rho^{n+1-i}, \\ &\rho = \max\left\{ \tau, \left(\frac{\kappa}{L} \right)^{\frac{1}{n+1}} \right\}, \end{aligned} \tag{2.76}$$

where the coefficients μ_i only depend on the differentiator parameters $\lambda_0, \ldots, \lambda_n$.

Proof *Using HIDD, the estimation error dynamics can be obtained from Equation (2.68):*

$$\begin{aligned} \varepsilon_{i,k+1} \in{}& \varepsilon_{i,k} + \tau \Psi_{i,n} \left(\varepsilon_{0,k} + [-\kappa, \kappa] \right) + \frac{\tau^{n-i+1}}{(n-i+1)!} [-L, L] + \ldots \\ &\ldots + \sum_{j=1}^{n-i} \frac{\tau^j}{j!} \varepsilon_{j+i,k} + \frac{\tau^{j+1}}{(j+1)!} \Psi_{j+i,n} \left(\varepsilon_{0,k+1} + [-\kappa, \kappa] \right), \\ \varepsilon_{n,k+1} \in{}& \varepsilon_{n,k} + \tau \Psi_{n,n} \left(\varepsilon_{0,k+1} + [-\kappa, \kappa] \right) + \tau [-L, L], \end{aligned} \tag{2.77}$$

with $i = 0, 1, \ldots, n$. *By defining* $\bar{\varepsilon}_{i,k} = \varepsilon_{i,k}/L$, *the inclusion* (2.77) *can be rewritten as:*

$$\begin{aligned}
\bar{\varepsilon}_{i,k+1} \in \bar{\varepsilon}_{i,k} + \tau \frac{\Psi_{i,n}\left(\bar{\varepsilon}_{0,k+1} + \left[-\frac{\kappa}{L}, \frac{\kappa}{L}\right]\right)}{L^{\frac{i+1}{n+1}}} + \frac{\tau^{n-i+1}}{(n-i+1)!}[-1,1] + \ldots \\
\ldots + \sum_{j=1}^{n-i} \frac{\tau^j}{j!}\bar{\varepsilon}_{j+i,k} + \frac{\tau^{j+1}}{(j+1)!}\frac{\Psi_{j+i,n}\left(\bar{\varepsilon}_{0,k+1} + \left[-\frac{\kappa}{L}, \frac{\kappa}{L}\right]\right)}{L^{\frac{j+i+1}{n+1}}}, \\
\bar{\varepsilon}_{n,k+1} \in \bar{\varepsilon}_{n,k} + \tau \frac{\Psi_{n,n}\left(\bar{\varepsilon}_{0,k+1} + \left[-\frac{\kappa}{L}, \frac{\kappa}{L}\right]\right)}{L} + \tau[-1,1].
\end{aligned} \tag{2.78}$$

As in the proof of Theorem 2.3.1, the piecewise linear continuous function $\boldsymbol{s}(t) = [s_0(t) \;\; s_1(t) \;\; \cdots \;\; s_n(t)]^T$ *is defined such that* $\boldsymbol{s}(t)$ *describes the solution of* (2.78) *(with* $\boldsymbol{s}_k = \boldsymbol{s}(t_k) = \bar{\varepsilon}(t_k)$*), i.e.,*

$$\begin{aligned}
\boldsymbol{s}(t) &= \boldsymbol{s}_k + (t - t_k)\boldsymbol{w}_k, \\
\boldsymbol{w}_k &\in \boldsymbol{G}(s_{0,k+1}, \boldsymbol{s}_k, \tau),
\end{aligned} \tag{2.79}$$

with $\boldsymbol{G}(s_{0,k+1}, \boldsymbol{s}_k, \tau) = [G_0(s_{0,k+1}, \boldsymbol{s}_k, \tau) \;\; G_1(s_{0,k+1}, \boldsymbol{s}_k, \tau) \;\; \cdots \;\; G_n(s_{0,k+1}, \boldsymbol{s}_k, \tau)]^T$, *and* $t \in [t_k, t_{k+1})$

$$\begin{aligned}
G_i(s_{0,k+1}, \boldsymbol{s}_k, \tau) = \frac{\Psi_{i,n}\left(s_{0,k+1} + \left[-\frac{\kappa}{L}, \frac{\kappa}{L}\right]\right)}{L^{\frac{i+1}{n+1}}} + \frac{\tau^{n-i}}{(n-i+1)!}[-1,1] \ldots \\
\ldots + \sum_{j=1}^{n-i} \frac{\tau^{j-1}}{j!}s_{j+i,k} + \frac{\tau^j}{(j+1)!}\frac{\Psi_{j+i,n}\left(s_{0,k+1} + \left[-\frac{\kappa}{L}, \frac{\kappa}{L}\right]\right)}{L^{\frac{j+i+1}{n+1}}}, \\
G_n(s_{0,k+1}, \boldsymbol{s}_k, \tau) = \frac{\Psi_{n,n}\left(s_{0,k+1} + \left[-\frac{\kappa}{L}, \frac{\kappa}{L}\right]\right)}{L} + [-1,1].
\end{aligned}$$

Let the disturbance intensity ρ *be defined as* $\rho = \max\left\{\tau, (\kappa/L)^{\frac{1}{n+1}}\right\}$, *then any solution of* (2.79) *almost everywhere satisfies the differential inclusion* (2.49). *Hence, one can apply similar arguments as the proof of Theorem 2.3.1 to conclude the proof.*

From Theorem 2.3.2, one can see that the HIDD preserves the asymptotic accuracy as its continuous-time counterpart, if $E_{3,k} = 0$. It becomes optimal for $\tau = 0$ and $E_{3,k} = 0$. From the definition of b_k^N, θ_k and Equation (2.58):

$$b_k^N = -\varepsilon_{0,k} + \sum_{l=0}^{n} \frac{\tau^{l+1}}{(l+1)!}\Psi_{l,n}(\varepsilon_{0,k} - \theta_k). \tag{2.80}$$

Note that the right-hand side of the following inclusion is homogeneous with respect to the transformation $(\tau, \kappa, \varepsilon_0, \ldots, \varepsilon_n) \mapsto (\alpha\tau, \alpha^{n+1}\kappa, \alpha^{n+1}\varepsilon_0, \ldots, \alpha\varepsilon_n)$, for all $\alpha \in \mathbb{R}^+$.

$$b_k^N \in -\varepsilon_{0,k} + \sum_{l=0}^{n} \frac{\tau^{l+1}}{(l+1)!}\Psi_{l,n}(\varepsilon_{0,k} + [-\kappa, \kappa]). \tag{2.81}$$

Equation (2.80) and the results of Theorem 2.3.2 allow deducing that after the finite-time transient mentioned in Theorem 2.3.2, b_k^N is bounded. Therefore, after this finite-time transient, r_0 is bounded. Furthermore, from the above fact and as

$b_k^N = -\sigma_{0,k} + \sum_{l=1}^{n} \frac{\tau^l}{l!} z_{l,k}$, one can deduce that $\sigma_{0,k}$ almost compensates $\sum_{l=1}^{n} \frac{\tau^l}{l!} z_{l,k}$ after the finite-time transient. Moreover, in the ideal case, the generalized equation (2.22) becomes:

$$\varepsilon_{0,k} + a_n \lfloor \varepsilon_{0,k} \rceil^{\frac{n}{n+1}} + a_{n-1} \lfloor \varepsilon_{0,k} \rceil^{\frac{n-1}{n+1}} + \cdots + a_1 \lfloor \varepsilon_{0,k} \rceil^{\frac{1}{n+1}} + b_k \in -a_0 \text{sign}(\varepsilon_{0,k}), \quad (2.82)$$

and both sides of inclusion (2.82) are homogeneous with respect to the transformation $(\tau, \varepsilon_0, \ldots, \varepsilon_n) \mapsto (\alpha\tau, \alpha^{n+1}\varepsilon_0, \ldots, \alpha\varepsilon_n)$, for all $\alpha \in \mathbb{R}^+$.

Remark 2.3.3 *It is important to note that for HEDD $\boldsymbol{z}_k$ estimates $\boldsymbol{x}_k$, whereas for HIDD $\boldsymbol{z}_{k+1}$ estimates $\boldsymbol{x}_k$. Therefore, $\varepsilon_{i,k}$ is the estimation error between $z_{i,k+1}$ and $x_{i,k}$ at time t_k. Nevertheless, $z_{i,k+1}$ is available at time t_k plus the time required to compute $z_{i,k+1}$. On the other hand, as $\sigma_{0,k}$ almost compensates $\sum_{l=1}^{n} \frac{\tau^l}{l!} z_{l,k}$, it could tend to infinity for signals with unbounded derivatives. However, Theorem 2.3.2 implies, under its respective assumptions, that $\varepsilon_{i,k}$ converges to a vicinity defined by (2.76).*

Remark 2.3.4 *If there exists a known constant $m > n$ such that $|f_0^{(m+1)}(t)| \leq L$, then a better accuracy can be obtained using a differentiator of order m (instead of n) for both HEDD and HIDD, i.e., $|z_{i,k} - x_{i,k}| \leq \mu_i L \rho^{m+1-i}$ ($|z_{i,k+1} - x_{i,k}| \leq \mu_i L \rho^{m+1-i}$).*

2.4 Toward an efficient implementation of the implicit differentiator

Recall that there is no analytical expression for the roots of polynomials of high degree and since the implicit differentiator requires to calculate the roots of a polynomial, an adequate root finding method is needed. After selecting an adequate root finding method in Subsection 2.4.1, methods to reduce time complexity of HIDD are studied in Subsection 2.4.2.

2.4.1 Interpolation methods

As it is mentioned previously, since there is no analytical expression for the roots of polynomials of high degree, a root-finding method is needed to implement the implicit differentiator. Here, the following interpolation methods are considered: the modified Newton-Raphson method [McDougall & Wotherspoon 2014], the Euler's method [Melman 1997] and the Halley's method [Scavo & Thoo 1995]. It is important to mention that the secant method was avoided because it can diverge. The above depends on the initial condition used. Hereafter, the order of convergence is used to compare the convergence rate of the interpolation methods [Varona 2002, Weerakoon & Fernando 2000], as described in the following definition.

Definition 2.1 *[Weerakoon & Fernando 2000] Let $r_0 \in \mathbb{R}$ the root of a polynomial, $r_{0,j} \in \mathbb{R}$ the estimation of r_0 at iteration j, $j = 0, 1, 2, \cdots$. A sequence $\{r_{0,j}\}$ is said to converge to r_0 if*

$$\lim_{j \to \infty} |r_{0,j} - r_0| = 0. \quad (2.83)$$

If, in addition, there exist a constant $c \geq 0$*, an integer* $j_0 \geq 0$ *and* $d \geq 0$ *such that for all* $j > j_0$

$$|r_{0,j+1} - r_0| \leq c\,|r_{0,j} - r_0|^d\,, \tag{2.84}$$

then $\{r_{0,j}\}$ *is said to converge to* r_0 *with q-order at least d. If* $d = 2$ *or* 3*, the convergence is said to be q-quadratic or q-cubic, respectively.*

The modified Newton-Raphson method is an iteration function with an order of convergence $1+\sqrt{2}$, which uses the same number of derivatives and function evaluations as the Newton-Raphson method (with an order of convergence 2). Since the Euler's method needs the calculation of a square root at each iteration, and Halley's method presents an order of convergence 3, Euler's method is not implemented. The modified Newton-Raphson and Halley's methods were experimentally tested to find the positive root of the polynomial (2.37). Here, the following parameters are considered $\tau = 0.1$, $n = 3$, $\lambda_0 = 1.1$, $\lambda_1 = 3.06$, $\lambda_2 = 4.16$, $\lambda_3 = 3$, $L = 2$, $b_k = -a_0 - 0.1$ and an initial condition $r_{0,0} = -(a_0 + b_k)/2$. The modified Halley's method reaches an absolute error estimate less than 1.111×10^{-16} after 6 iterations, while this accuracy is obtained with the modified Newton-Raphson method after 16 iterations, as shown in Figures 2.2-2.3. It can be seen a significant increase in the estimation error when $j = 1$. To avoid the above behavior for the Halley's method, the following lemma is used.

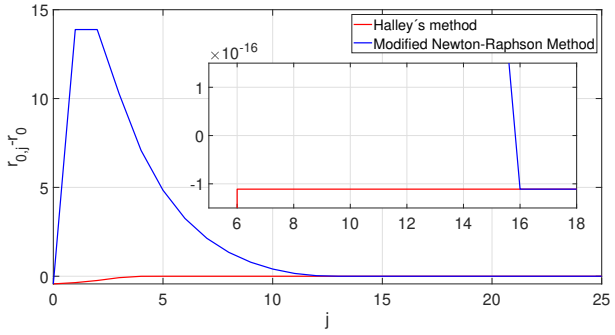

Figure 2.2: Roots obtained with two different interpolation methods.

Lemma 2.4 *[Melman 1997] Let* $\frac{d^3p(r)}{dr^3}$ *be continuous,* $\frac{dp(r)}{dr} \neq 0$*, and* $\frac{d^2\left((\eta\frac{dp(r)}{dr})^{-1/2}\right)}{dr^2} \geq 0$ *on an interval* J *containing the root* r_0 *of* $p(r)$ *with* $\eta = sign(\frac{dp(r)}{dr})$*. Then, the Halley's method [Scavo & Thoo 1995] converges monotonically to* r_0 *from any point in* J *using the following formula:*

$$r_{0,j+1} = r_{0,j} - \frac{2\frac{dp(r)}{dr}|_{r=r_{0,j}}p(r_{0,j})}{2(\frac{dp(r)}{dr}|_{r=r_{0,j}})^2 - \frac{d^2p(r)}{dr^2}|_{r=r_{0,j}}p(r_{0,j})} \tag{2.85}$$

As $\frac{dp(r)}{dr} > 0$ for polynomials (2.36) and (2.37) on the intervals $J = \left[0, (b_k - a_0)^{\frac{1}{n+1}}\right]$ and $J = \left[0, (-b_k - a_0)^{\frac{1}{n+1}}\right]$ respectively, then $\eta = 1$. Therefore,

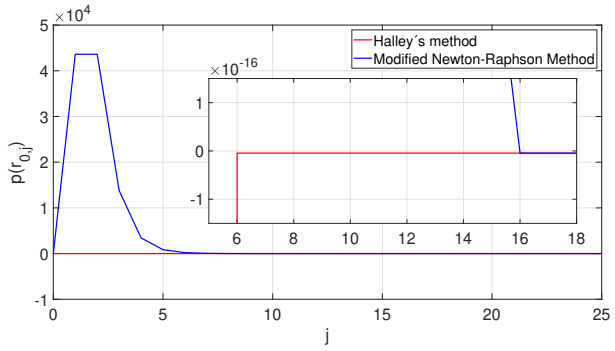

Figure 2.3: Evaluation of the polynomial using the estimated roots using two different interpolation methods.

the condition $\frac{d^2\left((\eta\frac{dp(r)}{dr})^{-1/2}\right)}{dr^2} \geq 0$ is equivalent to:

$$\left(\frac{3}{2}\left(\frac{d^2p(r)}{dr^2}\right)^2 - \frac{dp(r)}{dr}\frac{d^3p(r)}{dr^3}\right) \geq 0. \tag{2.86}$$

For $n < 8$, the above condition is invariant with respect to τ and L for polynomials (2.36) and (2.37). For the parameter λ_i given in [Levant 2018], condition (2.86) is fulfilled. Furthermore, for simple roots, the Halley's method is a third-order method [Scavo & Thoo 1995, McNamee & Pan 2013], which implies that:

$$|r_{0,j+1} - r_0| \leq c\,|r_{0,j} - r_0|^3\,, \tag{2.87}$$

with an error constant given as follows:

$$c = \frac{3\left(\frac{d^2p(r)}{dr^2}|_{r=r_0}\right)^2 - 2\frac{dp(r)}{dr}|_{r=r_0}\frac{d^3p(r)}{dr^3}|_{r=r_0}}{12\left(\frac{dp(r)}{dr}|_{r=r_0}\right)^2}. \tag{2.88}$$

2.4.2 Methodologies to reduce the time complexity

Here, we analyse the time complexity of the implicit differentiator in order to find an efficient way for its implementation, the results in this subsection were published in [Carvajal-Rubio *et al.* 2021b]. In specific, in this subsection the time complexity of HIDD will be reduced. First, the variables ϕ_i and $\bar{b}^*_{i,j}$ are defined as:

$$\begin{aligned}\phi_i &= \frac{\tau^{i-1}}{(i-1)!},\\ \bar{b}^*_{i,j} &= \frac{\tau^{j+1-i}}{(j+1-i)!}\lambda_{n-j+1}L^{\frac{j}{n+1}},\end{aligned} \tag{2.89}$$

for $i = 1, 2, \cdots, n+1$ and $j = i, i+1, i+2, \cdots, n+1$. It allows to rewrite (2.42) as follows:

- If $b_k > a_0$,

$$\begin{aligned} z_{i,k+1} &= z_{i,k} + \bar{b}^*_{i+1,i+1} r_0^{n-i} + \dots \\ &\quad \dots + \sum_{j=i+1}^{n} \phi_{j-i+1} z_{j,k} + \bar{b}^*_{i+1,j+1} r_0^{n-j}, \\ i &= 0, 1, \cdots, n. \end{aligned} \tag{2.90}$$

- If $b_k \in [-a_0, a_0]$,

$$\begin{aligned} z_{0,k+1} &= z_{0,k} + b_k + \sum_{j=1}^{n} \phi_{j+1} z_{j,k}, \\ z_{i,k+1} &= z_{i,k} + \bar{b}^*_{i+1,n+1} \left(\frac{b_k}{a_0} \right) + \sum_{j=i+1}^{n} \phi_{j-i+1} z_{j,k}, \\ i &= 1, 2, \cdots, n. \end{aligned} \tag{2.91}$$

- If $b_k < -a_0$,

$$\begin{aligned} z_{i,k+1} &= z_{i,k} - \bar{b}^*_{i+1,i+1} r_0^{n-i} + \dots \\ &\quad \dots + \sum_{j=i+1}^{n} \phi_{j-i+1} z_{j,k} - \bar{b}^*_{i+1,j+1} r_0^{n-j}, \\ i &= 0, 1, \cdots, n. \end{aligned} \tag{2.92}$$

Direct Evaluation

The number of additions and subtractions, N_{A1}, and the number of multiplications and divisions, N_{M1}, needed to evaluate $z_{0,k+1}$, $z_{1,k+1}$, $z_{0,k+1}$ and $z_{n,k+1}$ directly, after obtaining r_0, are as follows:

$$\begin{aligned} N_{A1}(n) &= (n+1)^2, \\ N_{M1}(n) &= \frac{n^3}{6} + n^2 - \frac{1}{6} n - 1. \end{aligned} \tag{2.93}$$

Therefore, taking into account the $(n+1)$ assignments of the states $z_{i,k+1}$, the time complexity is given as:

$$T_1(n) = \frac{n^3}{6} + 2n^2 + \frac{17}{6} n + 1, \tag{2.94}$$

which is a cubic time. On the other hand, the Halley's method is used recursively at each iteration. To evaluate the derivatives, one could store the following variables to reduce the number of operations,

$$\begin{aligned} c_{n+1} &= n+1, \\ c_i &= i a_i, \qquad \text{for } \; i = 1, 2, \cdots, n, \\ d_{n+1} &= n(n+1), \\ d_i &= i(i-1) a_i, \quad \text{for } \; i = 2, 3, \cdots, n. \end{aligned} \tag{2.95}$$

Furthermore, $\bar{j}$ is defined as the number of iterations used to estimate r_0. Then the number of additions, subtractions, multiplications and divisions used to evaluate the polynomials and its derivatives are given as:

$$\begin{aligned} N_{A2}(n) &= \bar{j}\,(3n+1)\,, \\ N_{M2}(n) &= \bar{j}\left(\frac{3}{2}n^2+\frac{3}{2}n\right). \end{aligned} \tag{2.96}$$

In the following, we consider that $\bar{j}=3$. Therefore, taking into account the value assignments, the evaluation of (2.85) yields to the time complexity

$$T_2(n)=\frac{9}{2}n^2+\frac{27}{2}n+46. \tag{2.97}$$

where one of the operations is a $(n+1)$-th root and a for-loop is considered. Hence, the complexity of the algorithm is cubic and is defined as:

$$T(n)=\frac{n^3}{6}+\frac{13}{2}n^2+\frac{110}{6}n+48. \tag{2.98}$$

where the multiplications and subtraction needed to evaluate $b_k$are taken into account. It is important to note that time complexity (2.98) is defined for $b_k \notin [-a_0, a_0]$.

Horner Method

Although the use of variables ϕ_i, $\bar{b}^*_{i,j}$, c_i, d_i reduces the number of basic operations, it does not reduce the time complexity of the discrete-time realization (2.42) with respect to n. Based on the Horner's method, one could calculate $z_{i,k+1}$ as follows:

- If $b_k > a_0$

$$\begin{aligned} z_{i,k+1} &= z_{i,k}+\sum_{j=i+1}^{n}\phi_{j-i+1}z_{j,k}+\dots \\ &\dots+(\cdots((\bar{b}^*_{i+1,i+1})r_0+\bar{b}^*_{i+1,i+2})\cdots)r_0+\bar{b}^*_{i+1,n+1}. \\ &i=0,1,\cdots,n. \end{aligned} \tag{2.99}$$

- If $b_k < -a_0$

$$\begin{aligned} z_{i,k+1} &= z_{i,k}+\sum_{j=i+1}^{n}\phi_{j-i+1}z_{j,k}-\dots \\ &\dots-(\cdots((\bar{b}^*_{i+1,i+1})r_0+\bar{b}^*_{i+1,i+2})\cdots)r_0-\bar{b}^*_{i+1,n+1}. \\ &i=0,1,\cdots,n. \end{aligned} \tag{2.100}$$

This methodology presents the following number of basic operations:

$$\begin{aligned} N_{A3}(n) &= (n+1)^2, \\ N_{M3}(n) &= n(n+1). \end{aligned} \tag{2.101}$$

As $\boldsymbol{\Phi}(\tau)$ and $\boldsymbol{B}(\tau)$ are Toeplitz matrices [Bai *et al.* 2000], the time complexity to evaluate $z_{i,k+1}$ could be reduce to a linearithmic one ($n \log n$) using the discrete Fourier transform. This alternative could be analyzed in the future. To evaluate the polynomials and its derivatives, n is considered greater than one. In the following, two methodologies based on Horner's method are analyzed. The first one is based on the evaluation of the polynomials and its derivatives as follows:

$$\begin{aligned} p\left(r\right) &= (\cdots((r+a_n)r+a_{n-1})\cdots)r+a_0 \pm b_k, \\ \frac{dp(r)}{dr} &= (\cdots((c_{n+1}r+c_n)r+c_{n-1})\cdots)r+c_1, \\ \frac{d^2p(r)}{dr^2} &= (\cdots((d_{n+1}r+d_n)r+d_{n-1})\cdots)r+d_2. \end{aligned} \tag{2.102}$$

The methodology (2.102) needs the following number of basic operations:

$$\begin{aligned} N_{A4}(n) &= \bar{j}\left(3n+1\right), \\ N_{M4}(n) &= \bar{j}\left(3n-1\right). \end{aligned} \tag{2.103}$$

Similar to (2.97), one obtains:

$$T_4(n) = 18n + 43. \tag{2.104}$$

However, one could take advantage of the evaluation of $p(r)$ to evaluate $\frac{dp(r)}{dr}$ and $\frac{d^2p(r)}{dr^2}$ with the following methodology for $n \geq 2$:

$$\begin{aligned} F_{i+1} &= rF_i + a_{n-i-1}, \\ dF_{i+1} &= rdF_i + F_{i+1}, \\ ddF_{i+1} &= rddF_i + dF_{i+1}, \end{aligned} \tag{2.105}$$

for $i = 0, \cdots, n-3$, with $F_0 = r + a_n$, $dF_0 = r + F_0$, $ddF_0 = r + dF_0$. Using these variables, one gets:

$$\begin{aligned} F_{n-1} &= rF_{n-2} + a_1, \\ p(r) &= rF_{n-1} + a_0 \pm b_k, \\ \frac{dp(r)}{dr} &= rdF_{n-2} + F_{n-1}, \\ \frac{d^2p(r)}{dr^2} &= 2ddF_{n-2}. \end{aligned} \tag{2.106}$$

It increases the number of assignments and additions but reduces the number of multiplications. Therefore, one obtains the following time complexity:

$$T_5(n) = 36n + 55. \tag{2.107}$$

Using the methodologies (2.99), (2.100) and (2.102) a quadratic time complexity is obtained, i.e.

$$T(n) = 2n^2 + 24n + 46. \tag{2.108}$$

If (2.106) is used instead of (2.102), the quadratic time complexity is given as:

$$T(n) = 2n^2 + 42n + 58. \tag{2.109}$$

Shaw–Traub Algorithm

Similar to the methodology (2.106), an algorithm was proposed in [Shaw & Traub 1974] to compute the normalized derivatives, $\frac{1}{i!}\frac{d^i p(r)}{dr^i}$. Note that the Horner's method is a special case of this algorithm. It allows to reduce the number of multiplications while increasing the number of divisions, assignments and additions. In the following, a modified algorithm which relies on the Shaw–Traub algorithm is described:

$$\begin{aligned}
&t_1 = r, \;\; t_i = t_{i-1} r, \;\; \text{for} \;\; i = 2, 3, \cdots, n; \\
&T_i^{-1} = a_{n-i} t_{n-i}, \;\; \text{for} \;\; i = 0, 1, \cdots, n-1; \\
&T_n^{-1} = a_0 \pm b_k, \\
&T_0^0 = t_n r, \;\; T_1^1 = T_0^0, \;\; T_2^2 = T_0^0; \\
&T_i^j = T_{i-1}^{j-1} + T_{i-1}^j, \;\; \text{for} \;\; j = 0, 1, 2; \; i = j+1, \cdots, n+1; \\
&p(r) = T_{n+1}^0, \;\; \frac{dp(r)}{dr} = \frac{T_{n+1}^1}{t_1}, \;\; \frac{d^2 p(r)}{dr^2} = 2\frac{T_{n+1}^2}{t_2}.
\end{aligned} \tag{2.110}$$

Since $T_0^0 = T_1^1 = T_2^2$, two assignments could be avoided if T_0^0 is used instead of T_1^1 and T_2^2. Then, algorithm (2.110) presents a linear time complexity given as:

$$T_6(n) = 30n + 70. \tag{2.111}$$

Applying the algorithms (2.99), (2.100) and (2.110), HIDD presents a quadratic time complexity, given as:

$$T(n) = 2n^2 + 36n + 74. \tag{2.112}$$

It is important to mention that in [Shaw & Traub 1975], the best parameters for the family of algorithms presented in [Shaw & Traub 1974] were founded. Then, the time complexity (2.112) could be reduced tuning its parameters but not its order. As the Halley's method does not use higher-order derivatives, we do not consider the algorithm presented in [De Jong & Van Leeuwen 1975], which improves the algorithm proposed in [Shaw & Traub 1974] for the $n+1$ normalized derivatives.

2.4.3 Simulation results using the interpolation methods in terms of complexity

In this subsection, we only focus on the complexity analysis for the proposed algorithms. Hereafter, two numerical studies are presented. The first one corresponds to a comparison of the number of required basic operations for each algorithm. The second one is a comparison of the computing time for the four methodologies proposed in this work. The methodology given by (2.85), (2.90), (2.91), (2.92) and a direct evaluation of the polynomials is referenced as direct evaluation, the methodology given by (2.85), (2.91) (2.99), (2.100) and (2.102) is referenced as half-Horner algorithm, the methodology given by (2.85), (2.91), (2.99), (2.100) and (2.106) is referenced as full-Horner algorithm and (2.85), (2.91), (2.99), (2.100) and (2.110) is referenced as Shaw-Traub algorithm.

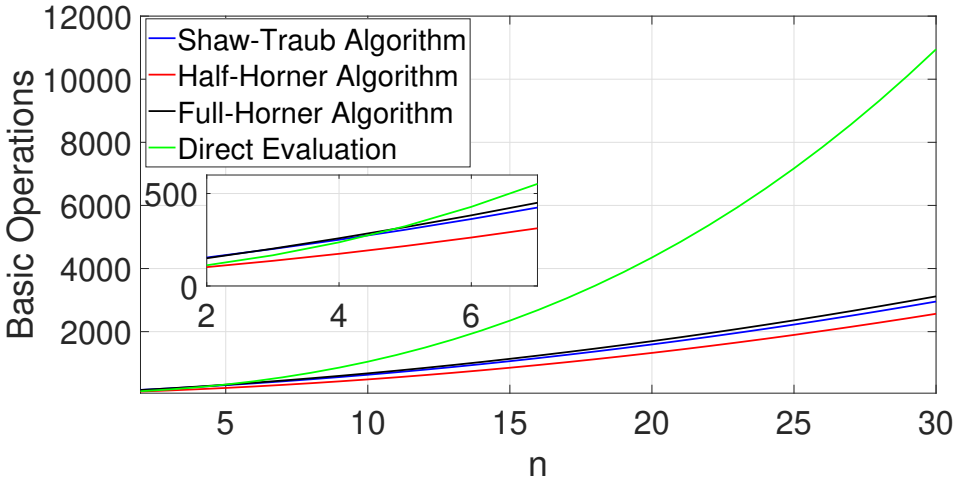

Figure 2.4: Comparison of the number of required basic operations for each algorithm.

Simulation 1

The time complexity of the different methodologies are evaluated for $2 \leq n \leq 30$. The results are presented in Figure 2.4. One can see that the algorithm with less basic operations is the half-Horner algorithm. Furthermore , the Shaw-Traub and full-Horner algorithms have less basic operations than the direct evaluation for $n > 4$. It is important to highlight the huge difference between the direct evaluation and the other algorithms for a large value of n.

Simulation 2

Now, the time complexity of the algorithms are compared. Furthermore, an algorithm which does not use the parameters defined in Equations (2.89) and (2.95) is simulated. It is similar as the direct evaluation without the parameters ϕ_i, $\bar{b}^*_{i,j}$, c_i and d_i. In the following, $n = 3$, $n = 7$ and $n = 10$ are considered. The noisy signal and the constants defined in (2.89) and (2.95) are computed offline. The sampling time is selected as $\tau = 0.001\,\text{sec}$ and the simulated time is selected as $t = 2000,\ 10000,\ 25000,\ 50000\,\text{sec}$. Simulations are performed using MATLAB, with a computer processing unit Intel Core i7-9750H and RAM memory of 8GB. The results are presented in Tables 2.1-2.3. The most efficient methods with respect to the computing time are the half-Horner and full-Horner algorithms. They both present a similar performance for $n = 3$, $n = 7$ and $n = 10$. They reduce the computing time more than 25 times for $n = 10$ as seen in Table 2.3. For $n = 3$, the direct evaluation has a better performance than the Shaw-Traub algorithm whereas for $n = 10$, the Shaw-Traub algorithm reduces the computing time compared to the direct evaluation. The above facts match with the computed time complexity.

	2000 sec	10000 sec	25000 sec	50000 sec
Evaluation without ϕ_i, $\bar{b}^*_{i,j}$, c_i and d_i	0.5963 sec	2.990 sec	7.470 sec	15.059 sec
Direct Evaluation	0.3578 sec	1.783 sec	4.475 sec	9.027 sec
Half-Horner	0.3494 sec	1.753 sec	4.411 sec	8.896 sec
Full-Horner	0.3496 sec	1.756 sec	4.407 sec	8.908 sec
Shaw-Traub	0.3852 sec	1.922 sec	4.813 sec	9.661 sec

Table 2.1: Computing time of the algorithms for $n = 3$ and $\tau = 0.001$ sec.

	2000 sec	10000 sec	25000 sec	50000 sec
Evaluation without ϕ_i, $\bar{b}^*_{i,j}$, c_i and d_i	6.791 sec	33.808 sec	85.045 sec	169.95 sec
Direct Evaluation	0.486 sec	2.414 sec	6.035 sec	12.51 sec
Half-Horner	0.466 sec	2.286 sec	5.729 sec	11.61 sec
Full-Horner	0.457 sec	2.293 sec	5.763 sec	11.51 sec
Shaw-Traub	0.503 sec	2.46 sec	6.210 sec	12.718 sec

Table 2.2: Computing time of the algorithms for $n = 7$ and $\tau = 0.001$ sec.

	2000 sec	10000 sec	25000 sec	50000 sec
Evaluation without ϕ_i, $\bar{b}^*_{i,j}$, c_i and d_i	14.312 sec	71.6 sec	179.37 sec	358.09 sec
Direct Evaluation	0.831 sec	4.192 sec	10.33 sec	20.527 sec
Half-Horner	0.5437 sec	2.75 sec	6.858 sec	13.692 sec
Full-Horner	0.5631 sec	2.807 sec	6.997 sec	14.139 sec
Shaw-Traub	0.6101 sec	3.097 sec	7.767 sec	15.464 sec

Table 2.3: Computing time of the algorithms for $n = 10$ and $\tau = 0.001$ sec.

From the above results, the Half-Horner method is used in the next subsection.

2.5 Comparative simulation results between the proposed discrete-time differentiators and existing ones

This section aims to show a comparison study between the proposed HEDD, HIDD, and other existing discrete-time differentiators. The first one is the HDD, given in eq. (1.81), which preserves the asymptotic accuracy. The second one is the GHDD,

given in eq. (1.87), which also preserves the asymptotic accuracy. The last one is the Matching differentiator, given in eq. (1.84), which uses a nonlinear eigenvalue placement. Although it preserves the asymptotic accuracy for the noise-free case and is insensitive to an overestimation of L, a convergence proof has not been investigated in the presence of noise.

In the following simulations, $\sigma_{i,k}$ is used for HEDD, HDD, GHDD, and Matching, whereas $\varepsilon_{i,k}$ is used for HIDD because for the first differentiators $\boldsymbol{z}_k$ gives an estimate of $\boldsymbol{x}_k$ whereas for HIDD $z_{i,k+1}$ gives an estimate of $x_{i,k}$. To compare these differentiators, indexes Y_i and y_i are proposed, i.e., the maximum absolute error (MAE)

$$\begin{aligned} Y_i &= \max\left\{|\sigma_{i,k}| \in \mathbb{R} | t_{min} \leq t_k \leq t_{max}\right\}, \\ Y_i &= \max\left\{|\varepsilon_{i,k}| \in \mathbb{R} | t_{min} \leq t_k \leq t_{max}\right\}, \end{aligned} \tag{2.113}$$

while y_i is the root mean square error (RMSE), which is given as:

$$y_i = \sqrt{\sum_{l=k_{\min}}^{k_{\max}} \frac{(\sigma_{i,l})^2}{k_{\max} - k_{\min} + 1}}, \tag{2.114}$$

or for HIDD

$$y_i = \sqrt{\sum_{l=k_{\min}}^{k_{\max}} \frac{(\varepsilon_{i,l})^2}{k_{\max} - k_{\min} + 1}}, \tag{2.115}$$

where $\tau k_{\max} = t_{\max}$ and $\tau k_{\min} = 10\,\text{sec}$.

From the results presented in Subsection 2.4.1, the Halley's method [Scavo & Thoo 1995] is used as an iteration function to implement the HIDD. Furthermore, $r_{0,k}$ is calculated recursively using only 3 iterations, with initial conditions $r_{0,0} = ((b_k - a_0)/2)^{1/(n+1)}$ and $r_{0,0} = ((-b_k - a_0)/2)^{1/(n+1)}$ for Cases 1 and 3, respectively.

2.5.1 Simulation I: Noise-free case

This simulation shows the performance of the five previously mentioned differentiators in a noise-free case with a constant sampling time $\tau = 0.1\,\text{sec}$. The noise-free signal is $f_0(t) = \sin(t) - \cos(0.5t)$ for $t \in [0\,\text{sec}, 80\,\text{sec}]$. Here and in the following simulations, the functions $f_0^{(i)}(t)$ are calculated analytically. For the differentiator, the parameters are $n = 3$, $L = 2$, $\lambda_0 = 1.1$, $\lambda_1 = 3.06$, $\lambda_2 = 4.16$, $\lambda_3 = 3$, $p_0 = -1.15849269 + 0.56444913i$, $p_1 = -1.15849269 - 0.56444913i$, $p_2 = -0.6253073 + 0.96639542i$, and $p_3 = -0.6253073 - 0.96639542i$, where p_i are the poles assigned for the Matching differentiator [Koch & Reichhartinger 2018]. Here, the previous p_i are used because it allows to perform a fair comparison. The initial condition for each differentiator is $\boldsymbol{z}_0 = [0, 0, 0, 0]^T$.

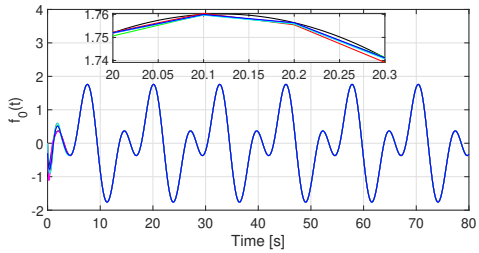

(a) Estimation of the signal.

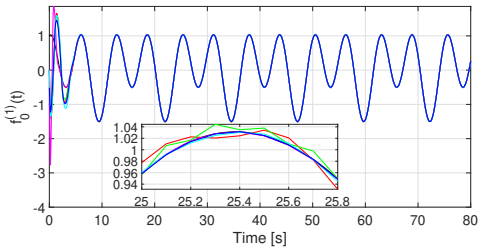

(b) Estimation of the first derivative.

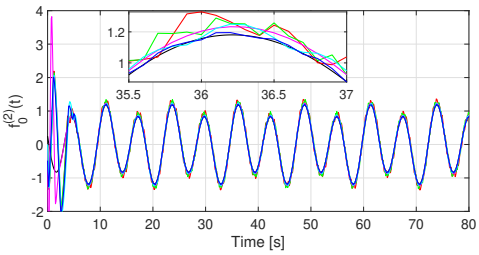

(c) Estimation of the second derivative.

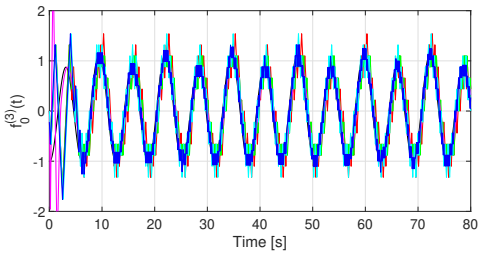

(d) Estimation of the third derivative.

Figure 2.5: Estimation of $f_0(t)$ and its first 3 derivatives, where the functions are shown with a black line, HIDD with a blue line, HEDD with a green line, HDD with a red line, GHDD with a cyan line and Matching with a magenta line.

The corresponding results are presented in Figures 2.5a-2.5d. Here, the discrete-time differentiator errors converge to a vicinity of the origin at a similar time. This can be better seen in Figures 2.6a-2.6d.

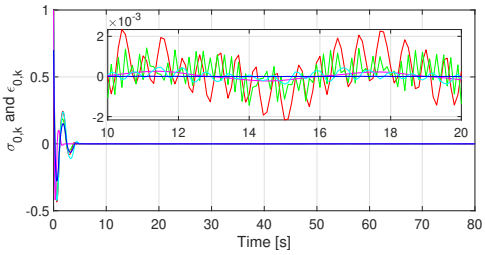

(a) Estimation error of the signal.

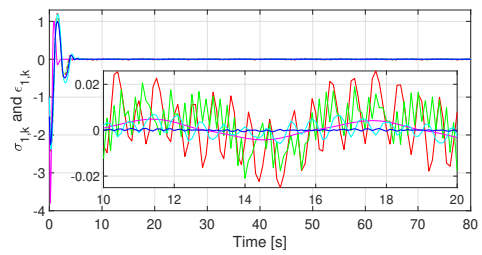

(b) Estimation error of the first derivative.

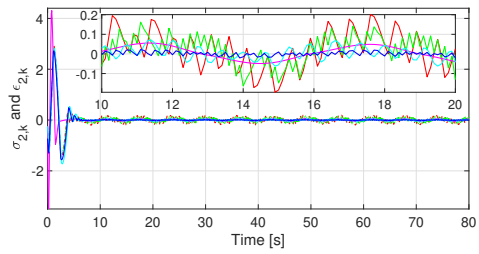

(c) Estimation error of the second derivative.

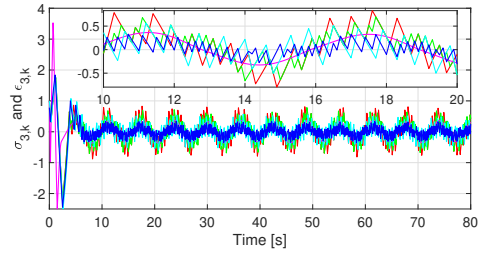

(d) Estimation error of the third derivative.

Figure 2.6: Estimation error of the signal and its first 3 derivatives (HIDD blue line, HEDD green line, HDD red line, GHDD cyan line, Matching magenta line)

Table 2.4 presents a numerical comparison. Here, the smallest maximum absolute error and RMSE are the metrics in consideration. Each column shows the results of those two error metrics for the HIDD, HEDD, HDD, GHDD, and the matching pole method. For this case, HIDD presents the best performance, except for the last time derivative. Moreover, HEDD presents better results than those obtained using the HDD. Nevertheless, GHDD enables to obtain better results than HEDD.

	HIDD	**HEDD**	**HDD**	**GHDD**	**Matching**
Y_0	1.23×10^{-5}	1.51×10^{-3}	2.34×10^{-3}	5.73×10^{-4}	2×10^{-3}
Y_1	9.16×10^{-4}	2.13×10^{-2}	2.582×10^{-2}	8.51×10^{-3}	2.28×10^{-2}
Y_2	2.25×10^{-2}	0.17	0.21	8.06×10^{-2}	0.15
Y_3	0.351	0.79	0.83	0.6	0.54
y_0	3.91×10^{-6}	7.39×10^{-4}	1.03×10^{-3}	2.06×10^{-4}	9.8×10^{-4}
y_1	3.59×10^{-4}	1.01×10^{-2}	1.23×10^{-2}	3.27×10^{-3}	1.18×10^{-2}
y_2	1.09×10^{-2}	7.78×10^{-2}	9.2×10^{-2}	3.44×10^{-2}	8.24×10^{-2}
y_3	0.15	0.33	0.37	0.24	0.34

Table 2.4: Indexes Y_i and y_i for each discrete-time differentiator.

2.5.2 Simulation II: Noise-free case with different sampling times

To show the asymptotic accuracy of the differentiators in the noise-free case, it is performed a sequence of simulations with $f_0(t) = \sin(t) - \cos(0.5t)$ under different sampling times $\tau \in [0.00001\,\text{sec}, 1\,\text{sec}]$, logarithmically spaced points were used, 50 for each figure. For each simulation, the maximum absolute error is computed while considering τ as constant. The parameters λ_i, L, n, p_i and initial conditions $\boldsymbol{z}_0$ are the same as in Simulation I. Here, $t_{max} = 50\,\text{sec}$. The corresponding results are depicted in Figures 2.7a-2.7d.

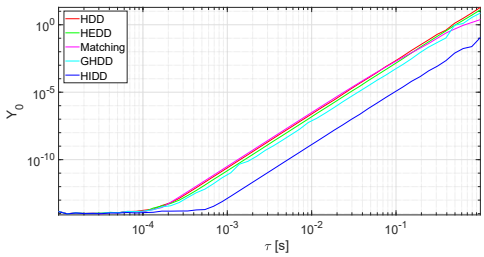

(a) Maximum absolute error for the signal.

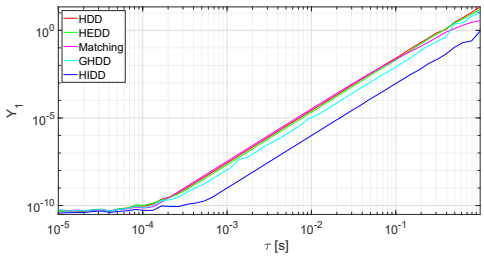

(b) Maximum absolute error for the first derivative.

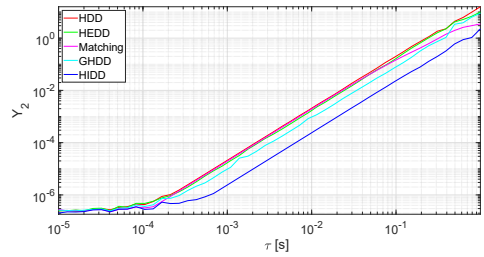

(c) Maximum absolute error for the second derivative.

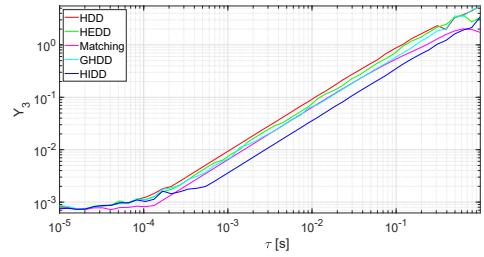

(d) Maximum absolute error for the third derivative.

Figure 2.7: Maximum absolute error of the discrete-time differentiators for each estimation under different sampling times.

For a sampling time in $[0.0007\,\text{sec}, 1\,\text{sec}]$, a reduction of the sampling time corresponds to a reduction of Y_i for each differentiator, as it can be seen from the asymptotic accuracy. Furthermore, the smallest Y_0, Y_1, Y_2 are obtained using HIDD for almost each sampling time. Concerning Y_3, for $\tau \in [0.0003\,\text{sec}, 0.65\,\text{sec}]$, the smallest value is obtained using HIDD, whereas for $\tau > 0.7\,\text{sec}$ and $\tau \in [0.00002\,\text{sec}, 0.0002\,\text{sec}]$, it is obtained with the Matching approach. One can note that for the function and its first two derivatives, one can obtain with HIDD and a given sampling time a similar accuracy as the one obtained using other differentiators with a lower sampling time. Finally, below $\tau = 0.0001\,\text{sec}$, a similar accuracy is obtained using any differentiator. Moreover, a sampling time lower than $0.0001\,\text{sec}$ does not present a significant improvement in terms of accuracy of the differentiators due to the accuracy of the class double from MATLAB.

2.5.3 Simulation III: Differentiation with measurement noise and different sampling times

Here, the performance of the differentiators with measurement noise and under different sampling times is studied. The parameters, initial conditions, and $f_0(t)$ are the same as in the previous subsection. The noise is given as $\Delta(t) \sim$ i.i.d. $\mathcal{N}(0, 0.01^2)$. This simulation is performed as in Simulation II, i.e., the maximum absolute error Y_i is computed for each sampling time. The corresponding results are shown in Figures 2.8a-2.8d. It can be seen that the discrete-time differentiators present asymptotic accuracy. As in the previous simulation, they present a similar Y_i for $\tau < 0.01\,\text{sec}$. For

$f_0(t)$, its first two derivatives, and $\tau > 0.003\,\text{sec}$, the best performance is obtained using HIDD.

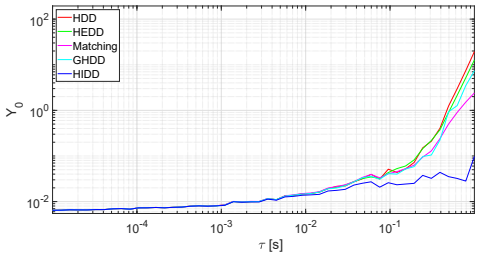

(a) Maximum absolute error of the signal.

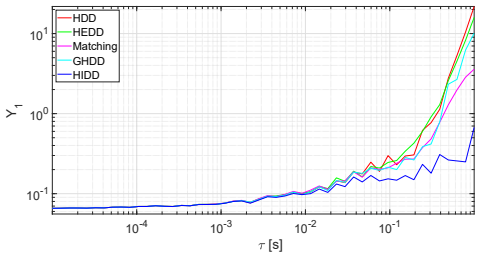

(b) Maximum absolute error of the first derivative.

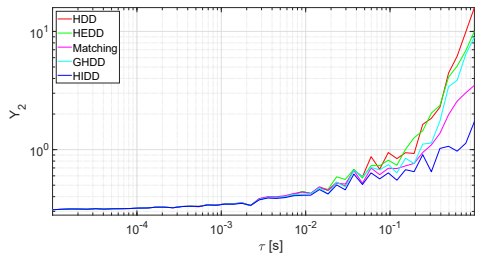

(c) Maximum absolute error of the second derivative.

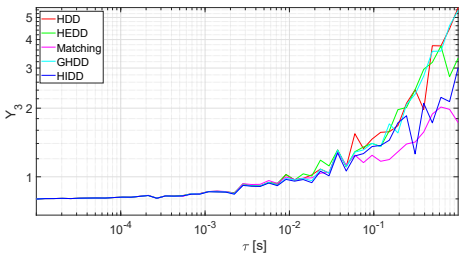

(d) Maximum absolute error of the third derivative.

Figure 2.8: Maximum absolute errors vs sampling time.

2.6 Conclusion

In this Chapter, we have introduced and analyzed two discrete-time realizations of the homogeneous differentiator, i.e. an explicit and an implicit one, namely HEDD and HIDD. They are based on the methodology used to obtain an exact discretization of linear systems with a zero-order hold. It was shown that the error dynamics of both discrete-time differentiators are homogeneous to their respective transformations, and they preserve the accuracy of their continuous-time counterparts after a finite time. An implementation strategy was proposed for the implicit discrete-time realization, which is non-anticipative and includes a root-finding method based on Halley's method. Different methodologies were also discussed to obtain an efficient implementation, in terms of time complexity, of the implicit discrete-time differentiator which rely on the Horner's method and the Shaw-Traub algorithm. Simulation results using the proposed interpolation methods were carried out to show a noticeable improvement compared to a direct implementation. At last, a detailed comparative study with HDD (1.81), GHDD (1.87) and Matching differentiator (1.84) was performed in simulation. It was shown that HIDD exhibits the best performance for a free-noise case and in the presence of noise. Furthermore, HIDD supersedes HEDD, consistent with the implicit and explicit time discretization of other continuous-time systems.

In the next Chapter, we will investigate the discrete-time realization of the fil-

tering differentiator to improve the performances in terms of rejection of the effects of large measurement noises.

CHAPTER 3

Explicit and implicit discretizations of the filtering differentiator

3.1 Introduction

As discussed in the previous Chapter, it is of paramount importance to be able to differentiate a noisy signal. Recently, in [Levant & Livne 2019], a continuous-time filtering differentiator (a sliding mode differentiator coupled to a filter) has been investigated to improve the accuracy compared with the standard one (discussed in the previous Chapter), under a specific class of noises. Mainly, for bounded noises, it presents the same accuracy as the standard one. In contrast to the standard differentiator, the robust exact filtering differentiator rejects the effects of some large noises after a finite time. Furthermore, this differentiator can filter out unbounded noises composed of signals of global filtering order $j \in \mathbb{N}$, where j is less than or equal to the filtering order of the differentiator.

As for the homogeneous differentiator, a discrete-time version of the robust exact filtering differentiator is needed for the implementation on a digital device. For instance, the discrete-time filtering differentiator, proposed in [Levant & Livne 2019], corresponds to an Euler discretization with Taylor-like terms for the states that estimate the signal derivatives. Similarly, the scheme presented in [Hanan *et al.* 2020] preserves the accuracy of the filtering differentiator. Furthermore, in the absence of noise, with an overestimated value of the Lipschitz constant of the n-th derivative of a signal and using enough large algorithm parameters, it presents the same properties as with the non-overestimated value of the Lipschitz constant of its n-th derivative.

The main contribution of this Chapter is to derive and study novel explicit and implicit realizations for the continuous-time robust exact filtering differentiator [Levant & Livne 2019]. First, a time discretization of the robust exact filtering differentiator based on the Matching approach is investigated. It relies on the stabilization of a pseudo linear discrete-time system. Then, an explicit discrete-time filtering differentiator, based on the exact discretization of linear systems with a zero-order holder, is introduced. However, the presence of high-order terms in the filter dynamics may cause instability of the estimation error for signals with unbounded derivatives. Hence,

a modified explicit discrete-time filtering differentiator is proposed, aiming to remove such a drawback of the exact discretization. Based on this scheme, an implicit version is derived. It will shown, using the homogeneity property, that after a finite time, the explicit and implicit discrete-time filtering differentiators preserve the accuracy of the continuous-time one despite the presence of measurement noise. Finally, some simulation results include comparisons between the proposed implicit and explicit discrete-time realizations with other existing schemes, highlighting that the implicit scheme supersedes the explicit one.

3.2 Discretization of the Robust Exact Filtering Differentiator Based on the Matching Approach

In this section, a differentiator is proposed using the differentiator (1.69) and the methodology proposed in [Koch & Reichhartinger 2018]. The results in section were published in [Carvajal-Rubio *et al.* 2020a]. As in [Koch & Reichhartinger 2018], for a free-noise case ($\Delta(t) = 0$), the error system can be given as a pseudo linear system [Ghane & Menhaj 2013]:

$$\begin{aligned}
\begin{bmatrix} \dot{\boldsymbol{w}} \\ \dot{\boldsymbol{\sigma}} \end{bmatrix} &= \boldsymbol{E} \begin{bmatrix} \boldsymbol{w} \\ \boldsymbol{\sigma} \end{bmatrix} - \boldsymbol{e}_{m+1} f_0^{(n+1)}(t), \\
\boldsymbol{E} &= \begin{bmatrix}
-\lambda_m L^{\frac{1}{m+1}} |w_1|^{\frac{-1}{m+1}} & 1 & 0 & \cdots & 0 \\
-\lambda_{m-1} L^{\frac{2}{m+1}} |w_1|^{\frac{-2}{m+1}} & 0 & 1 & \cdots & 0 \\
\vdots & \vdots & \vdots & \cdots & \vdots \\
-\lambda_1 L^{\frac{m}{m+1}} |w_1|^{\frac{-m}{m+1}} & 0 & 0 & \cdots & 1 \\
-\lambda_0 L |w_1|^{-1} & 0 & 0 & \cdots & 0
\end{bmatrix},
\end{aligned} \tag{3.1}$$

where $\boldsymbol{E} \in \mathbb{R}^{(m+1)\times(m+1)}$, $\boldsymbol{w} = \begin{bmatrix} w_1 & w_2 & \cdots & w_{n_f} \end{bmatrix}^T$ and $\boldsymbol{\sigma} = [\sigma_0 \ \sigma_1 \ \cdots \ \sigma_n]^T$. The characteristic equation of $\boldsymbol{E}$ is $P(s) = s^{m+1} + \lambda_m L^{\frac{1}{m+1}} |w_1|^{\frac{-1}{m+1}} s^m + \lambda_{m-1} L^{\frac{2}{m+1}} |w_1|^{\frac{-2}{m+1}} s^{m-1} + \cdots + \lambda_0 L |w_1|^{-1}$. Its roots can be calculated by using the equation:

$$\left(|w_1|^{\frac{1}{m+1}} s \right)^{m+1} + \lambda_m L^{\frac{1}{m+1}} \left(|w_1|^{\frac{1}{m+1}} s \right)^m + \cdots + \lambda_0 L = 0. \tag{3.2}$$

Therefore, the $m+1$ roots s_j of (3.2) can be calculated from the following polynomial:

$$Q(b) = b^{m+1} + \lambda_m L^{\frac{1}{m+1}} b^m + \cdots + \lambda_0 L. \tag{3.3}$$

Then, s_j is calculated as $s_j = |w_1|^{\frac{-1}{m+1}} b_j$, where b_j corresponds to the roots of polynomial (3.3).

Now, $z_{j,k+1}$ is proposed as a copy of $x_{j,k+1}$ in the discrete-time system (2.1) with an injection term $\Gamma_{j+n_f+1,k} w_{1,k}$:

$$\begin{aligned}
z_{j,k+1} &= \sum_{l=j}^{n} \frac{\tau^{l-j}}{(l-j)!} z_{l,k} + \Gamma_{j+n_f+1,k} w_{1,k}, \\
j &= 0, 1, 2, \cdots, n.
\end{aligned} \tag{3.4}$$

Obviously, $h_{j,k}(\tau)$ in (2.4), is omitted because it is not available. Please note that $\Gamma_{j+n_f+1,k}$ will be defined later. Based on Euler discretization, $w_{j,k+1}$ is proposed as:

$$\begin{aligned} w_{j,k+1} &= w_{j,k} + \tau w_{j+1,k} + \Gamma_{j,k} w_{1,k}, \\ w_{n_f,k+1} &= w_{n_f,k} + \tau(z_{0,k} - f(t)) + \Gamma_{n_f,k} w_{1,k}, \\ j &= 1, 2, \cdots, n_f - 1. \end{aligned} \tag{3.5}$$

Using equations (3.4)-(3.5), the discrete-time differentiator is summarized as:

$$\begin{bmatrix} \boldsymbol{w}_{k+1} \\ \boldsymbol{z}_{k+1} \end{bmatrix} = \boldsymbol{\Sigma}(\tau) \begin{bmatrix} \boldsymbol{w}_k \\ \boldsymbol{z}_k \end{bmatrix} - \tau \boldsymbol{e}_{n_f,m} f(t) + \boldsymbol{\Gamma}_k w_{1,k}, \tag{3.6}$$

where $\boldsymbol{w}_k = \begin{bmatrix} w_{1,k} & w_{2,k} & \cdots & w_{n_f,k} \end{bmatrix}^T$, $\boldsymbol{z}_k = \begin{bmatrix} z_{0,k} & z_{1,k} & \cdots & z_{n,k} \end{bmatrix}^T$, $\boldsymbol{\Gamma}_k = \begin{bmatrix} \Gamma_{1,k} & \Gamma_{1,k} & \cdots & \Gamma_{m+1,k} \end{bmatrix}^T$, $\boldsymbol{\Sigma}(\tau)$ is given as:

$$\boldsymbol{\Sigma}(\tau) = \begin{bmatrix} 1 & \tau & 0 & \cdots & 0 & 0 & 0 & 0 & \cdots & 0 \\ 0 & 1 & \tau & \cdots & 0 & 0 & 0 & 0 & \cdots & 0 \\ \vdots & \vdots & \vdots & \ldots & \vdots & \vdots & \vdots & \vdots & \ldots & \vdots \\ 0 & 0 & 0 & \cdots & 1 & \tau & 0 & 0 & \cdots & 0 \\ 0 & 0 & 0 & \cdots & 0 & 1 & \tau & \frac{\tau^2}{2!} & \cdots & \frac{\tau^n}{n!} \\ 0 & 0 & 0 & \cdots & 0 & 0 & 1 & \tau & \cdots & \frac{\tau^{(n-1)}}{(n-1)!} \\ \vdots & \vdots & \vdots & \ldots & \vdots & \vdots & \vdots & \vdots & \ldots & \vdots \\ 0 & 0 & 0 & \cdots & 0 & 0 & 0 & 0 & \cdots & 1 \end{bmatrix}, \tag{3.7}$$

with $\boldsymbol{\Sigma}(\tau) \in \mathbb{R}^{(m+1)\times(m+1)}$. Note that the first n_f rows of $\boldsymbol{\Sigma}(\tau)$ only present 1, 0 and τ terms. Similarly to the continuous-time system error, the discrete-time error system (3.6) can be represented as:

$$\begin{bmatrix} \boldsymbol{w}_{k+1} \\ \boldsymbol{\sigma}_{k+1} \end{bmatrix} = \left(\boldsymbol{\Sigma}(\tau) + \boldsymbol{\Gamma}_k \boldsymbol{e}_{1,m}^T \right) \begin{bmatrix} \boldsymbol{w}_k \\ \boldsymbol{\sigma}_k \end{bmatrix} - \begin{bmatrix} \boldsymbol{0} \\ \boldsymbol{h}_k(\tau) \end{bmatrix}, \tag{3.8}$$

where $\boldsymbol{\sigma}_k = \begin{bmatrix} \sigma_{0,k} & \sigma_{1,k} & \cdots & \sigma_{n,k} \end{bmatrix}^T$, and $\boldsymbol{h}_k(\tau) = \begin{bmatrix} h_{0,k}(\tau) & h_{1,k}(\tau) & \cdots & h_{n,k}(\tau) \end{bmatrix}^T$. Let d_j be the desired eigenvalues of the discrete-time system. Then, the desired polynomial is given as $P_d(r) = \prod_{j=1}^{m+1} (r - d_j)$ and for a matrix case $P_d(\boldsymbol{\Sigma}(\tau)) = \prod_{j=1}^{m+1} (\boldsymbol{\Sigma}(\tau) - d_j \boldsymbol{I})$. The desired polynomial evaluated at $\boldsymbol{\Sigma}(\tau) + \boldsymbol{\Gamma}_k \boldsymbol{e}_{1,m}^T$ is given by $P_d(\boldsymbol{\Sigma}(\tau) + \boldsymbol{\Gamma}_k \boldsymbol{e}_{1,m}^T) = (\boldsymbol{\Sigma}(\tau) + \boldsymbol{\Gamma}_k \boldsymbol{e}_{1,m}^T)^{m+1} + \sum_{j=0}^{m} \alpha_j (\boldsymbol{\Sigma}(\tau) + \boldsymbol{\Gamma}_k \boldsymbol{e}_{1,m}^T)^j$. Therefore, we obtain the following equation:

$$P_d(\boldsymbol{\Sigma}(\tau) + \boldsymbol{\Gamma}_k \boldsymbol{e}_{1,m}^T) = P_d(\boldsymbol{\Sigma}(\tau)) + \begin{bmatrix} * & \cdots & * & \boldsymbol{\Gamma}_k \end{bmatrix} \boldsymbol{S}. \tag{3.9}$$

Due to the Cayley–Hamilton theorem $P_d(\boldsymbol{\Sigma}(\tau) + \boldsymbol{\Gamma}_k \boldsymbol{e}_{1,m}^T) = \boldsymbol{0}$ and therefore, $\boldsymbol{\Gamma}_k$ can be calculated as:

$$\boldsymbol{\Gamma}_k = -P_d(\boldsymbol{\Sigma}(\tau)) \boldsymbol{S}^{-1} \boldsymbol{e}_{m+1,m}, \tag{3.10}$$

where

$$\boldsymbol{S} = \begin{bmatrix} \boldsymbol{e}_{1,m}^T \\ \boldsymbol{e}_{1,m}^T \Psi(\tau) \\ \boldsymbol{e}_{1,m}^T \Psi^2(\tau) \\ \vdots \\ \boldsymbol{e}_{1,m}^T \Psi^m(\tau) \end{bmatrix} \tag{3.11}$$

Now, the objective is to select adequate roots d_j. In order to emulate the behavior of the continuous-time system, a mapping of the continuous-time domain to the discrete-time domain is used. One can use different approaches, Euler with $d_j = 1 + \tau s_j$, matching with $d_j = e^{\tau s_j}$ and bilinear with $d_j = \frac{1+s_j\tau/2}{1-s_j\tau/2}$ ones, to name a few [Perdikaris 1991]. As $s_j = |w_1|^{\frac{-1}{m+1}} b_j$, Euler and bilinear approaches have a singularity at $w_1 = 0$. Hence, the Matching approach is used:

$$d_j = e^{\tau s_j} = e^{\tau |w_1|^{\frac{-1}{m+1}} b_j}. \tag{3.12}$$

3.3 Explicit discrete-time realization of the robust exact filtering differentiator (EDFD and MEDFD)

Assumptions 1.3.1, 1.3.3, 1.3.4 and 2.1.1, are not enough to obtain an adequate realization of the filtering differentiator. Similar to [Levant & Livne 2019], the following assumption is considered.

Assumption 3.3.1 *The sampled measurement noise consists of $n_f + 1$ components, $\Delta_k = \Delta(t_k) = \Delta_{0,k} + \Delta_{1,k} + \cdots + \Delta_{n_f,k}$, where each $\Delta_{j,k}$, $j = 0, 1, \cdots, n_f$ (possibly unbounded), is a discretely sampled signal of global filtering order j and jth-order integral magnitude $\varepsilon_j \geq 0$.*

Definition 3.1 *A discretely sampled signal $\Delta_{j,k} : \mathbb{R}_+ \to \mathbb{R}$ is said to be a signal of global sampling filtering order $j \geq 0$ and global jth order integral sampling magnitude $\varepsilon_j \geq 0$ if for each admissible sequence t_k there exists a discrete vector signal $\boldsymbol{\beta}_{j,k} = \begin{bmatrix} \beta_{j,k}^0 & \beta_{j,k}^1 & \cdots & \beta_{j,k}^j \end{bmatrix}^T \in \mathbb{R}^{j+1}$, $k = 0, 1, \cdots$, which satisfies:*

$$\begin{aligned} &\beta_{j,k+1}^l - \beta_{j,k}^l = \tau \beta_{j,k}^{l+1}, \quad l = 0, 1, \cdots, j-1, \\ &\beta_{j,k}^j = \Delta_{j,k}, \quad \left|\beta_{j,k}^0\right| \leq \varepsilon_j. \end{aligned} \tag{3.13}$$

With respect to the parameter $\beta_{j,k}^l$, the superscript l of $\beta_{j,k}^l$ does not indicate an exponentiation or differentiation. It is important mentioning that a discretely sampled signal of the global filtering order j is defined using difference equations whereas a signal of the global filtering order j is defined using differential equations.

Similar to HEDD, the following explicit differentiator, which is called EDFD, is obtained:

$$\begin{aligned} w_{j_f,k+1} &= \frac{\tau^{(n_f-j_f+1)}}{(n_f-j_f+1)!}(z_{0,k}-f_k)+\sum_{l=j_f}^{n_f}\frac{\tau^{(l-j_f)}}{(l-j_f)!}w_{l,k}+\dots \\ &\dots+\sum_{l=1}^{n}\frac{\tau^{n_f-j_f+l+1}}{(n_f-j_f+l+1)!}z_{l,k}+\sum_{l=j_f}^{m+1}\frac{\tau^{(l-j_f+1)}}{(l-j_f+1)!}\Psi_{l-1,m}\left(w_{1,k}\right), \\ z_{j_d,k+1} &= \sum_{l=j_d}^{n}\frac{\tau^{(l-j_d)}}{(l-j_d)!}z_{l,k}+\frac{\tau^{(l-j_d+1)}}{(l-j_d+1)!}\Psi_{n_f+l,m}\left(w_{1,k}\right), \\ j_f &= 1,2,\cdots,n_f. \quad j_d=0,1,2,\cdots,n. \end{aligned} \tag{3.14}$$

Note that the consideration of constant input using a zero-order hold is only used to derive equation (3.14). It is clear that such assumption does not hold in practice. Hence, (3.14) is not an exact discretization of (1.69). Furthermore, it is important to highlight that this discrete-time scheme contains the terms $\frac{\tau^{(l-j_d)}}{(l-j_d)!}z_{l,k}$ in the equations of $z_{j_d,k+1}$. It was shown that such terms are important to obtain an adequate discretization of the standard differentiator [Livne & Levant 2014, Koch *et al.* 2020, Carvajal-Rubio *et al.* 2019]. Contrary to the standard differentiator, the high-order terms $\frac{\tau^{n_f-j_f+l+1}}{(n_f-j_f+l+1)!}z_{l,k}$ in the equations of the filtering part may cause instability of the estimation error for signals with unbounded derivatives. This will be detailed in the next section. To remove this drawback, these terms are omitted and the following modified explicit discrete-time filtering differentiator, referenced as MEDFD, is obtained,

$$\begin{aligned} w_{j_f,k+1} =& \frac{\tau^{(n_f-j_f+1)}}{(n_f-j_f+1)!}(z_{0,k}-f_k)+\sum_{l=j_f}^{n_f}\frac{\tau^{(l-j_f)}}{(l-j_f)!}w_{l,k}+\dots \\ &\dots+\sum_{l=j_f}^{m+1}\frac{\tau^{(l-j_f+1)}}{(l-j_f+1)!}\Psi_{l-1,m}\left(w_{1,k}\right), \\ z_{j_d,k+1} =& \sum_{l=j_d}^{n}\frac{\tau^{(l-j_d)}}{(l-j_d)!}z_{l,k}+\frac{\tau^{(l-j_d+1)}}{(l-j_d+1)!}\Psi_{n_f+l,m}\left(w_{1,k}\right), \\ j_f =& 1,2,\cdots,n_f. \quad j_d=0,1,2,\cdots,n. \end{aligned} \tag{3.15}$$

The properties of the discrete-time system (3.15) will be presented and analyzed in detail in the following sections of this chapter.

3.4 Implicit discrete-time realization of the robust exact filtering differentiator (MIDFD)

3.4.1 Design of MIDFD

Taking into consideration the explicit discrete-time realization (3.15), its implicit counterpart is given as:

$$\begin{aligned} w_{j_f,k+1} =& \frac{\tau^{(n_f-j_f+1)}}{(n_f-j_f+1)!}(z_{0,k}-f_k)+\sum_{l=j_f}^{n_f}\frac{\tau^{(l-j_f)}}{(l-j_f)!}w_{l,k}+\sum_{l=j_f}^{m+1}\frac{\tau^{(l-j_f+1)}}{(l-j_f+1)!}\Psi_{l-1,m}\left(w_{1,k+1}\right), \\ z_{j_d,k+1} =& \sum_{l=j_d}^{n}\frac{\tau^{(l-j_d)}}{(l-j_d)!}z_{l,k}+\frac{\tau^{(l-j_d+1)}}{(l-j_d+1)!}\Psi_{n_f+l,m}\left(w_{1,k+1}\right), \\ j_f =& 1,2,\cdots,n_f. \quad j_d=0,1,2,\cdots,n. \end{aligned} \tag{3.16}$$

To implement (3.16), $w_{1,k+1}$ needs to be calculated at time t_k. From (3.16), one obtains

$$w_{1,k+1}=\frac{\tau^{n_f}}{n_f!}(z_{0,k}-f_k)+\sum_{l=1}^{n_f}\frac{\tau^{(l-1)}}{(l-1)!}w_{l,k}+\sum_{l=1}^{m+1}\frac{\tau^{l}}{l!}\Psi_{l-1,m}\left(w_{1,k+1}\right). \tag{3.17}$$

Since the right-hand side of Equation (3.17) depends on $w_{1,k+1}$, it cannot be used to implement (3.16). Let a_j and b_k be defined as:

$$a_j=\frac{\tau^{m-j+1}}{(m-j+1)!}\lambda_j L^{\frac{m-j+1}{m+1}},\ \ b_k=-\frac{\tau^{n_f}}{n_f!}\left(z_{0,k}-f_k\right)-\sum_{l=1}^{n_f}\frac{\tau^{(l-1)}}{(l-1)!}w_{l,k}, \tag{3.18}$$

with $j=0,1,2,\cdots,m$. Therefore, one obtains the following generalized equation with an unknown $w_{1,k+1}$

$$w_{1,k+1}+a_m\left\lfloor w_{1,k+1}\right\rceil^{\frac{m}{m+1}}+\cdots+a_1\left\lfloor w_{1,k+1}\right\rceil^{\frac{1}{m+1}}+b_k\in-a_0\mathrm{sign}(w_{1,k+1}). \tag{3.19}$$

Now, a new support variable $\xi_k\in\mathrm{sign}(w_{1,k+1})$ is introduced. The variable ξ_k represents a selection of the set-valued function $\mathrm{sign}(w_{1,k+1})$. To obtain equations that allow to calculate $w_{1,k+1}$ and ξ_k at time t_k, the following generalized equations need to be solved

$$\chi_m\left(w_{1,k+1}\right)\in-a_0\mathrm{sign}(w_{1,k+1}),\ \chi_m^{-1}\left(-a_0\xi_k\right)\in\mathcal{N}_{[-1,1]}\left(\xi_k\right),\ \xi_k\in\mathrm{sign}(w_{1,k+1}). \tag{3.20}$$

For $\zeta\in\mathbb{R}$, $\chi\left(\zeta\right)$ is defined as:

$$\chi_m\left(\zeta\right)=\zeta+a_m\left\lfloor\zeta\right\rceil^{\frac{m}{m+1}}+\cdots+a_1\left\lfloor\zeta\right\rceil^{\frac{1}{m+1}}+b_k, \tag{3.21}$$

Similar to the HIDD, the following lemma allows to calculate $w_{1,k+1}$ and ξ_k at the time t_k.

Lemma 3.1 *Let $a_j>0$, $w_{1,k+1}\in\mathbb{R}$ and $\xi_k\in[-1,1]$. Then the unique solution of the inclusions (3.20) is the pair $(w_{1,k+1},\xi_k)$ which is defined in the following three cases:*

- *If* $b_k > a_0$, *then* $\xi_k = \{-1\}$ *and* $w_{1,k+1} = -(r_0)^{m+1}$, *where* r_0 *is the unique positive root of the following polynomial:*

$$p(r) = r^{m+1} + a_m r^m + \cdots + a_1 r + (-b_k + a_0). \tag{3.22}$$

- *If* $b_k \in [-a_0, a_0]$, *then* $w_{1,k+1} = 0$ *and* $\xi_k = \left\{-\frac{b_k}{a_0}\right\}$.

- *If* $b_k < -a_0$, *then* $\xi_k = \{1\}$ *and* $w_{1,k+1} = r_0^{m+1}$, *where* r_0 *is the unique positive root of the following polynomial:*

$$p(r) = r^{m+1} + a_m r^m + \cdots + a_1 r + (b_k + a_0). \tag{3.23}$$

The proof is similar to the proof of Lemma 2.2. The proposed implicit discrete-time realization of the homogeneous continuous-time differentiator (1.69), referenced as MIDFD, is given as:

$$\begin{aligned}
w_{j_f,k+1} &= \frac{\tau^{(n_f-j_f+1)}}{(n_f-j_f+1)!}(z_{0,k} - f_k) + \sum_{l=j_f}^{n_f} \frac{\tau^{(l-j_f)}}{(l-j_f)!} w_{l,k} + \dots \\
&\dots + \sum_{l=j_f}^{m+1} \frac{\tau^{(l-j_f+1)}}{(l-j_f+1)!} \bar{\Psi}_{l-1,m}(w_{1,k+1}), \\
z_{j_d,k+1} &= \sum_{l=j_d}^{n} \frac{\tau^{(l-j_d)}}{(l-j_d)!} z_{l,k} + \frac{\tau^{(l-j_d+1)}}{(l-j_d+1)!} \bar{\Psi}_{n_f+l,m}(w_{1,k+1}), \\
\bar{\Psi}_{j,m}(w_{1,k+1}) &= -\lambda_{m-j} L^{\frac{j+1}{m+1}} |w_{1,k+1}|^{\frac{m-j}{m+1}} \xi_k, \quad j_f = 1, 2, \cdots, n_f. \\
j_d &= 0, 1, 2, \cdots, n.
\end{aligned} \tag{3.24}$$

where the pair $(w_{1,k+1}, \xi_k)$ is calculated according to Lemma 3.1. Note that at $w_{1,k+1} = 0$, $\bar{v}_{0,m}(w_{1,k+1}) = \left\{\frac{\lambda_0 L b_k}{a_0}\right\} = \left\{\frac{(m+1)! b_k}{\tau^{m+1}}\right\}$ whereas $v_{0,m}(w_{1,k+1}) \in [-\lambda_0 L, \lambda_0 L]$. Furthermore, as r_0 is positive, then for $b_k \notin [-a_0, a_0]$, $\bar{v}_{j,m}$ has the alternative form $\bar{v}_{j,m}(w_{1,k+1}) = -\lambda_{m-j} L^{\frac{j+1}{m+1}} r_0^{m-j} \xi_k$. With this form, one avoids to calculate the roots $|w_{1,k+1}|^{\frac{j}{m+1}}$.

Remark 3.4.1 *It is important to mention that MIDFD and Lemma 3.1, are valid for* $n_f > 0$. *In the case of* $n_f = 0$, *HIDD (2.42) is used instead of it.*

Remark 3.4.2 *Similar to other implicit realizations [Huber et al. 2019], at* $w_{1,k+1} = 0$, *the injection terms* $\bar{v}_{j,m}(w_{1,k+1})$ *are insensitive to* L *and* λ_j.

Remark 3.4.3 *The main difference between MEDFD, MIDFD, and the presented in [Levant & Livne 2019, Hanan et al. 2020] are the high-order terms* $\frac{\tau^{(l-j_f)}}{(l-j_f)!} w_{l,k}$ *and its inputs. Contrary to the differentiator presented in [Hanan et al. 2020], the differentiators MEDFD, EDFD, MIDFD and [Levant & Livne 2019] do not add new tuning parameters.*

3.4.2 Implementation of MIDFD

In this subsection, an implementation scheme of the MIDFD differentiator is presented as follows:

Require: $n, n_f \geq 0$, L, λ_i, τ
  $m \leftarrow 0$
  while $m \leq n + n_f$ **do**
    $a_m \leftarrow \frac{\tau^{n-m+1}}{(n-m+1)!}\lambda_m L^{\frac{n-m+1}{n+1}}$
    $m \leftarrow m + 1$
  end while
  $m \leftarrow 0$
  while $m \leq n$ **do**
    $z_m \leftarrow 0$ ▷ The states z_i are initialized.
    $m \leftarrow m + 1$
  end while
  $m \leftarrow 0$
  while $m \leq n_f$ **do**
    $w_m \leftarrow 0$ ▷ The states w_i are initialized.
    $m \leftarrow m + 1$
  end while
  $m \leftarrow 0$
  while $m\tau \leq t_{max}$ **do**
    $f_k \leftarrow f(m\tau)$ ▷ The measurement of $f(t)$ is obtained.
    $b_k \leftarrow -\frac{\tau^{n_f}}{n_f!}(z_0 - f_k) - \sum_{l=1}^{n_f} \frac{\tau^{(l-1)}}{(l-1)!} w_l$
    if $b_k > a_0$ **then**
      $r \leftarrow \left(\frac{b_k - a_0}{2}\right)^{1/(n+n_f+1)}$
      $j \leftarrow 0$
      while $j < 3$ **do** ▷ The positive root is calculated using Halley's method.
        $p \leftarrow r^{n+n_f+1} + a_{n+n_f} r^{n+n_f} + \cdots + a_1 r + (-b_k + a_0)$
        $dp \leftarrow (n + n_f + 1)\, r^{n+n_f} + (n + n_f) a_{n+n_f} r^{n+n_f-1} + \cdots + a_1$
        $ddp \leftarrow (n + n_f)\,(n + n_f + 1)\, r^{n+n_f-1} + \cdots + 2a_2$
        $r \leftarrow r - \frac{2p(dp)}{2(dp)^2 - p(ddp)}$
        $j \leftarrow j + 1$
      end while
      $\xi_k \leftarrow -1$
    end if
    if $b_k < -a_0$ **then**
      $r \leftarrow \left(\frac{-b_k - a_0}{2}\right)^{1/(n+n_f+1)}$
      $j \leftarrow 0$
      while $j < 3$ **do** ▷ The positive root is calculated using Halley's method.
        $p \leftarrow r^{n+n_f+1} + a_{n+n_f} r^{n+n_f} + \cdots + a_1 r + (b_k + a_0)$
        $dp \leftarrow (n + n_f + 1)\, r^{n+n_f} + (n + n_f) a_{n+n_f} r^{n+n_f-1} + \cdots + a_1$
        $ddp \leftarrow (n + n_f)\,(n + n_f + 1)\, r^{n+n_f-1} + \cdots + 2a_2$
        $r \leftarrow r - \frac{2p(dp)}{2(dp)^2 - p(ddp)}$

$j \leftarrow j+1$
end while
$\xi_k \leftarrow 1$
end if
if $b_k > -a_0$ and $b_k < a_0$ **then**
$r \leftarrow 0$
$\xi_k \leftarrow -\frac{b_k}{a_0}$
end if
$j \leftarrow 0$
while $j \leq n+n_f$ **do**
$u_j \leftarrow -\lambda_{n+n_f-j} L^{\frac{j+1}{n+n_f+1}} r^{n+n_f-j} \xi_k$
$j \leftarrow j+1$
end while
$j \leftarrow 1$
while $j \leq n_f$ **do**
$w_{j,M} \leftarrow \frac{\tau^{(n_f-j+1)}}{(n_f-j+1)!}(z_0 - f_k) + \sum_{l=j}^{n_f} \frac{\tau^{(l-j)}}{(l-j)!} w_l + \sum_{l=j}^{n+n_f+1} \frac{\tau^{(l-j+1)}}{(l-j+1)!} u_{l-1}$
$j \leftarrow j+1$
end while
$j \leftarrow 0$
while $j \leq n$ **do** ▷ The estimation at the time $t = (m+1)\tau$ are obtained
$z_{j,M} = \sum_{l=j}^{n} \frac{\tau^{l-j}}{(l-j)!} z_{l,k} + \frac{\tau^{l-j+1}}{(l-j+1)!} u_l$
$j \leftarrow j+1$
end while
$j \leftarrow 0$
while $j \leq n$ **do** ▷ The states are updated for the next measurement.
$w_j = w_{j,M}$
$z_j = z_{j,M}$
$j \leftarrow j+1$
end while
end while

3.5 Stability analysis of the differentiator based on the standard differentiator

In this section, the stability of the matching discrete-time filtering differentiator, the explicit discrete-time realization (EDFD and MEDFD) and the implicit one (MIDFD) are studied.

3.5.1 Stability analysis of the matching discrete-time filtering differentiator

Theorem 3.5.1

Let the matching discrete-time differentiator (3.6) with $\mathbf{\Gamma}_k$ defined as (3.10), d_j defined as (3.12). Under Assumptions 1.3.1, 1.3.4 and considering no measurement noise $\Delta(t) = 0$, if $\mathcal{RE}(b_j) < 0$, then the trajectories of the observation error system (3.8) converge to a neighborhood of the origin and remain within this neighborhood, defined as:

$$\left\| \begin{bmatrix} \boldsymbol{w}_k \\ \boldsymbol{\sigma}_k \end{bmatrix} \right\| \leq K \left\| \boldsymbol{h}_k(\tau) \right\|. \tag{3.25}$$

where K is defined in the proof.

Note that the roots b_j can be selected independently of λ_j and L from Theorem 3.5.1. This allows to implement the differentiator even if L is unknown. Furthermore, if b_j are selected as $b_1 = b_2 = b_3 = \cdots = b_{m+1}$, $\mathbf{\Gamma}_k$ presents a less complex equation than with $b_j \neq b_{j+1}$.

Proof *Let* $\boldsymbol{E} = \left(\mathbf{\Sigma}(\tau) + \mathbf{\Gamma}_k e_{1,m}^T\right)$. *Consider the candidate Lyapunov function defined as:*

$$V_k = \begin{bmatrix} \boldsymbol{w}_k \\ \boldsymbol{\sigma}_k \end{bmatrix}^T \boldsymbol{P} \begin{bmatrix} \boldsymbol{w}_k \\ \boldsymbol{\sigma}_k \end{bmatrix}, \tag{3.26}$$

where $\boldsymbol{P}$ *is a real positive definite matrix defined such that*

$$\boldsymbol{E}^T \boldsymbol{P} \boldsymbol{E} - \boldsymbol{P} = -\boldsymbol{Q}, \tag{3.27}$$

with $\boldsymbol{Q}$ *be a real positive definite matrix and* $\lambda_{\min}(Q) > 1$. *From Equations* (3.8) *and* (3.26), *one gets*

$$\begin{aligned} V_{k+1} - V_k = &- \begin{bmatrix} \boldsymbol{w}_k \\ \boldsymbol{\sigma}_k \end{bmatrix}^T \boldsymbol{Q} \begin{bmatrix} \boldsymbol{w}_k \\ \boldsymbol{\sigma}_k \end{bmatrix} + \begin{bmatrix} \mathbf{0} \\ \boldsymbol{h}_k(\tau) \end{bmatrix}^T \boldsymbol{P} \begin{bmatrix} \mathbf{0} \\ \boldsymbol{h}_k(\tau) \end{bmatrix} - \dots \\ &\dots - 2 \begin{bmatrix} \boldsymbol{w}_k \\ \boldsymbol{\sigma}_k \end{bmatrix}^T \boldsymbol{E}^T \boldsymbol{P} \boldsymbol{E} \begin{bmatrix} \mathbf{0} \\ \boldsymbol{h}_k(\tau) \end{bmatrix}. \end{aligned} \tag{3.28}$$

Using inequality $\boldsymbol{C}^T\boldsymbol{D} + \boldsymbol{D}^T\boldsymbol{C} \leq \boldsymbol{C}^T\mathbf{\Lambda}\boldsymbol{C} + \boldsymbol{D}^T\mathbf{\Lambda}^{-1}\boldsymbol{D}$, *where* $\boldsymbol{C}$, $\boldsymbol{D} \in \mathbb{R}^{n\times m}$ *and* $\mathbf{\Lambda} \in \mathbb{R}^{n\times n}$ *is any positive definite matrix, the following inequality is obtained:*

$$V_{k+1} - V_k \leq \left(\lambda_{\max}(\boldsymbol{E}) + \lambda_{\max}(\boldsymbol{P})\right) \left\| \boldsymbol{h}_k(\tau) \right\|^2 - \left(\lambda_{min}(Q) - 1\right) \left\| \begin{bmatrix} \boldsymbol{w}_k, & \boldsymbol{\sigma}_k \end{bmatrix} \right\|^2. \tag{3.29}$$

Therefore with the condition

$$\begin{aligned} \left\| \begin{bmatrix} \boldsymbol{w}_k \\ \boldsymbol{\sigma}_k \end{bmatrix} \right\| &> K \left\| \boldsymbol{h}_k(\tau) \right\|, \\ K &= \sqrt{\frac{\lambda_{\max}(\boldsymbol{E}) + \lambda_{\max}(\boldsymbol{P})}{\lambda_{\min}(\boldsymbol{Q}) - 1}}, \end{aligned} \tag{3.30}$$

one obtains $V_{k+1} - V_k < 0$. *This concludes the proof.*

3.5.2 Stability analysis of the modified explicit discrete-time filtering differentiator (MEDFD)

Contrary to [Levant & Livne 2019] where the following change of variables is proposed

$$\bar{\omega}_{j_f,k} = \left(w_{j_f,k} + \sum_{l=0}^{j_f-1} \beta^l_{n_f+l-j_f+1,k} \right) / L, \qquad j_f = 1, \cdots, n_f, \tag{3.31}$$

the following one is used in this work,

$$\begin{aligned} &\omega_{n_f-j_f+1,k} = w_{n_f-j_f+1,k} + \sum_{j=1}^{j_f} d^j_{j_f} \frac{\tau^{j_f-j}}{(j_f-j+1)!} \sum_{l=j}^{n_f} \beta^{l-j}_{l,k}, \\ &j_f = 1, \cdots, n_f. \end{aligned} \tag{3.32}$$

Constants $d^j_{j_f}$ are given in Table 3.1 for $j_f \leq 8$. The summations $\sum_{l=1}^{n_f} \beta^{l-1}_{l,k}$ are added to cancel the noise components $\beta^1_{1,k}, \beta^2_{2,k}, \cdots, \beta^{n_f}_{n_f,k}$ in the equation $\omega_{n_f,k+1}$. At the same time, the noise components and the above summations except $\tau\beta^0_{1,k}$ and $\frac{\tau^2}{2!}\beta^0_{0,k}$, have to be canceled in the equation of $\omega_{n_f-1,k+1}$. They are canceled with two summations in the change of variables of $w_{n_f-1,k}$. Regarding the remainder $w_{n_f-j_f+1,k}$, they are proposed recursively in a similar way.

	$j=1$	$j=2$	$j=3$	$j=4$	$j=5$	$j=6$	$j=7$	$j=8$
$j_f=1$	1	—	—	—	—	—	—	—
$j_f=2$	1	1	—	—	—	—	—	—
$j_f=3$	1	2	1	—	—	—	—	—
$j_f=4$	1	$\frac{7}{2}$	3	1	—	—	—	—
$j_f=5$	1	6	$\frac{15}{2}$	4	1	—	—	—
$j_f=6$	1	$\frac{31}{3}$	18	13	5	1	—	—
$j_f=7$	1	18	43	40	20	6	1	—
$j_f=8$	1	$\frac{127}{4}$	$\frac{207}{2}$	$\frac{243}{2}$	75	$\frac{57}{2}$	7	1

Table 3.1: Value of $d^j_{j_f}$ for $1 \leq j_f \leq 8$.

Theorem 3.5.2

Let $\boldsymbol{z}_k$ be generated with the modified explicit discrete-time filtering differentiator (3.15) with $n_f > 0$. Under Assumptions 1.3.1, 1.3.4, 3.3.1, there exist constants $\mu_{j_d} > 0$ such that after a finite-time transient, the following inequalities are verified:

$$|z_{j_d,k} - x_{j_d,k}| \leq \mu_{j_d} L \rho^{n+1-j_d}, \quad \rho = \max\left\{\tau, \max_{0\leq j\leq n_f}\left(\frac{\varepsilon_j}{L}\right)^{\frac{1}{n+j+1}}\right\}, \tag{3.33}$$

where $j_d = 0, 1, \cdots, n$ and the coefficients μ_{j_d} only depend on the parameters $\lambda_0, \ldots, \lambda_m$.

Proof *From the systems (2.1) and (3.15), the error dynamics are given as:*

$$\begin{aligned}
w_{j_f,k+1} =& \frac{\tau^{(n_f-j_f+1)}}{(n_f-j_f+1)!}(\sigma_{0,k} - \Delta_k) + \sum_{l=j_f}^{n_f}\frac{\tau^{(l-j_f)}}{(l-j_f)!}w_{l,k} + \sum_{l=j_f}^{m+1}\frac{\tau^{(l-j_f+1)}}{(l-j_f+1)!}\Psi_{l-1,m}\left(w_{1,k}\right),\\
\sigma_{j_d,k+1} =& -h_{j,k} + \sum_{l=j_d}^{n}\frac{\tau^{(l-j_d)}}{(l-j_d)!}\sigma_{l,k} + \frac{\tau^{(l-j_d+1)}}{(l-j_d+1)!}\Psi_{n_f+l,m}\left(w_{1,k}\right),\\
j_f =& 1, 2, \cdots, n_f, \quad j_d = 0, 1, 2, \cdots, n.
\end{aligned} \tag{3.34}$$

Then, with the change of variables (3.32), and with $\bar{\omega}_{j,k} = \omega_{j,k}/L$ and $\bar{\sigma}_{j,k} = \sigma_{j,k}/L$, one obtains the following inclusions:

$$\begin{aligned}
&\bar{\omega}_{j_f,k+1} \in \bar{\omega}_{j_f,k} + \tau\frac{\Psi_{j_f-1,m}(\cdot)}{L^{\frac{j_f}{m+1}}} + \frac{\tau^{n_f-j_f+1}}{(n_f-j_f+1)!}\left(\bar{\sigma}_{0,k} + \left[-\frac{\varepsilon_0}{L}, \frac{\varepsilon_0}{L}\right]\right) + \ldots\\
&\ldots + \sum_{l=j_f+1}^{n_f}\frac{\tau^{l-j_f}}{(l-j_f)!}\left(\bar{\omega}_{l,k} + d_{n_f-j_f+1}^{n_f-l+2}\left[-\frac{\varepsilon_{n_f-l+1}}{L}, \frac{\varepsilon_{n_f-l+1}}{L}\right]\right) + \ldots\\
&\ldots + \sum_{l=j_f+1}^{m+1}\frac{\tau^{l-j_f+1}}{(l-j_f+1)!}\frac{\Psi_{l-1,m}(\cdot)}{L^{\frac{l}{m+1}}},\\
&\bar{\omega}_{n_f,k+1} \in \bar{\omega}_{n_f,k} + \tau\frac{\Psi_{n_f-1,m}(\cdot)}{L^{\frac{n_f}{m+1}}} + \tau\left(\bar{\sigma}_{0,k} + \left[-\frac{\varepsilon_0}{L}, \frac{\varepsilon_0}{L}\right]\right) + \ldots\\
&\ldots + \sum_{l=n_f+1}^{m+1}\frac{\tau^{l-n_f+1}}{(l-n_f+1)!}\frac{\Psi_{l-1,m}(\cdot)}{L^{\frac{l}{m+1}}},\\
&\bar{\sigma}_{j_d,k+1} \in \bar{\sigma}_{j_d,k} + \tau\frac{\Psi_{n_f+j_d,m}\left(\cdot\right)}{L^{\frac{n_f+j_d+1}{m+1}}} + \frac{\tau^{n+1-j_d}}{(n+1-j_d)!}\left[-1, 1\right] + \ldots\\
&\ldots + \sum_{l=j_d+1}^{n}\frac{\tau^{(l-j_d)}}{(l-j_d)!}\bar{\sigma}_{l,k} + \frac{\tau^{(l-j_d+1)}}{(l-j_d+1)!}\frac{\Psi_{n_f+l,m}\left(\cdot\right)}{L^{\frac{n_f+l+1}{m+1}}},\\
&\bar{\sigma}_{n,k+1} \in \bar{\sigma}_{n,k} + \tau\frac{\Psi_{m,m}\left(\cdot\right)}{L} + \tau\left[-1, 1\right],\\
&j_f = 1, 2, \cdots, n_f - 1, \quad j_d = 0, 1, 2, \cdots, n-1.
\end{aligned} \tag{3.35}$$

From the change of variable for $w_{1,k}$ and Definition 3.1, the argument of $\Psi_{j,m}(\cdot)$ in Equation (3.35) is given as:

$$\bar{\omega}_{1,k} + \sum_{l=1}^{n_f} g_l^{n_f} \tau^{n_f - l} \left[-\frac{\varepsilon_l}{L}, \frac{\varepsilon_l}{L} \right], \tag{3.36}$$

where the constants $g_l^{n_f}$, for $1 \leq n_f \leq 6$, are presented in Table 3.2. Moreover, the following equations are applied with the purpose of obtain only $\beta_{j,\cdot}^0$ in the argument of $\Psi_{j,m}(\cdot)$

$$\begin{aligned} \tau\beta_{j,k}^1 =& \beta_{j,k+1}^0 - \beta_{j,k}^0, \\ \tau^2\beta_{j,k}^2 =& \tau(\beta_{j,k+1}^1 - \beta_{j,k}^1) = \beta_{j,k+2}^0 - 2\beta_{j,k+1}^0 + \beta_{j,k}^0, \\ \tau^3\beta_{j,k}^3 =& \beta_{j,k+3}^0 - 3\beta_{j,k+2}^0 + 3\beta_{j,k+1}^0 - \beta_{j,k}^0, \\ &\vdots \end{aligned} \tag{3.37}$$

	$l=1$	$l=2$	$l=3$	$l=4$	$l=5$	$l=6$
$n_f=1$	1	—	—	—	—	—
$n_f=2$	$\frac{1}{2}$	$\frac{3}{2}$	—	—	—	—
$n_f=3$	$\frac{1}{6}$	1	1	—	—	—
$n_f=4$	$\frac{1}{24}$	$\frac{7}{12}$	$\frac{8}{3}$	1	—	—
$n_f=5$	$\frac{1}{120}$	$\frac{1}{4}$	$\frac{5}{4}$	$\frac{121}{6}$	$\frac{51}{40}$	—
$n_f=6$	$\frac{1}{120}$	$\frac{31}{360}$	$\frac{3}{4}$	$\frac{13}{6}$	$\frac{5}{4}$	$\frac{91}{90}$

Table 3.2: Value of $g_l^{n_f}$ for $1 \leq n_f \leq 6$.

Let $\boldsymbol{s}(t)$ be a piecewise linear continuous-time function, which is given as $\boldsymbol{s}(t) = [s_0(t)\ s_1(t)\ s_2(t) \cdots\ s_m(t)]$, and describes the solution of (3.35) ($s_{j_f-1,k} = s_{j_f-1}(t_k) = \bar{\omega}_{j_f,k}$ and $s_{n_f+j_d,k} = s_{n_f+j_d}(t_k) = \bar{\sigma}_{j_d,k}$ for $j_f = 1, 2, \ldots, n_f$ and $j_d = 0, 1, \cdots, n$). Therefore, $\boldsymbol{s}(t)$ can be expressed as $\boldsymbol{s}(t) = \boldsymbol{s}_k + (t - t_k)\Omega_k$, $\Omega_k \in \boldsymbol{G}(\boldsymbol{s}_k, \tau)$,

where $t \in [t_k, t_{k+1})$ *and* $\boldsymbol{G}(\boldsymbol{s}_k, \tau) = [G_0(\boldsymbol{s}_k, \tau) \;\; G_1(\boldsymbol{s}_k, \tau) \;\; \cdots \;\; G_m(\boldsymbol{s}_k, \tau)]^T$ *is given as:*

$$
\begin{aligned}
&G_{j_f-1,k+1} \in \frac{\Psi_{j_f-1,m}(\cdot)}{L^{\frac{j_f}{m+1}}} + \left(s_{j_f,k} + d_{n_f-j_f+1}^{n_f-j_f+1} \left[-\frac{\varepsilon_{n_f-j_f}}{L}, \frac{\varepsilon_{n_f-j_f}}{L} \right] \right) + \dots \\
&\dots + \sum_{l=j_f+2}^{n_f+1} \frac{\tau^{l-j_f-1}}{(l-j_f)!} \left(s_{l-1,k} + d_{n_f-j_f+1}^{n_f-l+2} \left[-\frac{\varepsilon_{n_f-l+1}}{L}, \frac{\varepsilon_{n_f-l+1}}{L} \right] \right) + \dots \\
&\dots + \sum_{l=j_f+1}^{m+1} \frac{\tau^{l-j_f}}{(l-j_f+1)!} \frac{\Psi_{l-1,m}(\cdot)}{L^{\frac{l}{m+1}}}, \\
&G_{n_f-1,k+1} \in \frac{\Psi_{n_f-1,m}(\cdot)}{L^{\frac{n_f}{m+1}}} + s_{n_f,k} + \left[-\frac{\varepsilon_0}{L}, \frac{\varepsilon_0}{L} \right] + \sum_{l=n_f+1}^{m+1} \frac{\tau^{l-n_f}}{(l-n_f+1)!} \frac{\Psi_{l-1,m}(\cdot)}{L^{\frac{l}{m+1}}}, \quad (3.38) \\
&G_{n_f+j_d,k+1} \in \frac{\Psi_{n_f+j_d,m}(\cdot)}{L^{\frac{n_f+j_d+1}{m+1}}} + \frac{\tau^{n-j_d}}{(n+1-j_d)!} [-1,1] + \dots \\
&\dots + \sum_{l=j_d+1}^{n} \frac{\tau^{(l-j_d-1)}}{(l-j_d)!} s_{n_f+l,k} + \frac{\tau^{(l-j_d)}}{(l-j_d+1)!} \frac{\Psi_{n_f+l,m}(\cdot)}{L^{\frac{n_f+l+1}{m+1}}}, \\
&G_{m,k+1} \in \frac{\Psi_{m,m}(\cdot)}{L} + [-1,1], \\
&j_f = 1, 2, \cdots, n_f - 1, \;\; j_d = 0, 1, 2, \cdots, n-1.
\end{aligned}
$$

As $\boldsymbol{s}(t)$ *presents a piecewise constant derivative,* $\boldsymbol{s}(t)$ *satisfies the inclusion* $\dot{\boldsymbol{s}} \in \boldsymbol{G}(\boldsymbol{s}_k, \tau)$ *for* $t \neq t_k$*. Each solution of* $\dot{\boldsymbol{s}} \in \boldsymbol{G}(\boldsymbol{s}_k, \tau)$ *satisfies the following inclusions*

almost everywhere:

$$
\begin{aligned}
&\dot{s}_{j_f-1}(t) \in s_{j_f}\left(t-\rho[0,1]\right)+\frac{\Psi_{j_f-1,m}(\cdot)}{L^{\frac{j_f}{m+1}}}+\sum_{l=j_f+1}^{n_f+1} d_{n_f-j_f+1}^{n_f-l+2}\frac{\rho^{m+1-j_f}}{(l-j_f)!}\left[-1,1\right]+\ldots\\
&\ldots+\sum_{l=j_f+2}^{n_f+1}\frac{\rho^{l-j_f-1}}{(l-j_f)!}s_{l-1}(t-\rho[0,1])[-1,1]+\sum_{l=j_f+1}^{m+1}\frac{\rho^{l-j_f}}{(l-j_f+1)!}\frac{\Psi_{l-1,m}(\cdot)}{L^{\frac{l}{m+1}}}[-1,1],\\
&\dot{s}_{n_f-1}(t) \in \frac{\Psi_{n_f-1,m}(\cdot)}{L^{\frac{n_f}{m+1}}}+s_{n_f}(t-\rho[0,1])+\rho^{n+1}[-1,1]+\ldots\\
&\ldots+\sum_{l=n_f+1}^{m+1}\frac{\rho^{l-n_f}}{(l-n_f+1)!}\frac{\Psi_{l-1,m}(\cdot)}{L^{\frac{l}{m+1}}}[-1,1],\\
&\dot{s}_{n_f+j_d}(t) \in \frac{\Psi_{n_f+j_d,m}\left(\cdot\right)}{L^{\frac{n_f+j_d+1}{m+1}}}+s_{n_f+j_d+1}\left(t-\rho[0,1]\right)+\frac{\rho^{n-j_d}}{(n+1-j_d)!}\left[-1,1\right]+\ldots\\
&\ldots+\sum_{l=j_d+2}^{n}\frac{\rho^{(l-j_d-1)}}{(l-j_d)!}s_{n_f+l}\left(t-\rho[0,1]\right)\left[-1,1\right]+\ldots\\
&\ldots+\sum_{l=j_d+1}^{n}\frac{\rho^{(l-j_d)}}{(l-j_d+1)!}\frac{\Psi_{n_f+l,m}\left(\cdot\right)}{L^{\frac{n_f+l+1}{m+1}}}[-1,1],\\
&\dot{s}_{m-1}(t) \in \frac{\Psi_{m-1,m}\left(\cdot\right)}{L^{\frac{m}{m+1}}}+s_m\left(t-\rho[0,1]\right)+\frac{\rho}{2!}\left[-1,1\right]+\frac{\rho}{2!}\frac{\Psi_{m,m}\left(\cdot\right)}{L}[-1,1],\\
&\dot{s}_m(t) \in \frac{\Psi_{m,m}\left(\cdot\right)}{L}+\left[-1,1\right],\\
&\rho=\max\left\{\tau,\max_{0\leq j\leq n_f}\left(\frac{\varepsilon_j}{L}\right)^{\frac{1}{n+j+1}}\right\},\quad j_f=1,2,\cdots,n_f-1,\quad j_d=0,1,2,\cdots,n-2.
\end{aligned}
\tag{3.39}
$$

where the argument of $\Psi_{j,m}\left(\cdot\right)$ *in* (3.39) *is*

$$
s_0(t-\rho[-1,1])+\sum_{l=1}^{n_f} g_l^{n_f}\rho^{m+1}\left[-1,1\right]. \tag{3.40}
$$

As in the previous stability analysis, there are two key points in this structure. The first one is that if $\rho=0$*, the above inclusions becomes the inclusion* (1.68) *with* m *instead of* n*. The second one is that the above inclusion can be represented as:*

$$
\dot{\boldsymbol{s}}(t)\in\boldsymbol{C}_m\left(\boldsymbol{s}(t-\rho[0,1]),\boldsymbol{\Gamma}(\rho,\boldsymbol{s}(t-\rho[0,1]))\right), \tag{3.41}
$$

where $\boldsymbol{\Gamma}(\rho,\boldsymbol{s}(t))=[\Gamma_0(\rho,\boldsymbol{s}(t))\ \ \Gamma_1(\rho,\boldsymbol{s}(t))\ \ \cdots\ \ \Gamma_m(\rho,\boldsymbol{s}(t))]^T$ *with*

$$
\begin{aligned}
&\Gamma_0(\rho,\boldsymbol{s}(t-\rho[0,1]))=\sum_{l=1}^{n_f} g_l^{n_f}\rho^{m+1}\,[-1,1]\,,\\
&\Gamma_{j_f}(\rho,\boldsymbol{s}(t-\rho[0,1]))=\sum_{l=j_f+2}^{n_f+1}\frac{\rho^{l-j_f-1}}{(l-j_f)!}s_{l-1}(t-\rho[0,1])[-1,1]+\ldots\\
&\ldots+\sum_{l=j_f+1}^{n_f+1} d_{n_f-j_f+1}^{n_f-l+2}\frac{\rho^{m+1-j_f}}{(l-j_f)!}\,[-1,1]+\sum_{l=j_f+1}^{m+1}\frac{\rho^{l-j_f}}{(l-j_f+1)!}\frac{\Psi_{l-1,m}(\cdot)}{L^{\frac{l}{m+1}}}[-1,1],\\
&\Gamma_{n_f}(\rho,\boldsymbol{s}(t-\rho[0,1]))=\rho^{n+1}[-1,1]+\sum_{l=n_f+1}^{m+1}\frac{\rho^{l-n_f}}{(l-n_f+1)!}\frac{\Psi_{l-1,m}(\cdot)}{L^{\frac{l}{m+1}}}[-1,1],\\
&\Gamma_{n_f+j_d+1}(\rho,\boldsymbol{s}(t-\rho[0,1]))=\frac{\rho^{n-j_d}}{(n+1-j_d)!}\,[-1,1]+\ldots\\
&\ldots+\sum_{l=j_d+2}^{n}\frac{\rho^{(l-j_d-1)}}{(l-j_d)!}s_{n_f+l}\,(t-\rho[0,1])\,[-1,1]+\sum_{l=j_d+1}^{n}\frac{\rho^{(l-j_d)}}{(l-j_d+1)!}\frac{\Psi_{n_f+l,m}\,(\cdot)}{L^{\frac{n_f+l+1}{m+1}}}[-1,1],\\
&\Gamma_m(\rho,\boldsymbol{s}(t-\rho[0,1]))=\frac{\rho}{2!}\,[-1,1]+\frac{\rho}{2!}\frac{\Psi_{m,m}\,(\cdot)}{L}[-1,1],\\
&\rho=\max\left\{\tau,\max_{0\leq j\leq n_f}\left(\frac{\varepsilon_j}{L}\right)^{\frac{1}{n+j+1}}\right\},\quad j_f=1,2,\cdots,n_f-1,\quad j_d=0,1,2,\cdots,n-2.
\end{aligned}
\tag{3.42}
$$

Note that $\Gamma_j(\rho,\boldsymbol{s}(t))$ *satisfies the homogeneity condition, i.e., for all* $\alpha>0$, $\rho\geq 0$ *and* $\boldsymbol{s}(t)\in\mathbb{R}^{m+1}$, $\Gamma_j(\alpha^{-q}\rho,\alpha^{m+1}s_0(t),\alpha^m s_1(t),\cdots,\alpha s_m(t))=\alpha^{m-j+1}\Gamma_j(\rho,s_0(t),s_1(t),\cdots,s_m(t))$ *with* $q=-1$ *and* $j=0,\cdots,m$. *Although* $\Gamma_j(\rho,s_0(t),s_1(t),\cdots,s_m(t))$ *was used instead of* $\Gamma_j(\rho,\boldsymbol{s}(t))$, *hereafter only* $\Gamma_j(\rho,\boldsymbol{s}(t))$ *is used and* $\deg(s_j(t))=m+1-j$. *Furthermore, it is straightforward to see that for all* $\boldsymbol{s}(t)\in\mathbb{R}^{m+1}$, $\Gamma_j(\rho,\boldsymbol{s}(t))$ *satisfies the same properties as in Theorem 2.3.1 and 2.3.2.*

On the other hand, the undisturbed inclusion (3.41) satisfies the same properties than unperturbed system in the proofs of Theorem 2.3.1 y 2.3.2. Additionally, the inclusion (3.41) is not affected by the state values for $t<0$. *Hence, using Theorem 1 from [Levant & Livne 2016] and the properties of* $\boldsymbol{C}_m(\boldsymbol{s}(t),\boldsymbol{\Gamma}(\rho,\boldsymbol{s}(t)))$ *and* $\Gamma_j(\rho,\boldsymbol{s}(t))$, *one can deduce that after a finite-time transient, all indefinitely extendable solutions of the perturbed differential inclusion (3.41) enter and remain inside the region* $|s_j(t)|\leq\mu_j\rho^{m+1-j}$ *with* $\mu_j>0$. *Therefore,* $|\bar{\sigma}_{j,k}|\leq\mu_j\rho^{n+1-j}$ *and the accuracy (3.33) is obtained.*

From Theorem 3.5.2, one can deduce that MEDFD presents the same accuracy as the robust exact filtering differentiator for enough small sampling time. For bounded noise and enough small sampling time, MEDFD has an asymptotically optimal accuracy. Finally, it is shown that the proposed explicit discrete-time realization (3.15) preserves the homogeneity property of its continuous-time counterpart. To this end,

let $\bar{\rho}$ be defined as

$$\bar{\rho} = \max\left\{\left(\frac{\varepsilon_0}{L}\right)^{\frac{1}{n+1}}, \ \left(\frac{\varepsilon_1}{L}\right)^{\frac{1}{n+2}}, \ \cdots, \ \left(\frac{\varepsilon_{n_f}}{L}\right)^{\frac{1}{m+1}}\right\}. \tag{3.43}$$

Similar to (3.35), one obtains that $\bar{\omega}_{j_f,k}$ and $\bar{\sigma}_{j_d,k}$ satisfy the inclusion

$$\begin{aligned}
&\bar{\omega}_{j_f,k+1} \in \bar{\omega}_{j_f,k} + \tau\frac{\Psi_{j_f-1,m}(\cdot)}{L^{\frac{j_f}{m+1}}} + \frac{\tau^{n_f-j_f+1}}{(n_f-j_f+1)!}\left(\bar{\sigma}_{0,k} + \bar{\rho}^{n+1}[-1,1]\right) + \ldots \\
&\ldots + \sum_{l=j_f+1}^{n_f}\frac{\tau^{l-j_f}}{(l-j_f)!}\left(\bar{\omega}_{l,k} + d_{n_f-j_f+1}^{n_f-l+2}\bar{\rho}^{m+2-l}[-1,1]\right) + \ldots \\
&\ldots + \sum_{l=j_f+1}^{m+1}\frac{\tau^{l-j_f+1}}{(l-j_f+1)!}\frac{\Psi_{l-1,m}(\cdot)}{L^{\frac{l}{m+1}}}, \\
&\bar{\omega}_{n_f,k+1} \in \bar{\omega}_{n_f,k} + \tau\frac{\Psi_{n_f-1,m}(\cdot)}{L^{\frac{n_f}{m+1}}} + \tau\left(\bar{\sigma}_{0,k} + \bar{\rho}^{n+1}[-1,1]\right) + \ldots \\
&\ldots + \sum_{l=n_f+1}^{m+1}\frac{\tau^{l-n_f+1}}{(l-n_f+1)!}\frac{\Psi_{l-1,m}(\cdot)}{L^{\frac{l}{m+1}}}, \\
&\bar{\sigma}_{j_d,k+1} \in \bar{\sigma}_{j_d,k} + \tau\frac{\Psi_{n_f+j_d,m}(\cdot)}{L^{\frac{n_f+j_d+1}{m+1}}} + \frac{\tau^{n+1-j_d}}{(n+1-j_d)!}[-1,1] + \ldots \\
&\ldots + \sum_{l=j_d+1}^{n}\frac{\tau^{(l-j_d)}}{(l-j_d)!}\bar{\sigma}_{l,k} + \frac{\tau^{(l-j_d+1)}}{(l-j_d+1)!}\frac{\Psi_{n_f+l,m}(\cdot)}{L^{\frac{n_f+l+1}{m+1}}}, \\
&\bar{\sigma}_{n,k+1} \in \bar{\sigma}_{n,k} + \tau\frac{\Psi_{m,m}(\cdot)}{L} + \tau[-1,1], \\
&j_f = 1,2,\cdots,n_f-1, \ \ j_d = 0,1,2,\cdots,n-1,
\end{aligned} \tag{3.44}$$

where the argument of $\Psi_{\cdot,m}(\cdot)$ is given as

$$\bar{\omega}_{1,k} + \sum_{l=1}^{n_f} g_l^{n_f}\tau^{n_f-l}\bar{\rho}^{n+l+1}[-1,1]. \tag{3.45}$$

Lemma 3.2 *The explicit discrete-time realization* (3.15) *preserves the homogeneity property of its continuous-time counterpart.*

Proof *With the transformation*

$$\left(\tau,\bar{\rho},\bar{\omega}_1,\cdots,\bar{\omega}_{n_f},\bar{\sigma}_0,\cdots,\bar{\sigma}_n\right) \mapsto \left(\alpha\tau,\alpha\bar{\rho},\alpha^{m+1}\bar{\omega}_1,\ldots,\alpha^{n+2}\bar{\omega}_{n_f},\alpha^{n+1}\bar{\sigma}_0,\ldots,\alpha\bar{\sigma}_n\right), \tag{3.46}$$

for all $\alpha > 0$, the following equalities are obtained

$$
\begin{aligned}
&\sum_{l=1}^{n_f} g_l^{n_f} (\alpha\tau)^{n_f-l} (\alpha\bar{\rho})^{n+l+1} [-1,1] = \alpha^{m+1} \sum_{l=1}^{n_f} g_l^{n_f} \tau^{n_f-l} \bar{\rho}^{n+l+1} [-1,1], \\
&\Psi_{j,m} \left(\alpha^{m+1} \left(\bar{\omega}_{1,k} + \sum_{l=1}^{n_f} g_l^{n_f} \tau^{n_f-l} \bar{\rho}^{n+l+1} [-1,1] \right) \right) = \dots \\
&\alpha^{m-j} \Psi_{j,m} \left(\bar{\omega}_{1,k} + \sum_{l=1}^{n_f} g_l^{n_f} \tau^{n_f-l} \bar{\rho}^{n+l+1} [-1,1] \right), \\
&(\alpha\tau)^{n_f-j_f+1} \alpha^{n+1} \left(\bar{\sigma}_{0,k} + \bar{\rho}^{n+1}[-1,1] \right) = \alpha^{m+2-j_f} \tau^{n_f-j_f+1} \left(\bar{\sigma}_{0,k} + \bar{\rho}^{n+1}[-1,1] \right), \\
&\sum_{l=j_f+1}^{n_f} \frac{(\alpha\tau)^{l-j_f}}{(l-j_f)!} \alpha^{m+2-l} \left(\bar{\omega}_{l,k} + d_{n_f-j_f+1}^{n_f-l+2} \bar{\rho}^{m+2-l} [-1,1] \right) = \dots \\
&\alpha^{m+2-j_f} \sum_{l=j_f+1}^{n_f} \frac{\tau^{l-j_f}}{(l-j_f)!} \left(\bar{\omega}_{l,k} + d_{n_f-j_f+1}^{n_f-l+2} \bar{\rho}^{m+2-l} [-1,1] \right), \\
&\sum_{l=j_d+1}^{n} \frac{(\alpha\tau)^{(l-j_d)}}{(l-j_d)!} \alpha^{n+1-l} \bar{\sigma}_{l,k} = \alpha^{n+1-j_d} \sum_{l=j_d+1}^{n} \frac{\tau^{(l-j_d)}}{(l-j_d)!} \bar{\sigma}_{l,k}, \\
&\frac{(\alpha\tau)^{n+1-j_d}}{(n+1-j_d)!} [-1,1] = \alpha^{n+1-j_d} \frac{\tau^{n+1-j_d}}{(n+1-j_d)!} [-1,1].
\end{aligned}
\tag{3.47}
$$

Therefore, both sides of the inclusions (3.44) *have the same homogeneity degree with the same transformation.*

3.5.3 Stability analysis of the modified implicit discrete-time filtering differentiator (MIDFD)

The modified implicit discrete-time filtering differentiator (3.24) requires an estimation of r_0 (i.e., the roots of polynomials (3.22) and (3.23)). However, since there is no analytical expression for these roots, an interpolation method is needed to estimate r_0. Let the estimate of r_0 denoted as $\hat{r}_0$ and the associated estimation error as:

$$E_{1,k} = r_0 - \hat{r}_0. \tag{3.48}$$

From Lemma 3.1, it is clear that there exists an estimation error for $w_{1,k}$. Let the estimate of $w_{1,k}$ denoted as $\hat{w}_{1,k+1}$ and the associated estimation error as

$$E_{2,k} = w_{1,k+1} - \hat{w}_{1,k+1}. \tag{3.49}$$

It can be expressed as

$$E_{2,k} = \begin{cases} -(r_0)^{m+1} + (r_0 - E_{1,k})^{m+1} & \text{if} \quad b_k > a_0 \\ 0 & \text{if} \quad b_k \in [-a_0, a_0] \\ (r_0)^{m+1} - (r_0 - E_{1,k})^{m+1} & \text{if} \quad b_k < -a_0 \end{cases},$$
$$E_{2,k} = \begin{cases} E_{1,k}\left(e_1^m r_0^m + \cdots + e_m^m E_{1,k}^{m-1} r_0 + E_{1,k}^m\right) & \text{if} \quad b_k > a_0 \\ 0 & \text{if} \quad b_k \in [-a_0, a_0] \\ -E_{1,k}\left(e_1^m r_0^m + \cdots + e_m^m E_{1,k}^{m-1} r_0 + E_{1,k}^m\right) & \text{if} \quad b_k < -a_0 \end{cases}, \tag{3.50}$$

where e_j^m are the coefficients of the well-known Pascal's triangle with a respective change of sign, i.e., $e_j^m = (-1)^j \frac{(m+1)!}{j!(m-j+1)!}$. From Equation (3.50), one can deduce that $E_{2,k}$ is a continuous function of $E_{1,k}$ and is equal to zero if $E_{1,k} = 0$. Therefore, for any $\kappa \geq 0$ and r_0, there is a maximum tolerable error $M_{E_{1,k}} > 0$ such that $|E_{2,k}| \leq \kappa$ if $|E_{1,k}| \leq M_{E_{1,k}}$. Indeed, $M_{E_{1,k}}$ depends on b_k and a_j. Hence, it depends on $w_{j,k}$, σ_0, Δ_k, τ, L, n_f, λ_j and m. Taking into account the estimation error of r_0, the following assumption is presented.

Assumption 3.5.1 *It is assumed that $\hat{r}_0 > 0$ and that the estimation error $E_{2,k}$ is bounded by a constant $\kappa > 0$, i.e., $|E_{2,k}| \leq \kappa$.*

With the previous assumption, the following theorem can be derived.

Theorem 3.5.3

Let $\boldsymbol{z}_k$ be generated with the modified implicit discrete-time filtering differentiator (3.24) with $n_f > 0$. Under Assumptions 1.3.1, 1.3.4, 3.3.1, 3.5.1, there exist constants $\mu_{j_d} > 0$ such that after a finite-time transient, the following inequalities are verified:

$$|z_{j_d,k} - x_{j_d,k}| \leq \mu_{j_d} L \rho^{n+1-j_d}, \rho = \max\left\{\tau,\ \left(\frac{\kappa}{L}\right)^{\frac{1}{m+1}},\ \max_{0\leq j\leq n_f}\left\{\left(\frac{\varepsilon_j}{L}\right)^{\frac{1}{n+j+1}}\right\}\right\}, \tag{3.51}$$

where $j_d = 0, 1, \cdots, n$ and the coefficients μ_{j_d} only depend on the differentiator parameters $\lambda_0, \ldots, \lambda_m$.

Proof *Similarly to Theorem 3.5.2, for systems (2.1) and (3.24), the error dynamics*

are given as:

$$
\begin{aligned}
&w_{j_f,k+1} = \frac{\tau^{(n_f-j_f+1)}}{(n_f-j_f+1)!}(\sigma_{0,k}-\Delta_k) + \sum_{l=j_f}^{n_f}\frac{\tau^{(l-j_f)}}{(l-j_f)!}w_{l,k} + \dots \\
&\dots + \sum_{l=j_f}^{m+1}\frac{\tau^{(l-j_f+1)}}{(l-j_f+1)!}\bar{\Psi}_{l-1,m}\left(\hat{w}_{1,k+1}\right), \\
&\sigma_{j_d,k+1} = -h_{j,k} + \sum_{l=j_d}^{n}\frac{\tau^{(l-j_d)}}{(l-j_d)!}\sigma_{l,k} + \frac{\tau^{(l-j_d+1)}}{(l-j_d+1)!}\bar{\Psi}_{n_f+l,m}\left(\hat{w}_{1,k+1}\right), \\
&\bar{\Psi}_{j,m}\left(\hat{w}_{1,k+1}\right) = -\lambda_{m-j}L^{\frac{j+1}{m+1}}\left|\hat{w}_{1,k+1}\right|^{\frac{m-j}{m+1}}\xi_k, \quad j_f = 1,2,\cdots,n_f. \\
&j_d = 0,1,2,\cdots,n.
\end{aligned}
\tag{3.52}
$$

Due to the inclusion $\xi_k \in sign(\hat{w}_{1,k+1})$ *and the fact that* ξ_k *is not affected by* $E_{1,k}$, $\bar{\Psi}_{j,n}\left(\hat{w}_{1,k+1}\right) = \Psi_{j,n}\left(\hat{w}_{1,k+1}\right)$ *and* $\bar{\Psi}_{m,m}\left(\hat{w}_{1,k+1}\right) \in \Psi_{m,m}\left(\hat{w}_{1,k+1}\right)$ *for* $j = 0,1,2,\cdots,m-1$. *Hence, using the change of variables* (3.32), *one can obtain:*

$$
\begin{aligned}
&\bar{\omega}_{j_f,k+1} \in \bar{\omega}_{j_f,k} + \tau\frac{\Psi_{j_f-1,m}(\cdot)}{L^{\frac{j_f}{m+1}}} + \frac{\tau^{n_f-j_f+1}}{(n_f-j_f+1)!}\left(\bar{\sigma}_{0,k} + \left[-\frac{\varepsilon_0}{L},\frac{\varepsilon_0}{L}\right]\right) + \dots \\
&\dots + \sum_{l=j_f+1}^{n_f}\frac{\tau^{l-j_f}}{(l-j_f)!}\left(\bar{\omega}_{l,k} + d_{n_f-j_f+1}^{n_f-l+2}\left[-\frac{\varepsilon_{n_f-l+1}}{L},\frac{\varepsilon_{n_f-l+1}}{L}\right]\right) + \dots \\
&\dots + \sum_{l=j_f+1}^{m+1}\frac{\tau^{l-j_f+1}}{(l-j_f+1)!}\frac{\Psi_{l-1,m}(\cdot)}{L^{\frac{l}{m+1}}}, \\
&\bar{\omega}_{n_f,k+1} \in \bar{\omega}_{n_f,k} + \tau\frac{\Psi_{n_f-1,m}(\cdot)}{L^{\frac{n_f}{m+1}}} + \tau\left(\bar{\sigma}_{0,k} + \left[-\frac{\varepsilon_0}{L},\frac{\varepsilon_0}{L}\right]\right) + \dots \\
&\dots + \sum_{l=n_f+1}^{m+1}\frac{\tau^{l-n_f+1}}{(l-n_f+1)!}\frac{\Psi_{l-1,m}(\cdot)}{L^{\frac{l}{m+1}}}, \\
&\bar{\sigma}_{j_d,k+1} \in \bar{\sigma}_{j_d,k} + \tau\frac{\Psi_{n_f+j_d,m}\left(\cdot\right)}{L^{\frac{n_f+j_d+1}{m+1}}} + \frac{\tau^{n+1-j_d}}{(n+1-j_d)!}\left[-1,1\right] + \dots \\
&\dots + \sum_{l=j_d+1}^{n}\frac{\tau^{(l-j_d)}}{(l-j_d)!}\bar{\sigma}_{l,k} + \frac{\tau^{(l-j_d+1)}}{(l-j_d+1)!}\frac{\Psi_{n_f+l,m}\left(\cdot\right)}{L^{\frac{n_f+l+1}{m+1}}}, \\
&\bar{\sigma}_{n,k+1} \in \bar{\sigma}_{n,k} + \tau\frac{\Psi_{m,m}\left(\cdot\right)}{L} + \tau\left[-1,1\right],
\end{aligned}
\tag{3.53}
$$

where $j_f = 1,2,\cdots,n_f$, $j_d = 0,1,2,\cdots,n$ *and the argument of* $\upsilon_{j,m}(\cdot)$ *in* (3.53) *is given as*

$$
\bar{\omega}_{1,k+1} + \left[-\frac{\kappa}{L},\frac{\kappa}{L}\right] + \sum_{l=1}^{n_f} g_l^{n_f}\tau^{n_f-l}\left[-\frac{\varepsilon_l}{L},\frac{\varepsilon_l}{L}\right], \tag{3.54}
$$

with constant $g_l^{n_f}$ *as in Table 3.2. Similarly to proof of Theorem 3.5.2, using the homogeneity property, one can easily deduce inequality* (3.51).

From Theorem 3.5.3, one can deduce that MIDFD presents the same accuracy as the robust exact filtering differentiator for enough small sampling time and κ. Furthermore, with the above conditions and a discretely sampled signal of global filtering order 0 (bounded noise), MIDFD has an asymptotically optimal accuracy. Ultimately, it is showed that MIDFD preserves the homogeneity property of its continuous-time counterpart. Similar to (3.35) and (3.44), the following inclusion is obtained:

$$\begin{aligned}
&\bar{\omega}_{j_f,k+1} \in \bar{\omega}_{j_f,k} + \tau \frac{\Psi_{j_f-1,m}(\cdot)}{L^{\frac{j_f}{m+1}}} + \frac{\tau^{n_f-j_f+1}}{(n_f-j_f+1)!}\left(\bar{\sigma}_{0,k} + \bar{\rho}^{n+1}[-1,1]\right) + \dots \\
&\dots + \sum_{l=j_f+1}^{n_f} \frac{\tau^{l-j_f}}{(l-j_f)!}\left(\bar{\omega}_{l,k} + d^{n_f-l+2}_{n_f-j_f+1}\bar{\rho}^{m+2-l}[-1,1]\right) + \dots \\
&\dots + \sum_{l=j_f+1}^{m+1} \frac{\tau^{l-j_f+1}}{(l-j_f+1)!}\frac{\Psi_{l-1,m}(\cdot)}{L^{\frac{l}{m+1}}}, \\
&\bar{\omega}_{n_f,k+1} \in \bar{\omega}_{n_f,k} + \tau \frac{\Psi_{n_f-1,m}(\cdot)}{L^{\frac{n_f}{m+1}}} + \tau\left(\bar{\sigma}_{0,k} + \bar{\rho}^{n+1}[-1,1]\right) + \dots \\
&\dots + \sum_{l=n_f+1}^{m+1} \frac{\tau^{l-n_f+1}}{(l-n_f+1)!}\frac{\Psi_{l-1,m}(\cdot)}{L^{\frac{l}{m+1}}}, \\
&\bar{\sigma}_{j_d,k+1} \in \bar{\sigma}_{j_d,k} + \tau \frac{\Psi_{n_f+j_d,m}(\cdot)}{L^{\frac{n_f+j_d+1}{m+1}}} + \frac{\tau^{n+1-j_d}}{(n+1-j_d)!}[-1,1] + \dots \\
&\dots + \sum_{l=j_d+1}^{n} \frac{\tau^{(l-j_d)}}{(l-j_d)!}\bar{\sigma}_{l,k} + \frac{\tau^{(l-j_d+1)}}{(l-j_d+1)!}\frac{\Psi_{n_f+l,m}(\cdot)}{L^{\frac{n_f+l+1}{m+1}}}, \\
&\bar{\sigma}_{n,k+1} \in \bar{\sigma}_{n,k} + \tau \frac{\Psi_{m,m}(\cdot)}{L} + \tau[-1,1], \quad j_f = 1,2,\cdots,n_f-1, \\
&j_d = 0,1,2,\cdots,n-1.
\end{aligned} \tag{3.55}$$

where the arguments of $\Psi_{\cdot,m}(\cdot)$ and $\bar{\rho}$ are given as:

$$\begin{aligned}
&\bar{\omega}_{1,k+1} + \bar{\rho}^{m+1}[-1,1] + \sum_{l=1}^{n_f} g_l^{n_f}\tau^{n_f-l}\bar{\rho}^{n+l+1}[-1,1], \\
&\bar{\rho} = \max\left\{\left(\frac{\kappa}{L}\right)^{\frac{1}{m+1}}, \max_{0\le j\le n_f}\left\{\left(\frac{\varepsilon_j}{L}\right)^{\frac{1}{n+j+1}}\right\}\right\}.
\end{aligned} \tag{3.56}$$

Lemma 3.3 *The implicit discrete-time filtering differentiator (3.24) preserves the homogeneity property of its continuous-time counterpart.*

Proof *The proof is similar to the presented one for Lemma 3.2.*

Remark 3.5.1 *b_k can be represented as a function of $\bar{\omega}_{j_f,k}$, $\bar{\sigma}_{0,k}$, τ and $\beta^0_{j,\cdot}$. Then, b_k satisfies an inclusion which is homogeneous. Hence, after the finite-time transient mentioned in Theorem 3.5.3, b_k and r_0 are bounded.*

3.5.4 Stability analysis of the explicit discrete-time filtering differentiator (EDFD)

In this subsection, it is assumed that $|x_{j,k}| \leq D_j$ for $j = 1, \cdots, n$ where D_j is a constant. It should be highlighted that MEDFD and MIDFD do not require this assumption.

Theorem 3.5.4

Let $\boldsymbol{z}_k$ be generated with the explicit discrete-time filtering differentiator (3.14), with $n_f > 0$. Furthermore, let $x_{l,k}$ be bounded by D_l with $l = 1, \cdots, n$. Under Assumptions 1.3.1, 1.3.4, 3.3.1, there exist constants $\mu_{j_d} > 0$ such that after a finite-time transient, the following inequalities are fulfilled:

$$\begin{aligned} &|z_{j_d,k} - x_{j_d,k}| \leq \mu_{j_d} L \rho^{n+1-j_d}, \\ &\rho = \max\left\{\tau, \max_{0\leq j\leq n}\left\{\left(\frac{D_j}{L}\right)^{\frac{1}{n+j+1}}\right\}, \max_{0\leq j\leq n_f}\left\{\left(\frac{\varepsilon_j}{L}\right)^{\frac{1}{n+j+1}}\right\}\right\}, \end{aligned} \tag{3.57}$$

where $j_d = 0, 1, \cdots, n$ and the coefficients μ_{j_d} only depend on the differentiator parameters $\lambda_0, \ldots, \lambda_m$.

Proof *From Equations (2.1) and (3.14), the following discrete-time error system is obtained*

$$\begin{aligned} w_{j_f,k+1} &= -\frac{\tau^{(n_f-j_f+1)}}{(n_f-j_f+1)!}\Delta_k + \sum_{l=j_f}^{m+1}\frac{\tau^{(l-j_f+1)}}{(l-j_f+1)!}\upsilon_{l-1,m}\left(w_{1,k}\right) + \ldots \\ \ldots &+ \sum_{l=j_f}^{n_f}\frac{\tau^{(l-j_f)}}{(l-j_f)!}w_{l,k} + \sum_{l=1}^{n}\frac{\tau^{n_f-j_f+l+1}}{(n_f-j_f+l+1)!}\left(\sigma_{l,k}+x_{l,k}\right), \\ z_{j_d,k+1} &= \sum_{l=j_d}^{n}\frac{\tau^{(l-j_d)}}{(l-j_d)!}z_{l,k} + \frac{\tau^{(l-j_d+1)}}{(l-j_d+1)!}\upsilon_{n_f+l,m}\left(w_{1,k}\right), \end{aligned} \tag{3.58}$$

with $j_f = 1, 2, \cdots, n_f$, $j_d = 0, 1, 2, \cdots, n$. The remainder of the proof is similar to the proofs presented in Theorems 3.5.2 and 3.5.3.

It is evident that the terms $\frac{\tau^{n_f-j_f+l+1}}{(n_f-j_f+l+1)!}z_{l,k}$ in the equations of filtering part may cause instability of the estimation error for signals with unbounded derivatives. In such case, the EDFD loses the accuracy of the continuous-time robust exact the the filtering differentiator. Nevertheless, if D_j and the sampling time are sufficiently small, EDFD presents the same accuracy as the robust exact filtering differentiator. At last, one can mention that an implicit scheme can be proposed based on EDFD. However, it will depend on D_j.

3.6 Comparison between the discrete-time differentiator based on the robust exact filtering differentiator

The realizations obtained from the differentiator (1.69) are compared in this section, which are EDFD (3.14), MEDFD (3.15) and MIDFD (3.24). Additionally, the discrete-time differentiators presented in [Levant & Livne 2019] and [Hanan *et al.* 2020], are added to this comparison. They are the differentiator DFD [Levant & Livne 2019] and ADFD [Hanan *et al.* 2020].

3.6.1 Simulation I: Noise-free case

In this simulation, $f_0(t) = t^4 + \sin(t)$ and $\Delta(t) = 0$. The simulation parameters are $n_f = 7$, $n = 3$, $\tau = 0.005\,\text{sec}$, $L = 25$ and $k_L = 1000$. The parameters λ_j are selected as in [Jbara *et al.* 2020], $\lambda_0 = 1.1$, $\lambda_1 = 36.3354$, $\lambda_2 = 586.7823$, $\lambda_3 = 5025.3982$, $\lambda_4 = 19894.4668$, $\lambda_5 = 31601.1491$, $\lambda_6 = 24295.4978$, $\lambda_7 = 8907.9978$, $\lambda_8 = 1908.4659$, $\lambda_9 = 251.9857$ and $\lambda_{10} = 20$. In this simulation, $t_{max} = 100\,\text{sec}$ and the same initial conditions $\begin{bmatrix}\boldsymbol{w}_0^T & \boldsymbol{z}_0^T\end{bmatrix}$ are used for each differentiator, $\begin{bmatrix}\boldsymbol{w}_0^T & \boldsymbol{z}_0^T\end{bmatrix} = [\mathbf{0} \quad \mathbf{0}]$. For the two performance indexes, it is selected $t_{min} = 25\,\text{sec}$ (i.e., at this time, the discrete-time differentiation errors, except for the EDFD, have already converged to a vicinity of the origin). The corresponding results are given in Figure 2.6 and Table 3.3.

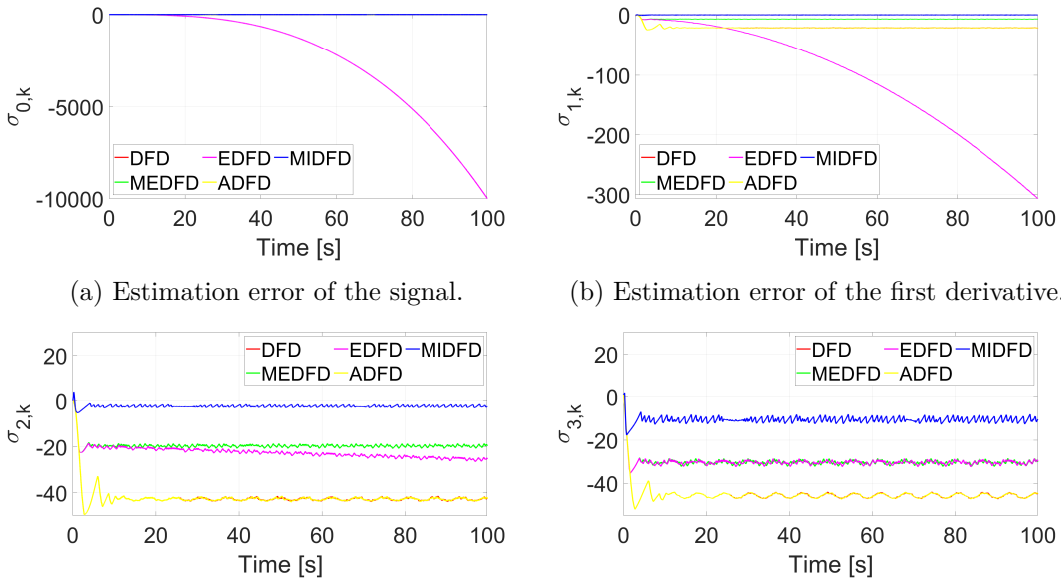

(a) Estimation error of the signal.

(b) Estimation error of the first derivative.

(c) Estimation error of the second derivative.

(d) Estimation error of the third derivative.

Figure 3.1: Estimation error of the signal and its derivatives in Simulation I.

MAE/RMSE	DFD	EDFD	MEDFD	MIDFD	ADFD
Y_0	5.19	9999.16	1.25	2.32×10^{-2}	5.2
Y_1	21.88	306.87	7.33	0.37	21.94
Y_2	43.99	26.56	20.8	2.98	44.15
Y_3	47.3	32.44	32.28	12.65	47.44
y_0	4.97	4364.33	1.19	1.58×10^{-2}	4.97
y_1	21.32	160.75	6.95	0.27	21.32
y_2	42.81	23.4	19.62	2.32	42.81
y_3	45.75	30.44	30.39	10.58	45.75

Table 3.3: Indexes Y_j and y_j for each discrete-time differentiator in Simulation I.

Note that the ADFD is mainly useful when L is overestimated, which is not the case in this simulation. According to Theorems 3.5.2 and 3.5.3, the estimation errors for MEDFD and MIDFD converge to a vicinity of the origin after a finite time. Furthermore, as shown in Figure 3.2, b_k and r_0 remain bounded according to Remark 3.5.1. Furthermore, as $x_{1,k}$, $x_{2,k}$ and $x_{3,k}$ are unbounded, the estimation error for EDFD increases as t increases, conforming to Theorem 3.5.4. As it can be seen in Table 3.3, the best estimations are obtained with the proposed MIDFD, followed by MEDFD.

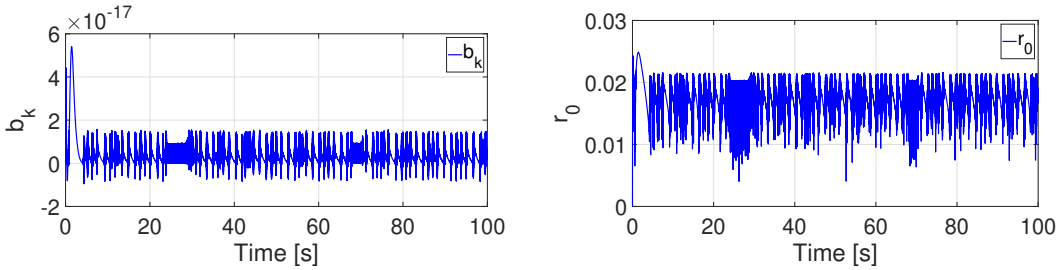

(a) b_k. (b) r_0.

Figure 3.2: b_k and r_0 for MIDFD in Simulation II.

3.6.2 Simulation II: Differentiation with measurement noise

In this simulation, $x_0(t) = \sin(3t) + \cos(2t) - sin(t)$. The simulation parameters are $n_f = 7$, $n = 3$, $\tau = 0.002\,\text{sec}$, $\Delta(t) \sim$ i.i.d. $\mathcal{N}(0, 0.1^2)$, $k_L = 300$ and $L = 90$. The parameters λ_j and initial conditions $\begin{bmatrix} \boldsymbol{w}_0^T & \boldsymbol{z}_0^T \end{bmatrix}$ are selected as in the previous simulation. $t_{min} = 2\,\text{sec}$ and $t_{max} = 10\,\text{sec}$. The corresponding results are presented in Figure 3.3 and Table 3.4.

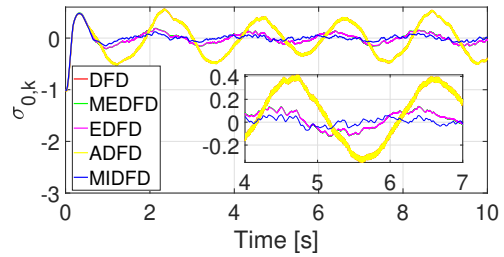

(a) Estimation error of the signal.

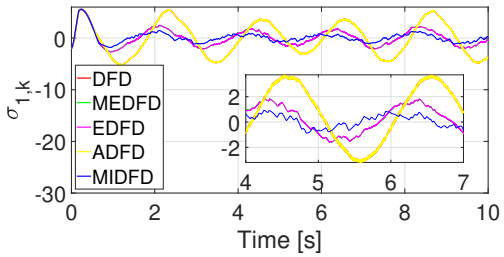

(b) Estimation error of the first derivative.

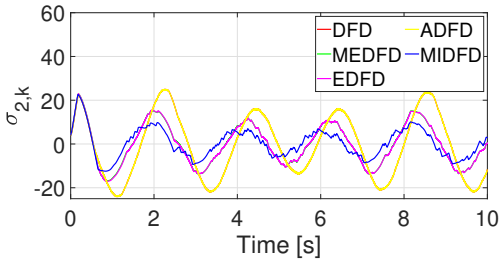

(c) Estimation error of the second derivative.

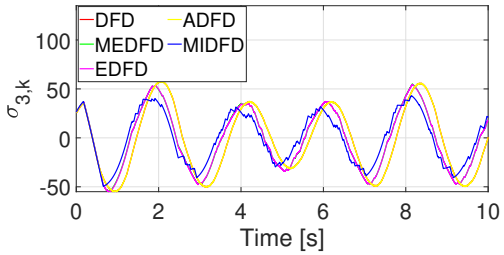

(d) Estimation error of the third derivative.

Figure 3.3: Estimation error of the signal and its derivatives in Simulation II.

MAE/RMSE	DFD	EDFD	MEDFD	MIDFD	ADFD
Y_0	0.56	0.18	0.19	0.12	0.56
Y_1	5.53	2.43	2.42	1.46	5.53
Y_2	25.01	15.18	15.15	10.04	25.01
Y_3	57.8	54.66	55.06	42.99	57.80
y_0	0.32	9.04×10^{-2}	9.42×10^{-2}	4.51×10^{-2}	0.32
y_1	3.11	1.30	1.31	0.65	3.11
y_2	14.26	8.58	8.58	5.32	14.26
y_3	33.06	29.28	29.29	23.92	33.06

Table 3.4: Indexes Y_j and y_j for each discrete-time differentiator in Simulation II.

The behavior of the estimation errors for MEDFD, MIDFD, and EDFD corresponds to the theoretical results given in Theorems 3.5.2, 3.5.3, 3.5.4. Indeed, the estimation errors for MEDFD, MIDFD, EDFD converge to a vicinity of the origin after a finite time. As it can be seen in Table 3.4 and Figure 3.3, the best performance is obtained using MIDFD.

3.6.3 Simulation III: Differentiation with measurement noise and different sampling times

In this simulation, $f_0(t) = \sin(3t) + \cos(2t) - \sin(t)$ with $\Delta(t) = 5\cos(10^8 t)$ and under different sampling times $\tau \in [0.000005\,\text{sec}, 0.1\,\text{sec}]$, in specific, 25 logarithmically spaced points were used. Contrary to the previous simulations, Y_j is plotted with different sampling times. The simulation parameters are $n_f = 3$, $n = 3$, $k_L = 10^5$, $L = 90$, $\lambda_0 =$

1.1, $\lambda_1 = 9.91$, $\lambda_2 = 43.6484$, $\lambda_3 = 101.9548$, $\lambda_4 = 110.0817$, $\lambda_5 = 47.6904$, $\lambda_6 = 10$, $t_{min} = 5\,\text{sec}$ and $t_{max} = 15\,\text{sec}$. Initial conditions are selected as $\begin{bmatrix} \boldsymbol{w}_0^T & \boldsymbol{z}_0^T \end{bmatrix} = [\mathbf{0}\ \ \mathbf{0}]$. The corresponding results are presented in Figure 3.4. As it can be seen in Figure 3.4, the best performance is obtained using MIDFD for almost any signal and sampling time.

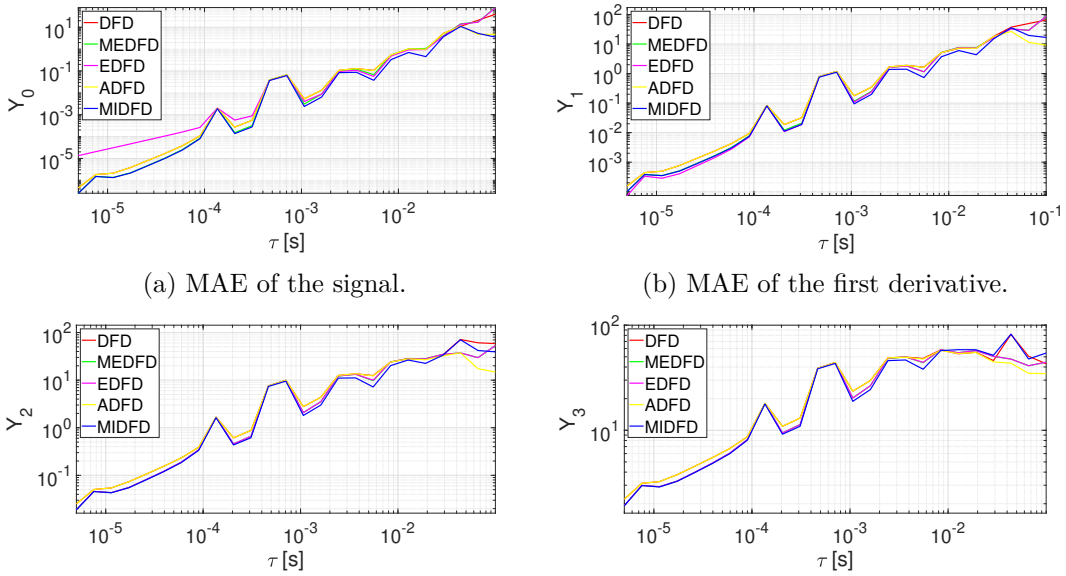

(a) MAE of the signal.

(b) MAE of the first derivative.

(c) MAE of the second derivative.

(d) MAE of the third derivative.

Figure 3.4: Maximum Absolute Error.

3.6.4 Simulation IV: Differentiation with large measurement noise

This simulation aims to show that the differentiator MIDFD has a better performance than DFD, in the noise case. In this simulation, the differentiator and filtering order are selected as $n = 3$ and $n_f = 4$, with the parameters $T = 0.001$s, $L = 2$, $\lambda_0 = 1.1$, $\lambda_1 = 14.13$, $\lambda_2 = 88.78$, $\lambda_3 = 295.74$, $\lambda_4 = 455.4$, $\lambda_5 = 281.37$, $\lambda_6 = 84.14$ and $\lambda_7 = 12$. The input signal is $f_0(t) = \text{sen}(()t) - \cos(0.5t)$ and the measurement noise is defined with $\beta_{j,k}^0 = \varepsilon_0(-1)^k$, with $\varepsilon_0 = 0.01$. As it can been seen in Figure 3.5, MIDFD obtains has a good estimation of the signal and its derivatives, in contrast to DFD, which has a constant error when they obtains its respective accuracy. However, it is important to mention that DFD improve its accuracy reducing the sampling time.

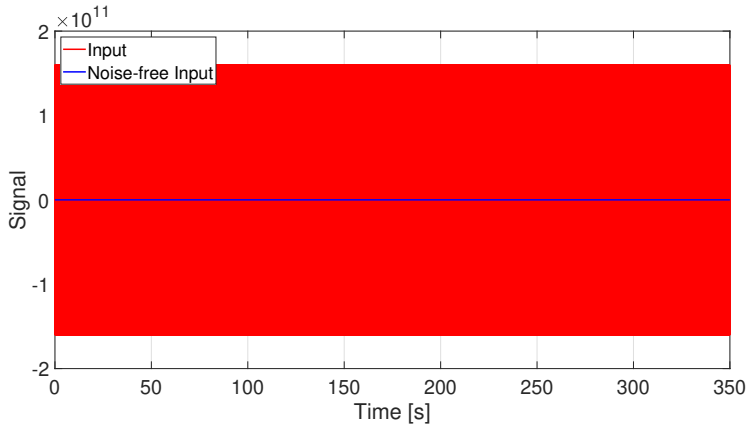

Figure 3.5: Input of the differentiator.

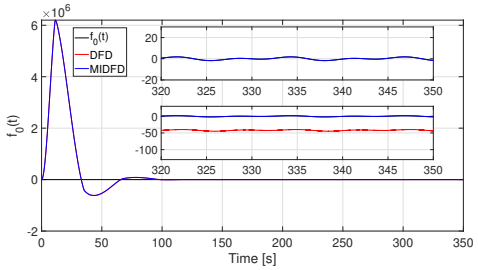

(a) Estimation of the signal.

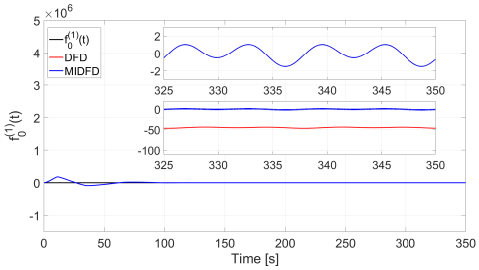

(b) Estimation of the first derivative.

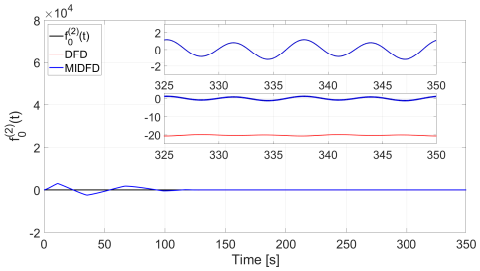

(c) Estimation of the second derivative.

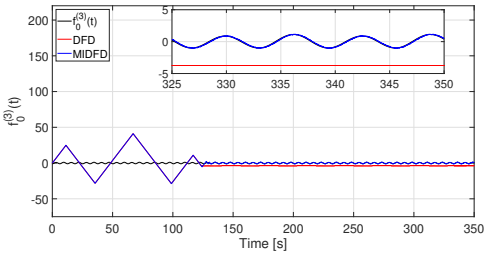

(d) Estimation of the third derivative.

Figure 3.6: Estimation of the input and its derivatives.

3.6.5 Simulation V: Simulation with different signals

This simulation is used to show the performance of the differentiators with different signals, then $f_0(t)$ is defined as:

$$f_0(t) = \begin{cases} \frac{t^4}{25} & \text{if} \quad t < 5\text{s} \\ 25 + \ln\left(\frac{1}{t-4}\right) & \text{if} \quad 5\text{s} \leq t < 15\text{s} \\ 22.6021 + 5\text{sen}(t-15) & \text{if } 15\text{s} \leq t < 40\text{s} \\ 1.9403 + 20e^{-\frac{t}{2}+20} & \text{if } 40\text{s} \leq t \end{cases} \tag{3.59}$$

The initial conditions, parameters λ_j, n_f and n are selected as in Simulation I and II. $L = 10$ and $\Delta(t) = 0$. Concerning the functions, they have a bounded forth derivative

for almost any time ($t \neq 5, 15, 40$). Moreover, since, there is a switch of functions, its estimations errors are changing. The results are presented in Figures 3.7-3.8, where the best estimations are obtained with MIDFD.

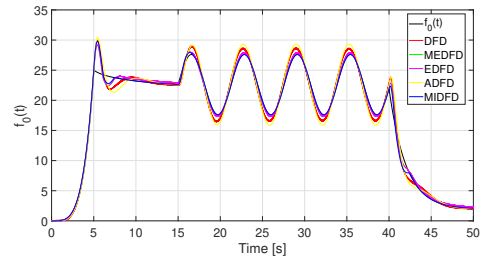

(a) Estimation of the signal.

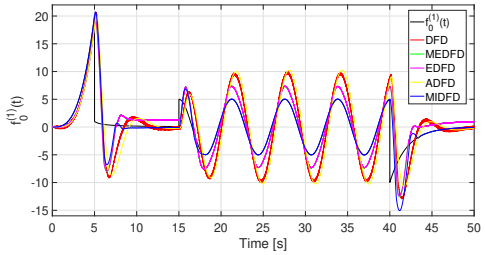

(b) Estimation of the first derivative.

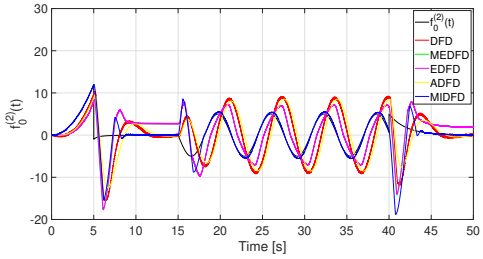

(c) Estimation of the second derivative.

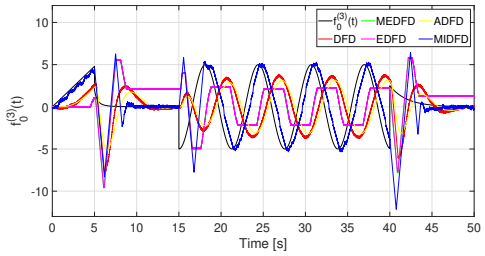

(d) Estimation of the third derivative.

Figure 3.7: Estimation of the input and its derivatives.

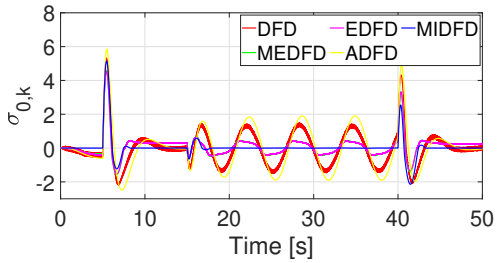

(a) Estimation error of the function.

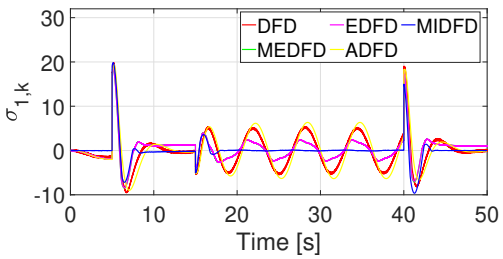

(b) Estimation error of the first derivative.

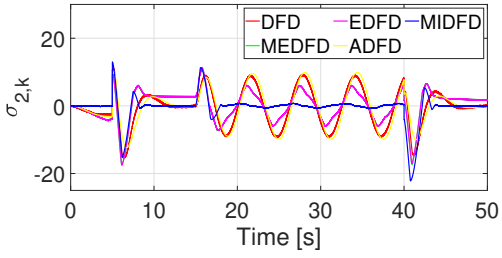

(c) Estimation error of the second derivative.

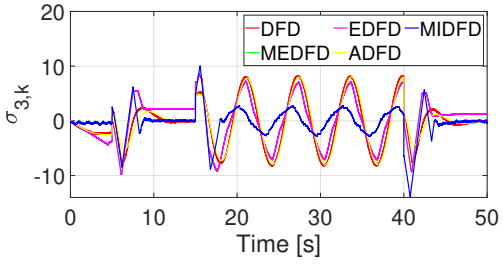

(d) Estimation error of the third derivative.

Figure 3.8: Estimation errors of the input and its derivatives.

3.7 Conclusion

In this Chapter, we have introduced and analyzed four discrete-time realizations of the robust exact filtering differentiator, i.e. explicit and implicit ones, namely MIDFD, MEDFD, EDFD and Matching ones. A time discretization, relying on the stabilization of a pseudo linear discrete-time system has been proposed using the matching approach. EDFD, based on the methodology used to obtain an exact discretization of linear systems with a zero-order hold, has been investigated. It does not preserve the continuous-time differentiator properties for signals with unbounded derivatives due to high-order terms in the filter dynamics. Hence, MEDFD and MIDFD has been proposed to preserve the homogeneity property and the accuracy of its continuous-time counterpart after a finite-time. MIDFD is an implicit discrete-time realization that is non-anticipative. At last, a detailed comparative study with DFD [Levant & Livne 2019] and ADFD [Hanan *et al.* 2020], was performed in simulation, highlighting that the implicit scheme supersedes the explicit one.

In the next Chapter, we will investigate the design of an appropriate output feedback controller using the proposed discrete-time realization of the robust exact filtering differentiator.

CHAPTER 4

Output Feedback Stabilization of Integrator Chains using MIDFD

4.1 Introduction

Many control engineering applications require a real-time estimate of the time derivatives of a noisy sampled signal. Indeed, a control law often needs the derivatives of noisy signals (i.e., the measurements). Hence, several works consider the design of sliding mode differentiator-based controllers due to finite-time property (see [Oliveira *et al.* 2017, Castañeda *et al.* 2021] for instance). However, differentiators require high gains to deal with the system uncertainties when they are used in a closed-loop. It is even more difficult when high-order differentiators are needed since it yields the sensitivity of the closed-loop system with respect to measurement noise and discretization effect. It should be highlighted that the sampled-data sliding mode differentiator-based control design is not well-investigated in the literature.

In this Chapter, we will restrict our study to the stabilization problem for perturbed chain of integrators using sampled noisy measurements. A discrete-time observer is needed to design a sampled-data output feedback controller. In the previous Chapter, a discrete-time version of the filtering differentiator [Levant & Livne 2019] is derived to compensate for the effects of some large noises after a finite time. In this Chapter, we include some additional terms related to the control input in the discrete-time differentiator. This enables to avoid to increase the value of L. Furthermore, the convergence of the observer to a vicinity of the origin is ensured for any initial conditions. Besides, it can be proved, using the homogeneity property, that the proposed discrete-time realization preserves the accuracy of the continuous-time robust exact filtering differentiator despite measurement noise. Then, the sampled-data sliding mode differentiator based controller is designed. From this design, various challenging issues arise:

- How can we design an appropriate saturated output feedback controller to guarantee that the associated closed-loop discrete-time system is stable?

- What is the link between the accuracy of the observer and the convergence region for the trajectories of the closed-loop system?

In this Chapter, we will give answers to these questions. The main contributions are as follows:

- A sampled-data implicit sliding mode differentiator-based observer is investigated.
- The link between the disturbance bound and the observer parameters of the filtering differentiator is discussed.
- A stability analysis of the closed-loop system combining the robust exact filtering observer and a saturated output feedback controller is provided for integrator chains with sampled data.
- A comparison between the implicit discrete-time closed-loop differentiator and the explicit one [Levant & Livne 2019] is given to highlight the advantages in terms of accuracy of the proposed scheme.
- Experiments are conducted on the DC-DC buck converter to show the effectiveness of the proposed scheme.

The results presented in this Chapter were published in [Alarcón-Carbajal *et al.* 2022] and [Carvajal-Rubio *et al.* 2022]. The organization of this Chapter is as follows. In Section 4.2, the considered problem (i.e., stabilization problem for perturbed chain of integrators using sampled noisy measurements) is mathematically formalized. Section 4.3 is focused on the design of the output feedback control law. First, an implicit discrete-time realization of the robust exact filtering differentiator will be derived to include some additional terms related to the control input. The temporal discretization of the continuous-time closed-loop system will be also introduced. The stability of the closed-loop system is studied in Section 4.4. In order to show its performance, simulations and experimental results are presented in Section 4.5 and Section 4.6, respectively. The conclusion is presented in Section 4.6.

4.2 Problem statement

Let us consider the stabilization problem for perturbed chain of integrators, described by the following dynamics

$$\dot{\boldsymbol{x}} = \boldsymbol{A}\boldsymbol{x} + \boldsymbol{e}_{n+1}\left(d(t) + u(t)\right); \quad y(t_k) = \bar{x}_{0,k} = x_0(t_k) + \Delta(t_k), \tag{4.1}$$

where the state is $\boldsymbol{x} = \begin{bmatrix} x_0 & x_1 & x_2 & \cdots & x_n \end{bmatrix}^T \in \mathbb{R}^{n+1}$, the control input is $u(t) \in \mathbb{R}$ and the discrete-time output measurement is $y(t_k) \in \mathbb{R}$. The measurement noise $\Delta_k = \Delta(t_k)$ satisfies Assumption 3.3.1 and the perturbation $d(t)$ is bounded by a known constant, i.e., $|d(t)| \leq D$.

Remark 4.2.1 *It can be noted that system (4.1) includes motorized actuators or robotic arms with $n = 2$ [Bhat & Bernstein 1998]. Higher order sliding mode control can also be seen as the stabilization problem of an auxiliary system described as a perturbed chain of integrators built from the output and its higher time derivatives [Emel'Yanov et al. 1996].*

The control objective is to stabilize system (4.1) using the discrete-time noisy measurement $y(t_k)$. Therefore, the states of the system can be estimated using the MIDFD differentiator.

4.3 Output feedback control design

To achieve the control objective, let us consider the implicit discrete-time realization of the robust exact filtering differentiator (MIDFD) given in (3.24). Here, in order to avoid the increase of L, we include some additional terms related to the control input in the discrete-time differentiator. The proposed differentiator becomes as follows:

$$\begin{aligned} w_{j_f,k+1} =& \frac{\tau^{(n_f-j_f+1)}}{(n_f-j_f+1)!}(z_{0,k}-y(t_k)) + \sum_{l=j_f}^{n_f}\frac{\tau^{(l-j_f)}}{(l-j_f)!}w_{l,k} + \sum_{l=j_f}^{m+1}\frac{\tau^{(l-j_f+1)}}{(l-j_f+1)!}\bar{\Psi}_{l-1,m}\left(w_{1,k+1}\right), \\ z_{j_d,k+1} =& \frac{\tau^{(n-j_d+1)}}{(n-j_d+1)!}u_k + \sum_{l=j_d}^{n}\frac{\tau^{(l-j_d)}}{(l-j_d)!}z_{l,k} + \frac{\tau^{(l-j_d+1)}}{(l-j_d+1)!}\bar{\Psi}_{n_f+l,m}\left(w_{1,k+1}\right), \\ j_f =& 1,2,\cdots,n_f. \quad j_d = 0,1,2,\cdots,n. \end{aligned} \tag{4.2}$$

with

$$\bar{\Psi}_{j,m}\left(w_{1,k+1}\right) = -\lambda_{m-j}L^{\frac{j+1}{m+1}}\left|w_{1,k+1}\right|^{\frac{m-j}{m+1}}\xi_k$$

The observer is implemented according to Lemma 3.1, where a_j and b_k are calculated using Equations (3.18). Moreover, L is selected such that $L \geq D$. This requires to ensure that the control input $u(t)$ remains bounded in order to stabilize system (4.1) using the noisy signal $y(t_k)$. With the estimation $z_{j,k}$ obtained in (4.2), an output feedback saturated controller is proposed as,

$$u(t) = \begin{cases} C & if \quad v_k \geq C, \\ v_k & if \quad -C < v_k < C, \\ -C & if \quad v_k \leq -C, \end{cases} \quad \forall t \in [t_k, t_{k+1}), \tag{4.3}$$

(4.4)

with

$$v_k = \boldsymbol{K}\boldsymbol{Z}_k. \tag{4.5}$$

Without the saturation constraint given by $|u(t)| \leq C$, the controller becomes $u(t) = v_k \ \forall t \in [t_k, t_{k+1})$. Vector $\boldsymbol{Z}_k = [z_{I,k} \ \ z_{0,k} \ \ z_{1,k} \ \ \cdots \ \ z_{n,k}]^T \in \mathbb{R}^{n+2}$ is defined using the estimated state obtained from the implicit discrete-time filtering observer (4.2). Furthermore, variable $z_{I,k}$ is an approximation of $\int_0^t x_0(\alpha)d\alpha$ using a forward Euler integration, i.e.,

$$z_{I,k+1} = z_{I,k} + \tau z_{0,k}, \tag{4.6}$$

with $z_{I,0} = 0$. The control parameters are given by $\boldsymbol{K} = [k_I \ \ k_0 \ \ k_1 \ \ \cdots k_n] \in \mathbb{R}^{n+1}$. Note that v_k in (4.5) is a classical PID control law for the case of $n = 1$.

Remark 4.3.1 *Although a forward Euler integration is used in (4.6), one can use other approximations.*

Since $d(t)$ is bounded, one can set the observer parameter $L = D$. In this case, the implicit discrete-time differentiator (4.2) estimates in finite-time the states $x_{j,k}$ (i.e., the n time derivatives of x_0). Furthermore, one can use a differentiator order greater than n, if $\ddot{x}_n(t)$ is bounded and its bound is known.

To select an adequate gain, $\boldsymbol{K}$, a discrete-time analysis is performed. From Taylor's series [Apostol 1967], one obtains the following realizations of $x_i(t)$:

$$\begin{aligned}
x_0(t_{k+1}) &= x_0(t_k) + (t_{k+1}-t_k)x_1(t_k) + \cdots + \frac{(t_{k+1}-t_k)^n}{n!}x_n(t_k) + \frac{(t_{k+1}-t_k)^{n+1}}{(n+1)!}\dot{x}_n(t_k),\\
x_1(t_{k+1}) &= x_1(t_k) + (t_{k+1}-t_k)x_2(t_k) + \cdots + \frac{(t_{k+1}-t_k)^{n-1}}{(n-1)!}x_n(t_k) + \frac{(t_{k+1}-t_k)^{n}}{n!}\dot{x}_n(t_k),\\
&\vdots\\
x_n(t_{k+1}) &= x_n(t_k) + (t_{k+1}-t_k)\dot{x}_n(t_k).
\end{aligned} \tag{4.7}$$

The above equations can be rewritten as follows:

$$\begin{aligned}
x_0(t_{k+1}) &= x_0(t_k) + \tau x_1(t_k) + \cdots + \frac{\tau^n}{n!}x_n(t_k) + \frac{\tau^{n+1}}{(n+1)!}\left(u(t_k)+d(t_k)\right),\\
x_1(t_{k+1}) &= x_1(t_k) + \tau x_2(t_k) + \cdots + \frac{\tau^{n-1}}{(n-1)!}x_n(t_k) + \frac{\tau^{n}}{n!}\left(u(t_k)+d(t_k)\right),\\
&\vdots\\
x_n(t_{k+1}) &= x_n(t_k) + \tau\left(u(t_k)+d(t_k)\right).
\end{aligned} \tag{4.8}$$

The addition of the terms u_k on the discrete-time observer (4.2) allows to obtain the same discrete-time error than the discrete-time differentiator (3.16) in the previous Chapter. Therefore, from Theorem 3.5.3, the discrete-time observer converges to a vicinity of the origin in finite-time and preserves its accuracy. L does not depends on $u(t)$. From equations (4.8) and (4.6), the following discrete-time realization is obtained:

$$\begin{aligned}
\boldsymbol{X}_{k+1} &= \boldsymbol{\Phi}(\tau)\boldsymbol{X}_k + \boldsymbol{B}(\tau)\left(u_k + d_k\right) + \tau\sigma_{0,k}\boldsymbol{e}_1,\\
\boldsymbol{X}_k &= \left[z_I(t_k)\ \ x_0(t_k)\ \ x_1(t_k)\ \ \cdots x_n(t_k)\right]^T,
\end{aligned} \tag{4.9}$$

where $\boldsymbol{\Phi}(\tau)$ and $\boldsymbol{B}(\tau)$ are defined as:

$$\boldsymbol{\Phi}\left(\tau\right) = \begin{bmatrix}
1 & \tau & 0 & 0 & \cdots & 0 & 0\\
0 & 1 & \tau & \frac{\tau^2}{2!} & \cdots & \frac{\tau^{n-1}}{(n-1)!} & \frac{\tau^n}{n!}\\
0 & 0 & 1 & \tau & \cdots & \frac{\tau^{n-2}}{(n-2)!} & \frac{\tau^{n-1}}{(n-1)!}\\
\vdots & \vdots & \vdots & \vdots & \ddots & \vdots & \vdots\\
0 & 0 & 0 & 0 & \cdots & 1 & \tau\\
0 & 0 & 0 & 0 & \cdots & 0 & 1
\end{bmatrix}, \quad \boldsymbol{B}\left(\tau\right) = \begin{bmatrix}
0\\ \frac{\tau^{n+1}}{(n+1)!}\\ \frac{\tau^n}{n!}\\ \vdots\\ \frac{\tau^2}{2!}\\ \tau
\end{bmatrix}^T. \tag{4.10}$$

As the implicit discrete-time observer (4.2) is implemented with a constant sampling time, the control law (4.3) is implemented using the same sampling time. Additionally, without saturation constraint, the closed-loop system (4.9) can be represented

as follows:

$$\boldsymbol{X}_{k+1} = \boldsymbol{\Omega}(\tau)\boldsymbol{X}_k + \boldsymbol{F}_k, \tag{4.11}$$

with

$$\boldsymbol{\Omega}(\tau) = \begin{bmatrix} 1 & \tau & \cdots & 0 \\ \frac{\tau^{n+1}}{(n+1)!}k_I & \left(1 + \frac{\tau^{n+1}}{(n+1)!}k_0\right) & \cdots & \left(\frac{\tau^n}{n!} + \frac{\tau^{n+1}}{(n+1)!}k_n\right) \\ \frac{\tau^n}{n!}k_I & \frac{\tau^n}{n!}k_0 & \cdots & \left(\frac{\tau^{n-1}}{(n-1)!} + \frac{\tau^n}{n!}k_n\right) \\ \vdots & \vdots & \ddots & \vdots \\ \frac{\tau^2}{2!}k_I & \frac{\tau^2}{2!}k_0 & \cdots & \left(\tau + \frac{\tau^2}{2!}k_n\right) \\ \tau k_I & \tau k_0 & \cdots & (1 + \tau k_n) \end{bmatrix}, \tag{4.12}$$

and

$$\boldsymbol{F}_k = \begin{bmatrix} \tau\sigma_{0,k} & \frac{\tau^{n+1}}{(n+1)!}(E_k + d_k) & \cdots & \tau(E_k + d_k) \end{bmatrix}^T, \tag{4.13}$$

where $E_k = k_0\sigma_{0,k} + k_1\sigma_{1,k} + \cdots + k_n\sigma_{n,k}$. Note that each element of matrix $\boldsymbol{F}_k$ is bounded after a finite-time and their bounds are defined by the parameters μ_j, which depend on the parameters λ_j and the methodology used to estimate $x_{j,k}$. Then, $\boldsymbol{K}$ is selected such that the magnitude of the $n+1$ eigenvalues of $\boldsymbol{\Omega}(\tau)$ have norm lower than 1 and $k_I < 0$, $k_0 < 0$, $k_1 < 0$, $\cdots$, $k_n < 0$.

4.4 Stability analysis of the output feedback controller

Before anaylis the propoerties of the proposed output feedback controller, let us introduce the following definitions:

- t_{k_0} is the lowest time instant such that $u(t)$ is saturated for any measurement time greater to t_{k_0} and previous t_{k_2}, i.e., $|v_k| \geq C$ for any t_k with $t_{k_0} \leq t_k < t_{k_2}$.
- t_{k_1} is the time instant when the discrete-time filtering observer (4.2) obtains and keeps the accuracy (3.51).
- t_{k_2} is the time instant such that v_k is unsaturated and for the previous measurement time v_k was saturated, i.e., $|v_{k_2}| < C$ at t_{k_2} and $|v_k| \geq C$ for t_k with $t_{k_0} \leq t_k < t_{k_2}$.
- t_{k_3} is the time instant when $|v_{k_3}| < C$ and the discrete-time filtering observer (4.2) obtains and keeps the accuracy (3.51).
- $\bar{v}(t)$ is the continuous-time function analogous to v_k, defined as:

$$\begin{aligned} \bar{v}(t) &= \boldsymbol{K}\begin{bmatrix} \bar{z}_I(t) & x_0(t) & x_1(t) & \cdots & x_n(t) \end{bmatrix}^T, \\ \bar{z}_I(t) &= z_{I,k}, \quad \text{for } t \in [t_k, t_{k+1}). \end{aligned} \tag{4.14}$$

- t_f is the time instant after t_{k_0} and t_{k_1} such that $\bar{v}(t_f) < C$.

Time instants t_{k_0}, t_{k_1}, t_{k_2} and t_{k_3} are measurement times but t_f could not be a measurement time. As it will be demonstrated hereafter, t_{k_1}, t_{k_3} and t_f are finite. On the other hand, t_{k_2} is finite due to the results presented in Theorem 3.5.3. Furthermore, t_{k_0}, t_{k_1} and t_{k_2} satisfy that $t_{k_0} \leq t_{k_1} < t_{k_2}$. Now, the main results are presented:

Theorem 4.4.1

Let system (4.1) under the controller $u(t)$ defined as in (4.3) and using the implicit discrete-time filtering observer (4.2). $\boldsymbol{K}$ is selected such that the magnitude of the $n+1$ eigenvalues of $\boldsymbol{\Omega}(\tau)$ have norm lower than one and $k_I < 0$, $k_1 < 0$, $\cdots$, $k_n < 0$. If $|v_k| \geq C$ at the time instant t_{k_1}, $|\sigma_{j_d,k}|$ and τ are such that:

$$|\bar{v}(t_{k_2})| + |E_k| \ < C, \tag{4.15}$$

with $j_d = 0, 1, \cdots, n$ and E_k at time t_{k_2}, then $|v_k| < C$ at time t_{k_2}.

Proof *Let us consider the case $v_k \geq C$ at time t_{k_1}. Then, on the time interval $t_{k_0} \leq t < t_{k_2}$, one can see that the state $x_n(t)$ satisfies the differential equation $\dot{x}_n(t) = d(t) + C$ and, as $|d(t)| \leq D$ and $u(t) = C$, one obtains:*

$$\begin{gathered}(C+D) \geq \dot{x}_n(t) \geq (C-D), \\ (C+D)(t-t_{k_0}) + x_n(t_{k_0}) \geq x_n(t) \geq (C-D)(t-t_{k_0}) + x_n(t_{k_0}).\end{gathered} \tag{4.16}$$

Since $\dot{x}_{n-1} = x_n$ and integrating $\dot{x}_{n-1}$:

$$\begin{aligned}x_{n-1}(t) &\leq (C+D)\frac{(t-t_{k_0})^2}{2} + (t-t_{k_0})x_n(t_{k_0}) + x_{n-1}(t_{k_0}), \\ x_{n-1}(t) &\geq (C-D)\frac{(t-t_{k_0})^2}{2} + (t-t_{k_0})x_n(t_{k_0}) + x_{n-1}(t_{k_0}).\end{aligned} \tag{4.17}$$

The above process can be repeated and one obtains:

$$\begin{aligned}x_{n-i}(t) &\geq \frac{(C-D)\,(t-t_{k_0})^{i+1}}{(i+1)!} + \sum_{j=0}^{i}\frac{(t-t_{k_0})^{i-j}}{(i-j)!}x_{n-j}(t_{k_0}), \\ x_{n-i}(t) &\leq \frac{(C+D)\,(t-t_{k_0})^{i+1}}{(i+1)!} + \sum_{j=0}^{i}\frac{(t-t_{k_0})^{i-j}}{(i-j)!}x_{n-j}(t_{k_0}).\end{aligned} \tag{4.18}$$

for $i = 0, 1, 2, \cdots, n$. For all t_k, with $t_{k_2} \geq t_k \geq t_{k_1}$, $z_{I,k}$ satisfies:

$$\begin{aligned}z_{I,k+1} - z_{I,k} &\geq \tau\left(\frac{(C-D)\,(t_k-t_{k_0})^{n+1}}{(n+1)!} + \sum_{j=0}^{n}\frac{(t_k-t_{k_0})^{n-j}}{(n-j)!}x_{n-j}(t_{k_0})\right) + \tau\sigma_{0,k}, \\ z_{I,k+1} - z_{I,k} &\leq \tau\left(\frac{(C+D)\,(t_k-t_{k_0})^{n+1}}{(n+1)!} + \sum_{j=0}^{n}\frac{(t_k-t_{k_0})^{n-j}}{(n-j)!}x_{n-j}(t_{k_0})\right) + \tau\sigma_{0,k}.\end{aligned} \tag{4.19}$$

Due to inequalities (4.18) and (4.19), $C-D>0$ and $C+D>0$, then $\bar{v}(t)<C$ at time t_f, which is finite. Now, it is considered the value of v_k for the measurement time after t_f, which is t_{k_2}. Note that $t_{k_2}\in[t_f,t_f+\tau]$. The estimation errors $|\sigma_{j_d,k}|$, with $j_d=0,1,\cdots,n$, and the sampling time τ have to be small enough to satisfy the following condition:

$$|\bar{v}(t_{k_2})|+|E_k| \ <C. \tag{4.20}$$

The above condition implies that $|v_k|<C$ at the time instant t_{k_2}. Furthermore, this condition can be rewritten as two conditions:

$$\begin{aligned}
&\left|k_I z_{I,k}+\sum_{i=0}^{n}k_{n-i}(C-D)\frac{(t_{k_2}-t_{k_0})^{i+1}}{(i+1)!}+k_{n-i}\sum_{j=0}^{i}\frac{(t_{k_2}-t_{k_0})^{i-j}}{(i-j)!}x_i(t_{k_0})\right| \ +|E_k|\leq C\\
&\left|k_I z_{I,k}+\sum_{i=0}^{n}k_{n-i}(C+D)\frac{(t_{k_2}-t_{k_0})^{i+1}}{(i+1)!}+k_{n-i}\sum_{j=0}^{i}\frac{(t_{k_2}-t_{k_0})^{i-j}}{(i-j)!}x_i(t_{k_0})\right| \ +|E_k|\leq C
\end{aligned} \tag{4.21}$$

A similar demonstration can be done for the case $v_k\leq -C$ at time t_{k_1}.

Theorem 4.4.1 shows that after the discrete-time observer (4.2) obtains the asymptotic accuracy and if $u(t)$ is saturated at time t_{k_1} then $|v_k|<C$ after a finite time t_{k_2}. The following step gives the required conditions to keep unsaturated $u(t)$ and system (4.9) stable. These conditions are presented in the following theorem.

Theorem 4.4.2

Let system (4.1) under the controller $u(t)$ defined as in (4.3), where $\boldsymbol{K}$ is given in Theorem 4.4.1. Let $\boldsymbol{P}$ and $\boldsymbol{Q}$ be symmetric positive definite matrix of dimensions $(n+1)\times(n+1)$, with $\boldsymbol{\Omega}(\tau)^T\boldsymbol{P}\boldsymbol{\Omega}(\tau)-\boldsymbol{P}=-\boldsymbol{Q}$ and $\boldsymbol{P}$ such that $\lambda_{min}(\boldsymbol{Q})>1$. If $|v_k|<C$ at time t_{k_3}, and C satisfies the following conditions:

$$\begin{aligned}
C&>|E_k|+|k_I+k_0+k_1+\cdots+k_n|\sqrt{\frac{(\lambda_{\max}(\boldsymbol{P}\boldsymbol{\Omega}(\tau)\boldsymbol{\Omega}(\tau)^T\boldsymbol{P}+\boldsymbol{P}))}{(\lambda_{\min}(\boldsymbol{Q})-1)}}\,\|\boldsymbol{F}_k\|_2\,,\\
C&>\left|\boldsymbol{K}\boldsymbol{\Omega}^i(\tau)\boldsymbol{X}_{k_3}+\sum_{j=0}^{i-1}\boldsymbol{K}\boldsymbol{\Omega}^j(\tau)\boldsymbol{F}_{k_3+i-j-1}\right|.
\end{aligned} \tag{4.22}$$

for all $t_k>t_{k_3}$ and $i=0,1,2,\ldots$, then the discrete-time system (4.9) is stable and $|v_k|<C$ for all $t_k\geq t_{k_3}$.

Proof *Let us consider the discrete-time Lyapunov function*

$$V_k=\boldsymbol{X}_k^T\boldsymbol{P}\boldsymbol{X}_k. \tag{4.23}$$

From the Lyapunov function, one obtains

$$V_{k+1}-V_k=\boldsymbol{X}_k^T\left(\boldsymbol{\Omega}(\tau)^T\boldsymbol{P}\boldsymbol{\Omega}(\tau)-\boldsymbol{P}\right)\boldsymbol{X}_k+2\boldsymbol{X}_k^T\boldsymbol{\Omega}(\tau)^T\boldsymbol{P}\boldsymbol{F}_k+\boldsymbol{F}_k\boldsymbol{P}\boldsymbol{F}_k. \tag{4.24}$$

One can deduce that

$$\begin{aligned} V_{k+1} - V_k \leq & - \boldsymbol{X}_k^T \boldsymbol{Q} \boldsymbol{X}_k + \boldsymbol{X}_k^T \boldsymbol{X}_k + \boldsymbol{F}_k^T \left(\boldsymbol{P} \boldsymbol{\Omega}(\tau) \boldsymbol{\Omega}(\tau)^T \boldsymbol{P} + \boldsymbol{P} \right) \boldsymbol{F}_k, \\ V_{k+1} - V_k \leq & - \left(\lambda_{min}(\boldsymbol{Q}) - 1 \right) \left\| \boldsymbol{X}_k \right\|_2^2 + \left(\lambda_{max}(\boldsymbol{P} \boldsymbol{\Omega}(\tau) \boldsymbol{\Omega}(\tau)^T \boldsymbol{P}) + \lambda_{max}(\boldsymbol{P}) \right) \left\| \boldsymbol{F}_k \right\|_2^2 . \end{aligned} \tag{4.25}$$

It implies that $V_{k+1} - V_k$ is negative if:

$$\left\| \boldsymbol{X}_k \right\|_2 \geq \sqrt{\frac{\left(\lambda_{max}(\boldsymbol{P} \boldsymbol{\Omega}(\tau) \boldsymbol{\Omega}(\tau)^T \boldsymbol{P} + \boldsymbol{P}) \right)}{\left(\lambda_{min}(\boldsymbol{Q}) - 1 \right)}} \left\| \boldsymbol{F}_k \right\|_2 . \tag{4.26}$$

Equation (4.26) defines the convergence region of the discrete-time system. Therefore, to keep an unsaturated control law, C must satisfy at least the following condition:

$$\begin{aligned} C > |v_k| = |\boldsymbol{K} \boldsymbol{Z}_k| = |k_I z_{I,k} + k_0 x_{0,k} + k_1 x_{1,k} + \cdots + k_n x_{n,k} + E_k| \\ C > |E_k| + |(k_I + k_0 + k_1 + \cdots + k_n)| \sqrt{\frac{\left(\lambda_{max}(\boldsymbol{P} \boldsymbol{\Omega}(\tau) \boldsymbol{\Omega}(\tau)^T \boldsymbol{P} + \boldsymbol{P}) \right)}{\left(\lambda_{min}(\boldsymbol{Q}) - 1 \right)}} \left\| \boldsymbol{F}_k \right\|_2 \end{aligned} \tag{4.27}$$

The above inequality has to be satisfied for all $t_k > t_{k_3}$, but $|E_k|$ and $\|\boldsymbol{F}_k\|_2$ are bounded for those time instants. Furthermore, without saturation, the solution of the discrete-time system (4.11) is given as

$$\boldsymbol{X}_{k_3+i} = \boldsymbol{\Omega}^i(\tau) \boldsymbol{X}_{k_3} + \sum_{j=0}^{i-1} \boldsymbol{\Omega}^j(\tau) \boldsymbol{F}_{k_3+i-j-1}, \tag{4.28}$$

where $\boldsymbol{X}_{k_3}$ is $\boldsymbol{X}_k$ at the measurement time t_{k_3} and $i = 1, 2, \cdots$. From Equations (4.5) and (4.28)

$$v_{k_3+i} = E_{k_3+i-1} + \boldsymbol{K} \boldsymbol{\Omega}^i(\tau) \boldsymbol{X}_{k_3} + \sum_{j=0}^{i-1} \boldsymbol{K} \boldsymbol{\Omega}^j(\tau) \boldsymbol{F}_{k_3+i-j-1}. \tag{4.29}$$

To keep an unsaturated control law $u(t)$, C has to satisfy:

$$C > \left| \boldsymbol{K} \boldsymbol{\Omega}^i(\tau) \boldsymbol{X}_{k_3} + \sum_{j=0}^{i-1} \boldsymbol{K} \boldsymbol{\Omega}^j(\tau) \boldsymbol{F}_{k_3+i-j-1} \right| + |E_{k_3+i-1}|. \tag{4.30}$$

for $i = 1, 2, \cdots$. This concludes the proof.

Remark 4.4.1 *Considering the case of an unbounded $u(t)$ and $\boldsymbol{K}$ is selected as in Theorem 4.4.2, the implicit discrete-time observer (4.2) converges to a vicinity of the origin for any initial condition $\boldsymbol{x}(0) \in \mathbb{R}^n$ with $L > D$. Therefore the closed loop system (4.1)-(4.6) is globally stable. Additionally, if $d(t)$ and $u(t)$ are n_1 times differentiable, one can use $n + n_1$ instead of n, which improves the accuracy of the discrete-time observer (4.2). Furthermore, for a given C, the linear system cannot be stabilized globally using the controller (4.5) if the input is limited.*

Equation (4.26) implies that $\|\boldsymbol{X}_k\|_2$ is bounded. Theorems 4.4.1 and 4.4.2 allow to show the stability of the continuous-time system (4.1) using the discrete-time law control (4.3). Furthermore, if for t_{k_1} the conditions in Theorem 4.4.2 are satisfied, then t_{k_2} becomes t_{k_3}. However, a small enough sampling time is required because $\boldsymbol{E}_k$ and $\boldsymbol{F}_k$ depend on it. It is important to note that there is not a value of C such that the discrete-time system is stable for any initial condition $\boldsymbol{X}_{k_3}$, it comes from the conditions in Theorem 4.4.1. On the other hand, reducing the value of $|k_I + k_0 + k_1 + \cdots + k_n|$ allows to reduce the minimum value of C.

4.5 Simulation results

To show the effectiveness of the proposed sampled-data sliding mode differentiator based controller, several scenarios are investigated. In this section, the root mean square value of the states and its maximum absolute value are selected as indexes of comparison. The maximum absolute value (MAV) of a state $x_i(t)$ after 50 sec is given as:

$$MAV = \max\left\{|x_i(t_j)| \in \mathbb{R} | t_j = 50\,\text{sec} + j\tau_s\right\}, \tag{4.31}$$

where τ_s is the simulation time, $j = 1, \cdots, (t_{\max} - 50)/\tau_s$, and $t_{\max}$ is the maximum time of simulation. In Simulation I and II, τ_s is selected such that $\tau_s < \tau$, $\tau_s = 0.00005\,\text{sec}$ and $\tau_s = 0.00001\,\text{sec}$ are used in Simulation I and II respectively. The root mean square value (RMSV) of $x_i(t)$ after 50 sec is defined as follows:

$$RMSV = \sqrt{\sum_{j=1}^{(t_{\max}-50)/\tau_s} \frac{(x_i(j\tau_s + 50))^2}{(t_{\max} - 50)/\tau_s}}. \tag{4.32}$$

On the other hand, two new index are related to the controller (4.3). They are defined as $ME = \max\left\{|E_k| \in \mathbb{R} | 50\,\text{sec} < t_k \leq t_{\max}\right\}$ and $MF = \max\left\{\|\boldsymbol{F}_k\|_2 \in \mathbb{R} | 50\,\text{sec} < t_k \leq t_{\max}\right\}$.

4.5.1 Simulation I: Second Order System

In this simulation, the following uncertain system is studied:

$$\begin{aligned} \dot{x}_0(t) &= x_1(t), \\ \dot{x}_1(t) &= d(t) + u(t), \\ y(t_k) &= x_0(t_k) + \Delta(t_k), \end{aligned} \tag{4.33}$$

where the state is $\boldsymbol{x} = \begin{bmatrix} x_0 & x_1 \end{bmatrix}^T \in \mathbb{R}^2$, the control input is $u(t) \in \mathbb{R}$ and the discrete-time output measurement is $y(t_k) \in \mathbb{R}$. The measurement noise $\Delta_k = \Delta(t_k)$ is normally distributed random signal with mean 0 and variance 5 and the perturbation is $d(t) = 0.5\sin(0.01t)$. The sampling period is constant, i.e., $\tau = t_{k+1} - t_k = 0.001\,\text{sec}$.

The output feedback saturated controller is given by

$$\begin{aligned} u(t) &= \begin{cases} C & if \quad v_k \geq C \\ v_k & if \quad -C \leq v_k \leq C \\ -C & if \quad v_k \leq -C \end{cases}, \quad \forall t \in [t_k, t_{k+1}), \\ v_k &= k_I z_{I,k} + k_0 z_{0,k} + k_1 z_{1,k}, \\ z_{I,k+1} &= z_{I,k} + \tau z_{0,k}. \end{aligned} \tag{4.34}$$

Vector $\boldsymbol{Z}_k = [z_{I,k} \;\; z_{0,k} \;\; z_{1,k}]^T \in \mathbb{R}^3$ is defined using the estimated state obtained from the implicit discrete-time filtering observer (4.2) with $L = 0.5$, $n = 1$, $n_f = 1$ and λ_j are selected as in [Hanan *et al.* 2021], which is given as:

$$\begin{aligned} w_{1,k+1} =& w_{1,k} + \tau\left(z_{0,k} - \bar{x}_{0,k}\right) - \tau\lambda_2 L^{\frac{1}{3}} \left|w_{1,k+1}\right|^{\frac{2}{3}} \xi_k - \frac{\tau^2}{2}\lambda_1 L^{\frac{2}{3}} \left|w_{1,k+1}\right|^{\frac{1}{3}} \xi_k - \frac{\tau^3}{6}\lambda_0 L \xi_k, \\ z_{0,k+1} =& z_{0,k} + \tau z_{1,k} + \frac{\tau^2}{2} u_k - \tau\lambda_1 L^{\frac{2}{3}} \left|w_{1,k+1}\right|^{\frac{1}{3}} \xi_k - \frac{\tau^2}{2}\lambda_0 L \xi_k, \\ z_{1,k+1} =& z_{1,k} + \tau u_k - \tau\lambda_0 L \xi_k, \end{aligned} \tag{4.35}$$

where ξ_k and $w_{1,k+1}$ are calculated according to Lemma 3.1, its respective polynomials are defined as:

$$\begin{aligned} p\left(r\right) &= r^3 + a_2 r^2 + a_1 r + \left(-b_k + a_0\right), \\ p\left(r\right) &= r^3 + a_2 r^2 + a_1 r + \left(b_k + a_0\right), \end{aligned} \tag{4.36}$$

with $a_0 = \frac{\tau^3}{6}\lambda_0 L$, $a_1 = \frac{\tau^2}{2}\lambda_1 L^{\frac{2}{3}}$, $a_2 = \tau\lambda_2 L^{\frac{1}{3}}$ and $b_k = -w_{1,k} - \tau\left(z_{0,k} - \bar{x}_{0,k}\right)$. Using Theorems 4.4.1 and 4.4.2, the controller parameters are selected as $C = 50$ and $\boldsymbol{K} = [k_I \;\; k_0 \;\; k_1]^T = [-0.1 \;\; -0.6 \;\; -0.4]^T$. Hence, eigenvalues of $\boldsymbol{\Omega}(\tau)$ are 0.9981, $0.9979 + 0.0069i$ and $0.9979 - 0.0069i$.

For comparison purposes, we have also depicted the results obtained by replacing the implicit discrete-time filtering observer (3.16) with the explicit discrete-time differentiator, which was presented in [Levant & Livne 2019], with the additional terms used in (4.2). It is important to note that both discrete-time observers have different inputs but the same $\Delta(t_k)$. The initial condition of the system is $\boldsymbol{X}_0 = [20 \;\; -5]^T$ and $\boldsymbol{Z}_0 = [0 \;\; 0 \;\; 0]^T$. Results are presented in Figures 4.1-4.2.

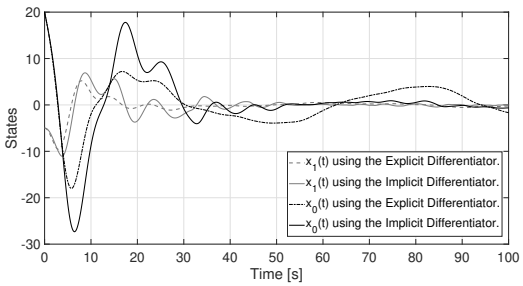

Figure 4.1: States of the system.

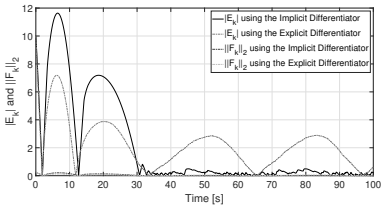

(a) $|E_k|$ and $\|\boldsymbol{F}_k\|_2$.

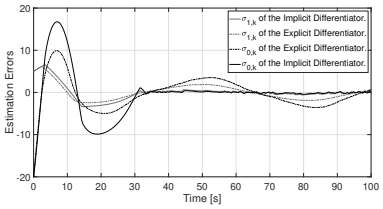

(b) Estimation errors of the states.

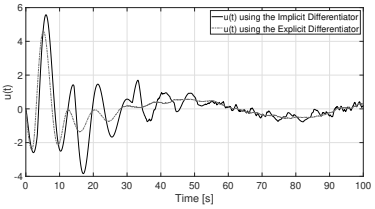

(c) State Feedback Control.

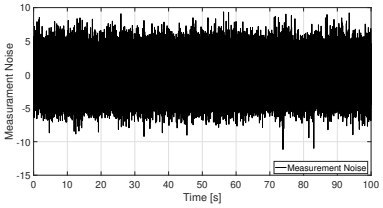

(d) Measurement noise.

Figure 4.2: Simulation results for the second-order system (4.33) with the control law (4.34) using the implicit and explicit observers.

Figure 4.2 shows that the discrete-time observers give a robust estimate in finite-time of $\boldsymbol{x}(t)$ in spite of the presence of measurement noise. Furthermore, it can be seen in Fig. 4.1 that the closed-loop system is stable. It is worth noting that the results with the implicit observer supersede the implicit one. In order to compare the results obtained with both discrete-time observers, the root mean square value of the states and its maximum absolute value after 50 sec are presented in Table 4.1. Furthermore, according to definition of $|E_k|$ and $\|\boldsymbol{F}_k\|_2$ both are bounded, then its maximum value after 50 sec is presented as ME and MF in Table 4.1.

RMSV	**Implicit Observer**	**Explicit Observer**
$x_0(t)$	0.5053	2.626
$x_1(t)$	0.1688	0.3108
MAV	**Implicit Observer**	**Explicit Observer**
$x_0(t)$	0.9034	3.9769
$x_1(t)$	0.5431	0.5603
	Implicit Observer	**Explicit Observer**
ME	0.4912	2.8915
MF	0.01077	0.04898

Table 4.1: Root mean square value and Maximum absolute value of the states.

4.5.2 Simulation II: Third Order System

The following third order uncertain system is analyzed:

$$\begin{aligned}\dot{x}_0(t) &= x_1(t),\\ \dot{x}_1(t) &= x_2(t),\\ \dot{x}_2(t) &= \sin\left(0.001x_1(t)\right) + u(t),\\ y(t_k) &= x_0(t_k) + \Delta(t_k),\end{aligned} \tag{4.37}$$

where the state is $\boldsymbol{x} = \begin{bmatrix} x_0 & x_1 & x_2 \end{bmatrix}^T \in \mathbb{R}^3$, $u(t) \in \mathbb{R}$ and $y(t_k) \in \mathbb{R}$. The measurement noise $\Delta_k = \Delta(t_k)$ is normally distributed random signal with mean 0 and variance 5 and the perturbation is $d(t) = \sin 0.001x_0(t)$. The sampling period is constant, i.e., $\tau = t_{k+1} - t_k = 0.0001s$. For the system (4.37), the discrete-time filtering differentiator based output feedback saturated controller is given by

$$\begin{aligned} u(t) &= \begin{cases} C & if \quad v_k \geq C \\ v_k & if \quad -C \leq v_k \leq C \\ -C & if \quad v_k \leq -C \end{cases}, \quad \forall t \in [t_k, t_{k+1}),\\ v_k &= k_I z_{I,k} + k_0 z_{0,k} + k_1 z_{1,k} + k_2 z_{2,k},\\ z_{I,k+1} &= z_{I,k} + \tau z_{0,k}. \end{aligned} \tag{4.38}$$

Similar to Simulation I, $\boldsymbol{Z}_k = [z_{I,k} \;\; z_{0,k} \;\; z_{1,k} \;\; z_{2,k}]^T \in \mathbb{R}^4$ is defined using the estimated state obtained from the implicit discrete-time filtering observer (4.2). Its parameters are given by $L = 1$, $n = 2$, $n_f = 1$ and λ_j given in [Hanan *et al.* 2021], which is given as:

$$\begin{aligned} w_{1,k+1} =& w_{1,k} + \tau\left(z_{0,k} - \bar{x}_{0,k}\right) - \tau\lambda_3 L^{\frac{1}{4}} \left|w_{1,k+1}\right|^{\frac{3}{4}} \xi_k - \frac{\tau^2}{2}\lambda_2 L^{\frac{2}{4}} \left|w_{1,k+1}\right|^{\frac{2}{4}} \xi_k - \ldots\\ & \ldots - \frac{\tau^3}{6}\lambda_1 L^{\frac{3}{4}} \left|w_{1,k+1}\right|^{\frac{1}{4}} \xi_k - \frac{\tau^4}{24}\lambda_0 L\xi_k,\\ z_{0,k+1} =& z_{0,k} + \tau z_{1,k} + \frac{\tau^2}{2} z_{2,k} + \frac{\tau^3}{6} u_k - \tau\lambda_2 L^{\frac{2}{4}} \left|w_{1,k+1}\right|^{\frac{2}{4}} \xi_k - \ldots\\ & \ldots - \frac{\tau^2}{2}\lambda_1 L^{\frac{3}{4}} \left|w_{1,k+1}\right|^{\frac{1}{4}} \xi_k - \frac{\tau^3}{6}\lambda_0 L\xi_k,\\ z_{1,k+1} =& z_{1,k} + \tau z_{2,k} + \frac{\tau^2}{2} u_k - \tau\lambda_1 L^{\frac{3}{4}} \left|w_{1,k+1}\right|^{\frac{1}{4}} \xi_k - \frac{\tau^2}{2}\lambda_0 L\xi_k,\\ z_{2,k+1} =& z_{2,k} + \tau u_k - \tau\lambda_0 L\xi_k, \end{aligned} \tag{4.39}$$

where ξ_k and $w_{1,k+1}$ are calculated according to Lemma 3.1, its respective polynomials are defined as:

$$\begin{aligned} p\left(r\right) &= r^4 + a_3 r^3 + a_2 r^2 + a_1 r + \left(-b_k + a_0\right),\\ p\left(r\right) &= r^4 + a_3 r^3 + a_2 r^2 + a_1 r + \left(b_k + a_0\right), \end{aligned} \tag{4.40}$$

with $a_0 = \frac{\tau^4}{24}\lambda_0 L$, $a_1 = \frac{\tau^3}{6}\lambda_1 L^{\frac{3}{4}}$, $a_2 = \frac{\tau^2}{2}\lambda_2 L^{\frac{2}{4}}$, $a_3 = \tau\lambda_3 L^{\frac{1}{4}}$ and $b_k = -w_{1,k} - \tau\left(z_{0,k} - \bar{x}_{0,k}\right)$.

Using Theorem 4.4.1 and 4.4.2, the controller parameters are selected as $C = 20$ and $\boldsymbol{K} = [k_I \;\; k_0 \;\; k_1 \;\; k_2]^T = [-0.2 \;\; -0.3 \;\; -1.2 \;\; -0.5]^T$. Due to the above

parameters, eigenvalues of $\boldsymbol{\Omega}(\tau)$ are $0.9988+0.0095i$, $0.9988-0.0095i$, $0.9986+0.0045i$, and $0.9986-0.0045i$. On the other hand, initial condition of the system and implicit observer are given by $\boldsymbol{X}_0 = [15 \quad -15 \quad 25]^T$ and $\boldsymbol{Z}_0 = [0 \quad 15 \quad -15 \quad 25]^T$. The results are presented in Figures 4.3-4.4.

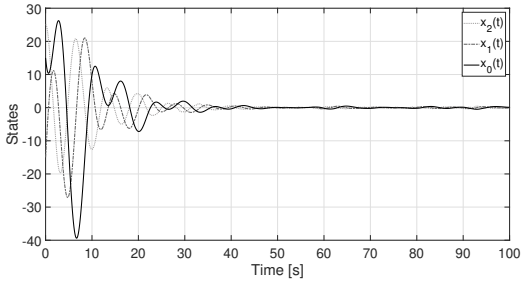

Figure 4.3: States of the system.

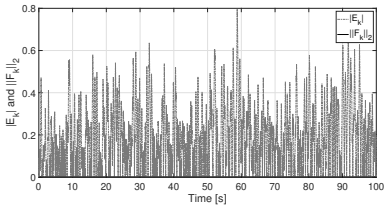

(a) States of the system.

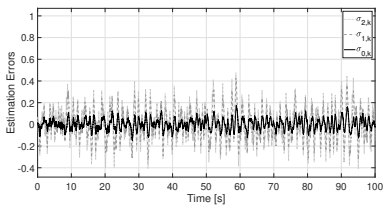

(b) Estimation errors of the states.

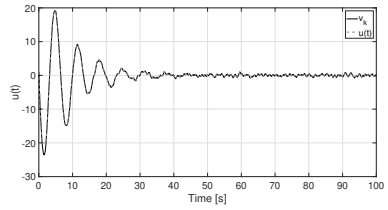

(c) State Feedback Control.

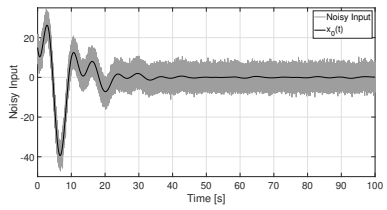

(d) Noisy Input.

Figure 4.4: Simulation results for the third-order system (4.37) with the control law (4.37) using the implicit observer.

4.5.3 Simulation III: Sampling time and initial conditions

In this simulation, the second-order system (4.33) is used with $\Delta(t) = 10\sin(10000t)$. The gains of Simulation I, the controller (4.34) and sampling time are kept as in Simulation I. First, Table 4.2 summarizes the behavior of the system with different initial conditions. As it can be seen in Figure 4.5, at time 2.543 sec the law control is saturated, according to Theorem 4.4.2, at time 3.408 sec the system is unsaturated with $\boldsymbol{X}_{k_3} = [-33.29 \quad 0.4681]^T$ and it is kept in this way. In the case of $\boldsymbol{X}_{k_3} = [200 \quad -100]^T$ the system is unstable.

Concerning the effects of the sampling time, they can be seen in Figure 4.6. If the sampling time is reduced then the bounds of the estimation errors are reduced, and

$(x_0(0), x_1(0))$	**RMSV** $x_0(t)$	**RMSV** $x_1(t)$	**MAV** $x_0(t)$
(20,-5)	0.371839	0.040175	0.568306
(30,5)	0.371783	0.043403	0.577819
(40,-10)	0.372305	0.043728	0.578355
(50,-25)	0.373469	0.047986	0.582988
(200,-100)	-	-	-
$(x_0(0), x_1(0))$	**MAV** $x_1(t)$	**ME**	**MF**
(20,-5)	0.080351	0.107837	0.000609
(30,5)	0.125534	0.108019	0.000609
(40,-10)	0.108718	0.107837	0.000609
(50,-25)	0.130512	0.107837	0.000609
(200,-100)	-	-	-

Table 4.2: Behavior of the system for initial conditions $\boldsymbol{X}_{k_3}$.

therefore the indexes of comparison are reduced. The above depends on the discrete-time signal $\boldsymbol{\beta}_{j,k}$ and its bounds δ_j.

4.6 Experimental Results

4.6.1 Problem statement

The DC-DC buck converter, depicted in Fig. 4.7, consists of a DC input source V_s, a controlled ideal switch W_s, a rectifier diode D_1, a filtering inductor L_i, a filtering capacitor C_p, a load resistance R, and the equivalent series resistances (ESR) R_c and R_{L_i} of the capatictor and the inductor, respectively.

Here, the control objective is that the output voltage $V_o(t)$ converges to a desired constant voltage V_{ref}. Let us define the output voltage error as

$$x_0(t) = V_o(t) - V_{\text{ref}}.$$

Based on the Kirchhoff's circuit laws, using the large-signal average model of the DC-DC buck converter [El Fadil *et al.* 2009, Moreno-Valenzuela 2020, Bacha *et al.* 2014], the dynamics of the output voltage error can be written as a chain of integrators as

$$\begin{aligned} \dot{x}_0(t) =& x_1(t), \\ \dot{x}_1(t) =& -\frac{1}{L_i C_p} x_0(t) - \frac{1}{RC_p} x_1(t) + \frac{V_s}{L_i C_p} u(t) - \frac{V_{ref}}{L_i C_p}, \\ y(t) =& V_o(t) + \Delta(t), \end{aligned} \tag{4.41}$$

$\frac{V_s}{L_i C_p} u(t)$ is the control input or duty cycle and $\Delta(t)$ represents measurement noise.

4.6.2 Experimental results

The experimental platform consists of the DC-DC buck converter, the digital control device and the signal conditioning subsystems (i.e. anti aliasing filter and MOSFET

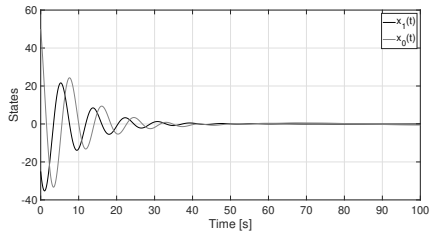

(a) States of the system.

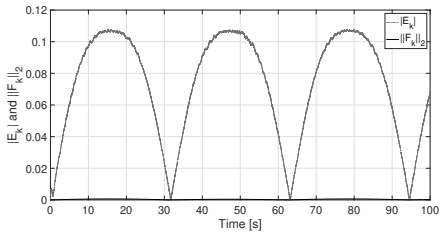

(b) State Feedback Control.

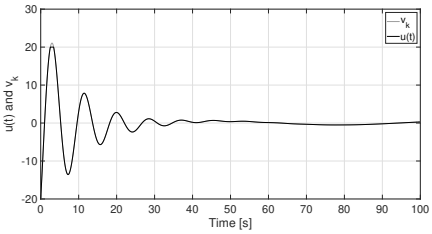

(c) $u(t)$ and v_k.

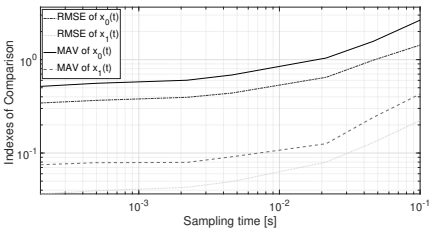

(d) Noisy input of the observer.

Figure 4.5: Simulation results for the second-order system (4.33).

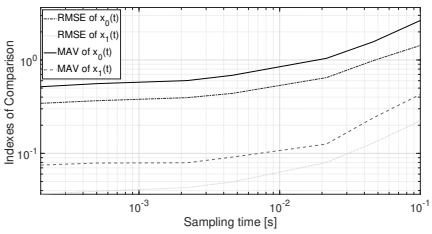

(a) RMSE and MAV of $x_0(t)$ and $x_1(t)$ for different sampling time.

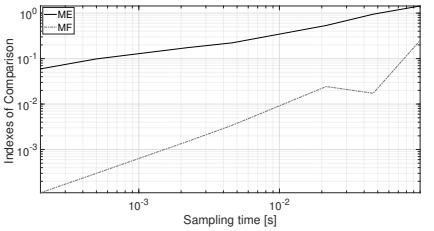

(b) State Feedback Control.

Figure 4.6: ME and MF for different sampling time.

drivers). The digital platform selected to execute the control algorithm is the dSPACE DS1104 Controller Board. A 16-bit resolution is used for analog-to-digital conversion, and the resolution of the digital pulse-width modulator is 50 ns. Serial communication between the dSPACE platform and ControlDesk software is used to monitor the DC-DC buck converter variables. In order to avoid frequency distortion in the voltage control loop due to the aliasing effect, a second-order Chebyshev low-pass filter with -20 dB of attenuation gain is used. The analog filter implementation is performed through a non-inverting Sallen–Key topology with OPA4187. The DC-DC buck converter switches are ultra-low on-resistance power MOSFET IRF3710 driven via dual low side driver IR4427 to minimize propagation times and a pair of 6N135 high-speed photo-coupler to isolate the control signal from the power section. The corresponding experimental setup is given in Fig. 4.8

In the following simulation, the system parameters are as follows: $R = 30\Omega$, $C_p = 512\mu$F, $L_i = 255.81\mu$H, $V_s = 12$V. This operating point is selected because the value of R produces that the current in the inductor decreases almost to zero (discontinuous

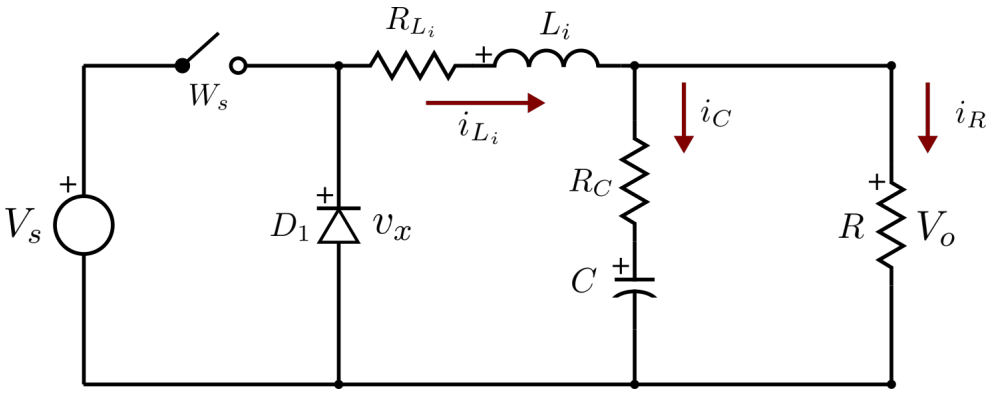

Figure 4.7: DC-DC buck converter.

conduction mode). The measurement noise is assumed to satisfy Assumption 3.3.1. The sampling period is constant, i.e., $\tau = t_{k+1} - t_k = 0.000025s$. The desired output voltage changes between $V_{re} = 3.3\text{V}$ and $V_{re} = 7\text{V}$.

The control parameters are chosen as $L = 750$, $C = \frac{V_s}{L_i C_p}$, $n = 1$, $n_f = 1$, λ_j are as in Simulation I and $\boldsymbol{K} = [k_I \;\; k_0 \;\; k_1]^T = [-0.5 \;\; -0.025 \;\; -0.00002]^T$. Note that in this case, C is a structural system constraint due to the maximum value of the duty cycle. From Theorem 4.4.2, system (4.41) under the controller $u(t)$ defined as in (4.3), with the implicit discrete-time differentiator (3.16), is stable.

The experimental results are presented in Figure 4.9. Despite the presence of measurement noise, one can see in Figure 4.9 that the proposed controller and observer allow to track the desired reference output voltage. Notice that the proposed scheme shows good performances (e.g. the settling time and overshoot are small enough). Additionally, one can note that the proposed controller enters the saturation region of $u_{k_{min}}$. Nevertheless, the control objective is still achieved.

4.7 Conclusion

In this Chapter, an output feedback controller has been proposed using an implicit discrete-time observer for perturbed chain of integrators using sampled noisy measurements. We have included some additional terms related to the control input in the discrete-time implicit robust exact filtering differentiator. The convergence of the observer to a vicinity of the origin has been ensured for any initial conditions. Then, the sampled-data sliding mode differentiator based controller has been designed. A convergence analysis has been performed, where some conditions on the control gains have been given. A comparison between implicit and explicit discrete-time schemes for a second-order system has been presented. Similar to the results obtained in the simulation of Chapters 2 and 3, the closed-loop implicit differentiator has shown better results than the explicit one. The behavior of the second-order system for different initial conditions and sampling times has been also investigated in the simulation, where the performance index improves if the sampling time is reduced. A simulation for a third-order system has been presented, where it has been showed to be stable

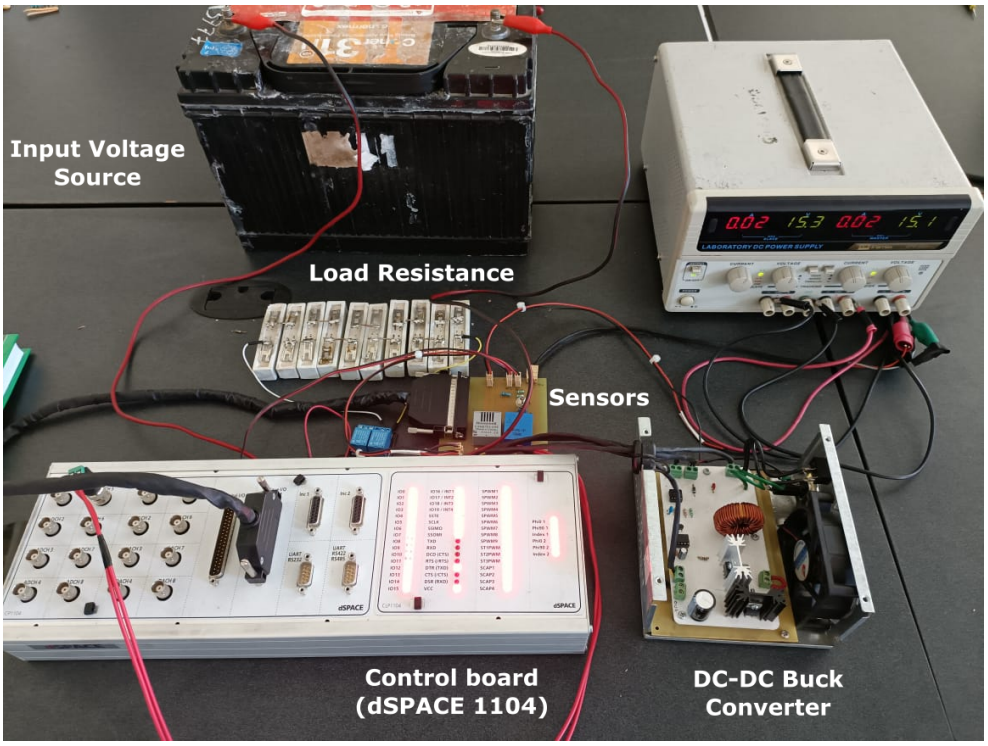

Figure 4.8: Experimental setup using the DC-DC buck converter.

for its respective initial conditions. Furthermore, the proposed controller and observer have been implemented for a DC-DC buck converter, where it has been shown that it successfully manages the control objective in spite of the presence of measurement noise.

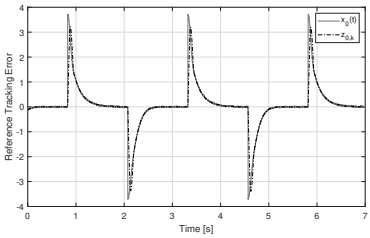

(a) Reference tracking error and its estimation.

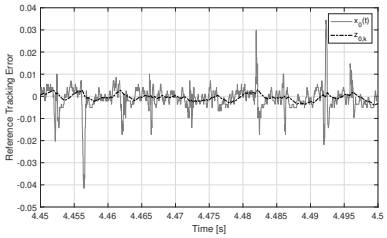

(b) Reference tracking error between 4.45 sec and 4.5 sec.

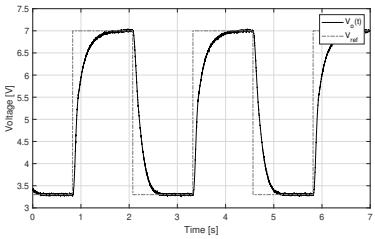

(c) Output voltage and reference.

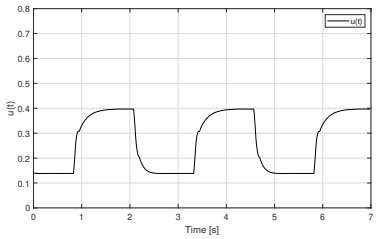

(d) State Feedback Control.

Figure 4.9: Experimental results with the DC-DC buck converter.

CHAPTER 5

General Conclusions and Perspectives

5.1 General conclusions

In this thesis, we have desgined discrete-time realizations for the continuous-time homogeneous differentiator (1.61) and filtering differentiator (1.69). Additionally, the generalized equations related to the implicit realizations are solved, it was demonstrated that they have a unique solution and the schemes are non-anticipative. The proposed discrete-time differentiators (HEDD, HIDD, MEDFD and MIDFD) preserve the continuous time properties of the continuous-time counterpart. They provide good robustness properties with respect to measurement noises and allow for large sampling periods without a significant decrease of the performances. Stability analysis has been given using homogeneity concept. Furthermore, a sampled-data sliding mode differentiator based controller has been designed. It has been guaranteed that the associated closed-loop discrete-time system is stable. As the implicit discrete-time differentiators require to estimate the roots of the polynomials, root finding methods have been proposed and studied. Simulation results showed that the Halley's method can be used with only three iterations and it was selected to implement the implicit differentiators. Furthermore, in this thesis, it was demonstrated that the Halley's method converge with a order of convergence 3 for the initial condition proposed in Chapter 2. Since the drawback of the implicit discretizations is the number of needed operations, methods to reduce the time complexity were investigated in Chapter 2, where the best methods was the Half-Horner method. As a root finding method is used, there exists an estimation error when the implicit differentiator is implemented. The above fact is taken into account in the convergence proof and its effects at time t_k are given in the variable θ_k in both discrete-time differentiators. The variable θ_k is attenuated by the sampling time. At last, both implicit discrete-time differentiators are robust to bounded numerical errors in the root-finding methods. Contrary to the implicit discrete-time differentiators presented in [Mojallizadeh *et al.* 2021], HIDD and MIDFD do not require that $f_{0,k}^{n+1} = 0$ to obtain a convergence of the estimation errors to the origin. Furthermore, in [Mojallizadeh *et al.* 2021], it was not demonstrated the convergence of the implicit discrete-time realizations based on the standard differentiator.

Numerical results were presented to show the performance of the differentiators

proposed in this thesis (HEDD, HIDD, EDFD, Matching, MEDFD, MIDFD) and in the literature (HDD, GHDD, Matching, DFD, ADFD). Different conditions were considered in terms of signal functions, sampling times and measurement noise. It can be seen in 2 and 3 that the implicit discrete-time differentiators supersede the explicit realizations. On the other hand, in 4 MIDFD has been modified and studied in closed-loop with an output feedback controller for perturbed chain of integrators using sampled noisy measurements. The convergence conditions of the closed-loop system were given. A comparison between implicit and explicit discrete-time schemes for a second-order system has been presented in 4. Similar to the results obtained in the simulation of Chapters 2 and 3, the closed-loop implicit differentiator has shown better results than the explicit one. Furthermore, the proposed controller and observer have been implemented for a DC-DC buck converter, where it has been shown that it successfully manages the control objective in spite of the presence of measurement noise.

5.2 Future perspectives

In this work, some problems related to implicit-time discretization were solved (e.g., implicit realizations of the robust standard differentiator and filtering differentiator for any order, stability proof taking into account measurement noises and numerical errors, closed-loop scheme combining a saturated controller and an implicit observer with its stability analysis, ...). However, as it is mentioned in [Brogliato & Polyakov 2020], there are still open problems related to our implicit discrete-time realization, for instance, the consideration of non-constant sampling time. Then, future works should be focused on the study of the behavior of the implicit differentiators with non-constant sampling time, and its behavior in closed loop systems using an appropriate discrete-time controller, which requires the estimation of the signal derivatives. An example of the above is the trajectory tracking problem.

Since, the implicit discrete-time realizations were compared with existing discrete-time realizations of the standard differentiator and the robust exact filtering differentiator, then, a comparative analysis of both realizations with other observers is important (e.g., Kalman filter, linear, non-homogeneous and Alien differentiators, ...).

Additionally, the implicit discrete-time realizations provide finite-time stability of the observation error. However, its convergence time depends on the initial condition. Hence, large values of initial errors ($|\sigma_{0,0}|$, $|\sigma_{1,0}|$, $\cdots$, $|\sigma_{n,0}|$) implies a large value of the settling-time. Then, one could attempt to obtain an implicit fixed-time or predefined stable differentiator to avoid large values of the settling time.

Systems with a large sampling time, appear in many real-time applications. In this thesis, it is shown that the performance of the implicit differentiators supersede to the performance of the explicit one. Although MIDFD was implemented for a DC-DC buck converter, one could consider many other applications, for instance, mobile robots with a limited sampling time.

One important fact is than the MIDFD takes a measurement at time t_k and an estimation is obtained for t_{k+1} and the HIDD obtains an estimation at time t_k. A

similar effect is obtained with the implicit differentiators obtained from the standard differentiator [Mojallizadeh *et al.* 2021], where they require to use a measurement at time t_{k+1} to be implemented. Then, is it possible to obtain a discrete-time differentiator from the standard differentiator? and what is the reason? It may be an other interesting research study.

List of Figures

List of Tables

Bibliography

[Acary *et al.* 2012] V. Acary, B. Brogliato and Y. V. Orlov. *Chattering-Free Digital Sliding-Mode Control With State Observer and Disturbance Rejection.* IEEE Transactions on Automatic Control, vol. 57, no. 5, pages 1087–1101, May 2012. (Cited on page 43.)

[Alarcón-Carbajal *et al.* 2022] Martin A. Alarcón-Carbajal, José E. Carvajal-Rubio, Juan D. Sánchez-Torres, David E. Castro-Palazuelos and Guillermo J. Rubio-Astorga. *An Output Feedback Discrete-Time Controller for the DC-DC Buck Converter.* Energies, vol. 15, no. 14, 2022. (Cited on page 106.)

[Aleksandrov *et al.* 1999] A.D. Aleksandrov, A.N. Kolmogorov and M.A. Lavrent'ev. Mathematics: Its content, methods and meaning, volume 1 of *Dover Books on Mathematics Series.* Dover Publications, 1999. (Cited on page 44.)

[Apostol 1967] T. Apostol. Calculus: One-variable calculus with an introduction to linear algebra, volume 1. John Wiley & Sons, 2 édition, 1967. (Cited on pages 41 and 108.)

[Atassi & Khalil 2000] A.N. Atassi and H.K. Khalil. *Separation results for the stabilization of nonlinear systems using different high-gain observer designs.* Systems & Control Letters, vol. 39, no. 3, pages 183–191, mar 2000. (Cited on pages 2 and 27.)

[Bacha *et al.* 2014] Seddik Bacha, Iulian Munteanu and Antoneta Iuliana Bratcu. Classical averaged model, pages 55–96. Springer London, London, 2014. (Cited on page 118.)

[Bachem *et al.* 2012] Achim Bachem, Martin Grötschel and Bernhard Korte. Mathematical programming the state of the art: Bonn 1982. Springer-Verlag Berlin Heidelberg, 1 édition, 2012. (Cited on page 10.)

[Bai *et al.* 2000] Zhaojun Bai, James Demmel, Jack Dongarra, Axel Ruhe and Henk van der Vorst. Templates for the solution of algebraic eigenvalue problems: a practical guide. Society for Industrial and Applied Mathematics (SIAM), 2000. (Cited on page 65.)

[Barbot *et al.* 2020] Jean-Pierre Barbot, Arie Levant, Miki Livne and Davin Lunz. *Discrete Differentiators Based on Sliding Modes.* Automatica, vol. 112, page 108633, 2020. (Cited on pages 3, 39, 41 and 50.)

[Bhat & Bernstein 1997] S. P. Bhat and D. S. Bernstein. *Finite-time Stability of Homogeneous Systems*. In Proceedings of the 1997 American Control Conference (Cat. No.97CH36041), volume 4, pages 2513–2514., June 1997. (Cited on pages 19 and 20.)

[Bhat & Bernstein 1998] Sanjay P Bhat and Dennis S Bernstein. *Continuous finite-time stabilization of the translational and rotational double integrators*. IEEE Transactions on automatic control, vol. 43, no. 5, pages 678–682, 1998. (Cited on page 106.)

[Brogliato & Polyakov 2020] Bernard Brogliato and Andrey Polyakov. *Digital implementation of sliding-mode control via the implicit method: A tutorial*. International Journal of Robust and Nonlinear Control, 2020. (Cited on page 124.)

[Brogliato *et al.* 2019] B. Brogliato, A. Polyakov and D. Efimov. *The Implicit Discretization of the Super-Twisting Sliding-Mode Control Algorithm*. IEEE Transactions on Automatic Control, pages 1–1, 2019. (Cited on pages 3 and 39.)

[Brogliato *et al.* 2020] B. Brogliato, A. Polyakov and D. Efimov. *The Implicit Discretization of the Supertwisting Sliding-Mode Control Algorithm*. IEEE Transactions on Automatic Control, vol. 65, no. 8, pages 3707–3713, 2020. (Cited on page 43.)

[Carvajal-Rubio *et al.* 2019] J. E. Carvajal-Rubio, A. G. Loukianov, J. D. Sánchez-Torres and M. Defoort. *On the Discretization of a Class of Homogeneous Differentiators*. In 2019 16th International Conference on Electrical Engineering, Computing Science and Automatic Control (CCE), pages 1–6., September 2019. (Cited on page 79.)

[Carvajal-Rubio *et al.* 2020a] J. E. Carvajal-Rubio, J. D. Sánchez-Torres, M. Defoort, A. G. Loukianov and M. Djemai. *Discretization of the Robust Exact Filtering Differentiator Based on the Matching Approach*. In 2020 17th International Conference on Electrical Engineering, Computing Science and Automatic Control (CCE), pages 1–6, 2020. (Cited on page 76.)

[Carvajal-Rubio *et al.* 2020b] J.E. Carvajal-Rubio, J.D. Sánchez-Torres, M. Defoort and A.G. Loukianov. *On the Discretization of Robust Exact Filtering Differentiators*. In 21st IFAC World Congress 2020 - 1st Virtual IFAC World Congress (IFAC-V 2020), 2020. (Cited on page 3.)

[Carvajal-Rubio *et al.* 2021a] J.E. Carvajal-Rubio, J.D. Sánchez-Torres, M. Defoort, M. Djemai and A.G. Loukianov. *Implicit and explicit discrete-time realizations of homogeneous differentiators*. International Journal of Robust and Nonlinear Control, vol. 31, no. 9, pages 3606–3630, mar 2021. (Cited on page 3.)

[Carvajal-Rubio *et al.* 2021b] Jose Eduardo Carvajal-Rubio, Juan Diego Sánchez-Torres, Michael Defoort, Mohamed Djemai and Alexander G. Loukianov. *On the Efficient Implementation of an Implicit Discrete-Time Differentiator*.

WSEAS Transactions on Circuits and Systems, vol. 20, pages 70–74, 2021. (Cited on page 62.)

[Carvajal-Rubio *et al.* 2022] J.E. Carvajal-Rubio, J.D. Sánchez-Torres, M. Defoort, M. Djemai and A.G. Loukianov. *Robust Discrete-Time Output Feedback Stabilization of Integrator Chains*. International Journal of Robust and Nonlinear Control, 2022. (Cited on page 106.)

[Castañeda *et al.* 2021] Herman Castañeda, Jonathan Rodriguez and José Luis Gordillo. *Continuous and smooth differentiator based on adaptive sliding mode control for a quad-rotor MAV*. Asian Journal of Control, vol. 23, no. 2, pages 661–672, 2021. (Cited on pages 3 and 105.)

[Clempner & Yu 17] Julio B Clempner and Wen Yu. New perspectives and applications of modern control theory. Lecture Notes in Control and Information Sciences. . Springer International Publishing, 1 édition, 2017. (Cited on page 34.)

[De Jong & Van Leeuwen 1975] Lieuwe De Jong and Jan Van Leeuwen. *An improved bound on the number of multiplications and divisions necessary to evaluate a polynomial and all its derivatives*. ACM SIGACT News, vol. 7, no. 3, pages 32–34, 1975. (Cited on page 66.)

[Drakunov & Utkin 1990] S.V. Drakunov and V.I. Utkin. *On Discrete-Time Sliding Modes*. In Nonlinear Control Systems Design 1989, . IFAC Symposia Series, pages 273–278. Pergamon, Oxford, 1990. (Cited on pages 2, 3 and 39.)

[Edwards & Spurgeon 1998] C. Edwards and S. Spurgeon. Sliding mode control: Theory and applications. Systems and Control. . Crc Press, London, 1 édition, 1998. (Cited on page 2.)

[El Fadil *et al.* 2009] Hassan El Fadil, Fouad Giri, Fatima-Zahra Chaoui and Ouadia El Magueri. *Accounting for Input Limitation in the Control of Buck Power Converters*. IEEE Transactions on Circuits and Systems I: Regular Papers, vol. 56, no. 6, pages 1260–1271, 2009. (Cited on page 118.)

[Emel'Yanov *et al.* 1996] SV Emel'Yanov, SK Korovin and A Levant. *High-order sliding modes in control systems*. Computational mathematics and modeling, vol. 7, no. 3, pages 294–318, 1996. (Cited on page 106.)

[Facchinei & Pang 2003] Francisco Facchinei and Jong-Shi Pang. Finite-dimensional variational inequalities and complementarity problems. Springer-Verlag New York, 1 édition, 2003. (Cited on pages 11, 12 and 13.)

[Filippov 88] A. F. Filippov. Differential equations with discontinuous righthand sides, volume 18 of *Mathematics and its Applications*. Springer Netherlands, 1 édition, 1988. (Cited on page 29.)

[Firey 1960] William J. Firey. *Remainder Formulae in Taylor's Theorem*. The American Mathematical Monthly, vol. 67, no. 9, pages 903–905, 1960. (Cited on page 40.)

[Franklin *et al.* 1998] Gene Franklin, Powell J. David and Workman Michael L. Digital control of dynamic systems. World Student Series. Addison-Wesley, 3 édition, 1998. (Cited on page 34.)

[Ghane & Menhaj 2013] Hamed Ghane and Mohammad Bagher Menhaj. *Eigenstructure-based analysis for non-linear autonomous systems.* IMA Journal of Mathematical Control and Information, vol. 32, no. 1, pages 21–40, 08 2013. (Cited on page 76.)

[Hanan *et al.* 2020] Avi Hanan, Adam Jbara and Arie Levant. *Non-chattering discrete differentiators based on sliding modes.* In 59th Conference on Decision and Control, December 14-18, Jeju Island, Republic of Korea, 2020. (Cited on pages 3, 75, 81, 97 and 103.)

[Hanan *et al.* 2021] Avi Hanan, Arie Levant and Adam Jbara. *Low-chattering discretization of homogeneous differentiators.* IEEE Transactions on Automatic Control, pages 1–1, 2021. (Cited on pages 114 and 116.)

[Hiriart-Urruty & Lemaréchal 2004] Jean-Baptiste Hiriart-Urruty and Claude Lemaréchal. Fundamentals of convex analysis. Grundlehren Text Editions. Springer Science & Business Media, 1 édition, 2004. (Cited on page 9.)

[Huber *et al.* 16] Olivier Huber, Bernard Brogliato, Vincent Acary, Ahcene Boubakir, Franck Plestan and Bin Wang. *Experimental Results on Implicit and Explicit Time-Discretization of Equivalent-Control-Based Sliding-Mode Control.* In Recent Trends in Sliding Mode Control, volume 102 of *IET Control, Robotics and Sensors Series*, pages 207–235. IET, Apr 2016. (Cited on page 39.)

[Huber *et al.* 2013] O. Huber, V. Acary and B. Brogliato. *Comparison Between Explicit and Implicit Discrete-Time Implementations of Sliding-Mode Controllers.* In 52nd IEEE Conference on Decision and Control, pages 2870–2875., 2013. (Cited on pages 3 and 39.)

[Huber *et al.* 2016a] O. Huber, V. Acary and B. Brogliato. *Lyapunov Stability and Performance Analysis of the Implicit Discrete Sliding Mode Control.* IEEE Transactions on Automatic Control, vol. 61, no. 10, pages 3016–3030, oct 2016. (Cited on page 39.)

[Huber *et al.* 2016b] Olivier Huber, Vincent Acary, Bernard Brogliato and Franck Plestan. *Implicit Discrete-Time Twisting Controller Without Numerical Chattering: Analysis and Experimental Results.* Control Engineering Practice, vol. 46, pages 129 – 141, 2016. (Cited on page 39.)

[Huber *et al.* 2019] O. Huber, V. Acary and B. Brogliato. *Lyapunov Stability Analysis of the Implicit Discrete-Time Twisting Control Algorithm.* IEEE Transactions on Automatic Control, pages 1–1, 2019. (Cited on pages 3, 39 and 81.)

[Iqbal *et al.* 2011] M. Iqbal, A. I. Bhatti, S. I. Ayubi and Q. Khan. *Robust Parameter Estimation of Nonlinear Systems Using Sliding-Mode Differentiator Observer.*

IEEE Transactions on Industrial Electronics, vol. 58, no. 2, pages 680–689, Feb 2011. (Cited on page 2.)

[Jbara *et al.* 2020] Adam Jbara, Arie Levant and Avi Hanan. *Filtering homogeneous observers in control of integrator chains*. International Journal of Robust and Nonlinear Control, 2020. (Cited on pages 30 and 97.)

[Jbara *et al.* 2021] Adam Jbara, Arie Levant and Avi Hanan. *Filtering homogeneous observers in control of integrator chains*. International Journal of Robust and Nonlinear Control, vol. 31, no. 9, pages 3658–3685, 2021. (Cited on page 27.)

[Kaveh & Shtessel 2008] Parisa Kaveh and Yuri B. Shtessel. *Blood Glucose Regulation Using Higher-Order Sliding Mode Control*. International Journal of Robust and Nonlinear Control, vol. 18, no. 4-5, pages 557–569, 2008. (Cited on page 2.)

[Kazantzis & Kravaris 1999] Nikolaos Kazantzis and Costas Kravaris. *Time-Discretization of Nonlinear Control Systems Via Taylor Methods*. Computers & Chemical Engineering, vol. 23, no. 6, pages 763 – 784, 1999. (Cited on page 41.)

[Kikuuwe & Fujimoto 2006] R. Kikuuwe and H. Fujimoto. *Proxy-Based Sliding Mode Control for Accurate and Safe Position Control*. In Proceedings of the 2006 IEEE International Conference on Robotics and Automation, 2006, pages 25–30., May 2006. (Cited on pages 2 and 39.)

[Kim 2010] I. Kim. *A Technique for Estimating the State of Health of Lithium Batteries Through a Dual-Sliding-Mode Observer*. IEEE Transactions on Power Electronics, vol. 25, no. 4, pages 1013–1022, April 2010. (Cited on page 2.)

[Koch & Reichhartinger 2018] S. Koch and M. Reichhartinger. *Discrete-Time Equivalent Homogeneous Differentiators*. In 2018 15th International Workshop on Variable Structure Systems (VSS), pages 354–359., July 2018. (Cited on pages 32, 34, 40, 41, 69 and 76.)

[Koch *et al.* 2020] S. Koch, M. Reichhartinger, M. Horn and L. Fridman. *Discrete-Time Implementation of Homogeneous Differentiators*. IEEE Transactions on Automatic Control, vol. 65, no. 2, pages 757–762, Feb 2020. (Cited on pages 3, 32, 34, 35, 39 and 79.)

[Kratz 1995] Werner Kratz. *Characterization of strong observability and construction of an observer*. Linear Algebra and its Applications, vol. 221, pages 31 – 40, 1995. (Cited on page 28.)

[Levant & Livne 2016] Arie Levant and Miki Livne. *Weighted Homogeneity and Robustness of Sliding Mode Control*. Automatica, vol. 72, pages 186–193, 2016. (Cited on pages 26, 50 and 90.)

[Levant & Livne 2019] Arie Levant and Miki Livne. *Robust Exact Filtering Differentiators*. European Journal of Control, 2019. (Cited on pages 2, 3, 4, 5, 6, 27, 28, 30, 75, 78, 81, 85, 97, 103, 105, 106 and 114.)

[Levant *et al.* 2017] Arie Levant, Miki Livne and Xinghuo Yu. *Sliding-Mode-Based Differentiation and Its Application.* IFAC-PapersOnLine, vol. 50, no. 1, pages 1699 – 1704, 2017. (Cited on page 29.)

[Levant 2003] Arie Levant. *Higher-Order Sliding Modes, Differentiation and Output-Feedback Control.* International Journal of Control, vol. 76, no. 9-10, pages 924–941, 2003. (Cited on pages 2, 27, 28, 29 and 30.)

[Levant 2005] Arie Levant. *Homogeneity Approach to High-Order Sliding Mode Design.* Automatica, vol. 41, no. 5, pages 823–830, 2005. (Cited on page 23.)

[Levant 2010] A. Levant. *Chattering Analysis.* IEEE Transactions on Automatic Control, vol. 55, no. 6, pages 1380–1389, June 2010. (Cited on page 2.)

[Levant 2018] A. Levant. *Filtering Differentiators and Observers.* In 2018 15th International Workshop on Variable Structure Systems (VSS), pages 174–179., July 2018. (Cited on pages 30 and 62.)

[Lienhardt *et al.* 2007] A. Lienhardt, G. Gateau and T. A. Meynard. *Digital Sliding-Mode Observer Implementation Using FPGA.* IEEE Transactions on Industrial Electronics, vol. 54, no. 4, pages 1865–1875, Aug 2007. (Cited on page 2.)

[Livne & Levant 2014] Miki Livne and Arie Levant. *Proper Discretization of Homogeneous Differentiators.* Automatica, vol. 50, no. 8, pages 2007–2014, 2014. (Cited on pages 2, 3, 32, 33, 39, 50, 53 and 79.)

[Luo *et al.* 2019] Dong Luo, Xiaogang Xiong, Shanhai Jin and Wei Chen. *Implicit Euler Implementation of Twisting Controller and Super-Twisting Observer without Numerical Chattering: Precise Quasi-Static MEMS Mirrors Control.* MATEC Web Conf., vol. 256, page 03004, 2019. (Cited on page 3.)

[McDougall & Wotherspoon 2014] Trevor J. McDougall and Simon J. Wotherspoon. *A Simple Modification of Newton's Method to Achieve Convergence of Order* $1 + \sqrt{2}$. Applied Mathematics Letters, vol. 29, pages 20 – 25, 2014. (Cited on page 60.)

[McNamee & Pan 2013] J. M. McNamee and Victor Pan. Numerical methods for roots of polynomials - part ii, volume 16 of *Studies in Computational Mathematics.* Elsevier Science, Amsterdam London, 2013. (Cited on page 62.)

[Melman 1997] A. Melman. *Classroom Note: Geometry and Convergence of Euler's and Halley's Methods.* SIAM Review, vol. 39, no. 4, pages 728–735, 1997. (Cited on pages 60 and 61.)

[Mojallizadeh *et al.* 2021] Mohammad Rasool Mojallizadeh, Bernard Brogliato and Vincent Acary. *Time-discretizations of differentiators: Design of implicit algorithms and comparative analysis.* International Journal of Robust and Nonlinear Control, vol. 31, no. 16, pages 7679–7723, aug 2021. (Cited on pages 3, 35, 36, 39, 123 and 125.)

[Moreno-Valenzuela 2020] J. Moreno-Valenzuela. *A Class of Proportional-Integral With Anti-Windup Controllers for DC–DC Buck Power Converters With Saturating Input*. IEEE Transactions on Circuits and Systems II: Express Briefs, vol. 67, no. 1, pages 157–161, 2020. (Cited on page 118.)

[Moreno 2021] Jaime A Moreno. *Arbitrary order fixed-time differentiators*. IEEE Transactions on Automatic Control, 2021. (Cited on page 27.)

[Moulay *et al.* 2022] Emmanuel Moulay, Vincent Léchappé, Emmanuel Bernuau, Michael Defoort and Franck Plestan. *Fixed-time sliding mode control with mismatched disturbances*. Automatica, vol. 136, page 110009, 2022. (Cited on page 27.)

[Oliveira *et al.* 2017] Tiago Roux Oliveira, Antonio Estrada and Leonid M Fridman. *Global and exact HOSM differentiator with dynamic gains for output-feedback sliding mode control*. Automatica, vol. 81, pages 156–163, 2017. (Cited on pages 3 and 105.)

[Othmane *et al.* 2021] Amine Othmane, Joachim Rudolph and Hugues Mounier. *Systematic comparison of numerical differentiators and an application to model-free control*. European Journal of Control, vol. 62, pages 113–119, 2021. (Cited on page 27.)

[Perdikaris 1991] George A. Perdikaris. Computer controlled systems: Theory and applications, volume 8 of *Intelligent Systems, Control and Automation: Science and Engineering*. Springer Netherlands, 1 édition, 1991. (Cited on page 78.)

[Polyakov *et al.* 2019] Andrey Polyakov, Denis Efimov and Bernard Brogliato. *Consistent Discretization of Finite-Time and Fixed-Time Stable Systems*. SIAM Journal on Control and Optimization, vol. 57, no. 1, pages 78–103, 2019. (Cited on pages 2, 3 and 39.)

[Polyakov 2011] Andrey Polyakov. *Nonlinear feedback design for fixed-time stabilization of linear control systems*. IEEE Transactions on Automatic Control, vol. 57, no. 8, pages 2106–2110, 2011. (Cited on page 22.)

[Polyakov 2020] Andrey Polyakov. Generalized homogeneity in systems and control. Springer, 2020. (Cited on page 22.)

[Reichhartinger *et al.* 2017] M. Reichhartinger, S.K. Spurgeon, M. Forstinger and M. Wipfler. *A Robust Exact Differentiator Toolbox for Matlab®/Simulink®*. IFAC-PapersOnLine, vol. 50, no. 1, pages 1711 – 1716, 2017. 20th IFAC World Congress. (Cited on page 30.)

[Ren *et al.* 2019] C. Ren, X. Li, X. Yang and S. Ma. *Extended State Observer-Based Sliding Mode Control of an Omnidirectional Mobile Robot With Friction Compensation*. IEEE Transactions on Industrial Electronics, vol. 66, no. 12, pages 9480–9489, Dec 2019. (Cited on page 2.)

[Rodrigues & Oliveira 2018] Victor Hugo Pereira Rodrigues and Tiago Roux Oliveira. *Global adaptive HOSM differentiators via monitoring functions and hybrid state-norm observers for output feedback*. International Journal of Control, vol. 91, no. 9, pages 2060–2072, 2018. (Cited on pages 2 and 27.)

[Scavo & Thoo 1995] T. R. Scavo and J. B. Thoo. *On the Geometry of Halley's Method*. The American Mathematical Monthly, vol. 102, no. 5, pages 417–426, 1995. (Cited on pages 60, 61, 62 and 69.)

[Shaw & Traub 1974] Mary Shaw and Joseph Frederick Traub. *On the number of multiplications for the evaluation of a polynomial and some of its derivatives*. Journal of the ACM (JACM), vol. 21, no. 1, pages 161–167, 1974. (Cited on page 66.)

[Shaw & Traub 1975] Mary Shaw and Joseph Frederick Traub. *Analysis of a family of algorithms for the evaluation of a polynomial and some of its derivatives*. Department of Computer Science Carnegie Mellon University, 1975. (Cited on page 66.)

[Shtessel *et al.* 14] Yuri Shtessel, Christopher Edwards, Leonid Fridman and Arie Levant. Sliding mode control and observation. Control Engineering. . Birkhäuser Basel, 1 édition, 2014. (Cited on pages 17, 28, 29 and 30.)

[Shtessel *et al.* 2007] Yuri B. Shtessel, Ilya A. Shkolnikov and Arie Levant. *Smooth Second-Order Sliding Modes: Missile Guidance Application*. Automatica, vol. 43, no. 8, pages 1470–1476, 2007. (Cited on page 2.)

[Su *et al.* 2000] W. C. Su, S. V. Drakunov and U. Ozguner. *An O(T/sup 2/) Boundary Layer in Sliding Mode for Sampled-data Systems*. IEEE Transactions on Automatic Control, vol. 45, no. 3, pages 482–485, March 2000. (Cited on pages 2 and 39.)

[Utkin *et al.* 2009] Vadim I. Utkin, Juergen Guldner and Jingxin Shi. Sliding mode control in electro-mechanical systems. CRC Press, 2 édition, 2009. (Cited on page 2.)

[Utkin 1994] Vadim I. Utkin. Sliding mode control in discrete-time and difference systems, pages 87–107. Springer, Berlin, Heidelberg, 1994. (Cited on pages 2 and 39.)

[Varona 2002] Juan L. Varona. *Graphic and Numerical Comparison Between Iterative Methods*. The Mathematical Intelligencer, vol. 24, pages 37–46, 2002. (Cited on page 60.)

[Vasiljevic & Khalil 2008] Luma K Vasiljevic and Hassan K Khalil. *Error bounds in differentiation of noisy signals by high-gain observers*. Systems & Control Letters, vol. 57, no. 10, pages 856–862, 2008. (Cited on page 27.)

[Wang *et al.* 2015] B. Wang, B. Brogliato, V. Acary, A. Boubakir and F. Plestan. *Experimental Comparisons Between Implicit and Explicit Implementations of Discrete-Time Sliding Mode Controllers: Toward Input and Output Chattering Suppression.* IEEE Transactions on Control Systems Technology, vol. 23, no. 5, pages 2071–2075, Sep 2015. (Cited on page 39.)

[Weerakoon & Fernando 2000] S. Weerakoon and T.G.I. Fernando. *A Variant of Newton's Method with Accelerated Third-Order Convergence.* Applied Mathematics Letters, vol. 13, no. 8, pages 87–93, 2000. (Cited on page 60.)

[Zubov 1958] Vladimir Ivanovich Zubov. *Systems of ordinary differential equations with generalized-homogeneous right-hand sides.* Izvestiya Vysshikh Uchebnykh Zavedenii. Matematika, pages 80–88, 1958. (Cited on page 17.)